GRAPHENE BASED SORBENTS AND SENSORS FOR ENVIRONMENTAL APPLICATIONS

Thesis submitted to
the University of Calicut in partial fulfillment of the
requirements for the award of the degree of

Doctor of Philosophy
in Chemistry under the Faculty of Sciences

by

ANJU M.

Under the guidance of

Dr. Renuka N.K.

DEPARTMENT OF CHEMISTRY
UNIVERSITY OF CALICUT
KERALA-673 635
DECEMBER 2017

CERTIFICATE

This is to certify that the thesis entitled "**GRAPHENE BASED SORBENTS AND SENSORS FOR ENVIRONMENTAL APPLICATIONS**" is an authentic record of the research work carried out by **Anju M.** under my guidance for the award of the degree of Doctor of Philosophy in Chemistry under the faculty of Sciences, University of Calicut, Kerala and the same has not been submitted elsewhere for any degree or diploma. Certified that all the modifications suggested by the examiners have been incorporated in the thesis.

Calicut University
13. 08. 2018

Dr. Renuka N.K
(Supervising Teacher)

DECLARATION

I hereby declare that the thesis entitled **"GRAPHENE BASED SORBENTS AND SENSORS FOR ENVIRONMENTAL APPLICATIONS"** is the bonafide report of the original work carried out by me under the supervision of Dr. N.K. Renuka, Asst. Professor, Department of Chemistry, University of Calicut for the award of the degree of Doctor of Philosophy in Chemistry Under the Faculty of Sciences, University of Calicut, Kerala. The content of this thesis have not been submitted to any other institute or University for the award of any degree or diploma.

Calicut University **Anju. M.**
13. 08. 2018

ACKNOWLEDGEMENT

Words fail to pen down my gratitude, love and respect to all those amazing people in my life who are responsible for the very existence of my Ph.D thesis. I have been blessed with dozens of wonderful human beings who have spun a web of love, care and support around me. The road to this acknowledgement page would not have been this much smoother without their presence.

At the outset, I would like to express my sincere respect, gratitude and love to my Research Guide, Dr. N.K. Renuka for her whole hearted and full-fledged guidance during my doctoral research endeavor for the past few years. Her observations and comments helped me to establish the overall direction of the research and were crucial in developing the content of my thesis. I respect and gratefully acknowledge all her contributions and suggestions for my work specially her patience during communication of articles, in preparation of presentations and during thesis correction. She was the only person who was responsible for creating a passion within me towards my research work. She gave all the required freedom that was instrumental in creating a good research atmosphere with full of graphene chemistry and decked with evergreen moments and smiles.

Besides my advisor, I would like to thank our present Head of the Department, Dr.P.Raveendran and our former HOD's who were instrumental in providing the working atmosphere and all basic instrumentation facilities for pursuing Ph.D. Heartfelt thanks are due to all other faculty members of the Department. My sincere thanks are also extended to all the non teaching staffs of our Department. Mr. K. Satheesan needs a special mention for his dedication and sincerity as

the technical assistant of our Department. With great appreciation, I would like to acknowledge the support and help extended by the Research Scholars of the Department. Many thanks and gratitude to my colleagues in Physical research Lab, Anju Ajayan, Shivanandan, Vineeth M, Jyothi P.R., Sarada Karangadan, Nusrath Riyas, Nadira, Sabira and Sumitha. Vintu M, Anjana P.K. and Pranav K.G needs special mention for always being a helping hand in times of need.

I ran short of words while beginning this paragraph. Words ain't enough to express my love, care and affection, I treasure deep within for my dear group members-my extended family: Dr.Divya T, Nikhila M.P., Arsha Kusumam T.V., Akhila A.K., Ansi V.A., Varsha R. and Thasleena. Their joy, enthusiasm, love and care were contagious and inspiring for me, even during the very tough times of my life. With an ecstatic smile, I do cherish every moment with them and those cute memories will remain afresh in me forever.

Dr.Divya T, Nikhila M.P, Arsha Kusumam T.V., Akhila A.K., Anu Antony and Bintu Thomas needs special mention. They were a source of constant support, love and care for me that made my only dream in life come true. Those talks, walks, mocks and the list goes on, which once seemed to be unending had come to a blissful ending.

In this juncture, I remember all my school teachers who have taught me the basics of Chemistry.

I gratefully acknowledge the financial assistance received from UGC. I extend my profound thanks to STIC Cochin, IIT Bombay, NIT Calicut, Department of Physics Vimala College, SAIF Mahatma Gandhi University, Department of Nanoscience and Technology and Department of Physics, University of Calicut for carrying out the analysis necessary for my research wok. I thank Bina Xerox for the neat processing of my thesis.

My warmest thanks and love to my dearest friend, my mentor and my better half Sijin. I pursued Ph.D for him and it was because of his love, patience, support, care, optimism and unwavering belief in me that had led to the completion of my thesis. He was my backbone and that had enabled me to overcome all the hurdles I had to face in my life. I greatly adore the love, support and encouragement shown by my Father-in-law, Mother-in-law and my dear Sis-in-law (Sini).

Last but nevertheless the least, I place this thesis before my parents, my Achan, Amma and my dearest Sisters Anu and Amritha. Looking back, even unhappiness acquires a glow with my sisters' smile. Words fail to convey the struggles they have gone through for me. I owe my life to my family for bringing me up to this stage, forever and ever.

All of you made it possible for me to reach this point and your roles cannot be measured by any wordy yardstick.

Realising the blessings of the omnipotent force, I wish to dedicate this thesis to my dear Achan. Indebted to his silent nod and support, for all the good that had come in my life till date.

Anju M.

PREFACE

The Super Carbon 'Graphene' has revolutionized scientific and technological world on account of its intriguing physiochemical properties. Devising Graphene as a scaffold for inclusion of various species like metal oxides, organic dyes, heteroatoms etc. have paved the way for Graphene nanohybrids. They have exemplified themselves as indispensible tools for a wide range of applications, wherein its unique electrical, optical, structural and mechanical features etc. have been exploited. These hybrids depict substantial enhancement in their multi functional aspects when compared to conventional composites. Present endeavour is focused on the environmental applications of Graphene hybrids; more precisely on sensing and adsorbing contaminants present in aqueous media.

Today, there is an ever growing need for an affirmative action to tackle the environmental pollution due to the unruly discharge of contaminants. Among the much celebrated decontamination technologies, adsorption occupies an esteemed position. Sorbents ought to be properly tailored for fast and effective adsorption-desorption dynamics in contaminants removal from aqueous solutions. Graphene based magnetic sorbents deserve citation in view of their multifarious application as adsorbents for a wide array of contaminants namely heavy metals, organic dyes, oils, organic solvents, industrial sewage etc. In this regard, well designed hybrids of Graphene-Iron Oxide nanostructure have been projected as an elite sorbent to mitigate

the perils of water pollution and their adsorption characteristics against Chromium (VI), Methylene Blue dye, Oils and Organic solvents are investigated in detail.

Driven by environmental and health concerns, there is presently a strong thrust towards the development of fast, inexpensive sensors for the detection of noxious and relevant analytes like heavy metals, anions, etc. in water bodies. The advancement of Graphene-dye based sensors has become an area of hot research due to their tunable optical and electric properties. By taking the advantage of preferential adsorption capacity of Graphene towards target analytes over dye molecules, interesting sensing application has been demonstrated, which could quantify Mercury ion and Fluoride ion in parts per trillion levels. The projected approach of building a simple Graphene-Dye based sensor depicted admirable detectivity and selectivity towards the test ions and these hybrids can further offer many opportunities that can be also tuned for other optical functionalities employing a variety of commercial dye molecules.

CONTENTS

ABBREVIATIONS

GRO	GRAPHENE OXIDE
GN	GRAPHENE
RGO	REDUCED GRAPHENE OXIDE
CNT	CARBON NANOTUBE
PU	POLYURETHANE
GPUF	GRAPHENE-POLYURETHANE-IRON OXIDE
GPU	GRAPHENE-POLYURETHANE
MB	METHYLENE BLUE
FPU	IRON OXIDE-POLYURETHANE
RD	RHODAMINE Dye
FLR	FLUORESCEIN Dye
GRD	GRAPHENE-RHODAMINE
GD	GRAPHENE-DYE
GFU	GRAPHENE-FLUORESCEIN
ppm	PARTS PER MILLION
ppb	PARTS PER BILLION
ppt	PARTS PER TRILLION

CHAPTER I
INTRODUCTION

Contents

Graphene, the elite member of carbon fraternity has received immense attention of the scientific community owing to its intriguing thermal, electrical, optical and mechanical properties. It is certain that Graphene and its hybrids will revolutionize current technological and scientific world. In this chapter, we have attempted to provide a general introduction to Graphene and its hybrids. Necessary basic information regarding the history and structure of Graphene is outlined in this chapter. Various synthetic methodologies adopted for the preparation of Graphene is briefly discussed. This chapter also presents a brief outline regarding the properties of Graphene and its applications in diverse fields. Towards the end of the chapter, the relevance, objectives and outline of the research work are highlighted.

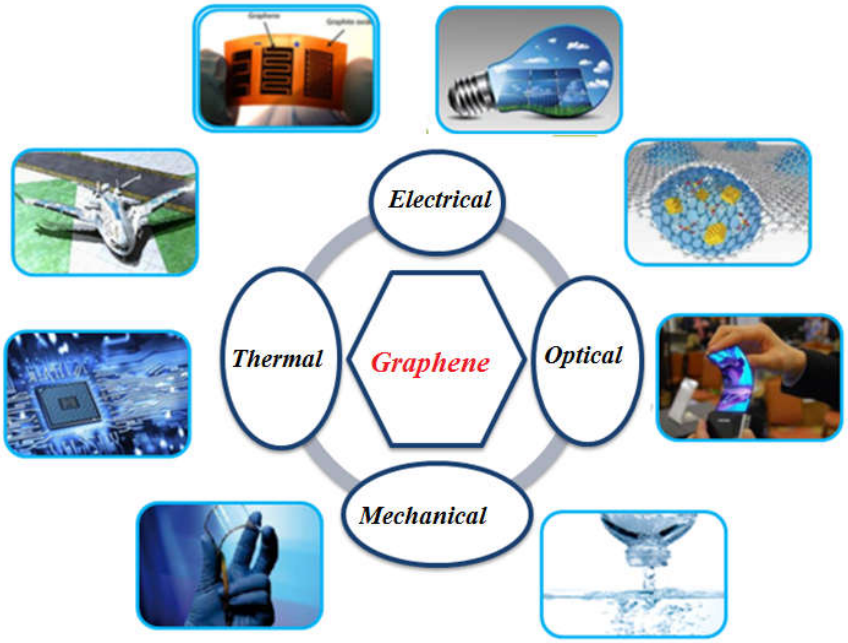

GRAPHENE - SUPER CARBON OF 21st CENTURY

1.1 Carbon

"Carbon has this genius of making a chemically stable, two-dimensional, one-atom-thick membrane in a three-dimensional world. And that, I believe, is going to be very important in the future of chemistry and technology in general." - Richard Smalley [Nobel Laureate for the discovery of Fullerenes].

This Genius Carbon [C], the sixth element belonging to Group IV of the periodic table is a wonder entity with many superlatives to its credit. The word Carbon is derived from the Latin word 'Carbo' which means Charcoal. It is the sixth most abundant element in the Earth's crust and can be represented by the electronic structure $1s^2 2s^2 2p_x^1 2p_y^1$. The uniqueness of carbon lies in its ability to bind with itself and other atoms to form networks which forms the basis of life. Atomic carbon is very short lived and it tends to stabilize in atomic structures with various configurations or allotropes like amorphous carbon, Graphite, Diamond, Fullerenes, Carbon Nanotubes, Graphene etc. Carbon is phenomenal in forming allotropes of every possible dimensionality viz. 0D Fullerenes, 1D nanotube, 2D Graphene, 3D Diamond etc.

1.2 Graphite

Before excavating the history of Graphene, one must note about Graphite. Graphite is the naturally occurring crystalline allotrope of carbon. Graphite can be regarded as a structure formed by stacking of Graphene layers in a 3D fashion. Graphite was familiar to mankind several centuries ago and historical records quote its use in

pottery for decoration and by shepherds to mark their sheep. However it was known as 'Plumbago' believing it to be a Lead ore until 1799, when Scheele demonstrated its identity to be a Carbon structure. In 1789, a German Scientist coined the term Graphite (Greek word for writing) and with the advancement of pencil industry, it has been used in pencils since the Eighteenth century.

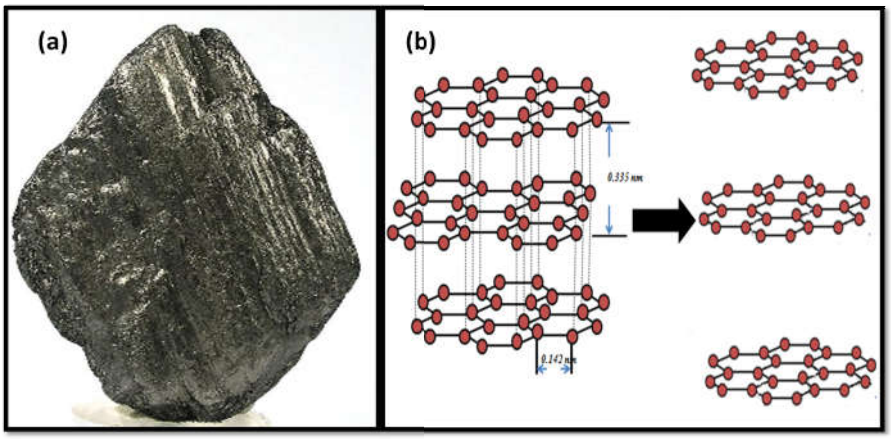

Figure 1. (a) Image of Graphite specimen [Adapted from https://en.wikipedia.org/wiki/Graphite] (b) Structure of Graphite depicting the interlayer distance and honeycomb arrangement of Carbon atom.

Graphite is characterised by layer and planar structure where the individual layers are separated and it constitutes Graphene. The Carbon atoms of the same plane in Graphite are separated by 0.142 nm and the separation between layers is 0.335 nm [Fig. 1]. The carbon atoms in graphite planes are covalently bonded satisfying only 3 of the 4 bonding sites. The non bonded fourth electron is free to traverse

through the plane and thus making graphite conducting. The layers are held together by Van der Waals forces which being weak allows the layers to slide past one another. On account of its weak dispersion forces, Graphite is also widely used as a lubricant. The high thermal, electrical stability and conductivity of graphene assist its extensive use as electrodes and refractories in high temperature applications. Graphite finds application in batteries, steel industries, for Brake lining etc.

1.3 Graphene

As per the definition recommended by IUPAC, Graphene term means "A single carbon layer of the graphite structure, describing its nature by analogy to a polycyclic aromatic hydrocarbon of quasi infinite size" [1]. This Magic Bullet in current scientific world is a one atom thick hexagonal carbon array known for its intriguing properties and exciting applications. Graphene, the elite allotrope in the carbon fraternity has received immense attention of the scientific community owing to its intriguing structure and properties. To be more precise, graphene is a flat monolayer allotrope of carbon with sp^2 hybridized atoms fashioned in a honeycomb like lattice. The honeycomb like lattice of Graphene can be moulded into other carbon allotropic structures and is considered as the mother of all graphitic forms. It can be wrapped to form 0D Fullerenes, rolled to 1D carbon nanotubes, stacked to form 3D graphite. Graphene is a dense material to such an extent that even the smallest Helium atom cannot pass through it. Graphene is known to be thinnest material known till date, and also

the strongest entity. It competes with Copper in its electrical conductivity and outshines all other materials in thermal conductivity. Pristine Graphene can be considered as a semi-metal or zero gap semiconductor with unique electronic, mechanical properties and with unexpectedly high opacity with an astonishingly low absorption ratio of (~2%) white light.

1.3.1 History of Graphene

The history of Graphene dates to 1859, when Benjamin Bordie synthesised a lamellar structure of graphene oxide by reacting graphite with concentrated nitric acid and Potassium chlorate. In 1919, the properties of Graphene oxide prepared by Brodie's method were investigated. Steps directed to prepare Graphene using similar adopted procedure for carbon nanotubes yielded thicker graphite films. The band theory of graphite was put forward by Wallace in 1947 [2]. Ruess and Vogt (1948) published the First TEM image of few layers of graphene [3], and in 1960, a single atom plane of graphite was isolated by Ubbelohde and Lewis which had higher basal conductivity [4]. Hanns-Peter Boehm and his coworkers in 1961, prepared single graphene sheets and characterised it by TEM and XRD [5]. The first report on the application of Chemical Vapour deposition method to achieve Graphene was done by Hess and Ban in 1996 [6]. Epitaxial growth of few layer graphene through the chemical vapor deposition of hydrocarbons on metal substrates were attempted by Land et al. (1992) [7] and Nagashima et al. (1993) [8]. Research on Graphene went in a snail's speed from 1960 to 2000 and the research interests were

mainly centered on graphite intercalation compounds. The beginning of twenty first century witnessed many significant discoveries with respect to graphene. The year 2004 created a jolt in Graphene research when Andre Geim and Kostya Novoselov at Manchester University, UK, extracted one-atom thick graphene sheets from graphite using Scotch type method [Fig.2]. They received the Nobel Prize in Physics in 2010 for their ground breaking discovery that had enough potential to revolutionize scientific world and is crowned as the Super Carbon by science fraternity [9-10]. In 2005, Quantum Hall Effect was discovered in Graphene by Novoselov et al. and Zhang et al. [11-13].

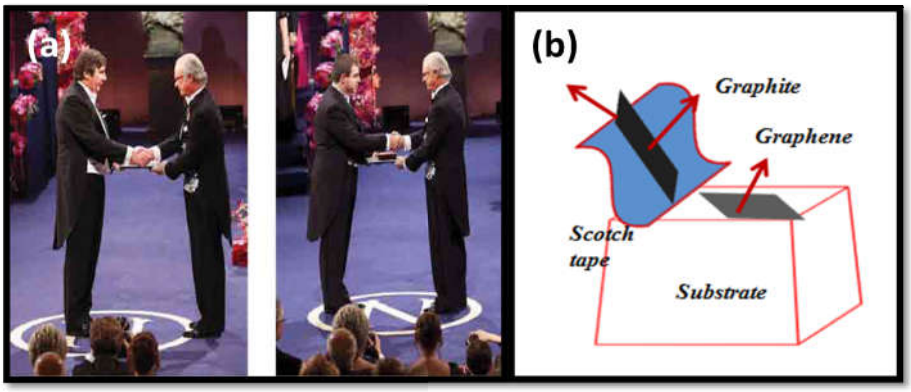

Figure 2. (a) Andre Geim and Kostya Novoselov receiving the Nobel Prize in Physics & (b) Pictorial depiction of Scotch type method.

By 2009, commercialization of Graphene started and more Graphene based systems were developed which finds its use in every walks of life such as in energy storage, sensors, environmental applications, transistors etc. Still there is ample room for the development of graphene based structures and their applications.

1.3.2 Graphene Family

The Graphene family comprises of those materials obtained in synthesis routes toward Graphene. Graphene family tree consists of Graphite Oxide, Graphene oxide and Reduced Graphene oxide which can be distinguished by the number of layers and by the oxidation level of carbon.

(i) *Graphite*: As mentioned earlier, Graphite is an allotrope of Carbon composed of hexagonal array of Carbon atoms in a planar condensed ring system. These layers are stacked one above the other in a 3D-fashion [14-15] [Fig.1]. Graphite is the most stable state of carbon and it exists in two forms, viz. alpha and rhombohedra form. These forms differ only in stacking of graphene layers. Alpha graphite may be either buckled or flattened.

(ii) *Graphite Oxide*: It is a heterogeneous product obtained by the oxidation of graphite and can be regarded as an assembly of several graphene oxide layers. Formerly, known as Graphitic acid or graphitic oxide it is constituted by Carbon, Oxygen and Hydrogen in different ratios. It is a yellow/brown coloured solid with carbon to oxygen ratio in the range of 2.1 to 2.9. Its structure and properties depend on the synthesis procedure adopted and the oxidation level [16-17]. Graphite oxide maintains the layer structure of its parent graphite. But the interlayer distance is about ten times higher than graphite.

(iii) *Graphene Oxide*: Graphene oxide (GRO) is exactly single layer of polycyclic carbon network with all the Carbon atoms arranged

hexagonally in a planar condensed ring system [Fig.3]. It depicts partial aromatic nature and is characterised by the presence of several oxygen functional groups [CO, OH, and COOH]. GRO has unique characteristic traits that distinguish it from graphene, owing to the presence of several oxygen containing functional groups like hydroxyl and epoxy group on the basal plane along with few carboxyl, carbonyl, phenol, lactone, and quinine groups at the edges [18-19]. The coverage of oxygen functional groups vary according to the preparation procedure and these functional groups inhibit the electron transfer process and hence conductivity of GRO is smaller than Graphene. It possesses a band gap greater than 1.5 eV, depending on the oxidation level. The C: O ratio is between 2 and 3. Due to the non-uniform oxygen coverage in the graphene basal plane, GRO exhibits small ordered sp^2 clusters isolated with sp^3 C-O matrix. Literature survey suggests that the thickness of GRO can be approximately 1 nm which is greater than pristine graphene due to the presence of oxygen functional moieties and adsorbed water molecules above and below the plane. The Lerf–Klinowski model has been widely accepted as the structural model of GRO [20]. Recently, Gao and co-workers have proposed a model of GRO with five- and six membered lactol rings adorning the edges and esters of tertiary alcohols decorating the surface. GRO sheets are hydrophilic and biocompatible in nature [21]. GRO demonstrates exquisite electronic, thermal, electrochemical and mechanical properties. In contrast to Graphene, GRO is fluorescent over a wide range of wavelength due to its heterogeneous structure

and hence GRO finds extensive application as optical sensors for a wide range of molecules.

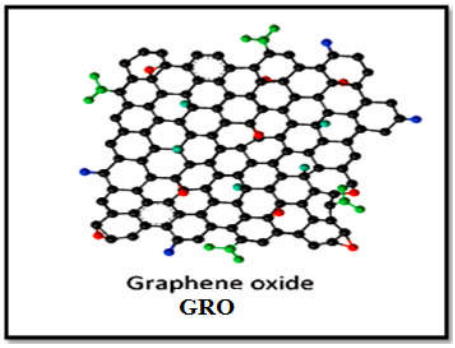

Figure 3. Structure of Graphene oxide

(iv) *Reduced Graphene Oxide (RGO)*: All the carbon atoms are arranged hexagonally in a single layer of polycyclic hydrocarbon framework forming a planar condensed ring system. It is mostly aromatic and mimics graphene in terms of its electrical, thermal and mechanical features. Normally chemical and thermal reduction of Graphene Oxide yield Reduced Graphene oxide (RGO) as the major product by removing the oxygen containing groups from the basal planes and the edges of the GRO sheets [Fig.4]. As a result of reduction of GRO, new sp^2 clusters is formed due to the removal of oxygen functional groups. The sp^2 domains already present in GRO will not increase in size on reduction, while the newly formed sp^2 clusters mediates and aid the electron transport by hopping. RGO is a disordered structure with the basal plane occupied by holes due to the

evolution of CO and CO_2 [22]. The oxygen groups specifically carbonyl groups and ether groups are almost fully reduced, and as a consequence defects arises in graphene basal plane. The electrical conductivity of GO is restored on reduction and the conductivity of RGO falls in the range of 200-42000 Sm^{-1} depending on the preparation procedure. RGO exhibits high specific capacitance, transparency and dispersibility than GRO. Being atomically thin, RGO is transparent in the visible spectrum and electronically it is a semi metal with finite density of states at Fermi level, like mono and multi layered graphene [23] .

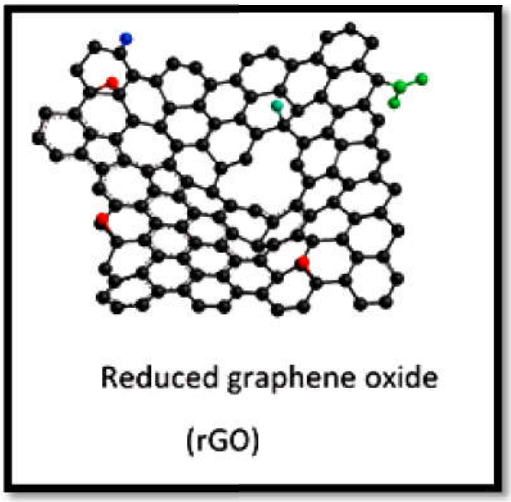

Figure 4. Structure of Reduced Graphene oxide

1.3.3 Structure of Graphene

In its pristine form, Graphene is a single layer of Carbon atoms covalently bonded to each other in a sp^2 bonded hexagonal aromatic

structure. It occurs in nature as the building block of graphite wherein each single graphene layers are held together by week Van der Waals force [24]. It can be considered as a single layer of carbon atom peeled off from graphite layers. The carbon-carbon bond length in graphene is 0.142 nm. The electronic configuration of Carbon is $1s^2 2s^2 2p_x^1 p_y^1 p_z^0$. 1s orbitals are lower in energy and the electrons will not participate in bonding, whereas, the 2s and 2p orbitals are of same energy undergo sp^2 hybridization and hold 4 electrons in their orbitals. The 4 valence electrons of carbon occupying the 2s and 2p orbitals will interact with the neighbouring orbitals of carbon atoms to form 3 covalent sp^2 σ bonds. These σ bonds are strong in nature and the electrons are localised in the plane containing carbon atoms. These bonds provide the honey comb framework and are responsible for the strength and mechanical properties of Graphene. The p_z orbitals hold the single electron and are normal to the graphene plane which is relatively free to move above and below the plane. The remaining p_z orbitals on every carbon atom overlap with its neighbouring carbon atoms to form a filled valence band and an empty conduction band. Dirac equation describes the charge carriers in graphene rather than Schrödinger equation. Owing to the presence of two equivalent carbon sub lattices in the graphene lattice, the cone like valence and conduction band intersect at the Fermi level at the K and K_0 points of its 2D Brillouin zone [Fig.5a and 5b] [25-26]. The energy bands disperse away from touching points and this distinctive topological feature is responsible for the extraordinary properties of graphene observed at low temperature. The out of plane interactions among the p_z orbitals

are weak and are involved in the progression of free charge and thermal carriers. These features lead to out of plane electrical and thermal conductivities

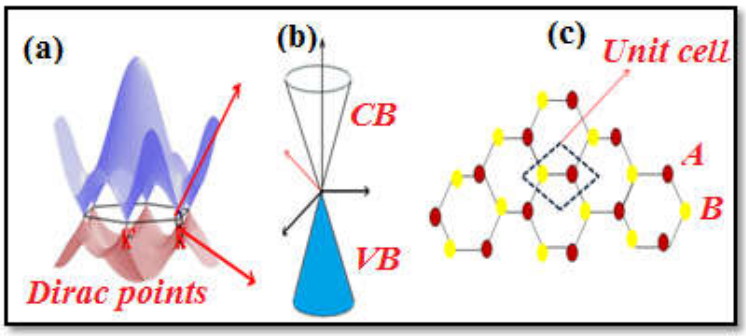

Figure 5. (a) & (b) Electronic band structure of single layer of graphene depicting the Dirac points. (c) Unit cell of Graphene

This unusual structure is responsible for the extraordinary properties of graphene such as high optical transparency, high carrier mobility, quantum hall effect, high theoretical specific surface area, high Youngs modulus and thermal conductivity [27-28]. The 3D structure of graphene lattice structure depicts a honeycomb net with unit cell comprising of two triangular sub lattices A and B. The honeycomb lattice is formed by two sub lattice contains two atoms per unit cell and each atom from sub lattice A is surrounded by three atoms from sub lattice B and vice versa [Fig.5c]. However, this honeycomb net cannot be considered itself as a Bravais lattice but can be represented as a 2D-triangular Bravais lattice. These two sub lattices of carbon atom in the graphene lattice are bonded by σ bonds, and the π orbital of each carbon atom constitutes the delocalized network of electrons. The electronic structure of Graphene is different

from other 3D materials. Fermi structure of graphene is constituted by two double cones as shown in Fig.5b. The structure of pristine graphene is free of defects as it is made up of same kind of atoms linked by strong and flexible bonds which is crucial in attributing extraordinary properties to graphene. P.R. Wallace has performed the first band structure calculations of graphene. The low energy band structure of graphene involves π electrons. Bonding π states forms the valence band while the conduction band is formed by anti bonding π* orbitals. These bonding and anti bonding states are orthogonal and the conduction and valence bands touch at six points known as Dirac points. Graphene is considered as a zero band gap semiconductor. Due to small effective mass and large intrinsic carrier mobility, its charge carriers will travel without scattering. Electrons will flow through graphene with more ease than in copper. The edges of graphene display an armchair or zigzag edge like form due to the lattice arrangement [29]. The structure of single layer of graphene sheets is presented in Fig.6.

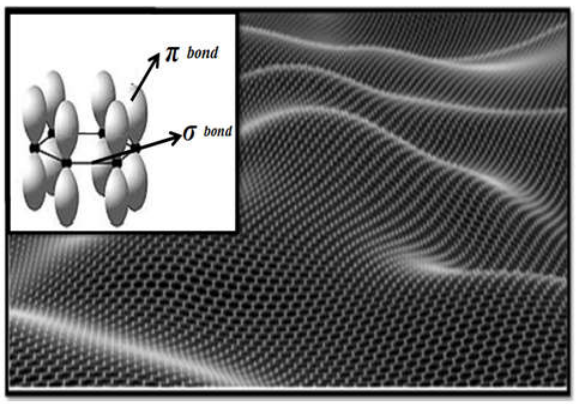

Figure 6. Structure of Graphene. The inset depicts the type of bonding possible between carbon atoms in graphene sheets.

1.3.4 Synthesis of Graphene

Synthesis of graphene refers to all those fabricating methods to derive Graphene sheets depending on the number of layers, purity and point of application. Ever since the isolation of this single Graphene sheets by Geim and coworkers by Scotch tape method, the explosion of research interests followed therein gave impetus to the synthesis of high quality, cost effective Graphene sheets. In spite of the continuing interests and experimental success by enthusiastic scientists worldwide, the wide spread application of GN has yet to occur. The main hinge for this advancement is due to the unavailability of reliable production techniques that can yield high quality GN samples in any scalable fashion. Graphene synthesis can be generally classified under two heads: (i) Top-down approach and (ii) Bottom up approach [Fig.7].

Top-down approach involves separating individual graphene layers in Graphite by overcoming Van der Waals force of attraction between the layers. The key hurdles in this method is to separate the layers efficiently without damage and also preventing the restacking of graphene sheets after exfoliation. Top down approaches result in low yields, tedious procedures and also have graphite as the prime source which is on the European list of scarce materials. Synthetic graphite can serve as an alternative but it is not apt for graphene production due to low levels of graphitization and disordered morphology.

Bottom down approach employs direct synthesis of Graphene using carbon precursors as building blocks to form graphene layers. Bottom up approach demands high quality graphitization which can be achieved only at high temperatures. Though procedures for bottom up methods are simpler than top up methods, these yield graphene with greater defects.

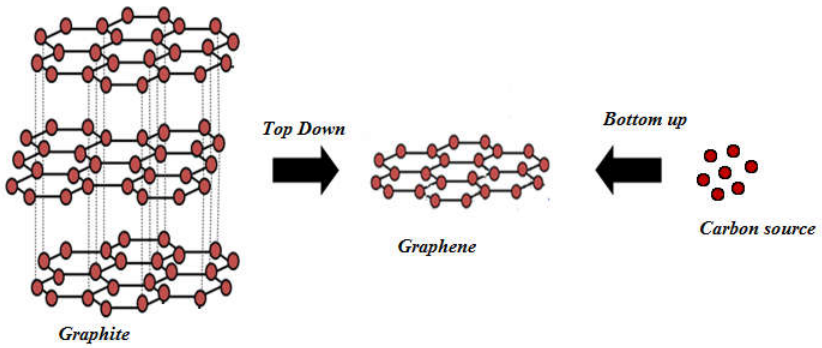

Figure 7. Schematic representation of top down and bottom up approaches

(a) Top-Down approach

(i) *Mechanical Exfoliation*:

Mechanical exfoliation has created a magical twist in the history of Graphene, when Geim isolated high quality single layer GN sheets using scotch tape. Till date, this is celebrated as a top notch technique to obtain graphene sheets of varying thickness (5 to 10 μm) [10]. This method employs the scotch tape repeatedly to peel off graphite crystals from bulk graphite into thinner pieces. This tape containing optically transparent flakes was then dissolved in acetone

and was deposited on a silicon substrate for further characterisation and applications. Further developments in this direction led to large sized graphene flakes which were visible to naked eyes. Later Jayasena et al. employed a similar strategy to create high quality GN sheets, wherein they used a diamond wedge to scrape off Graphene from ordered high quality pyrolitic graphite (HOPG) with the aid of ultrasonic oscillations [30]. As the frequency of ultrasonic oscillations and contact pressure can be controlled, this method has greater control leading to higher control over properties. Low scalability of this method holds back its widespread application. Graphite dispersed in stabilizing liquids can be exfoliated using sonication as suggested by Keith et al. which can yield high quality GN which can be scaled for industrial use [31]. Zhang et al. and McAllister et al. have employed a hot press at high pressures to obtain single to few layered GN sheets [32-33].

(ii) *Graphite intercalation*

Insertion of molecules between Graphite layers results in its reduction to graphene. Various strategies are adopted to exfoliate Graphite by intercalation. Solvent molecules can be intercalated on Graphite layers and exfoliation by ultrasonication yields Graphene. Thermal expansion of graphene intercalated compounds was reported. Due to heating, thermal decomposition of the intercalates into gaseous species which will push the layers apart resulting in the formation of Graphene [Fig.8]. Graphite intercalated with ionic liquids and Graphite co-intercalated with Nitromethane and $FeCl_3$ also promotes

the expansion of layers leading to graphene. Expanded graphite or exfoliated graphite can be used as a precursor for Graphene. Mono to few layer Graphene is reported by using expanded graphite [34]. Recently, critical carbon dioxide in super critical state has been employed to intercalate between the graphite layers and the depressurization results in the formation of Graphene layers. As the presence of chemical species between the graphitic layers increases the interlayer distance, this changes the electronic structure between the layers. Depending on the nature of the intercalates, various Graphene intercalated compounds can be achieved which finds applications, mainly in electric and magnetic fields.

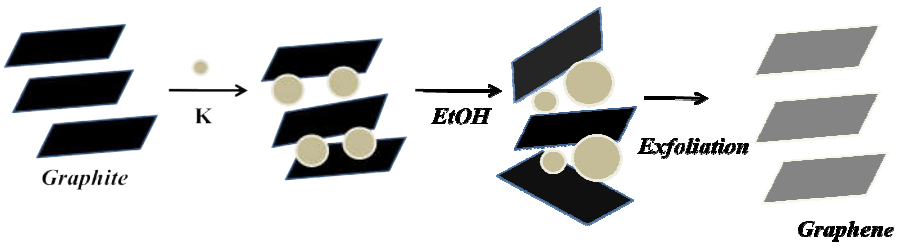

Figure 8. Graphite intercalation leading to the formation of Graphene sheets

(iii) *Exfoliation by solvents*

In 2008, Hernandez et al. and Blake et al. separately reported the exfoliation of graphite using suitable solvents [35-36]. Literature survey points out various studies in this regard and based on the investigations NMP was the best candidate to this effect. Another

strategy employs the use of surfactants to exfoliate graphite flakes thereby reducing the use of harmful solvents [37].

(iv) Nanotube slicing

Theoretically, carbon nanotubes can be sliced to form 2D graphene sheets wherein CNT acts as the source. Etching of CNT embedded in polymer matrix or in a solution of Potassium Permanganate and sulphuric acid can yield high quality GN sheets with high yields also. In a typical procedure adopted by Chen et al. [38] CNT was abraded between ground-glass surfaces under pressure leading to slicing of CNT's into GN sheets. GN obtained through this route finds applicability in interconnects, Field Effect Transistor etc. The major demerit associated with this technique is its non viable nature using costly CNT.

(v) Pyrolysis

This method offers facile production of Graphene but with low yields. As the name implies, it involves pyrolysis of typical carbon sources at high temperatures viz. Ethanol, biomass etc.

(vi) Exfoliation of Graphite oxide

This is regarded as one of the best techniques to obtain large quantity of Graphene sheets, involving production of graphite oxide by suitable oxidation techniques. This graphite oxide is then dispersed in suitable solvents by ultrasonication followed by reduction of graphene oxide to graphene using reducing agents. It is worthwhile to

mention here that graphite oxide can be exfoliated easily than graphite and hence it is used as the source for graphene. Strictly speaking, it is almost impossible to obtain pristine graphene sheets by this technique and the end product is mainly reduced graphene oxide (RGO). Graphite oxide can be obtained by the well acclaimed Brodie, Hummers and Staudenmaier methods can yield graphite oxide [39—41]. Before proceeding further, a brief description on the aforementioned methods is necessary.

- Brodie's Oxidation Method: This method involves oxidation of Graphite using concentrated nitric acid and Potassium Chlorate yielding a solid product containing carbon, Hydrogen and Oxygen. The limiting Carbon: Hydrogen: Oxygen percentage composition in the end of successive oxidation steps was found to be 61.04:1.85:37.11. The product obtained can be dispersed in water but not in acidic media and hence it is termed as Graphitic acid. The chemical formula of the compound was ascertained as $C_{11}H_4O_5$. This method is time consuming, tedious and produces several noxious gases.

- Staudenmaier method: This method can be considered as the improved version of Brodie's method, in which concentrated sulphuric acid was used as an extra additive apart from Conc.HNO_3 and Potassium Chlorate. Addition of aliquots of $KClO_3$ during the reaction course which lasted for weeks and the presence of Conc.H_2S0_4 leads to increase in oxidation and a highly oxidized graphite oxide is obtained. Though the

Staudenmaier method produces high quality Graphite oxide, it releases toxic gases and is time consuming.

- Hoffmann method: Hoffman method developed in 1937 uses a mixture of Conc. Sulphuric acid, Conc. Nitric Acid and $KClO_3$ as the oxidation mixture.

- Hummers' method: In 1958, Hummers' developed an alternative method to obtain Graphite Oxide wherein Graphite, Potassium Permanganate, Sodium Nitrate and Conc. Sulphuric acid were used as the oxidizing mixture. Currently, Hummers method and its modified versions are widely adopted to obtain highly oxidized graphite oxide to serve as an efficient precursor for Graphene. Reduction of graphite oxide can be achieved using several reducing agents like Hydrazine Hydrate, Sodium Borohydride, Hydroiodic acid, hydroquinone, amines, sulphur containing agents etc. are widely used [42-43]. Hydrazine Hydrate is commonly used as the reducing agent owing to its strong reducing property but is now replaced by green reducing agents like Vitamin C, amino acids, reducing sugar, alcohols, hydrohalous acids, tea, lysosomes etc. Apart from the reducing agents, several methods like Hydrothermal, thermal, solvothermal, microwave techniques have been adopted to reduce GRO to yield graphene sheets [44-45].

(b) *Bottom up approach*

(i) *Epitaxial growth on silicon carbide*

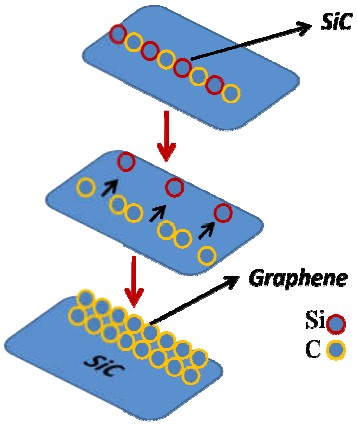

Figure 9. Epitaxial growth of Graphene on Silicon Carbide.

On annealing SiC substrate at high temperature, Si atoms will be desorbed from the surface leaving behind Carbon atoms to form Graphene sheets. Thin Graphene films of thickness less than 50 μM can be obtained by via preferential sublimation of Silicon from Silicon Carbide surface at higher temperatures (>1100 ^{0} C) and at ultra vacuum conditions under argon atmosphere [Fig.9]. Usually hexagonal phase silicon carbide is used for graphene synthesis and the size of graphene is dependent on the size of SiC wafers. The thickness, mobility and carrier density of graphene are greatly dependent on the surface of SiC. Graphene obtained through epitaxial method displays extremely high carrier mobility of charge carriers. Through this method, high quality graphene sheets are obtained but at the expense of SiC [46].

(ii) *Chemical vapour deposition*

Chemical vapour deposition (CVD) involves pyrolysis of carbon containing gases at high temperatures and leads to the deposition of large, thin graphene layers on transition metal substrates and this technique is regarded as one of the most efficient technique for Graphene synthesis. CVD method can proceed by 2 ways viz. surface catalysed and segregation techniques depending on the type of metal. In surface catalysed reactions, the decomposition of the carbon species and graphene formation occur at the surface of metal. This process is self limiting as once a layer is formed, the surface is passivated.

In segregation, the carbon dissolved in the bulk metal diffuses out to the metal surface upon cooling and is deposited on the surface. The number of layers formed depends on the rate of cooling and the carbon content. Graphene growth has been carried out on a wide range of metals, mainly Group 8-10 transition metals (Fe, Ru, Rh, Ni, Pd, Pt, Cu, Au etc) and alloys (Co-Ni, Au-Ni, stainless steel, Ni-Mo). Various factors are decisive in determining the quality of graphene layers like temperature, pressure, nature of metal etc. Copper and Nickel have been widely employed as the substrate for CVD of graphene. CVD process produces large graphene sheets which finds application on touch screens, solar cells, flexible OLED and LCD [47]. Though CVD techniques are scalable they are not cost effective. Dodecyl-functionalised single walled carbon tubes can serve as a substrate for production of nanotube-reinforced Graphene via spin coating and

annealing of Dodecyl-functionalised single walled carbon tubes. Flexible, stronger and highly conducting graphene sheets are formed through this technique. Reports on thermal decomposition of cookies, chocolate, grass and cockroach legs onto a Copper substrate have also been reported [48].

(iii) Miscellaneous methods

Literature survey points several other methods to prepare Graphene sheets of various thickness and morphologies. To quote a few methods: ash pyrolysis of the solvothermal product of Sodium and ethanol, ignition of Magnesium in dry ice, calcination of Aluminum Sulphide, calcination of Calcium Carbonate and Magnesium powder etc yields high quality few layered Graphene sheets of admirable quality[49]. A novel technique reported by Xu. et al. involves the synthesis of graphite by high temperature carbonization of metal phthalocyanine by microwave heating [50]. The formed graphite is then exfoliated by rapid cooling. In another report, heating electrically insulating substrates with solutions of poly aromatic hydrocarbons in chloroform leads to fusion of molecules and will synthesise graphene of different concentration depending on the concentration of hydrocarbon solution. Till date from its time of inception, graphene has created immense amount of fame and research attention on account of its extraordinary properties and potential. Graphene production still continues to be a tough task as majority of the methods adopted cannot be scaled up for large scale production. It is noteworthy to mention that current production techniques depends

on batch operation and suffers from the lack of consistency [Fig.10]. A huge quantum of research is currently devoted to synthesise high quality and large quantity consistently and it will be realized in the near future.

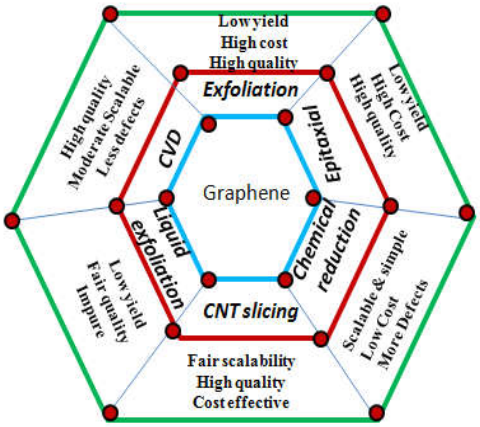

Figure 10. A brief comparison of some of the widely adopted graphene synthesis method.

1.3.5 Properties of Graphene

The unique properties of Graphene stem from the arrangement of Carbon atoms, giving birth to an entity possessing the most potential of the current century. These properties of graphene can be exploited for a plethora of fundamental and commercial applications.

(i) *Electrical properties*

A major portion of Graphene research focuses on its electrical properties. Graphene exhibits an unusually unique feature that it can sustain huge electrical currents. The π-bonds in graphene are

responsible for conductivity in graphene. The important characteristic feature of graphene is that the Dirac fermions which are the charge carriers in graphene behave as massless relativistic particles. Graphene is demonstrated as a zero band gap semi metal with a tiny overlap between the conduction band and valence band. Graphene conducts either by electrons or holes with a concentration as high as 10^{13} cm^{-2}. These Dirac fermions demonstrate outstanding properties. The charge carriers within graphene suffers minimum scattering under ambient conditions. Being a zero band gap two dimensional semiconductor, graphene exhibits well defined ambipolar electric field effect, large mean path and quasi particles. Being a zero band gap semiconductor, GN shows high electron mobility independent of temperature. The room temperature mobility of charge carriers was found to be approximately 10000 cm^2V^{-1} s^{-1} on application of gate voltage. Such high mobility arises due to the movement of electrons through the perfect honeycomb lattice of graphene [51]. Unlike in semiconductors, suspended graphene exhibits low temperature mobility of about 2, 00,000 $cm^2V^{-1}s^{-1}$ for carrier density below 5 x 10^9 cm^{-2}. In addition to this, electron and hole carriers in graphene exhibit an unusual half-integer quantum hall effect by adjusting the cell potential with the application of electric field effect. Owing to these properties, Graphene and its composites finds applications in super capacitors, Light emitting diodes, solar cells etc. The combination of its high conductivity and its low Johnson noise (noise due to thermal stir of charge carriers) makes it an adept entity for p: n junction diodes.

As suggested by Wallace, due to the large spacing of lattice planes in graphite (true for graphene also) as when compared to the hexagonal spacing in the layer, conduction usually occurs in the π plane and interaction of electrons between the planes can be ruled out. Novoselov et al. later demonstrated that the charge carriers in graphene can be defined by Dirac equation and the charge carriers behave as relativistic particles with zero rest mass and travels with the speed of light. Consequently, conductivity of graphene does not diminish to zero even when the concentration of charge drops to zero.

The thickness of graphene layers is decisive in tuning its electronic properties. In the case of monolayer graphene, the charge carriers are highly mobile, even then monolayer graphene cannot be regarded as high quality electronic material unless and until its band gap can be fine tuned. Graphene with zero band gap can be regarded as a car moving without any control. Graphene must conduct only when energy is provided and hence its band gap must be modulated to generate the desired output, similar to a semiconductor.

(ii) *Mechanical properties*

Graphene exhibits unique mechanical properties which makes it an ideal candidate for various applications. It is a very light material, weighing only about 0.77 mg/m^2. The mechanical properties of monolayer Graphene sheets are measured using atomic force microscope. The Youngs modulus of graphene was measured to be 1.0 TPa and the breaking strength was found to be 42 Nm^{-1}, which makes

graphene the strongest material ever observed. Studies suggest that external mechanical loads alter the electronic performance of graphene, like in field emission performance [52]. Response of various geometries of graphene towards the uptake of stress and compression buckling strains has been studied and it was found that the response is dependent on the Raman shift of the 2D phonons of graphene. The elastic deformation studies of functionalised graphene sheets and reduced graphene oxide sheets confirmed the pre existing kinks or defect lines in RGO and functionalised graphene sheets. Graphene sheets are highly flexible in nature and can be stretched like a balloon and it can also withstand pressure differences. It is impermeable to small atoms like Helium. Taming all these properties, graphene and graphene based composites can be employed in roof buildings, windows etc.

(iii) *Thermal properties*

The unmatched thermal properties of Graphene are due to its strong in-plane carbon bonds. Graphene is an excellent heat conductor. Graphene exhibits little or no phonon scattering. As low-energy phonons affects heat transfer and graphene offers higher thermal conductivity. The thermal conductivity of single layer suspended graphene was measured to be 3000-5000$Wm^{-1}K^{-1}$ at room temperature depending on the size of graphene sheets [53]. The thermal conductivity of graphene is found to be higher than any other carbon allotropes. Owing to the high thermal conductivity of graphene sheets, it is used as heat sinks in electronic circuit. Investigation on Graphene

sheets supported on silica (a case study for practical application) showed that the measured thermal conductivity was approximately 600Wm^{-1} K^{-1}. This reduction in conductivity can be ascribed to the leaking of phonons across graphene-silica interface and also due to intense interface scattering [54]. In addition to this, the thermal conductivity value is higher than copper (2 times) and silicon (50 times), which are indispensible in electronics.

(iv) *Optical properties*

The unique optical properties of graphene arising due to the inherent defects crown it as an indispensible entity for sensor and other related applications. Single layer graphene absorbs 2.3 % of white light with a mere reflectance of 0.01% and the absorbance varies linearly with the number of layers from 1 to 5.3. Graphene is transparent and hence finds application in photonic devices which demand conducting and transparent thin films. The observed and theoretical values are in good agreement with each other. Studies show that the visible range dynamic conductivity of graphene depends on the universal constants $G= \pi e^2/2h$. The transparency of graphene depends on the fine structure constant $\alpha = 2\pi e^2/hc$, which is related to the coupling between the light and relativistic electron. Monolayer graphene exhibits a flat absorption in the range of 300 to 2500 nm with a peak at around 250 nm in UV region which can be attributed to the inter band electronic transition from the unoccupied π-states [55]. The absorbance of n-layer graphene can be expressed as $n\pi a$. Deviations from this relation are observed when the energy of the

incident photons is less than 0.5eV, owing to the effect of doping, temperature and intra band transitions. Low resistivity of graphene alone with its high transparency makes it a suitable candidate for electrodes in liquid crystal devices. Carrier dynamics and relative relaxation time scale of graphene layers grown on SiC have been studied using ultrafast optical pump–probe spectroscopy. A 70-120 seconds initial fast relaxation followed by a slower relaxation process of 0.4-1.7 picoseconds can be attributed to the carrier-carrier intra band and carrier –phonon inter band scattering process respectively. Current smart era demands flexible transparent conductors, solid state lighting, printable electronics and thin film photovoltaics. Presently, the demand is met by Indium Oxide owing to its transparency and resistance. However, the sources of Indium Oxide are fast depleting and it is not cost effective. Moreover, it is brittle, crystalline and hence can be fractured easily. Graphene seems to be the best alternative for Indium Oxide owing to its transparency, flexibility, cost effectiveness and its mechanical strength [56]. It was demonstrated using infra red spectroscopy that the inter-band transitions and optical transitions of monolayer and double layer graphene depend on layers and can be tuned by means of electrical gating. This feature opens up new area for infrared optics and optoelectronics. On account of saturable absorption as well as nonlinear phase shift, multilayer graphene shows an increase in transmittance. It was found that graphene shows a nonlinear refractive index of 10^{-7} cm^2 W^{-1} which is much higher than bulk dielectrics, which makes graphene a suitable entrant in nonlinear photonics. It was established that graphene shows unusual

phenomenon like the Faraday Effect and the magneto-optical Kerr effect. These unique properties of graphene can be exploited to enable its application in optical communications and switching devices.

(v) *Chemical stability and reactivity*

Due to the presence of strong in-plane sp^2 hybrid bonds in graphene, it shows excellent stability and chemical inertness. Graphene can prevent oxidation of metal and metal alloys from oxidation. Moreover, graphene is expected to improve the durability of optoelectronic devices [57]. Graphene can interact with other molecular species on its surface and it exhibits the tendency to modulate its conductivity by proper choice of molecules.

1.3.6 Graphene Hybrids

As mentioned earlier, graphene is a wonder material with sizeable potentials that can revolutionise current scientific and technological world. The main hindrance in the development process of graphene world lies in the stability of graphene sheets. Free standing graphene sheets have a tendency to aggregate and restack back to graphite due to the Van der Waals force of attraction between the individual layers. In order to circumvent this obstacle and to exploit the maximum potential of graphene, graphene is incorporated with molecular species like metal, metal oxide, metal sulphides, metal selenides, metal nitrides, organic molecules, inorganic salts, polymers, dyes, nonmetals, clays etc and this have paved the road for an exciting area, i.e., Graphene Hybrids.

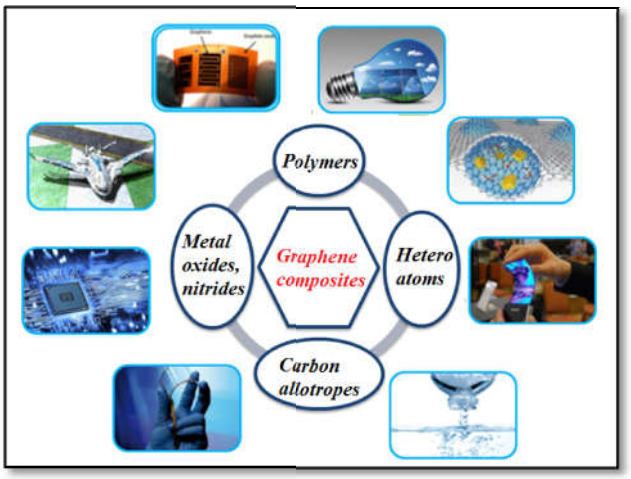

Figure 11. Graphene hybrids and their potential application in diverse fields.

Graphene-Hybrids are multiphase heterogeneous materials where either of the constituent can function as the dispersed phase or dispersion medium leading to the synergistic combination of the constituents. GN-Polystyrene nano composite reported by Ruoff et al. in 2006 [58] was the first GN based nanocomposites, which has enthused researchers and was consequently followed by tremendous development of novel Graphene-Hybrids. Shen et al. have classified GN hybrids based on (a) the nature of the additive involved and (b) the nature of the architecture involved as listed in Fig. 12 and Table 1 [59]. A variety of chemical and physical synthesis methods like solution deposition, sol-gel processing, hydrothermal/solvothermal, gas-phase deposition, template method can be employed to effectively synthesise graphene-hybrids at ambient conditions. Currently, intensive research has been carried to devise graphene hybrids and employ them in

interdisciplinary fields. The driving force for investigating the research on Graphene based hybrids is to synergistically combine the properties of graphene with the second component. The planar 2D structure of graphene allows a good decoration of nanomaterials of several hundred nanometers on graphene sheets. Graphene with high surface area improvises the interfacial contact with the other constituent and the large surface of graphene can hinder the aggregation of the secondary constituents and hence preserving its properties at nano dimension. The secondary constituents act as spacers between graphene sheets hence obstructing its tendency to form irreversible agglomerates. In addition to this, the presence of secondary components improves the overall thermal, mechanical, electrical and optical properties of graphene based hybrids and finds application in versatile fields [Fig.11].

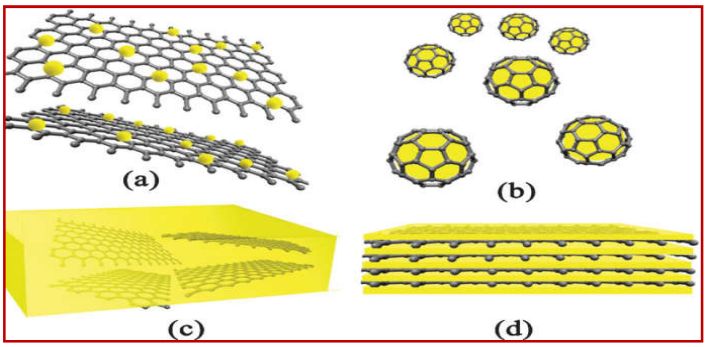

Figure 12. Illustration of GN composites based on architecctures [Adapted from reference. 59] .

Graphene based nanocomposites	Additives
GN-Polymer nanocomposites	*Polymer*
GN-Metal/metal compound nanocomposites	*Metals,Metal oxides,Nitrides and sulphides*
GN-Carbon nanocomposites	*Carbon Nanotubes,Fullerene*
GN-non metal nanocomposites	*Nitrogen, Phosphorous, Boron, Sulphur*

Table 1: Classification of Graphene based composites

1.3.7 Applications of graphene and graphene hybrids

The huge potential of graphene has ignited encouraging interests among scientists of all fields of science and technology. Herein, we will discuss briefly on the applications of graphene, spanning from advancement in conventional devices to applied biological applications. This mammoth possibility arises due to its intriguing properties, viz., it is flexible and strong still it is ultra light, it does not retains heat but is resistant to fire, it is an excellent conductor but is impermeable even to helium atom. It is to be noted here that the synthesis methodology greatly affects the properties and hence the utility of GN and its hybrids for various applications. Table 2 gives a correlation between the properties of GN hybrids and their point of use. The research community have now focused their attention to exploit the tremendous potential of graphene but only a very few applications have been commercialized. A fair number of applications are at the verge of completion and some exists as fantasies which may become reality in near future.

Feature	Electrical conductivity	Surface area	Strength	Thermal Conductance	Elasticity	Trans-parency	Inert-ness
Adsorbent	*No*	*Yes*	*Yes*	*In part*	*No*	*No*	*Yes*
Sensors	*Yes*	*In part*	*No*	*No*	*In part*	*In part*	*Yes*
Electrode	*Yes*	*No*	*In part*	*No*	*No*	*No*	*Yes*
Conduct-ive inks	*Yes*	*No*	*No*	*No*	*Yes*	*Yes*	*Yes*
Energy storage	*Yes*	*Yes*	*No*	*No*	*Yes*	*No*	*Yes*
Transistor	*Yes*	*Yes*	*No*	*No*	*No*	*No*	*Yes*

Table 2: Correlation between properties and applications of Graphene composites

(i) *Applications of graphene based on its high surface area*

Graphene exhibits a theoretical surface area as high as 2630 m^2/g, which grants its applications as an adsorbent, a catalyst etc. Graphene more precisely graphene oxide and reduced graphene oxide and their composites have been widely exploited as an adsorbent for a wide array of contaminants ranging from organic dyes, pesticides, organic compounds, oils etc [60]. Recently, scientists have developed atom-thick flakes of graphite oxide which are water soluble and can adsorb both natural and artificial radioactive materials from aqueous system and then condense them into clump of solids. After adsorption, the adsorbate can be recovered by skimming off the solids and burning the graphene oxide. Consequently, graphene oxide burns rapidly and leaves a cake of radioactive material which can be reused. The interplay of large surface area of graphene together with its fast adsorption kinetics has paved the way for this adsorbent property [61]. In similar direction, many contaminants can be removed by adsorption

and can be recycled if needed. Thus graphene can emerge as an alternative sorbent for a cleaner and safer environment in near future.

(ii) Applications of graphene related to its high specific strength

On account of the high strength of graphene, graphene can be employed in the production of light weight and strong aircraft. Owing to its strength, ultra light nature and its ability to withstand diamond cutters, graphene is now being considered for applications in blades of wind, turbine, flywheel, aerospace, transportation, high power transmission lines etc [62]. Graphene –epoxy composite is set to be an alternative to steel in aircrafts and hence the overall weight and efficiency will improve. Graphene can also be used to fabricate armor for military personnel and automobiles. Recently, HEAD company has developed YouTeK ^{TM} SPEED tennis racquet whose shaft is coated with graphene and is set to reach commercial markets in the near future

(iii) Applications of graphene related to its flexibility

The synergistic play of high electron mobility and the mechanical strength of graphene have enabled it as a superior material to fabricate flexible electronic circuits. Recently, approaches to deposit graphene over polymers for devising flexible screens, transistor and electronic components were fruitful and their commercial entry is expected soon. Researchers have developed solution of graphene with particle size less than 100 nm and this solution can be used as a conducting ink. This ink can be employed as a single layer sheet of graphene that can mimic all properties of graphene and can be used to make graphene sheets on any substrates like glass, polymers,

paper etc which can function at very high frequency range. Similarly, graphene of desired thickness can be deposited on a substrate using AC field, which finds application in transistors [63]. These transistors find application in flexible screen, electronic devices mounted on various fabrics etc. Several devices are available for sensing mercury ion in human muscles but their selectivity is always questionable. Recently, a liquid ion gated field-effect transistor (FET) fabricated using flexible graphene aptasensor for Hg^{2+} ion has been developed which exhibited excellent selectivity and sensitivity with detection time less than one second [64].

(iv) *Graphene for Electrical Energy Storage*

Storage of energy when not in use has always posed as a problem. Batteries can store energy effectively but unfortunately, if the battery delivers high power within a short time, the storage capacity and the life of battery decreases. Super capacitors are the solution in this direction. Super capacitors can provide high power for short duration and also it can be charged very quickly. The conjunction of a super capacitor with battery can store energy and can be effectively applied for several applications. On account of graphene's elastic, mechanical and electronic properties, it is being researched as an electrode material in super capacitors, as transparent conducting electrode in dye sensitized cells etc [65]. Intense research is being carried out to replace activated carbon which is used as an electrode in electrochemical double layer capacitor (EDLC) with single layer graphene, as single layer graphene has higher surface area than activated carbon. It was demonstrated that graphene based super

capacitor can be fabricated for developing grid-scale integrated electrochemical charge storage as the graphene coating passivated the surface charge traps on the electrode and provide an efficient electrode-electrolyte electrochemical interface, improving the energy density and performance [66]. It is believed that in the next decade, graphene based micro-super capacitor will be employed in lithium ion batteries, in personal computers, electrically powered vehicles etc. for much efficient energy related applications .

(v) Electronic and Optoelectronic Devices Using Graphene

The unique electronic and optical properties of graphene viz., high transmittance, high conductivity, and low resistance crown it as an elite component for optoelectronic devices. Extensive research is now being carried out to investigate the prospects of graphene and its composites for application in this direction (in integrated circuits, touch screens, liquid crystal displays (LCD) and foldable organic light emitting diodes (OLEDs) and its commercialization will be realized soon. Commercial applications of graphene were realized in 2008, wherein the smallest one-atom thick transistor was made and this was followed by fabricating an n-type transistor in 2009. IBM developed epitaxial grown graphene on SiC for mass production of integrated circuits in 2011. Due to the response of graphene to perpendicular electric field, graphene nanoribbons were employed for their application in Field Effect Transistor (FET) [67].

(vi) Graphene Film's Impermeability Related Applications

As mentioned earlier, monolayer graphene was found to be impermeable even to the smallest helium atom, and consequently many applications of graphene can be derived from this feature. To quote a few; graphene-sealed chambers can be employed to probe pressure changes and phase transitions during chemical reactions. Recently, the application of graphene membrane which can serve as selective barriers for ultra filtration is also projected. It was found that graphene oxide is permeable to water vapour, and impermeable to other liquids and gases. Exploiting this feature, graphene oxide membrane has been used to distill vodka at room temperature without employing any heating device for application [68]. Extending this methodology, graphene oxide membranes can be used to distill bio fuels, thereby reducing its overall cost. Graphene oxide sheets are biodegradable, and consequently can be used as a permeable barrier which will be of great aid in ground water remediation. Graphene sheets allow water to pass through but are impervious to other liquids and hence can be used as molecular sieves. Another standout property of graphene is its ability to filter NaCl from water and consequently can be employed for desalination of water [69]. Graphene can be applied as protective coatings on gadgets to prevent gases and moisture.

(vii) *Graphene for energy applications*

Due to the distinguished electrical properties of graphene, it finds application as a suitable electrode for fuel cells. The major demerit associated with the functioning of fuel cell is the diffusion of

the electrolyte to the outer side of the electrode which may results in shirt circuiting. Moreover, the reduction process occurring in the electrode of fuel cell can be assisted by the electro catalyst in the electrode (pores of the electrode incorporated with the electro catalyst). All these requirements can be met by making the pores of the electrode hydrophobic, simultaneously the hydrophobicity of the electrode must not hinder the electron transfer process [70-72]. This is where the prominence of graphene arises. Graphene can satisfy these criteria and hence can be employed as an excellent electrode in fuel cells.

(viii) Miscellaneous applications

Graphene can be employed for many engineering applications by integrating two dimensional templates of graphene with suitable materials with crystalline structure. For example, MoS_2/graphene template can be employed for fabrication of optical and electronic devices. Being transparent and oxidant resistant, graphene can be used as coating for anti corrosion applications. Being transparent in the visible and near-infrared regions, chemically inert and thin, graphene can be employed as a charge collector and transporter in photovoltaics [73]. Due to its optical transparency and conductivity, graphene can act as transparent conductive electrode in flat panel displays and cathode ray tubes touch screens etc. Graphene can also be used in holography. Recently, researchers are trying to develop graphene yarns without compromising its surface area and electrical properties. These yarns can be employed as electrodes for fuel cells and can be extended to

conducting cloth. Exploiting the large surface area, atom thickness, tunable chemistry and molecularity of graphene can be employed for fabricating bio devices which can be used for detection and diagnostic purposes in humans and microbial systems. In addition to this, graphene can be used as a drug carrier when coated with biocompatible molecules. Very high and efficient loading of anticancer drugs has been achieved on graphene surface by π-π stacking for drug delivery [74]. The efficient drug loading efficiency is due to large surface area of graphene. Researchers are projecting the application of dye labeled graphene based systems for bio imaging applications.

(ix) Graphene for sensor applications

The outstanding electrical, chemical, electrochemical and optical properties of graphene have driven its use in and as a sensor in diverse fields.

- *Graphene for Pressure-Sensors*

Graphene sheets can be employed to measure gas pressure as it is impermeable to gases. When suitable stress is applied on graphene sheet, it will develop a potential and the electric signal hence obtained can be used to measure the amount of pressure applied. Graphene based pressure sensors can be fabricated by depositing graphene over suitable substrates like SiO_2, Silicon nitride etc. The sensitivity of such sensors was found to be 20-100 times higher than conventional sensor materials [75].

- *Graphene for strain-guage*

Exploiting the piezo-resistive property of graphene, strain-gauge sensor can be developed. Herein, the developed resistance, on applying a strain on Graphene sheet supported over substrates like SiO_2 is measured. Detecting this deformation can serve to investigate and measure the internal activities of human bodies. It is projected that in future, the market for strain sensor based on graphene can be as high as 4.5 billion US dollars [76].

- *Graphene as biosensor*

Thanks to the extraordinary chemical, optical and electrochemical properties of graphene that have ignited its application as a biosensor for DNA oligomers, several enzymes, thrombin, hemin, in situ molecular probing and imaging, proteins etc. To quote a few examples: He. et al. have devised GO based DNA probes that could offer quick, selective and sensitive sensing for DNA. Owing to the high surface area and excellent electron mobility, graphene based devices are extremely sensitive to the presence of biomolecules and has been investigated for electrochemical sensing of biomolecules like glucose, proteins etc [77]. The major hurdle associated with graphene based biosensors lies in its reproducibility issue. However, the prospects of graphene based sensors are very high, which rely on its surface area, conductivity, strength, optical probes, and commercialization of efficient graphene based biosensors is expected in near future.

- *Graphene based chemical sensors*

Graphene and graphene based systems have emerged as top notch materials for sensing of chemical species due to its following qualities:

- Due to its high surface-to-volume ratio, graphene and graphene oxide can sense chemical species upto ppm, ppb, ppt and even ppq levels.
- Functionalisation of graphene with polymers, dyes, metal oxides, metal sulphides etc can tune its sensing signal and can improve its selectivity and sensitivity with analyte.
- Electronic and mechanical properties can be fine tuned to perform the transduction of the sensing signal.
- For electrochemical sensing, graphene being highly conducting, a small change in interactions of analyte will lead to a significant shift in carrier concentration. Due to this, analyte molecules at very low concentration can be detected accurately.
- Graphene, Graphene oxide and graphene based sensors are cost effective.
- Functionalisation of graphene with chemical species enhances the adsorption of analyte species, which can modulate the

electric response or optical response of the sensor and hence can lead to the detection of analyte molecules.

- *Graphene based gas sensors*

Due to the high surface to volume ratio and large surface area, graphene can be employed as gas sensors. Graphene can adsorb gases on large quantities which will change the concentration of surface states, consequently altering the surface resistance of graphene. These change in surface resistance can be measured and hence realizing a sensor. Various gases like NO_2, NH_3, H_2S, CO etc can be sensed using graphene and graphene based hybrids [78-79]. The sensitivity of graphene sensors can be enhanced by improving the patterning of graphene and graphene based systems.

1.4 Objectives of the study

This Research work aims at investigating the prospects of Graphene hybrids for environmental applications particularly for monitoring and removing the pollutants from water, thus maintaining the purity of water bodies.

- Synthesis of Graphene by chemical reduction of Graphene oxide by using Hydrazine Hydrate. Characterisation of the as synthesized Graphene sheets by adopting adept physiochemical characterisation techniques like X-Ray Diffraction analysis (XRD), UV-Visible spectroscopy, Fourier Transform Infra Red spectroscopy (FTIR), Scanning Electron Microscopy (SEM),

Transmission Electron Microscopy (TEM), Raman spectroscopy, Photoluminescence spectroscopy and Thermo Gravimetric Analysis (TGA).

- Synthesis of Graphene-Iron oxide nanotube hybrid by hydrothermal method. Characterisation of the prepared composite by various characterisation techniques like X-Ray Diffraction analysis (XRD), Fourier Transform Infra Red spectroscopy (FTIR), Scanning Electron Microscopy (SEM), Transmission Electron Microscopy (TEM), Raman spectroscopy, Thermo Gravimetric Analysis (TGA) and Vibration Sample Magnetometer Analysis (VSM). Application of the prepared composite for adsorptive removal of Chromium (VI) and Methylene blue dye.

- Preparation of Graphene-Iron oxide incorporated Polyurethane sponge by dip coating method, followed by characterisation of the hybrid using known characterisation techniques and investigation of the said hybrid for adsorptive removal of oils and organic solvents.

- Noncovalent functionalisation of Graphene using organic dyes and application of the Graphene-dye hybrids as sensor for toxic heavy metal, Mercury ion (Hg^{2+}) and Fluoride ion (F^-) in aqueous solution.

1.5 Present work

Graphene and its hybrids have revolutionsed the lane with which we have devised devices and strategies in various fields, ranging from environmental remediation, sensing to energy sector. Owing to the pertinacious and toxic nature of dyes, heavy metals, oils and organics, release of the aforesaid toxicants into aquatic systems has become an alarming issue. Hence to preserve the serene beauty and balance of our environment, it is of paramount importance to stop and/or reduce the concentration of toxicants before discharge into water [80-83]. Adsorption is hailed as an efficient and robust technique for the removal of pollutants. In this regard, Current research interests are rooted on Graphene and its hybrids as an efficient adsorbent for water contaminants. Moreover, integration of magnetic responsiveness onto Graphene scaffold by incorporation of magnetic materials has emerged as a proficient strategy for the separation of toxic contaminants from aqueous system. Such Graphene based magnetic sorbents combine the merit of adsorption efficacy of graphene as well as the ease of separation of adsorbate after sorption [84-85].

Water pollution stands as one of the most grievous environmental issue impairing environmental sustainability. As mentioned above, heavy metals, anions, organic compounds etc contributes to water pollution and hence the real time monitoring of these in environmental, biological and industrial samples has gained significant attention over the past few decades and continues to be a hot area of research. Currently, steps directed to devise prime sensors

for the detection of heavy metals, anions, organics etc is centered on graphene [86]. Recently, the application of non covalently functionalised Graphene-dye hybrids has gained unceasing interests ascribing to the tunable optoelectronic properties of graphene-dye hybrids. Literature review has suggested the extensive prospects of graphene-dye hybrids as potential sensors in aqueous systems.

Moved by the prevalent environmental deterioration and motivated by the mighty potential of the Super Carbon 'Graphene and its hybrids', we have framed our research problem in the direction of sensing and removing contaminants in aqueous medium. This thesis entitled 'Graphene based Sorbents and Sensors for Environmental Applications 'investigates the prospects of Graphene hybrids as an efficient sorbent and also as a dynamic sensor for relevant water toxicants.

This thesis is divided into six chapters:

- Chapter 1 provides a detailed introduction to Graphene, its synthesis methodologies, properties and applications. In addition to this, the prospects and applications of graphene hybrids are also discussed.

- Chapter 2 outlines the specifications of various materials used and includes the detailed description of the methodologies and the characterisation techniques adopted for the present research work.

- Chapter 3 explains the results of characterisation studies that pave way to the identification of graphene layer structure.

- Chapter 4 presents the application of graphene hybrid as an adsorbent. This chapter is divided into two parts: Part A deals with the synthesis, characterisation and application of Graphene-Iron oxide nanotube hybrid as a potential sorbent for Methylene Blue dye and Chromium (VI). Part B deals with the synthesis, characterisation and application of Graphene coated magnetic polyurethane foam as a potential sorbent for oils and organics in aqueous solution.

- Chapter 5 furnishes the application of graphene-dye hybrid as sensor. This chapter is further divided into two parts: Part A deals with the application of Graphene-dye units as sensor for Mercury ion (Hg^{2+}). Rhodamine and Fluorescein dye are opted as the model dyes. Part B deals with the application of Graphene-Rhodamine unit and Graphene-Fluorescein unit as sensor for Fluoride ion in aqueous system.

- Chapter 6 summarizes the highlights of the research work carried out, and projects the future scope and hope in extending the potential of graphene hybrids for several applications.

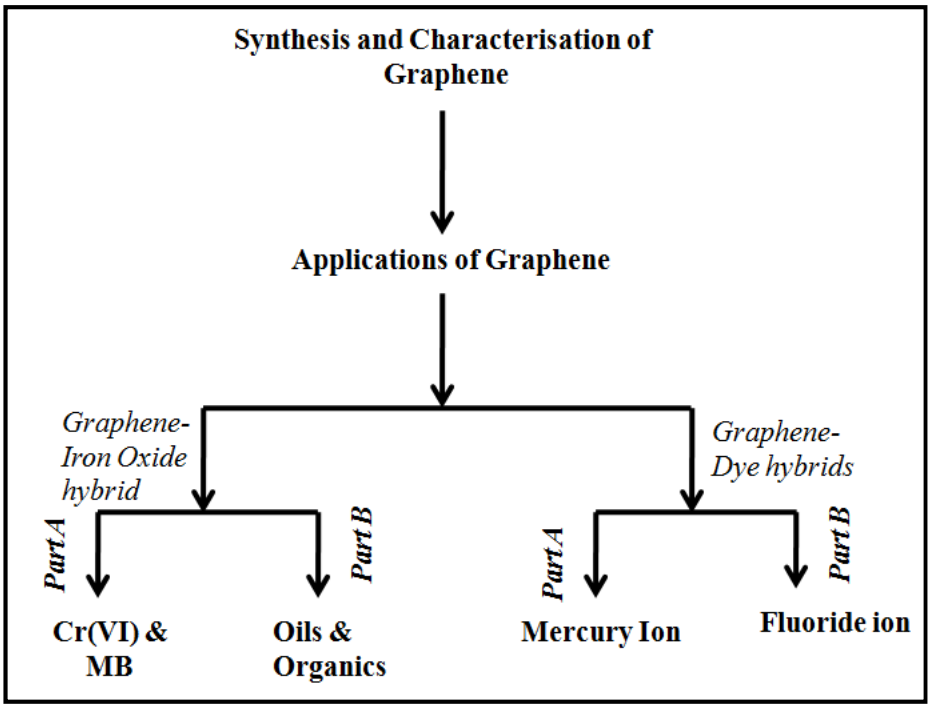

Framework of the Research Work

1.6 Relevance of the study

(i)Graphene-Iron Oxide nanotube Hybrid as a potential sorbent for environmental remediation

The inadequate access to safe and clean water continues to be one of the most pervasive problems affecting mankind. Across the globe, scores of contaminants including heavy metals, dyes, oils, organics, domestic sewage etc are dumped into water bodies indiscriminately [87-89]. Hence, the quest for highly efficient and cost effective techniques to decontaminate water from its origin to point of use is the need of the hour. The increase in flux of toxic pollutants due

to the haphazard release of agricultural, industrial, domestic, and municipal waste effluents into water bodies has raised serious apprehension. Polluted water alters the balance of our ecosystem and also invests billions of people at the risk of water borne diseases. Among the group, heavy metals, dyes and oil spills have invited gruesome concern owing to their far reaching impact on the whole ecosystem and hence this trio is chosen as our target entities [90]. Hence to protect the innate balance and serenity of our Earth especially of water bodies, it is important to prevent and/or reduce the toxicants amount before their discharge. A wide array of techniques like flocculation, bioremediation, membrane filtration, reverse osmosis, photocatalysis, adsorption etc have been adopted to reduce the toxicants in water [91-92].

Adsorption is widely acclaimed as an efficient water treatment technology on account of its extensive applicability, versatility, feasibility, that provides high quality treated water. Adsorption is a surface phenomenon and can be defined as the increase in concentration of any element at the surface or interface between the two constituents [93] .To decontaminate polluted water, various kinds of sorbents were employed, like clay, silica gel, alumina, polymeric materials, carbon materials etc. Among the aforesaid sorbents, Carbon based materials can be regarded as staple adsorbents for removing a bunch of pollutants from water. The carbon family comprising of the conventional activated carbon, carbon nanotubes, carbon nanofibers, Graphene have been investigated as high prolific adsorbents for water

purification [94-96]. Though these entities portray high adsorption capacities towards certain type of pollutants they are not efficient to other types. To quote an example, unmodified CNT displays unusually high adsorption capacity towards organic molecules while it is nearly ineffective for heavy metals [97-98]. Functionalisation of Carbon based materials increases their adsorption capacity towards ions but drastically reduces their affinity towards anionic dyes or negatively charged species [99]. Hence it is still a challenging task to devise and construct an adsorbent for a broad spectrum of pollutants. Recently, GN has aroused tremendous interests among researcher as an efficient adsorbent. High surface area of GN and its ease of functionalisation mould GN as a potential candidate for adsorptive removal. The adsorption capacity can be enhanced by functionalisation with oxygen functional groups as well as with other nanomaterials. It is to be noted here that, pristine GN cannot function as an efficient adsorbent for many adsorbate as it can only provide Van der Waals force to bind with adsorbate. In this similar ground, it is suffice to mention here that Graphene more scientifically RGO decorated with sufficient number of oxygen functional groups can provide various adsorptive forces to enable adsorption of anions, cations, heavy metals, oils, dyes etc [100-104] . Incorporation of various nanomaterials synergistically improvises the adsorption capacity as well as prevents the aggregation of GN sheets. Tailoring of various nanostructures onto graphene sheets is of great interest to the researchers and these have applications in various disciplines. Graphene nanocomposites have become an indispensible entity in

multidisciplinary applications such as sensors, electronics, super capacitors, hydrogen storage, catalysis etc [105]. Current research focus is to exploit the positive synergistic effect between graphene and the dopant.

Though several reports suggest the application of bare GN sheets alone as adsorbent for Heavy metals, Chromium and oils, it takes prolonged time to separate the pollutants after adsorption which limits its practical application. Here comes the merit of magnetic separation which is regarded as a rapid, effective technique for separating the pollutants after adsorption. Magnetic separation also ensures recyclability of the sorbent [106-108]. In this regard, integration of Iron Oxide nanomaterials has drawn considerable interests attributing to their promising applications in magnetic fluids, sensors, biomedicine and environmental remediation. Iron oxide is one of the most prominent transition metal oxides of technological and industrial significance. Additionally, iron oxide nanomaterials are less toxic, environmentally benign and cost effective. Literature reports portray iron minerals as an excellent media for the removal of various heavy metal ions, dyes and oils [109-111]. However, due to the quick oxidation /dissolution of iron oxide nanoparticles especially in acidic media, the recyclability issue works as a hurdle to their utility [112-113]. In order to overcome these hurdles iron oxide nanostructures have been incorporated /encapsulated onto a substrate, most commonly carbon based substrate like GN due to its low cost and high surface area. Moreover, presence of iron oxide nanostructures prevents the

aggregation of GN sheets. Hence, the integration of GN with iron oxide nanomaterials would pave the lane for novel hybrids with complementary behavior between the constituents.

In this piece of work, we have synthesied a novel hybrid based on Graphene-Iron oxide nanostructures and have exploited it as an adsorbent for a Heavy Metal, an Organic dye and Oils and organics. The target heavy metal and dye employed for the study are Chromium (VI) and Methylene Blue (MB). For Oil spill removal studies, commercially available oils and organic solvents were chosen. Graphene-Iron Oxide nanotube composite was employed as sorbent for removal of Cr (VI) and MB dye from aqueous solution. As our efforts to utilize Graphene-Iron Oxide nanocomposites as oil sorbent did not yield fruitful results, we incorporated Graphene-Iron Oxide nanocomposite onto Polyurethane foam and examined its applicability as sorbent for organic contaminants and oils.

(ii) Application of Graphene-Dye Hybrids as potential sensor

Owing to the intriguing optical, electrical, mechanical and structural properties of graphene and its derivatives have ignited exploding interests in the field of sensors. With the advancement of graphene chemistry, past few decades have witnessed the application of graphene materials as sensors which had enhanced the selectivity and sensibility and has been of prime significance to enhance the detection limits and had led to miniaturization of sensing devices.

Remarkably, due to the distinguished optoelectronic properties of Graphene, specifically Graphene oxide (GRO) and Reduced Graphene oxide (RGO), these duos serve as efficient sensing arena for a wide spectrum of molecules. RGO and GRO are suggested as "Super quenchers" of optical response with long range electron transfer feature. Exploiting this property, graphene based sensors can be classified under two heads i.e. "TURN ON and TURN OFF" sensor. As the name suggests, turn on (optical signal on) sensor works by restoring the quenched optical response either by means of complexation or displacement amongst the analyte, host and/or the indicator. Turns off sensors (optical signal off) are comparatively less sensitive than turn on sensors and functions by reducing the intensity of optical response with the advent of analyte molecule by means of complexation or displacement [114].

The sensing and recognition of major elements in water bodies have emerged as a key research theme owing to their implications on aquatic ecosystem. Recently, the design and sensing of receptors with potential of sensing ionic species (heavy metal cations and anions) constitutes an important scientific research area due to their vital role in industrial, biological and environmental field. Advancement of sensors has witnessed a surge in the past few decades owing to the fact that the sensors will facilitate environmental remediation measures besides serving as a diagnostic tool in medicinal field. Ionic elements viz. F^-,NO^{3-} ,So_4^{2-} ,PO_4^{3-} , Cu^{2+} , Zn^{2+} etc. play a dominant role in cell migration, cell proliferation and works as co-factors and enzyme

substrates in biological systems etc., while on the other hand Pb^{2+} , Hg^{2+} , CN^- are convicted as major toxicants. The techniques for trace detection of heavy metals and anions (in the ppb, ppt and ppq range) need sophisticated analytical instruments like atomic absorption spectroscopy (AAS), potentiometric methods, inductively coupled plasma-mass spectrometry (ICPMS), mass spectroscopy (MS), X-ray fluorescence spectroscopy (R-FS) etc which demand trained personal to carry out the analysis [115]. Due to this, methods like colorimetry, fluorimetry and voltammetry etc. are employed to allow the miniaturization and infield applications along with commendable sensing efficiency and cost effectiveness. Notably, development of colorimetric sensors and portable solid phase sensors is an acclaimed area for quantitative and qualitative sensing of the said targets. Among this array, Mercury and Fluoride ion require special mention. Fluoride ion plays a vital role in protecting teeth from dental cries and in osteoporosis. But an excess of fluoride ion concentration leads to urolithiasis, fluorisis, nephrotoxic changes and even to cancer. Alarmed by this issue, the US Environmental agency has laid down 2 ppm as the permissible limit of Fluoride ion in drinking water. The adverse and beneficial effects of fluoride ion have urged researchers to fabricate suitable sensors. Conventional methods like Willard–Winter method, ion chromatography demand tedious workup, costlier instrumentation and trained personals [116]. Hence as mentioned earlier, there is an impetus to the development of optical sensors. Similarly, another commonly encountered ion of potential toxicity even at low threshold is Mercury ion (Hg^{2+}). Mercury is ranked as the 6^{th} most

hazardous toxicant owing to its non biodegradability, persistence in atmosphere, bioaccumulation through food cycle etc. Mercury ion has far reaching impact on human health. Over exposure of mercury ion leads to neurodegenerative disorders, developmental delays etc. Optical sensors have a better edge over conventional instrumental intensive techniques on account of reasons stated earlier in this section. Summing up, prior emphasis has been placed on the fabrication of optical sensors that will specifically and selectively respond to the concentration of analyte ions. Graphene-based sensors are comparatively novel and have enough potential to meet the demand of quick in situ measurement of ionic analytes in water.

Among the several strategies adopted till date, we present a novel displacement strategy based on preferential adsorption of graphene - dye hybrids toward ionic analytes namely Mercury ion (Hg^{2+}) and Fluoride ion (F^-) as test ions. Rhodamine and Fluorescein dye were opted as the model dyes in this work. We also aim to fabricate solid phase sensors for the said ions that could serve as portable layman's read out tool for qualitative detection of Mercury ion and Fluoride ion in aqueous solution.

1.7 References

[1] W. Rüdorff, E. Stumpp, W. Spriessler and F. W. Siecke, *Angew. Chem.,* 1963, 2, 67.

[2] P. R Wallace, *Phys. Rev.*, 1947, 71, 622.

[3] G. Ruess and F. Vogt, *Monatshefte für Chemie. 1948,* 78, 222.

[4] A.R Ubbelohde and F.A. Lewis, *Graphite and its Crystal Compounds*, Oxford, Clarendon Press. (1960).

[5] H. P. Boehm, A. Clauss, G. Fischer and U. Hoffmann, *Proceedings of the Fifth Conference on Carbon,* Pergamon Press, 1962

[6] W. M. Hess and L. L. Ban, *Proc. 6th Int. Congr. on Electron Microscopy* (Kyoto), 1966, 1, 569.

[7] T. A. Land, T. Michely, R.J. Behm, J.C. Hemminger and G. Consa *Surf. Sci.*, 1992, 264, 261.

[8] A. Nagashima, K. Nuka, K .Satoh, H. Itoh and Ichinokawa, *Surf. Sci*., 1993, 93, 291.

[9] S. V. Morozov, K. S. Novoselov, F.Schedin, D. Jiang, A. A Firsov and A. K Geim. *Phys. Rev. B*, 2005, 72, 201401.

[10] K. S. Novoselov, A. K. Geim, S. V. Morozov, D.Jiang, Y.Zhang, S. V. Dubonos, I. V. Grigorieva and A. A. Firsov., *Science,* 2004,306, 666.

[11] K. S. Novoselov, A. K Geim, S. V Morozov, D.Jiang, M.I Katsnelson, I.V. Grigorieva , V. S. Dubonos and A. A.Firsov, *Nature,* 2005, 438, 197,

[12] K. S. Novoselov , D.Jiang, F.Schedin, J. Booth, V.V. Khotkevich, S.V. Morozov and A.K Geim., *Proceedings of the National Academy of Sciences of the United States of America,* 2005, 30, 10451.

[13] Y. Zhang, Y. W. Tan, H. L. Stormer and P. Kim, *Nature,* 2005,438, 7065.

[14] Gautam Anand and Prateek Saxena, *IOP Conf. Ser.: Mater. Sci. Eng*. 2016,012201,149.

[15] Y. Baskin and L. Meyer, *Physical Review Journals Archieve*, 1955,100,544.

[16] H G. Eda and M. Chhowalla, *Adv. Mater*., 2010, 22, 2392.

[17] D. C. Marcano, D. V. Kosynkin, J. M. Berlin, A. Sinitskii, Z. Z. Sun, A. Slesarev, L. B. Alemany, W. Lu and J. M. Tour, *ACS Nano*, 2010, 4, 4806.

[18] Boehm, R. Setton, and E. Stumpp. *Carbon*, 1986, 24, 241.

[19] K. Erickson, R. Erni, Z. Lee, N. Alem, W. Gannett and A. Zettl, *Adv. Mater*., 2010, 22, 4467.

[20] A. Lerf, H. He, M. Forster and J. Klinowski, *J. Phys. Chem. B*, 1998, 102, 4477.

[21] T. Gao, S. Xie, Y. Gao, M. Liu, Y. Chen, Y. Zhang and Z. Liu, *ACS Nano*, 2011, 5, 9194.

[22] G. Eda, C. Mattevi, H. Yamaguchi, H. Kim and M. Chhowalla, *J. Phys. Chem. C*, 2009, 113, 15768.

[23] Q. Y. He, S. X. Wu, S. Gao, X. H. Cao, Z. Y. Yin, H. Li, P. Chen and H. Zhang, *ACS Nano*, 2011, 5, 5038.

[24] A. K. Geim, *Science*, 2009, 324, 1530.

[25] A. K. Geim and K. S. Novosolov, *Nat. Mater*., 2007, 3, 183.

[26] M. I. Katsnelson, *Eur. J. Phys*., 2006, 51, 157.

[27] D. Li and R. B. Kaner, *Science*, 2008, 320, 1170.

[28] V. Singh, D. Joung, L. Zhai, S. Das, S. I. Khondaker and S. Seal, *Prog. Mater. Sci*., 2011, 56, 1178.

[29] B. Partoens and F. M. Peeters, *Phys. Rev. B: Condens. Matter Mater. Phys.,* 2006, 74, 075404.

[30] B.Jayasena and S.Subbiah, *Nanoscale Res Lett*., 2011,6,95.

[31] E. Varrla, K.R. Paton, C. Backes, Andrew Harvey, Ronan J. Smith, Joe McCauley and Jonathan N. Coleman, *Nanoscale*, 2014,6, 11810.

[32] Y.Zhang, D.Li, X.Tan, B.Zhang, X.Ruan and H.Liu, *Carbon*, 2013, 54, 143.

[33] M.J.Mcallister, J.-L.LI, D.H.Adamson, H.C.Schniepp, A.A Abduala. and J.Liu, *Chem. Mater*., 2007, 19, 4396.

[34] C. Vall´es, C. Drummond, H. Saadaoui, C. A. Furtado, M. He,O. Roubeau, L. Ortolani, M. Monthioux and A. Penicaud, *J. Am. Chem. Soc*., 2008, 130, 15802.

[35] P.Blake, P.D.Brimicombe, R.R.Nair, T.J.Booth, D.Jiang, F.Schedin, *Nano Lett*., 2008, 8 1704.

[36] K.Parvez, S.R.Li, Y.Puniredd Hernandez, F.Hinkel, S.Wang, *ACS Nano*, 7, 2013, 3598.

[37] Y. Hernandez, V. Nicolosi, M. Lotya, F. M. Blighe, Z. Sun, S. De, I. T. McGovern, B. Holland, M. Byrne, Y. K. Gun'ko, J. J. Boland, P. Niraj, G. Duesberg, S. Krishnamurthy, R. Goodhue, J. Hutchison, V. Scardaci, A. C. Ferrari and J. N. Coleman, *Nat. Nanotechnol*., 2008, 3, 563.

[38] J. Chen, L.Chen, Z. Zhang, J. Li, L. Wang and W. Jiang, *Carbon*, 2012,50 , 1934.

[39] B. C. Brodie, *Philosophical Transactions of the Royal Society of London*, 1859,149, 249.

[40] W. S. Hummers and R. E. Offeman, *J. Am. Chem. Soc.*, 1958, 80, 6, 1339.

[41] L. Staudenmaier and L. Ber, *Chem. Ges*., 1898, 31, 1481.

[42] H. J. Shin, K. K. Kim, A. Benayad, S. M. Yoon, H. K. Park, I. S.Jung, M. H. Jin, H. K. Jeong, J. M. Kim, J. Y. Choi and Y. H. Lee, *Adv. Funct. Mater*., 2009, 19, 1987.

[43] F. Yang, Y. Q. Liu, L. A. Gao and J. Sun, *J. Phys. Chem. C*, 2010,114, 22085.

[44] Y. Zhou, Q. L. Bao, L. A. L. Tang, Y. L. Zhong and K. P. Loh, *Chem. Mater*., 2009, 21, 2950.

[45] A. V. Murugan, T. Muraliganth and A. Manthiram, *Chem. Mater.,* 2009, 21, 5004.

[46] P. Sutter, *Nat. Mater.*, 2009, 8, 171.

[47] K. S. Novoselov, D. Jiang, F. Schedin, T. J. Booth, V. V. Khotkevich, S. V. Morozov and A. K. Geim, *Proc. Natl. Acad. Sci*.USA, 2005, 102, 10451.

[48] A. Reina, X. T. Jia, J. Ho, D. Nezich, H. B. Son, V. Bulovic, M. S.Dresselhaus and J. Kong, *Nano Lett*., 2009, 9, 30.

[49] A. Chakrabarti, J. Lu, J.C. Skrabutenas, T. Xu, Z. Xiao and J.A. Maguire, *J. Mater. Chem*., 2011, 21, 9491

[50] S. Bae, H. Kim, Y. Lee, X. Xu, J.-S. Park and Y. Zheng, *Nat. Nanotechnol*., 2010, 574, 574.

[51] S. V. Morozov, K. S. Novoselov, M. I. Katsnelson, F. Schedin, D. C. Elias, J. A. Jaszczak and A. K. Geim, *Phys. Rev. Lett*., 2008,100, 016602.

[52] C. Lee, X. D. Wei, J. W. Kysar and J. Hone, *Science*, 2008, 321,385.

[53] C. Soldano, A. Mahmood and E.Dujardin, *Carbon*, 2010, 48, 2127.

[54] A. A. Balandin, S. Ghosh, W. Z. Bao, I. Calizo, D. Teweldebrhan, F. Miao and C. N. Lau, *Nano Lett*., 2008, 8, 902.

[55] T. K. Hong, D. W. Lee, H. J. Choi, H. S. Shin and B. S. Kim, *ACS Nano,* 2010, 4, 3861.

[56] V. C. Tung, L. M. Chen, M. J. Allen, J. K. Wassei, K. Nelson, R. B. Kaner and Y. Yang, *Nano Lett.,* 2009, 9, 1949.

[57] Si Zhou and Angelo Bongiorno, *Sci.Reports* 3 : 2484 | DOI: 10.1038/srep02484

[58] M. D. Stoller, S. J. Park, Y. W. Zhu, J. H. An and R. S. Ruoff, *Nano Lett.*, 2008, 8, 3498.

[59] Song Bai and Xiaoping Shen, *RSC Advances*, 2012, 2, 64.

[60] Y. Li, Q. Du, T. Liu, X. Peng, J. Wang, J. Sun, Y. Wang, S. Wu, Z. Wang, Y. Xia and L. Xia, *Chem. Eng. Res. Des.*, 2013, 91,361.

[61] Mohammed Yusuf, F. M. Elfghi, Shabi Abbas Zaidi, E. C. Abdullahab and Moonis Ali Khan, *RSC Adv*., 2015, 5, 50392.

[62] Yongle Wu and Meijun Qu, *Scientific Reports,* 2016*,* 6, Article number: 31760 .

[63] G. C. Liang, N. Neophytou, D. E. Nikonov, and M. S. Lundstrom, *IEEE Trans. Electron. Dev.*, 2007, 54, 677.

[64] Y. H. Zhang1, Y. B. Chen, K. G. Zhou, C. H. Liu, J. Zeng, H. L. Zhang, and Y. Peng, *Nanotechnology*, 2009,20, 185504 .

[65] L. Kavan, J. H. Yum and M. Graztzel, *ACS Nano*, 2010, 5,165.

[66] L. L. Zhang, R. Zhou and X. S. Zhao, *J. Mater. Chem*., 2010, 20, 5983.

[67] 67. X. Li, X.Wang, L. Zhang, S. Lee, and H. Dai, *Science*, 2009, 319, 1229.

[68] R. R. Nair, H. A. Wu, P. N. Jayaram, I. V. Grigorieva and A. K. Geim, *Science* ,2012,335, 442.

[69] Yi You, Veena Sahajwalla, Masamichi Yoshimura and Rakesh K. Joshi, *Nanoscale*, 2016, 8, 117.

[70] Z. Fan, J. Yan, L. Zhi, Q. Zhang, T. Wei, J. Feng, M. Zhang, W. Qian and F. Wei, *Adv. Mater*., 2010, 22, 3723.

[71] B. Seger and P. V. Kamat, *J. Phys. Chem. C*, 2009, 113, 7990.

[72] Y. G. Guo, J.-S. Hu and L.-J. Wan, *Adv. Mater*., 2008, 20, 2878.

[73] Z. Yin, S. Wu, X. Zhou, X. Huang, Q. Zhang, F. Boey and H. Zhang, *Small*, 2010, 6, 307.

[74] X. Yang, X. Zhang, Y. Ma, Y. Huang, Y. Wang and Y. Chen, *J. Mater. Chem.*, 2009, 19, 2710.

[75] Sang-Hoon Bae, Young bin Lee, Bhupendra K. Sharma, Hak-Joo Lee , Jae-Hyun Kim and Jong-Hyun Ahn, *Carbon*, 2013,51, 232.

[76] O. Frank, G. Tsoukleri, K.P. John, A. C. Ferrari, Andre K. Geim, Kostya S. Novoselov and C. Galiotis, *Nature Communications,2011,* 2, 255

[77] Xiao Zhu , J. Li, Hanping He, Min Huang, Xi Zhang and S. Wang, *Biosensors and Bioelectronics*, 2015, 74, 113.

[78] T. Wang, D.Huang, Z. Yang, S. Xu, G. He, X.Lin. Nantao Hu, G.Yin, D. He and L. Zhang, *Nano-Micro Lett.* , 2016,8,95.

[79] Usman Latif and Franz. L. Dickert, *Sensors*, 2015, 15, 30504.

[80] P. Bradder, S. K. Ling, S. Wang and Liu, *J. Chem. Eng. Data*, 011, 56, 138.

[81] J. T. T. Wang, B. Tang, X. Hou, L. Sun and X. Wang, *ACSAppl. Mater. Interfaces*, 2012, 4, 3084.

[82] C. Wang, H. Luo, Z. Zhang, Y. Wu, J. Zhang and S. Chen, *J.Hazard. Mater.,* 2014, 268, 124.

[83] L. Li, L. Fan, H. Duan, X. Wang and C. Luo, *RSC Adv.*, 2014,4, 37114.

[84] Z. W. D. Dong, X. Liu, X. Pei, L. Chen and J. Jin, *J. Mater.Chem. A*., 2014, 2, 5034.

[85] M. Liu, C. Chen, J. Hu, X. Wu and X. Wang, *J. Phys. Chem. C*.,2011, 115, 25234.

[86] F. Marahel, M. A. Khan, M. Ehsan, B. Iman and H. Soraya, *Desalin. Water Treat.,* 2015, 53, 826.

[87] N. M. Julkapli, S. Bagheri and S. B. Abd Hamid, *Sci. World J.*, 2014, 25, 692307.

[88] H. Hou, R. Zhou, P. Wu and L. Wu, *Chem. Eng. J.*, 2012, 211, 336.

[89] M. M Matlock, B. S. Howerton and D. A. Atwood, *Ind. Eng. Chem. Res.,* 2002, 41, 1579.

[90] S. B. Yang, J.Hu, C. L. Chen, D. D. Shao, and X. K. Wang, *Environ. Sci. Technol.,* 2011, 45, 3621.

[91] T. Pradeep and Anshup, *Thin Solid Films*, 2009, 517, 6441.

[92] X. Ren, C. Chen, M. Nagatsu and X. Wang, *Chem. Eng. J*., 2011, 170, 395.

[93] H.W. Liang, X. Cao, W.J. Zhang, H.T. Lin, F. Zhou, L.F. Chen and S.-H. Yu, *Adv. Funct. Mater.,* 2011, 21, 3851.

[94] Y. Yao, S. Miao, S. Liu, L. P. Ma, H. Sun and S. Wang, *Chem.Eng. J.,* 2012, 184, 326.

[95] J.-L. Gong, B. Wang, G.-M. Zeng, C.-P. Yang, C.-G. Niu, Q.-Y. Niu, W.-J. Zhou and Y. Liang, *J. Hazard. Mater.*, 2009,164, 1517.

[96] D. Xu, X. Tan, C. Chen and X. Wang, *J. Hazard. Mater.*, 2008,154, 407.

[97] S. Park, K.-S. Lee, G. Bozoklu, W. Cai, S. T. Nguyen and R. S. Ruoff, *ACS Nano,* 2008, 2, 572.

[98] H. Bai, X. L. Wang, C. Li and G. Q. Shi, *J. Phys. Chem. C*, 2011, 115, 5545.

[99] Y. X. Xu, Q. Wu, Y. Q. Sun, H. Bai and G. Q. Shi, *ACS Nano*, 2010, 4, 7358.

[100] X. Huang, X. Qi, F. Boey and H. Zhang, *Chem. Soc. Rev*., 2012,41, 666.

[101] T.H. Liu, Y.H. Li, Q.J. Du, J.K. Sun, Y.Q. Jiao, G.M. Yang, Z.H. Wang, Y.Z. Xia,W. Zhang, K.L. Wang, H.W. Zhu and D.H. Wu, *Colloids Surf. B.*, 2012, 90, 197.

[102] F. Liu, S. Chung, G. Oh and T.S. Seo, *ACS Appl. Mater. Interfaces* 2012, 4,922.

[103] G.K. Ramesha, A. Vijaya Kumara, H.B. Muralidhara and S. Sampath, *J.Colloid Interface Sci.* 2011,361, 270.

[104] S.R. Kanel, J.M. Greneche and H. Choi, *Environ. Sci.Technol.*2006, 40, 2045.

[105] J. Fan, Y.H. Guo, J.J. Wang and M.H. Fan, *J. Hazard.Mater.* 2009,166,904.

[106] J. Gu, W.Jiang, F.Wang, M. Chen, J. Mao and T. Xie, *Applied Surface Science*, 2014,301,492.

[107] H.J. Zhu, Y.F. Jia, X. Wu and H. Wang, *J. Hazard. Mater*.2009, 172, 1591.

[108] Q. Wang, H.J. Qian, Y.P. Yang, Z. Zhang, C. Naman and X.H. Xu, *J. Contam. Hydrol*. 2010, 114, 35.

[109] Hu Liu, Mengyao Dong, Wenju Huang, Jiachen Gao, Kun Dai,Jiang Guo, Guoqiang Zheng, Chuntai Liu, Changyu Shena and Zhanhu Guo, *J. Mater. Chem. C*, 2017, 5, 73.

[110] Palanisamy Thanikaivelan, T. Narayanan, K. Bhabendra Pradhan, and Pulickel M. Ajayan, *Sci.Reports,* 2012, 2.

[111] M. Husseien, A.A. Amer, A. El-Maghraby and N. Hamedallah, *J.Anal.Appl.Pyrol*., 2009,86,360.

[112] D. C. Tuncaboylu and O. Okay, *Eur. Polym. J*., 2009, 45, 2033.

[113] G. Hayase, K. Kanamori, M. Fukuchi, H. Kaji and K. Nakanishi, *Angew. Chem. Int. Ed.*, 2013, 52, 1986.

[114] U.S. Environmental Protection Agency Framework for metals risk assessment. EPA 120/R-07/001. Office of the Science Advisor, Risk Assessment Forum, Washington, D.C. (2007)

[115] Jingbo Chang , Guihua Zhou , Erik R. Christensen , Robert Heideman and Junhong Chen, *Anal Bioanal Chem*, 2014, 406,3957.

[116] X. J. Zhu, S. T. Fu, W. K. Wong, H. P. Guo and W. Y. Wong, *Angew.Chem.* 2006, 118, 3222.

CHAPTER II

MATERIALS AND METHODOLOGIES

Contents

Chapter 2 deals briefly with the various materials and methodologies adopted for the present study. Various chemicals employed for the study are tabulated in this chapter. A detailed description about the experimental methodologies which are crucial in developing the working systems and decisive for their applications are outlined. The principles and experimental aspects of various physiochemical techniques like UV-Vis, PL, FTIR, XRD, TGA, VSM, SEM and TEM employed for characterization Graphene and its hybrids are discussed.

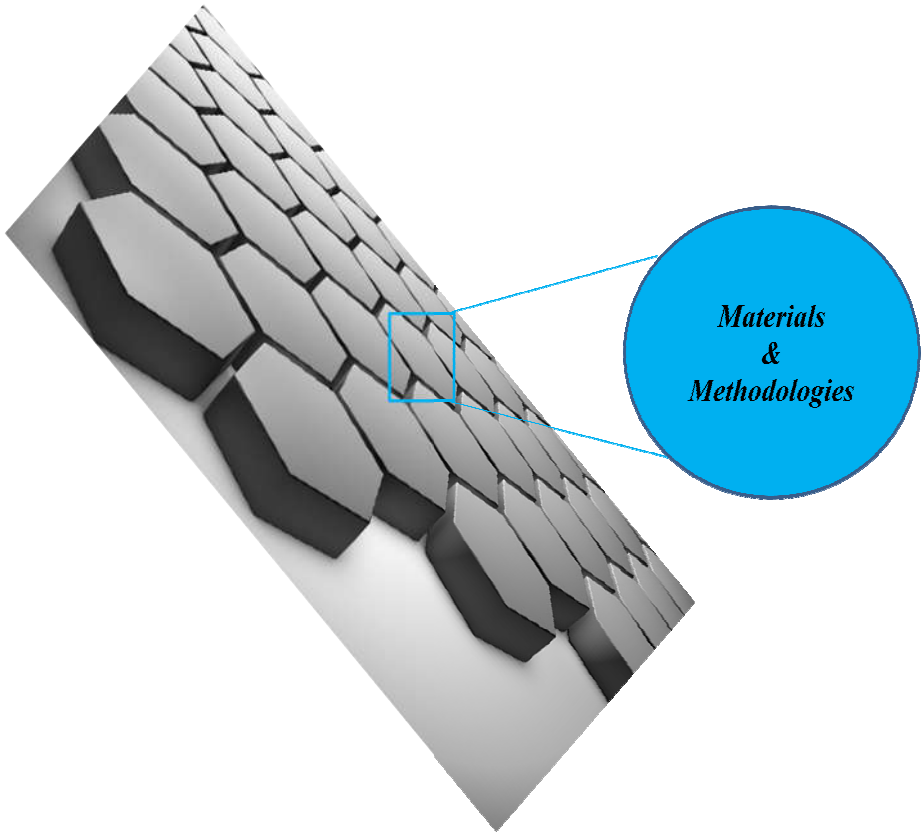
Materials
&
Methodologies

2.1 Introduction

The proper choice of materials and the adopted experimental techniques constitute the most vital steps for a research problem. The reaction conditions are crucial in determining the nature, morphology, stability and activity of the proposed systems. In addition to this, the very existence and the identity of the prepared systems lie on its characteristic features. In this direction, several physicochemical characterisation techniques are adopted to establish the identity of the material. This chapter describes the experimental methods adopted for the present work, and also furnishes a brief outline on the characterisation techniques employed for the present work.

2.2 Materials

The list of chemicals used in the work is listed in the Table 1. All the chemicals and materials employed were of analytical grade and were used without any further purification, unless specified.

Materials	***Company***
Graphite Powder	Acros Organics
Conc. sulphuric acid	Merck
Sodium nitrate	Sigma Aldrich
Potassium permanganate	Nice Chemicals
Conc. Hydrochloric acid	Merck
Sodium Borohydride	Merck
Hydrogen Peroxide	Nice Chemicals
Nitrates and Chlorides of Cd^{2+}, Pb^{2+}, Cu^{2+}, Fe^{3+}, Zn^{2+}, Cr^{3+}, Na^{+}, Ca^{2+}, Be^{2+}, Mg^{2+}, K^{+}, Sr^{2+}, Al^{3+}, Mn^{2+}, Cs^{2+}, Ba^{2+}, Ni^{2+}, Hg^{2+} and Co^{2+}	Merck
Potassium and Sodium salts of Cl^{-},Br^{-},I^{-},SO_4^{2-}	Merck

,NO_2^-,NO_3^-,CO_3^{2-},HCO_3^-,CH_3COO^-, F^-	
Hydrazine Hydrate	Merck
Fluorescein dye	Hi-Media
Rhodamine dye	Hi-Media
Ferrous sulphate	Hi-Media
Sodium acetate	Qualigens
Methylene Blue dye	Qualigens
Potassium Dichromate	Merck
Filter Paper	Whatmann
Poly Urethane	Local Market
Oil Blue	Sigma Aldrich
Organic Solvents	Merck

Table1: Chemicals used in the Research work

2.3 Experimental

This section describes the synthesis strategies adopted for preparing Graphene and its hybrids.

2.3.1 Synthesis of Graphene

Generally, Graphene is prepared by the reduction of graphene oxide obtained by oxidation of graphite. Graphite oxide is widely synthesied by oxidation of graphite by adopting the well appreciated Hummers' method [1]. Briefly, about 1g of graphite powder was mixed with 25 mL concentrated sulphuric acid and 1g of sodium nitrate and was kept in an ice bath. The reaction mixture was kept as such for about 3 hours, and was followed by the addition of 5g of potassium permanganate. After stirring the mixture vigorously for three hours, 100 mL of deionised water was added. Stirring was continued for two more hours. Subsequently 15 mL 30% H_2O_2 was added. The yellowish

cake formed was filtered and was washed with dilute HCl and deionised water. The final black residue was collected and dried in vacuum at 60^0C for 12 hours to get graphite oxide. Graphite oxide formed was exfoliated by ultrasonication by dispersing100 mg of graphite oxide in 100 mL of water for half an hour. This will lead to the formation of Graphene oxide. The pictorial representation of the synthetic route adopted is depicted in Fig.1. Graphene Oxide obtained by ultrasonication of Graphite oxide can be reduced chemically by any common reducing agent to yield Graphene sheets. In our work we have employed Hydrazine Hydrate as the reducing agent. It needs to be mentioned here that, it is almost impossible to obtain pristine Graphene sheets via chemical reduction and the actual product formed is Reduced Graphene oxide. ***However, throughout this work we have coined Reduced Graphene oxide as Graphene, which is scientifically Reduced Graphene Oxide.*** In brief, 20 µL of Hydrazine Hydrate and 104 µL of ammonia solution were added to GRO solution and were heated to 95° C for 1 h. The black dispersion obtained was filtered to obtain a stable black solution of GN. The obtained GN solution was quite stable and no aggregation was observed for one month [2, 3].

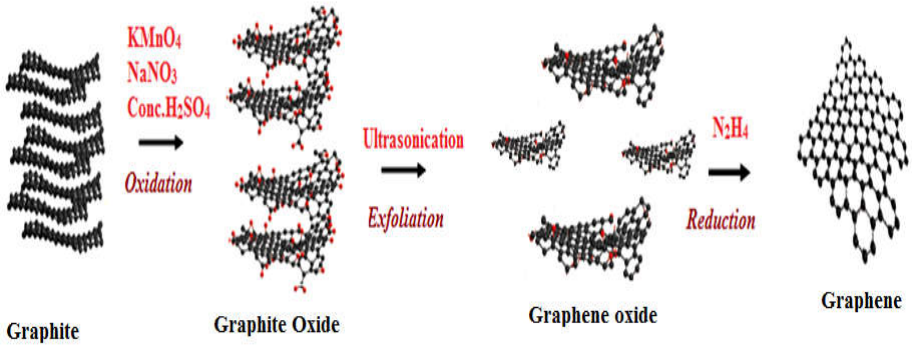

Figure 1. Pictorial representation of the preparation of Graphene sheets

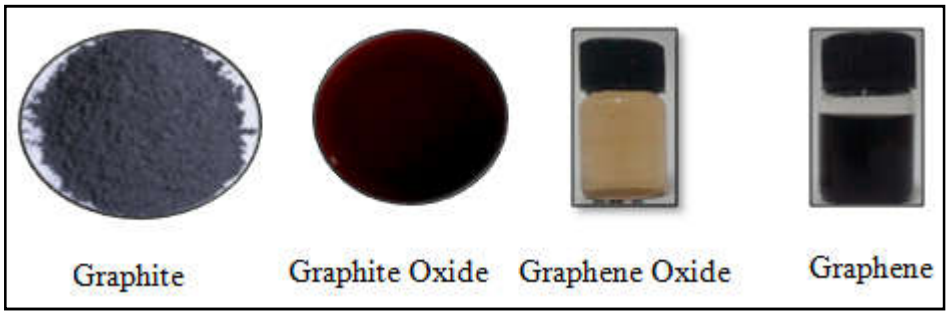

Figure 2. Graphene family. (a) Graphite powder, (b) Graphite oxide, (c) Graphene Oxide and (d) Graphene solution

(i)Probable reduction mechanism

As a result of oxidation of Graphite, a large number of oxygen functional groups such as hydroxyl, carboxyl, epoxide groups etc. decorate the graphite surface. These oxygen functionalities increase the '*d*' spacing of graphite sheets and leads to the formation of fully exfoliated graphene oxide in water on ultrasonication. Presence of these groups reduces the number of sp^2 carbons. Hydrazine Hydrate reduces nearly all the epoxide rings present in GRO. It opens the

epoxide rings to form hydrazino alcohols which react further to form an aminoaziridine moiety and consequently a double bond is formed due to the thermal elimination of diimide. It is to be noted that Hydrazine Hydrate cannot remove the carboxyl group completely as it reacts to form hydrazones. Hydrazine Hydrate is ineffective in removing the hydroxyl group even at higher temperatures. Hence the actual product obtained by reduction using Hydrazine Hydrate is Reduced Graphene Oxide, as supported by the characterisation techniques discussed below.

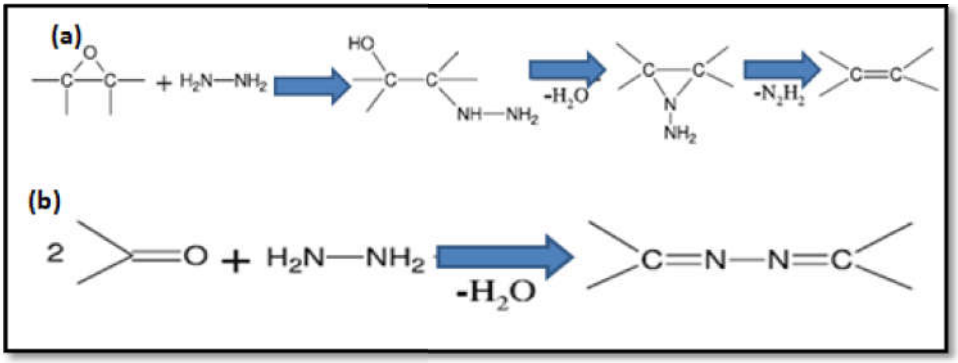

Scheme 1. Reduction of epoxide group (a) and Carbonyl group (b) with hydrazine Hydrate

2.3.2 Preparation of Graphene-Iron Oxide nanotube Hybrid

We have successfully incorporated hollow iron oxide nanotubes on graphene sheets via modification of a previously reported procedure [Fig.3] [4]. In a typical procedure, 0.03 g of graphene was dispersed in 30 mL of DI water by ultrasonication. Subsequently the above solution was mixed with 40 mL of 0.200 g of ferrous sulphate and 0.328 g of sodium acetate. The above mixture was stirred

vigorously for 30 minutes. The pH of the solution was maintained at 6.9 ±0.2, then autoclaved at 100 ^{0}C for 8 hours. The black precipitate formed was washed with DI water and ethanol and vacuum dried at 60 ^{0}C for 12 hours. The composite was obtained by heating the sample at 300 ^{0}C for 2 hours.

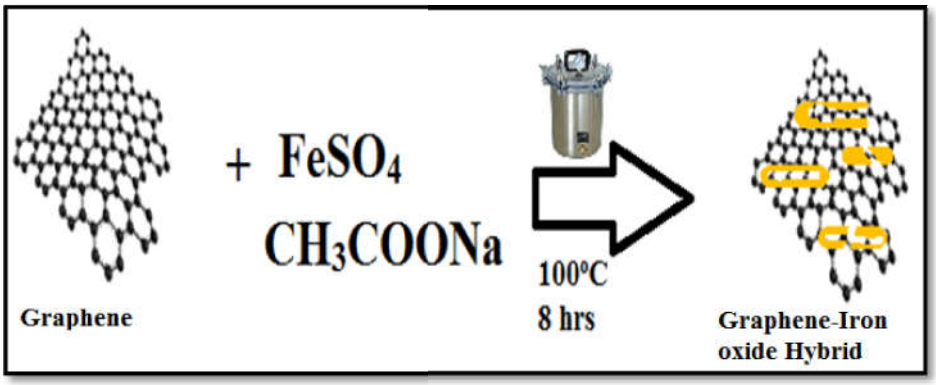

Figure 3. *Synthesis of Graphene –Iron oxide nanotube*

2.3.3Preparation of Graphene Iron oxide composite coated Poly Urethane sponge (GPUF)

As our efforts to employ GN-Iron Oxide nanotube as sorbent for oil spills did not yield fruitful results, we changed the due course by incorporating Graphene and mesoporous Iron oxide on to a 3D scaffold i.e. Poly Urethane foam to yield a hybrid of Graphene-mesoporous Iron Oxide decorated Polyurethane foam. Iron oxide was prepared by a modified route as reported by Poyraz et al. [5]. Prior to all experiments, PU sponges were ultrasonically cleaned in water and ethanol, followed by vacuum drying for 12 hrs.

Briefly 0.1g of Fe_3O_4 and 0.01 g of GRO were dispersed in 100 mL of water. The pH of metal oxide dispersed in water was adjusted in the range 5-6 using HCl and that of GRO to 7-8 using NaOH. These two solutions were mixed together and stirred for an hour. Consequently, 50 mg ascorbic acid was added followed by the immersion of the treated PU sponges. After 24 hrs, the sponges were taken out and washed with copious amount of deionised water and was dried at 30 ^{0} C. [Fig.4] As a control, graphene coated PU sponges (GPU) and Iron Oxide coated PU(FPU) sponges were prepared following the same procedure without the addition of iron oxide and graphene respectively.

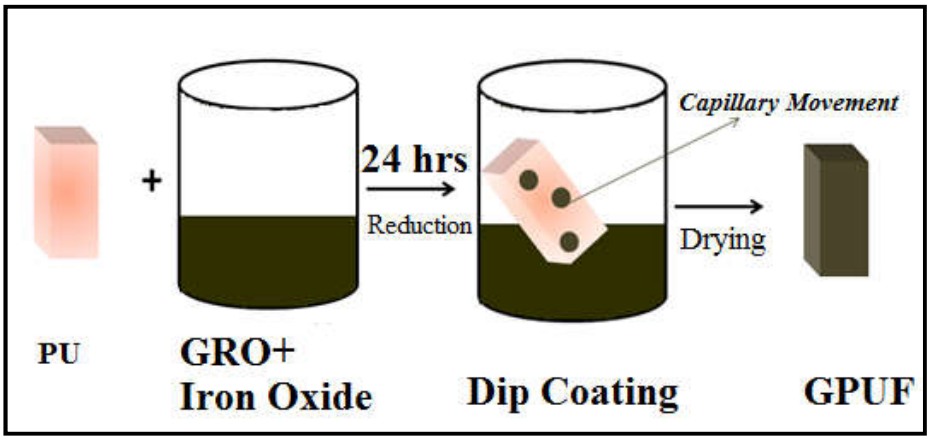

Figure 4. Preparation of GPUF by dip coating

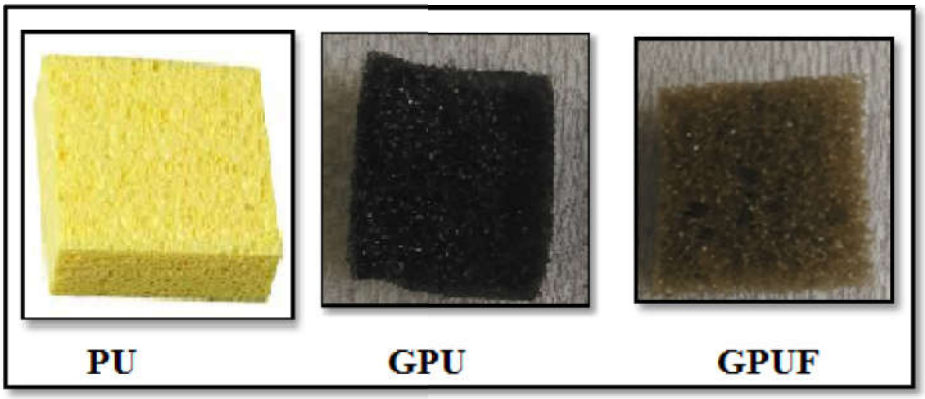

Figure 5. Digital images of Polyurethane (PU), Polyurethane/ Graphene (GPU) and Graphene/ Polyurethane/Iron oxide (GPUF)

2.4 Characterisation techniques

Characterisation of materials constitutes an inevitable part in scientific research. Currently several powerful and efficient techniques have been widely adopted to derive quantitative and qualitative information regarding the structure, morphology, and composition of the material under investigation. Generally, characterisation techniques can be classified into two main types: (1) Analysis by spectroscopic methods and (2) Imaging by Microscopic methods. Every analytical method involves two components viz. a stimulant and a signal. The stimulant is generally a part of electromagnetic radiation which on interacting with the material under investigation produces characteristic signals. These signals can be harnessed for deriving characteristic features of a specimen using specific instruments [Fig.6].

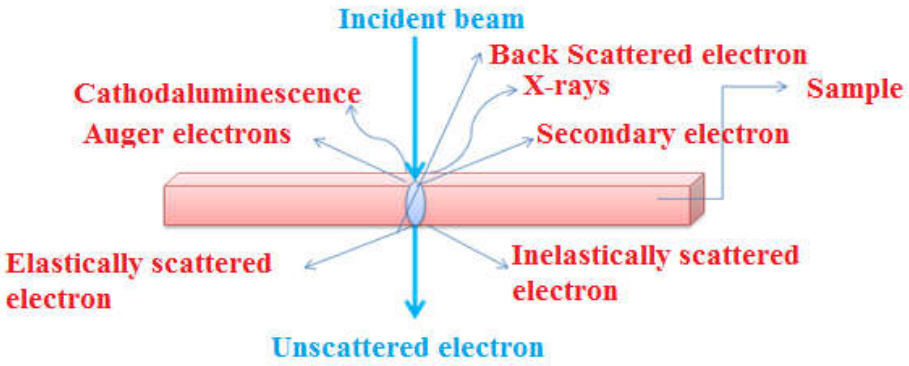

Figure 6. Modes of interaction of electromagnetic radiation with matter.

The instruments/equipments used for different analysis during the research are given below.

XRD	X-Ray Diffractometer
UV-Vis	UltraViolet-Visible Spectroscopy
PL	Photoluminescence Spectroscopy
FTIR	Fourier Transform Infrared Spectrometer
Raman	Raman Spectroscopy
SEM	Scanning Electron microscopy
TEM	Transmission Electron Micrpscopy
VSM	Vibrating Sampling Magnetometer
TG	ThermoGravimetric Analyzer

2.4.1 X-ray diffraction

X-ray Diffraction is an extensively used technique for the structural characterization of samples in powder as well as thin film form. Exploration of crystalline structures at the atomic level was made possible with the introduction of powder X-Ray diffraction by William Lawrence Bragg and William Henry Bragg in 1913. When the accelerated electrons from the cathode of a X-ray tube hits the anode, 2 types of processes may occur (a) the electrons are decelerated on interaction with the target material atoms giving rise to the emission of energy in the form of X-rays which is depicted as a continuous spectrum. In another case, the incident electrons can knock out electrons from the inner shells of target atoms and the resultant vacancies are filled by dropping down of electrons from the higher L and M shells and will give rise to K_α and K_β respectively, characteristic of the target material. Rooted on this principle, XRD analysis is a non destructive analytical tool to study crystallite nature of a material [6].

The 3-dimensional structure of a crystallite material is composed of regular, ordered arrangement of repeating atoms to form a crystal structure. As the incident X-ray beam interacts with these planes of atoms, a part of the X-ray beam is transmitted, some is absorbed, refracted scattered and a part is diffracted. The electron cloud around the atoms oscillate with same frequency as that of the incident beam and there will be destructive interference in all directions as majority of electron waves are out of phase. However, in crystals, due to perfect arrangement of atoms there will be constructive

interference in few directions [Fig.7]. Representing crystal as a set of discrete parallel planes with constant spacing 'd', when an X-ray radiation of wavelength λ is incident on a crystal plane at an angle θ, a Bragg's peak is formed if reflections from the different planes interfere constructively viz. there exists a phase change in multiples of 2π. Thus Bragg's law can be stated as

$$n\lambda = 2d\sin\theta$$

Where θ is the angle between the incident rays and the scattering planes, λ is the wavelength of incident radiation which is generally $CuK_{\alpha}1$ (1.54056Å) and $CuK_{\alpha}2$ (1.5444Å).

Briefly, for a particular d spacing, constructive interference occurs only at a specific θ value which is defined Bragg's angle while for all other angles it will be destructive interference and the intensity of diffracted X rays will be minimum. By scanning the sample through a whole range of 2θ, all possible diffraction patterns possible for the sample is collected and these diffracted X-rays are then detected and processed. Transformation of these diffraction peaks into d spacing helps in identifying a crystal structure.

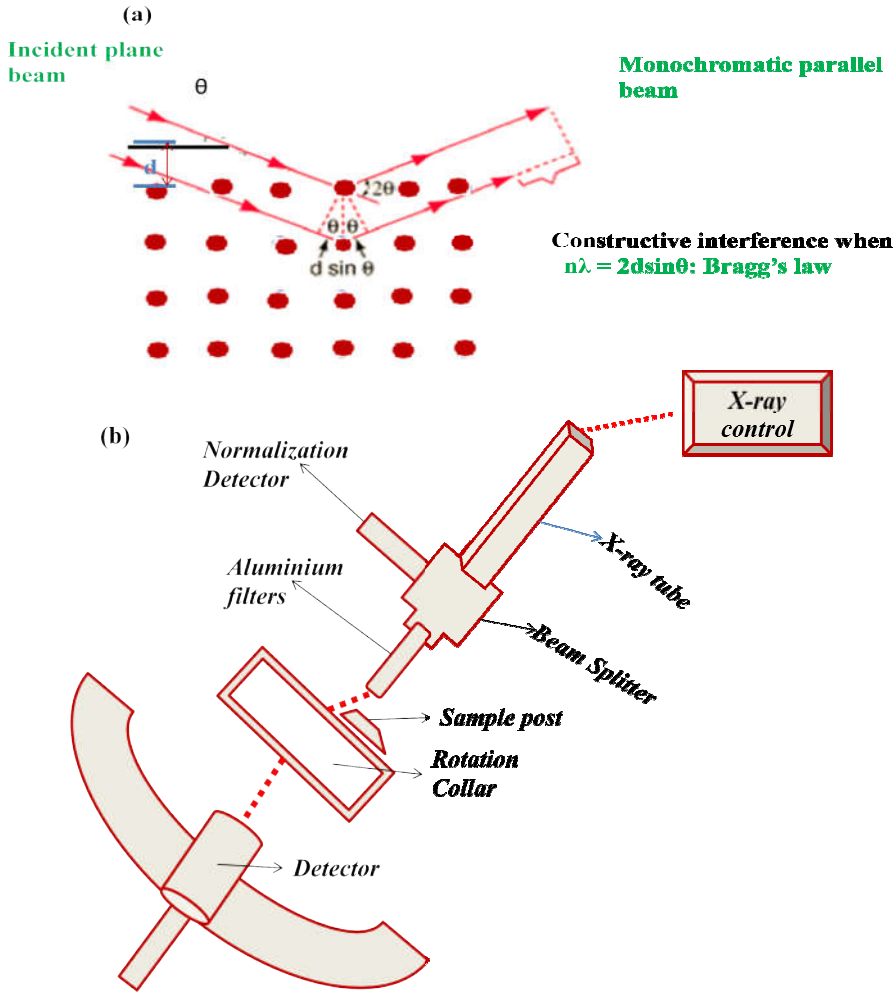

Figure 7. (a) Bragg diffraction of X-rays from various planes of crystalline material and (b) Ray diagram of XRD Diffractometer.

➢ *Instrumentation*

The main components of an X-ray diffarctometer are:

(a) X-ray source (usually a Copper target or anode giving CuK_{α})

(b) Goniometer for providing mechanical movements for source, specimen and detector

(c) Detector generally a scintillation counter. A detector measures the number of X-rays at each angle. The angle between the incident ray and detector is maintained at 2θ.

The data obtained from the detector constitutes of X-ray counts versus 2θ angle and is plotted as diffraction pattern. Conversion of these diffracted peaks into d spacing helps us to identify the crystal structure. The d-spacings can be can be compared with standard JCPDS diffraction file and can be indexed for identification of phases. The crystalline size can be calculated from the broadening of peaks based on Scherer formula, d= "Kλ/β cos θ" Where; d is mean particle size, K is a constant (0.89), β is the full width at half maximum and θ is Bragg angle.

➢ *Applications*

- The intensities and position of peaks can be employed to identify the crystal planes, crystal phase, and lattice parameters. By comparing the d spacings with standard JCPDS diffraction file, crystal phases can be identified.
- Moreover, the position of peaks can reveal information regarding the doping effects, internal strain and amount of stacking in stacking in layered structures.

- Intensity of peaks can be correlated to the types and position of atoms.

➢ *Specifications*

- Model-Rigaku miniflex 600 diffractometer
- Source- Cu kα radiation, λ=1.5404 Å

2.4.2 UV-Vis Spectroscopy

UV-Vis Spectroscopy refers to the study of interaction of UV-Vis radiation with molecules and the instrument used in UV-Vis spectroscopy is known as UV−Vis Spectrophotometer. The energy of UV-Visible radiation is sufficient for electronic transition from ground state to excited state in a molecule. Liquids, gases and solids can be analysed using Spectrophotometer by the use of radiant energy in the ultraviolet- visible regions of the electromagnetic spectrum by means of the spectrometer. Light is composed of tiny packets of energy called photons whose energy can be transferred upon collision. The energy transfer will occur only when the energy difference between the two states involved corresponds to the energy of incident light. This forms the basis of absorption spectroscopy. As light of certain wavelength and energy is incident on the sample a certain amount of light is absorbed by it. The energy of the transmitted light is measured by the photodetector. The wavelength of the incident light gives information regarding the chemical structure of the sample while the intensity of the absorbed light will provide information about the concentration of the sample [7]. A UV-Vis spectrum is a graphical depiction of the

amount of light absorbed or transmitted by the sample as a function of wavelength. Normally the measurements are carried in the range of 180-900 nm

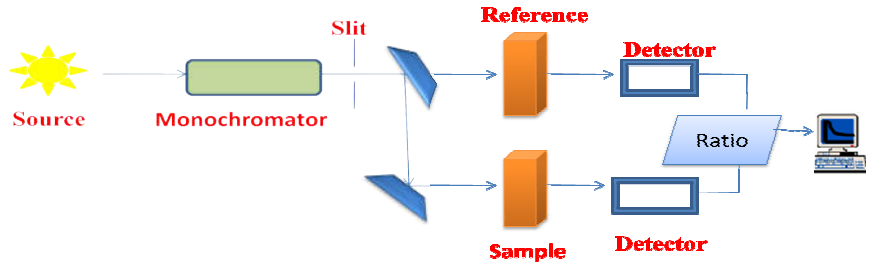

Figure 8. Pictorial representation of UV-Visible spectrometer.

➢ *Instrumentation*

The main components of an UV-Vis spectrophotometer are [Fig.9].

- Light Source- Tungsten filament or deuterium arc lamp is used as the radiation source. Recently, Light emitting diodes and Xenon arc lamps are used for visible wavelength.

- Monochromator – The monochromator splits the beam into two equally intense beams by half mirrored device before it reaches the specimen. One of the beams passes through the sample container usually a cuvette containing the solvent. While the second beam, passes through an identical cuvette containing only the reference solvent. The cuvette used must be transparent to the UV radiation and are made of quartz Quartz or fused silica. The intensity of the beam passed through the reference solvent is referred to as I_0 while that transmitted by

the sample is referred as I. From the I_0 and I values, the absorbance is calculated using Beer-Lambert's law. Absorbance= $\log I_o/I=KcL$; where K is called molar extinction coefficient, c is the concentration, L is the path length.

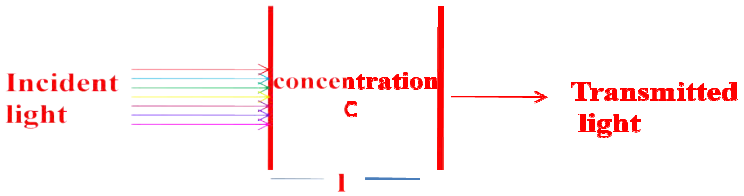

Figure 9. Absorption of radiation by sample.

- A detector- The detector must be light sensitive and measures the intensity of light transmitted from the cuvette and the value is displayed on the LCD screen.

➢ *Applications*

- Spectrophotometric determination of organic and inorganic compounds.
- Determination of concentration of unknown samples.
- Around 95 % of all quantitative determinations in health field are done using ultraviolet/visible spectroscopy.
- Determination of reaction kinetics

➢ *Specifications*

➢ Model-JascoV-550 spectrometer

➢ Source-Deuterium lamp

2.4.3 Photoluminescence Spectroscopy

Photoluminescence spectroscopy refers to versatile, nondestructive and powerful optical tool for investigating the electronic structure of substances. As light is absorbed by the sample, the molecule gets excited to higher energy states and the excited state energy is dissipated by emission. If the excitation is brought by photons, this process is called as photoluminescence. Photoluminescence refers to instantaneous emission of light from a substance by optical excitation. The energy of the emitted light corresponds to the energy difference between two electron states involved in the optical transition. This emitted light can be collected and can be analysed spectrally, spatially to derive various information regarding the electronic states of the substance [Fig.10 (a)]. The analytical instrument used to measure fluorescence of the material is called Spectrofluorometer [8].

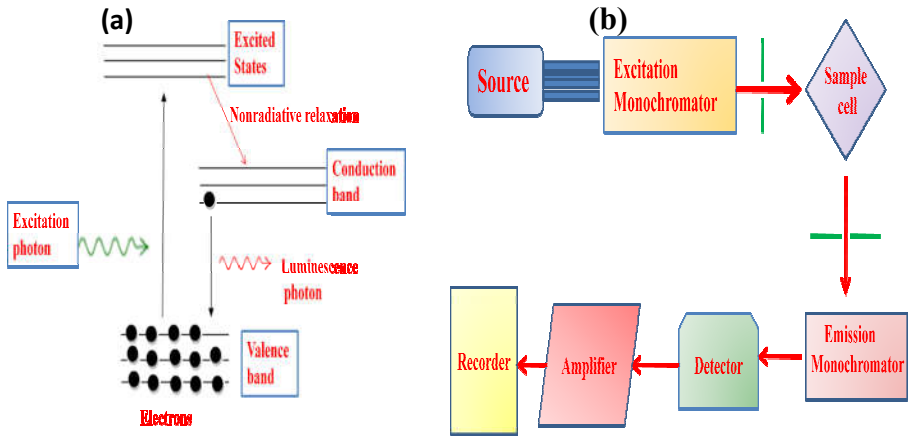

Figure 10. (a) Principle of Photoluminescence spectroscopy and (b) Ray Diagram of Fluorescence spectrometer

➢ *Instrumentation*

The essential parts of a spectrofluorometer are:

- Source: Normally ozone free Xenon lamp is employed as the source. An elliptical mirror collects the light from the source and is then focused on the entrance slit using excitation monochromator. A quartz window separates the lamp from the excitation monochromator which will a helps to minimize the heat and also the spherical aberration from the instrument

- Monochromators: An excitation and emission monochromator is present in spectrofluorometer. These chromators make use of reflective optics to reduce spherical aberrations and rediffraction.

- Gratings: Reflection grating which disperses the incident light by vertical grooves constitutes an essential part of a monochromator. A grating disperses the incident light by means of its vertical grooves and the spectrum is obtained by rotating the grating.

➢ Slits: Slits play a vital role in determining the band pass of light incident on the sample. The entrance and exit portion of each monochromator have adjustable slits. The intensity of the fluorescence signal is controlled by the emission monochromator slit. As the slit get narrowed, the resolution increases but at the expense of signal intensity.

- Shutters: Similar to slits, 2 types of shutters are present namely excitation shutter and emission shutter. Shutters protect the sample from photo bleaching and photo degradation due to prolonged exposure to light source.

- Sample compartment: Houses the sample and several optical fibers which will direct the excitation beam to the sample and brings back the emission beam to the emission monochromator.

- Detectors: A signal detector and reference detector constitutes the main components of Fluorometers. Signal detectors count the photons whereas the reference detector monitors the source lamp and corrects its wavelength etc.

- *Applications*

- Identification of unknown substances, contaminants etc.
- Helpful in cancer diagnosis
- Life time measurement of materials

- *Specifications*

- Model: PerkinElmer Fluorescence spectrometer

2.4.4 Fourier Transform Infrared (FTIR) spectroscopy

For characterizing a compound, it is essential to know the band of electromagnetic radiation absorbed by it and that left unadsorbed. In this regard, the source must cover a broad range of radiation and the

individual components must be examined after absorption. Infrared spectroscopy is a classical technique dealing with the interaction between infrared radiation and the vibrating dipole moments of molecules. Every substance has covalent bonds that absorb radiation in the infrared region of the electromagnetic spectrum and get excited to higher vibrational states. This absorption process corresponds to energy changes in the order of 8 to 40 KJ/mol. For a molecule to show IR spectrum, the vibrating motion of the bond in the molecule must undergo a change in its dipole moment as a function of time. Generally there are two types of IR spectrometers: (a) Dispersive and (b) Fourier transform.

Conventional dispersive spectrometers employ a grating or prism to disperse light into its constituent frequencies and a detector identifies the frequency that is passed from slit. Fourier Transform infrared spectroscopy is the 3rd generation IR spectroscopy which has revolutionized the scientific field. Fourier Transform infrared spectroscopy includes the absorption, reflection and emission spectrum obtained by Fourier transform of an Interferogram and involves analysis of any varying signal into its constituent components. Current IR spectrometers functions on a different approach known as Fourier transform, which can be mathematically represented as:

$$F(\omega) = \int_{-\infty}^{+\infty} f(x) e^{i\omega x} dx$$

where, F (ω) is the spectrum, f(x) is the Interferogram, ω is the angular frequency and X is the optical path difference. The experimentally obtained Interferogram [f(x)] is transformed to spectrum [F (ω)]] by Fourier transform.

In a conventional spectrometer, the desired energy falling on a sample is varied and the output obtained is plotted as a function of frequency of the incident radiation. At specific resonant frequencies, radiation will be absorbed by the sample that can be employed to identify the species. In FT, the sample is exposed to a single pulse of radiation comprising frequencies in a particular range and the output consists of rapidly decaying composite of all possible frequencies [9]. At resonance condition, certain frequencies will dominate and can be Fourier transformed to obtain the output. Hence yield the same spectra as that of conventional spectrometers but with a much shorter time.

- *Instrumentation*

Parts of an FTIR spectrometer: [Fig.11]

- An IR source- Common sources are electrically heated rods of Silicon Carbide (Globar),Mixtures of the oxides of Zr, Th, Ce, Y, Er, etc. (Nernst glower)
- Michelson Interferometer
- Detector: A detector must be quick in responding to the intensity changes occurring. Generally, photo detectors,

Pyroelectric detectors or liquid-cooled phonon detectors are employed.

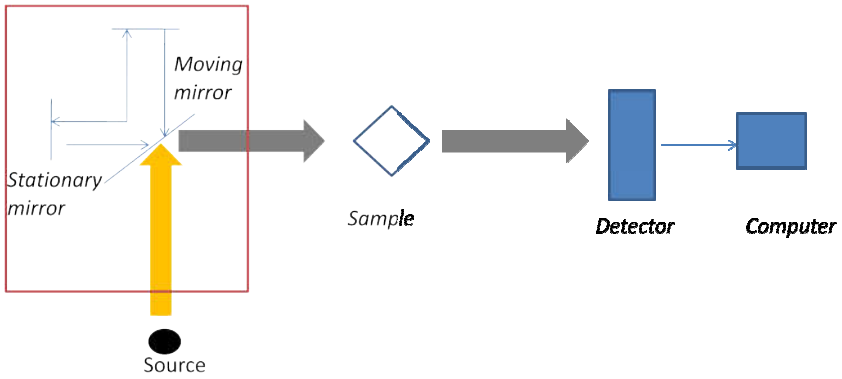

Figure 11. Fourier Transform Infrared spectrometer

- The Michelson Interferometer consisting of a broad-band light source which emits light covering the mid-IR range, a beam splitter (KBr or CsI) and two front surface coated mirrors – one moving and one fixed and a detector.

The infrared radiation is directed towards the beam splitter that reflects 50 % of the light and transmits the other. The transmitted light moves towards the moving mirror and is reflected back towards the mirror. While, the reflected light will be directed towards the fixed mirror where it will be reflected back to the beam splitter. Hence the detector can see 2 beams i.e. one from the fixed mirror and the other from the moving mirror. These two beams reaching the detector have fixed phase difference and hence they interfere constructively or destructively for a specific frequency depending on the positioning of the moving mirror. Suppose the moving mirror is scanned over a

range, a sinusoidal signal will be detected for that specific frequency with its maximum corresponding to constructive interference and minima to destructive interference. This sinusoidal signal generated is called Interferogram- plot of detector signal against optical path difference. From the Interferogram, the corresponding spectrum is obtained by computing by the Fourier transformation. The computing is so instantaneous that we may not realize that the transformation has occurred.

Depending on the nature of the sample, the sample techniques will vary. For eg., in gaseous samples, the analyte gas is introduced onto to a gas cell which houses infrared transparent windows that allow the cell to be mounted directly on the sample. For liquid samples, the liquid is squeezed as a thin film between two infrared transparent windows. In the case of solid samples, KBr disc method, mulls and deposited film methods are adopted. Throughout this study, KBr disc method was adopted which involves grinding 200 mg of KBr with 20 mg of the sample and then pelletizing the mixture at high pressure to form required pellets.

- *Applications of FTIR*

FTIR is one of the preliminary charcterisation techniques to identify the compound.

- Infrared spectra yield many bands characteristic of each molecule and these bands can serve as finger print of the molecule. The region from 900 cm^{-1} to 1400 cm^{-1} is generally

referred to as the finger print region of a molecule.IR data can function as a proof of identity for two molecules as compounds that give same infrared spectra are identical. Infrared spectra can be employed for quantitative estimation of unknown components in a mixture to a certain extent.

- Identification of transition phases of ceramics.
- Comparative chain length in polymers.
- FTIR spectroscopy can be employed to study the events that occur in blood-biomaterial interface.
- FTIR is widely used in the fields of toxicology, mutagenesis and general cellular research.
- *Specifications*
- Model- Jasco FTIR- 4100
- Sampling technique- KBr Disc Method

2.4.5 Raman Spectroscopy

Raman Spectroscopy is a powerful characterisation tool that can offer vibrational information regarding molecular structures and can also give information about surface characteristics of a material. Raman Spectroscopy can be operated in all phases viz. solids, liquids and gases over a wide range of temperatures and pressures. It is a straight forward, nondestructive and simple technique which does not require any sample preparation procedures. Raman Spectroscopy is

based on inelastic scattering of monochromatic light generally from a laser source usually in the UV-Visible and near infrared range. When the sample is irradiated with laser source, the scattered light is collected by a system of lens and subsequently forwarded through a spectrophotometer to obtain the Raman Spectrum. When the frequency of incident light is same as that of emitted light, the process is referred to as Rayleigh scattering and when the frequency of emitted light is higher or lower than the incident radiation, Raman scattering occurs. Stokes shift occurs when the frequency of emitted radiation is higher than the incident radiation and if the frequency of emitted radiation is lower than that of incident radiation, anti stokes shift occurs. The stokes shift and anti stokes shift together constitutes the Raman shift. The shift in frequency of emitted photons with respect to that of the incident radiation give rise to Raman signals and can be inferred to provide information regarding the rotational, vibrational and other low energy transitions. The Raman shift is unique feature of the material causing Raman Effect and does not depend on the frequency of the incident radiation. Generally the more intense Stokes lines are measured during Raman spectroscopy. The polarisability of the molecule must change during vibration for the molecule to be Raman active [10].

- *Instrumentation*

The major components of a Raman Spectrometer are:

- Excitation source (Laser) - A laser beam emits radiation in the Ultraviolet, Visible and near infrared range.

- Sample illumination system and light collection optics.
- Wavelength selector (Filter or Spectrophotometer).
- Detector (Photodiode array, CCD or PMT).

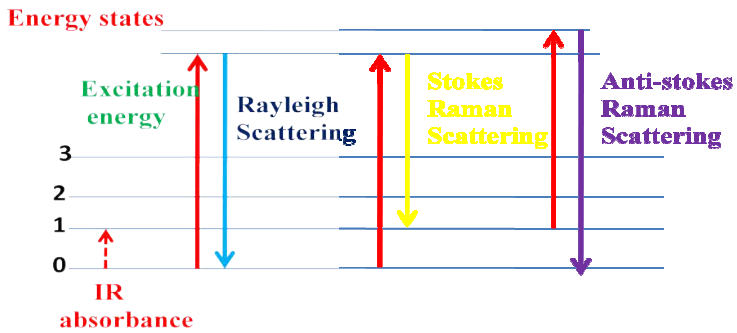

Figure 12. Modes of scattering of light

As the specimen is illuminated by laser beam, the emitted light is collected and is send to a spectrophotometer. Raman spectrometers are fitted with suitable filters and instruments like notch filters, tunable filters, laser stop apertures, double and triple spectrometric systems to reduce and filter the Rayleigh scattered signals, hence to obtain high quality Raman signals [Fig.13] . Charge Coupled Device (CCD) detectors are now been extensively employed in Raman spectrometer to obtain data quickly and with more precision. The advances in Raman spectrometers include Resonance Raman Effect (RRE) and Surface Enhanced Raman Spectra which strengthens the weak Raman signals. In order to reduce the damage to the sample caused by laser heating, Micro Raman Spectrometers are employed, wherein the spot size of light on the sample is reduced. Micro Raman Spectrometers are now widely employed in characterizing Graphene

based systems. Raman spectroscopy is extensively employed in multidisciplinary areas of chemistry, biology, physics etc. Raman Spectroscopy can be used to identify specimens quantitatively and qualitatively.

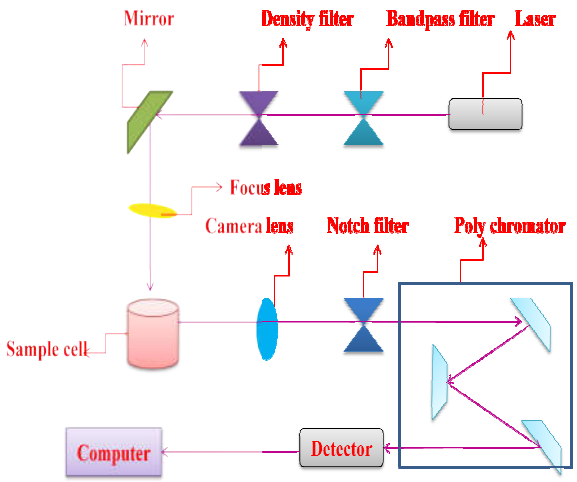

Figure 13. Ray diagram for Raman Spectrometer

➢ *Applications*

- Structural determinations of molecules
- Investigations of phase transitions
- Identification of defects in materials
- To investigate the number of layers in Graphene materials
- Study of polymer degradation and quantification of polymer composition.

➢ *Specifications*

- Sample: LabRamHR-Horiba Jobinyvon Spectrometer
- Source: 532 nm Nd: YAG

2.4.6 Vibrating Sample Magnetometer

Vibrating Sample Magnetometer is a powerful and effective method for investigating the magnetic properties of a material. The working of VSM is based on Faraday's law that states that the change in flux linking a coil generates an electromagnetic force. When a magnetic substance is placed in a constant magnetic field, it will get magnetized by aligning the magnetic domains in the direction of applied filed. The magnetic dipole moment of the sample will create a magnetic field around the sample which changes with the change in field as a function of time. This can be sensed by a pair of detection coils as stated by Faradays law of Induction. This signal from the coil is detected by a lock in the amplifier as it has a narrow bandwidth and a very high gain which in turn gives a dc voltage output. The output signal is detected by detection coils which are linked to a computer interface which will report the magnetization of sample [11]. The data is presented as a graph of magnetization against magnetic field.

➢ *Instrumentation*

- Sample Rod
- linear motor transport for vibrating the specimen

- Electronics for driving the motor
- Detection coil

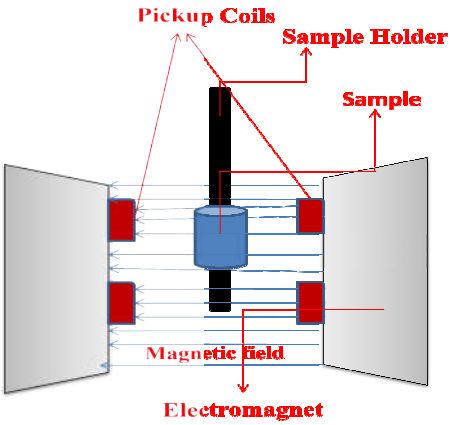

Figure 14. A Vibrating Sample Magnetometer

➢ *Applications*

- Interpretation of magnetic measurements from VSM identifies the magnetic nature of materials viz. paramagnetic, diamagnetic, super paramagnetic, ferromagnetic and ferromagnetic nature of materials.
- To examine superconducting properties of materials.
- VSM analysis finds varied applications in the field of medicine

➢ *Specifications*

- Model: Lake Shore model 7404

2.4.7 Transmission Electron Microscope

Electron Microscopy refers to that imaging technology which employs beam of electrons as a probe to form images of the sample. Unlike light microscopes, which use light for illuminating the specimen and optical lenses to magnify specimens, Electron Microscopy focuses electron beam through condenser lens to obtain the image. The shorter wavelength of electrons employed when compared to the wavelength of light in light microscopes gives electron microscopes a much higher edge over the latter [12]. Scanning electron microscope and Transmission electron microscope are the two basic types of electron microscopes.

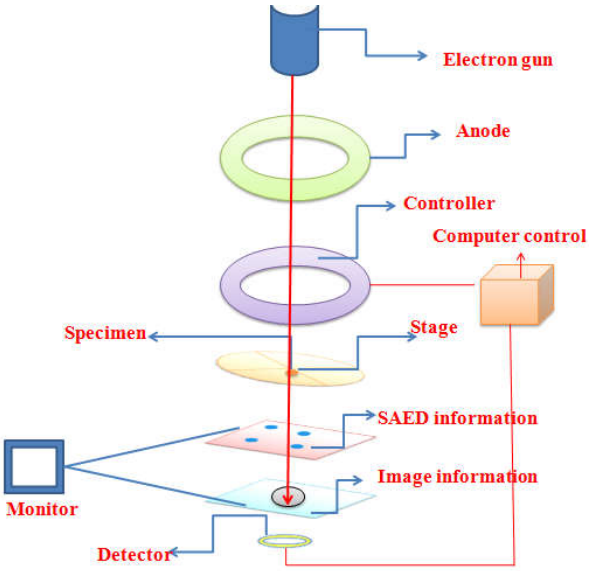

Figure 15. Ray Diagram of Transmission Electron Microscope

As the name suggests, TEM refers to microscopic technique wherein an electron beam is transmitted through an ultrathin sample which interacts with the sample as it passes through the specimen and consequently an image is formed which is magnified and focused on to an imaging device.TEM is capable of imaging the specimen at significantly higher resolution than light microscopes owing to the small de broglie wavelength of electron. As a function of thickness and composition of the specimen some of the electrons are absorbed which will lead to contrast in the image. The electrons scattered over small angles depending on the composition and structure of the specimen leading to phase contrast in the image. Scattering of electrons in very distinct direction causes diffraction contrast in the image. A few impinging electrons are deflected through large angles or reflected (backscattered) by sample nuclei whereas some impinging electrons can knock electrons from sample atoms which escape as low energy secondary electrons. Characteristic X-rays can be emitted from the specimen by the impinged electron and also photons can be emitted from the specimen. Ultimately, the transmitted electrons can be counted and sorted by the spectrometer according to the amount of energy lost in interactions with the specimen. All the elemental, chemical, electronic information regarding the specimen can be derived from analyzing this lost energy [Fig.15].

➢ *Instrumentation*

- Electron Gun- The main types of electron sources are used in electron microscopes: tungsten, lanthanum hexaboride.

- Electromagnetic lenses- condenser lenses to focus the electron beam on the sample, an objective lens and some intermediate lenses to magnify the image or the diffraction pattern on the fluorescent screen.

- Detector- A fluorescent screen and a film camera was employed for real-time imaging and recording the high resolution images of the specimen. Modern instruments rely on solid-state imaging devices, like CCD (charge-coupled device) camera for image capture.

➢ *Applications*

TEM has revolutionsed the analytical world of material and life sciences.

- The morphological, topographical, compositional and crystalline information about a specimen can be obtained from TEM images. Researchers can view specimens on a molecular scale helping to analyse structure and texture of the sample.

- TEMs can be used in semiconductor research and for manufacturing computer and silicon chips.

- Industries use TEM images to identify fractures and damages to micro-sized objects as the data obtained from TEM can help fix problems.

- TEM finds applications in all streams of research, namely, in tumor research, virology, material chemistry, environmental chemistry etc.

➢ *Specifications*

- Model: FEI TECNAI 30 G2, 300 kV

2.4.8 Scanning Electron Microscopy (SEM)

SEM is a genre of surface electron microscopy that images the sample by scanning it with a beam of electrons in a raster fashion. Typically in SEM, a focused mono-energetic electron beam is impinged on a specimen surface and is scanned back and forth. To obtain signals from a part, the electron beam is scanned over the specified region by two pairs of electromagnetic deflection coils and the signals are transferred from point to point and the signal map of the scanned area is displayed on a screen. Back scattered electrons and secondary electrons are exploited for SEM application which can be collected individually by the detectors and can be utilized to obtain information. The intensity of the electrons depends on the atomic number of the host atoms. The signals derived from electron-sample interactions provide information regarding the external morphology (texture), chemical composition, and crystalline structure and orientation of materials making up the sample [Fig.16]. Data are collected over a specified region of the surface of the specimen, and a 2-dimensional image is formed which show spatial variations in these properties. Areas ranging from approximately 1 cm to 5 microns in

width can be imaged in a scanning mode and can provide magnification upto 30,000 times. There is no special sample preparation process expect that for non conducting samples, gold sputtering is required to make it conductive. Field emission constitutes an advanced way of generating electrons. In the field emission, cathode is a thin wire with a sharp point (100 nm or less), generally supported by a tungsten filament. When a negative potential is applied to the cathode the tip concentrates the electric field, and when the magnitude of electric field strengthens to a magnitude of about 10 V/nm, tunneling occurs and electrons leave the cathode. The most prominent feature of electron gun performance is the Brightness of images. In FESEM, since the cathode current density is as high as 105 A/cm^2, images with a very high brightness are obtained. Field emission guns have lateral image resolution in nanometer scale [13]. In majority of SEM, an instrument is attached for Energy Dispersive Analysis (EDS). EDS analysis will make use of characteristic X-rays generated by atoms as electron beam is incident on the specimen and identifies the elemental composition of the sample imaged.

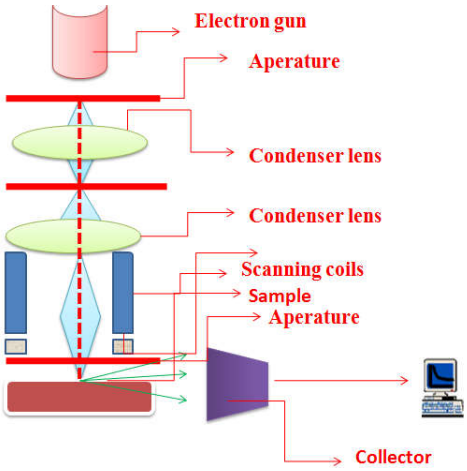

Figure 16. Ray Diagram of Scanning Electron Microscopy

- *Instrumentation*

  The essential parts of a SEM are similar to that of TEM.

- Electron gun-made of tungsten or LaB6 producing a stream of monochromatic beam of electrons.

- Condenser lens- A pair of condenser lens adjusts the energy of the electron beam and these works in conjunction with the condenser aperture and objective aperture to eliminate high angle electrons.

- Scanning coils-Scans the beam in a grid fashion

- Objective lens- focuses the scanning beam on to the desired region in the specimen. The beam then strikes the sample leading to various interactions which can be detected and analysed to form image on a long persistent phosphor CRT.

➢ *Applications*

- Topography of material and its structural defects.
- Shape and size of constituent particles.
- Composition of materials.
- Crystallographic information
- A useful research tool in the field of gemology, metallurgy, forensic science, biology etc.

➢ *Specification*

- Model JSM-6390LV

2.4.9 Thermogravimetry (TG)

Thermo gravimetric analysis (TGA) is a simple thermo analytical method which records the quantity and rate of change in the weight of a material as a function of temperature or time. This widely used thermo analytical technique can characterize compounds which exhibit weight loss or gain as a result of decomposition, dehydration or oxidation.TG measurements can be primarily employed to determine the thermal stability and composition of materials at temperatures upto 1000 ºC. The data obtained from TGA is called a thermo gram and is generally a plot of weight change against temperature. TGA curves yield information regarding the composition, thermal stability, oxidative stability, decomposition kinetics and moisture content of materials [14].

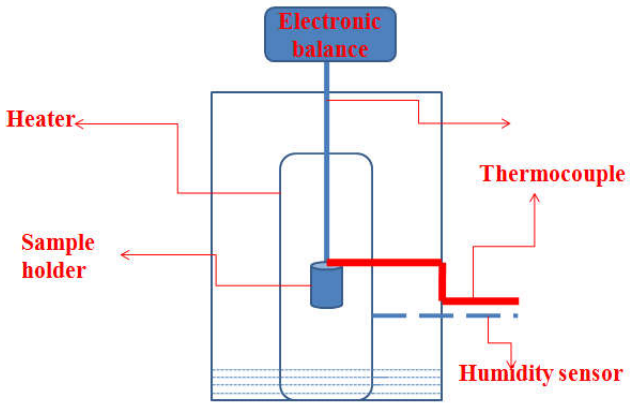

Figure 17. Pictorial depiction of Thermogravimetric Analyser

Thermobalance is the instrument employed in Thermogravimetry analysis [Fig.17]. It constitutes a sample pan kept in a furnace which is supported by a precision balance. The mass change during the analysis is monitored and a purge gas controls the sample environment. The gas purged may be inert or reactive which can prevent unwanted reactions.

➢ *Instrumentation*

The components of a thermo balance are:

- Balance - The balance made of Platinum must be accurate, responsive and reproducible. There are two types of balances (i) null type and (ii) deflection type. The sensor attached to the balance identifies the deviation and initiates the restoring force

to bring the beam balance to its equilibrium position. The restoring force is proportional to the mass change.

Deflection of the beam about the fulcrum is traced by recording the change by various techniques .The balances used in TGA instruments can measure mass ranging from 0.0001mg to 1g depending on sample containers used.

- Furnace: The temperature range of the furnace generally ranges from 150 ° C to 2000 °C depending on the models. Temperature measurements are done using thermocouples like Chromal-alumel and Pt-Rh thermocouple. The sample is heated isothermally using suitable thermocouple.

- Temperature Controller and recorder: The temperature is usually programmed controlled with two thermocouple arrangement. The recorders are automatic and measures mass as temperature changes. X−Y recorders are commonly employed and they plot weight directly against temperature. The data obtained are processed using personal computer and are plotted.

➢ *Applications*

- To analyse the purity and stability of sample

- To investigate the thermal degradation and identify products in the course of degradation.

- To examine the chemical process during the thermal process.

➢ *Specifications*

- Model: TGA Q50

2.5 Investigations *on the application of Graphene based Hybrids as sorbent and sensor*

The synthesied Graphene sheets were employed for devising versatile hybrids as sorbent and sensors for environmental applications. Inspired by potential of magnetic actuation for adsorptive removal, we have incorporated Iron Oxide onto GN sheets for the fabrication of Graphene-Iron Oxide nanocomposites and have employed it towards pollutant abatement. We have investigated the application of Graphene based hybrids as sorbent for common water pollutants viz. an organic Dye (Methylene Blue), a toxic heavy metal (Hexavalent Chromium) and Oil and are presented in Chapter 4. In the second working chapter, the prospects of Graphene-Dye hybrids as potential sensors for Mercury ion and Fluoride ion in aqueous solution are examined. The adopted methodology for the synthesis of these hybrids is discussed in detail below.

2.5.1 Graphene-Iron oxide nanotube Hybrid as an adsorbent

(i)Procedure for adsorptive removal of Chromium (VI)

Activity of the prepared composite in the adsorptive removal of toxic heavy metal Cr (VI) was studied. The standard method of colour development using diphenylcarbazide reagent was adopted for this estimation. Stock solution of chromium was prepared from K_2CrO_4.

pH of the solution was maintained at 7. The optimized dosage for the adsorption study was found to be 80 mg of adsorbent in 60 mg L^{-1} of Cr in potassium chromate solution. 25 mL of Cr (VI) solution of known concentration was added to the composite. The sorbent after sorption was recovered by an external magnet. The change in concentration of Cr (VI) ion due to adsorption by the prepared magnetic composite was determined colorimetrically by measuring the absorbance at 540 nm with the help of Shimadzu spectrophotometer.

$$\textit{Removal efficiency (\%)} = (C_o - C_e / V)\ 100$$

where C_0 is the Initial concentration of Cr (VI) (mg/L), C_e is the Equilibrium concentration of Cr (VI) (mg/L).

The amount of Cr (VI) adsorbed on the composite can be calculated as follows

$$\textit{Quantity of Cr (VI) adsorbed, } q_e = (C_0 - C_e)\ V / m$$

Where 'q_e' concentration of Cr (VI) adsorbed (mg/g), 'V' volume of the solution taken and 'm' mass of the composite.

For adsorption equilibrium experiment, a known dosage of the composite (80 mg) was weighed and transferred to 25 mL chromium solution of different concentrations. This mixture was shaken for 2 hours until equilibrium was obtained. The adsorbent was then separated with the aid of an external magnet and the absorbance of the remaining solution was measured using UV-vis spectrometer. In order to study the effect of solution pH on the adsorptive removal process,

the adsorption experiments were carried out at pH values ranging from 2-10. Acidic and alkaline pH was attained by adding required amounts of 1M HCl or 1M NaOH solutions. The pH of the solution was measured using a portable pH meter, Systronics μ pH 361. During the experiment all the other experimental conditions were kept constant.

To test the reusability of the prepared composite for the adsorptive removal of Cr (VI) ion, a definite amount (80mg) of the composite was added to 25 mL of chromium solution of known initial concentration (60 mg/L) and the mixture was shaken for 2 hours in a rotary shaker with 200 rpm. The adsorbed composite alone was collected via magnetic separation. Then the collected adsorbent was shaken with 25 mL of 0.5 M HCl. After shaking for 2 hours, the adsorbent was recovered and reused for adsorption. The adsorption experiment was again repeated by analyzing the supernatant solution using UV-VIS spectrometer. The cycles of adsorption-desorption were repeated for six successive cycles.

(ii)Procedure for adsorptive removal of Methylene Blue

Methylene blue adsorption experiment was carried out in glass bottles at room temperature. (The adsorption experiment was carried out at pH 6.6±0.3 as it is the pH corresponding to normal effluents from industries). The adsorption data were fitted with Freundlich and Langmuir adsorption models. The influence of contact time, the initial pH of the solution on the adsorption efficiency was investigated. To investigate the effect of time, 20 mg of the prepared sample was added to dye solution with initial concentration 25mg/L. At constant

intervals, 5mL dispersion was drawn and the composite was separated instantaneously from the dye solution with the help of an external magnet. Dye removal efficiency of the prepared composite was calculated by measuring the dye concentration before and after adsorption at room temperature. Different amount of Graphene-Fe_2O_3 hybrids were added to the dye solution (25 mg/L) and sonicated. Subsequently, the suspension was separated by a magnet. The concentrations of the remnant dye were determined by measuring the absorbance of solutions at 660 (Methylene Blue) by using UV-VIS spectrometer.

The removal efficiency of the dye were calculated using the equation

$$\text{Removal efficiency (\%)} = [(C_1-C_0)/C_0\,]*100$$

The amount of dye adsorbed was calculated using the equation (q_e)

$$q_e = [(C_0-C_e)\ V]*M$$

For adsorption equilibrium experiment, a known dosage of the composite [20mg] was weighed and transferred to 25 mL dye solution of different concentrations [25mg/L-120 mg/L].This mixture was shaken for 2 hours until equilibrium was obtained. Then the adsorbent was separated with the aid of an external magnet and the absorbance of the remaining solution was measured using UV-VIS spectrometer. The effect of pH on the adsorption of MB was examined in the pH range of 2-10. The pH was varied using 0.1 M HCl or 0.1 M NaOH.

To test the reusability of the prepared composite for MB dye, 20mg of the composite was added to 25 mL of MB dye solution [25mg/L], and the mixture was shaken for 2 hours. After magnetic separation, the adsorbent alone was collected. The adsorbent was then shaken with 25 mL of 0.5 M HCl. After shaking for 2 hours, the adsorbent was recovered and reused for adsorption. The adsorption-desorption cycles were repeated six times in order to examine the reusability.

(iii)Procedure for adsorptive removal of oil

The adsorption efficiency was evaluated in sets of batch adsorption systems; (i) In pure organic solvent and (ii) organic solvent/water. For sorption tests, 40 ml of organic liquid/oil was poured into a 100 ml beaker and then pre weighed GPUF was immersed in it for 15 minutes and its weight was recorded after draining for a few minutes. The adsorption capacity was calculated using the equation: $Q= (W_t-W_0)/W_0$; where: W_t is the weight of the sorbent after adsorption and W_0 is the initial weight of the sorbent. For organic solvent/water system, sponges were immersed in a mixture of solvent and water. Typically, (diesel oil and chloroform were taken as the representative pollutants) 4g of diesel oil/chloroform was added to 50 ml of Deionised water and as mentioned above the weight of the sponge before and after immersion were noted. Reusability is critical in scaling up an adsorbent to commercial level. Investigations on reusability were carried out by squeezing the saturated sponges manually and drying for 15 minutes and performing the adsorption

process. The cycle was repeated for around 150 times to charecterise the reusability of GPUF.

2.5.2 Graphene-Dye Hybrid as sensor

For investigating the prospects of Graphene hybrids as sensor for Mercury ion, Graphene sheets worked as the host matrix, while Rhodamine6G and Sodium salt of Fluorescein dye were opted as the indicators.

(i) Mercury ion sensing strategy

Stock solution of Rhodamine 6G (R6G) and Fluorescein (FLR) and corresponding metal salts were prepared in Deionised water. Aliquots of GN solution were added to the dye solution taken in a glass cuvette. Subsequently the change in absorption spectra was noted. Aliquots of metal ion solutions [Hg^{2+} (100 μM), all other metal ions at a concentration of 150 μM] were then titrated against GFU and the absorption spectra were recorded after every addition. The selectivity toward $Hg^{2+}$was checked in the presence of other competing metal ions (Cd^{2+} , Pb^{2+} , Cu^{2+} , Fe^{3+} , Zn^{2+} , Cr^{3+} , Na^{+} , Ca^{2+} , Be^{2+} , Mg^{2+} , K^{+} , Sr^{2+} , Al^{3+} , Mn^{2+} , Cs^{2+} , Ba^{2+} , Ni^{2+} , and Co^{2+}). The reversibility of the system was examined by the addition of EDTA (150 μL) as coordinating ligand. pH of the solution was 6.7 ± 0.4 for R6G system and 8.0 ± 0.4 for FLR system during the whole study. At the concentration of Hg^{2+} selected for the present study (ppt and ppb levels), no mercury-hydroxide formation is noticed even at higher pH values. Below this pH, Hydroxide formation is detected only at

mercury concentration > 120 ppm. Hence it is evident that the whole mercury is present as Hg^{2+} ions.

(a) Fabrication of solid phase sensors for Mercury ion (Hg^{2+})

The integration of sensing receptors into any solid substrate outshined proficient sensing designs. Immobilisation of sensing receptors onto filter paper strips showed a facile and extremely selective sensing strategy for various analytes. These strips with fair mechanical and chemical stability allowed easy and stable detection of analytes and transformed the sensing system into smart, stable and portable laboratory assays. These strips provided ion sensing recognition for both cost and energy saving systems. Indeed, these strips serve as efficient sensing strips targeting specifically for on-site applications. These miniaturized strips can serve as portable layman's tool for quick, cost effective sensing of various test ions.

In order to develop a solid phase sensor for Hg^{2+}, GD units were immobilized on filter paper (Whatmann 1, 90 mm) by soaking in GD solution for 4 h, followed by normal drying. Mercury ions were added on this paper strip and the fluorescence was monitored by placing the strip under UV illumination. Fig.18 depicts the pictorial representation for the fabrication of GD strips.

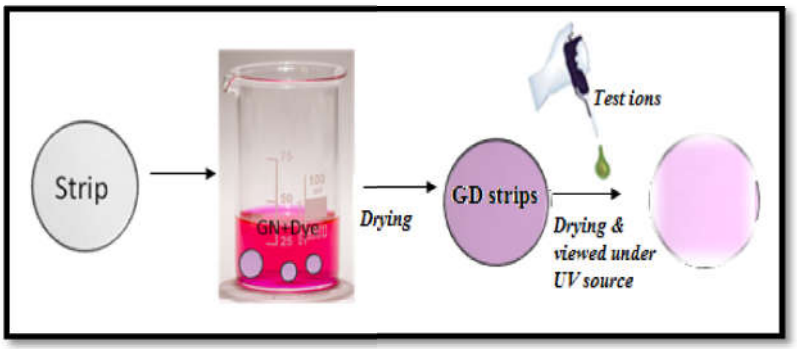

Figure 18. Fabrication of Graphene-dye strip sensor

(ii)Fluoride ion sensing strategy

Aliquots of Graphene solution was added to Rhodamine solution in a cuvette, recording the absorption and emission spectra of the solution after each addition, as mentioned earlier. Subsequently, titration of concerned anions (F^- Cl^-,Br^-,I^-,SO_4^{2-},NO_2^-,NO_3^-,CO_3^{2-},HCO_3^-,CH_3COO^- in the form of K and Na salts) against Graphene-dye unit (GRD & GFU) was done by following the absorbance and fluorescence in the same manner.

(a)Fabrication of solid phase sensors for Fluoride ion (F^-)

For the preparation of test strips, the cellulose acetate strips of desired shape were immersed in GD solution for 2 hours and were air dried. Fluoride solution of varying concentration was added to the test strip and the strip was imaged under a UV source.

2.6 References

[1] W. S. Hummers Jr and R. E. Offeman, *J. Am. Chem. Soc.,* 1958, 80, 1339.

[2] B. Zhao, R. Liu, X. Cai, Z. Jiao, M. Wu, X. Ling, B. Lu and Y. Jiang, *J. Appl. Electrochem.,* 2014, 44, 53.

[3] B. J. Li, H. Q. Cao, J. Shao, M. Z. Qu and J. H. Warner,*J. Mater. Chem*., 2011, 21, 5069.

[4] J. Guo, R. Wang, W. W. Tjiu, J. Pan and T. Liu, *J. Hazard.Mater.* 2012, 225, 63.

[5] A. S. Poyraz, C.H. Kuo, S. Biswas, C. K. King'ondu and S. L. Suib, *Nat. Commun.* 2013, 4, 2952

[6] B. D. Cullity, "Elements of X-ray Diffraction", Addison Wesley, Massachusetts.

[7] C. N. Banwell, E. M. McCash, *A Book: Fundamentals of Molecular Spectroscopy, 4th Ed., Tata McGraw Hill Publishing Co. Ltd.*, 2002.

[8] Wei W., Cui X., Chena W., Ivey D. G., *Chem. Soc. Rev*. 2011, 40, 1697.

[9] D. A. Long, *Raman Scattering, Mcgraw Hill Book Company, New York*, 1977.

[10] N. A. D. Burke, H. D. H. Stover, F. P. Dawson, *Chem. Mater*., 2002, 14, 4752.

[11] Williams, D.B., Carter, C.B., 2009. Transmission Electron Microscopy – A Textbook for Materials Science. Springer.

[12] K. Wang, L. Yu, S. Yin, H. Li, Pure Appl. Chem.81, 2009, 2327.

[13] REIMER, Ludwig. 2nd completely rev. and updated ed. Berlin: Springer, 1998. Springer series in optical sciences. ISBN 35-406-3976-4.

[14] Hatakeyama T. and Quinn F.X. Thermal Analysis: Fundamentals and Applications to Polymer Science, *John Wiley & Sons Ltd., England.*, 1994.

CHAPTER III

CHARACTERISATION OF GRAPHENE

Contents

This chapter analyses the results of the physiochemical techniques adopted to confirm the formation of Graphene sheets and to characterise its nature. The prepared Graphene sheets were characterised by various analytical techniques such as UV-Vis spectroscopy (UV-VIS), powder X-Ray diffraction analysis (XRD), Fourier transform infrared spectroscopy (FTIR), Raman spectroscopy, electron microscopic techniques; scanning electron microscopy (SEM) and transmission electron microscopy (TEM) .The results obtained from the analysis are discussed in detail.

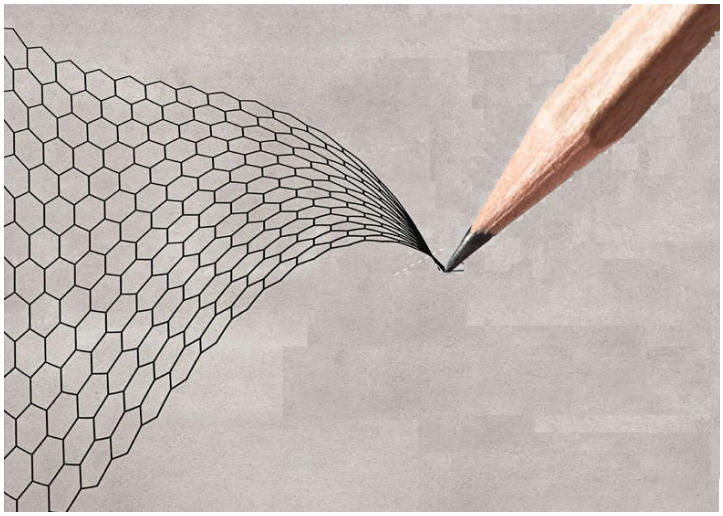

The Future lies on a pencil trace

3.1 Introduction

"A pencil and dream can take you anywhere". Literally, this is what Geim and his dedicated group did in 2004, by discovering GN sheets from Graphite using a simple Scotch tape technique. Graphene is a wonder super carbon with enough potential to revolutionize current scientific and technological world. Graphene and its derivatives stands as the centre of attraction of research community and if bibliometrics are to be trusted, the quantity of research papers on graphene will continue to increase rapidly over the next few decades. As mentioned in Chapter 1, several techniques are available to produce GN sheets for diverse applications. Moreover, proper characterisation of graphene and its derivatives must be carried out before proceeding to their application. It requires mentioning here that, chemical reduction routes always will yield Reduced Graphene Oxide (RGO), as it is almost impossible to reduce all the functional groups on Graphene oxide. Though, we have obtained RGO as our product, and have employed it for our studies, we have used Graphene for RGO throughout the thesis. In this research work, we have synthesised Graphene by chemical reduction of Graphene oxide, which was obtained by Hummers' method. Hydrazine Hydrate was employed as the reductant. The prepared Graphene sheets were characterised by various analytical techniques such as UV-Vis spectroscopy (UV-VIS), powder X-Ray diffraction analysis (XRD), Fourier transform infrared spectroscopy (FTIR), Raman spectroscopy, Electron microscopic techniques; Scanning electron microscopy (SEM) and Transmission electron microscopy (TEM). This chapter is devoted for the

characterisation of prepared Graphene sheets and the obtained results are discussed in detail.

3.2 X-ray Diffraction Analysis

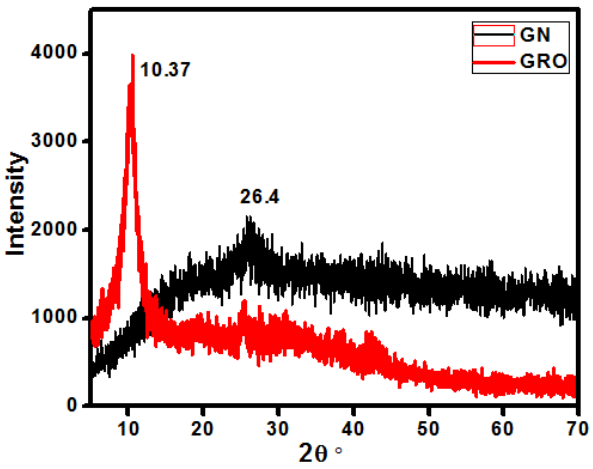

Figure 1. XRD pattern of Graphite oxide (GRO) and Graphene (GN)

XRD is an important characterisation technique for characterization of intercalation and exfoliation in composites made up of layered materials. The XRD pattern of graphite oxide (GRO) and Graphene (GN) is presented in Fig. 1. As shown in the XRD pattern, GRO exhibits its unique peak centered at 2θ value 10.37º which corresponds to the reflection from (001) plane of the material. The interlayer spacing estimated from Scherrer equation is around 8.61 Å. The interlayer distance in GO was fund to be much higher than that of Graphite sheets (0.354 nm) which can be ascribed to the presence of oxygen functional groups and adsorbed water molecules on GRO. On reduction of GRO, the peak at 10.37º disappears, affirming the

removal of oxygen functional groups and conversion to GN. The XRD pattern of GN shows a less intense peak at 2θ value 26.4º which can be attributed to the reflections from (002) planes and corresponds to an interlayer distance of 0.348 nm. Concerned data is provided in Table 1.The increase in FWHM of GN when compared to that of GRO underlines the increase in amorphous nature of GN sheets [1-2].

Sample	***Peak Position***	***d spacing(Å)***	***FWHM(nm)***
Graphene Oxide	*10.37*	*8.61*	*1.8*
Graphene	*26.4*	*3.48*	*5.7*

Table 1: Parameters obtained from XRD data

3.3 Ultraviolet-Visible Spectroscopy

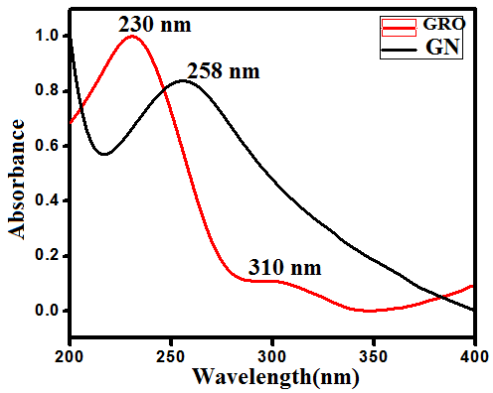

Figure 2. UV-Vis spectra of Graphene oxide (GRO) and Graphene (GN)

Fig.2 depicts the UV-Vis spectra of Graphene oxide and Graphene. The UV-Vis spectrum of Graphene oxide features a prominent peak at 230 nm and a shoulder peak at 310 nm, which are characteristic features of GO spectra. The peaks at 230 nm and at 310 nm arise due to the π–π* transition of aromatic C-C bonds and n → π* transitions of C=O bonds in sp^3 hybrid domains respectively. On adding Hydrazine Hydrate, the golden brown solution of GRO reduces to a black GN dispersion and consequently, there is a red shift in the absorption peak of GRO. An extended aromatic system is the characteristic feature of GN sheets and hence it can absorb light. The 26 nm shift of the peak of GRO towards the longer wavelength region on chemical reduction confirms the conversion of GRO to GN [3-4] .The red shift in the absorption spectra is due to restoration of aromatic structure of GN on reduction.

3.4 Photoluminescence Spectroscopy

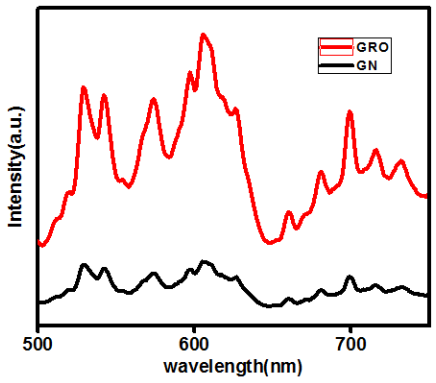

Figure 3. Fluorescence spectra of Graphene Oxide(GRO) and Graphene(GN)

The fluorescence spectra provided in Fig.3 shows the auto fluorescence of Graphene Oxide in the visible region. Several peaks arises due to presence of graphitic sp^2 in GRO, presence of oxygen functional groups, π-π transitions etc. The fluoresence intensity of GN is too low when compared to that of GRO owing to the removal of various functional groups [5,6] .

3.4.1Fluorescence Resonance Energy Transfer (FRET)

An important phenomenon exhibited by Graphene based materials is in its ability to quench the optical response of a species by means of Fluorescence Resonance Energy Transfer (FRET). FRET refers to distance dependant radiationless energy transfer from an excited donor molecule to a suitable acceptor. FRET is one among the very few techniques available for measuring nanometer distances and the change in distance between interacting molecular species. FRET mechanism involves a donor fluorophore in the excited electronic state, which upon excitation transfers its energy to an acceptor molecule in a non-radiative manner by means of long range dipole-dipole interactions. The exciting fluorophore can be regarded as an oscillating dipole capable of undergoing energy exchange with a second dipole of similar resonance energy or frequency. In this direction, the resonance energy transfer can be compared to that of coupled oscillators,e.g. a pair of tuning forks vibrating at same frequency. Resonance energy transfer reveals information about the donor acceptor couple. As mentioned earlier, in FRET, a donor fluorophore absorbs energy upon excitation, and then transfers the

energy to a nearby acceptor. Energy transfer is accompanied by the decrease in donor fluorescence (quenching of fluorescence) and decrease in excited state life time. Consequently, there occurs an increase in fluorescence intensity of the donor. Certain conditions must be satisfied for the occurrence of FRET; (i) the absorption spectra of the donor molecule must overlap with the emission spectrum of the donor species;(ii) The acceptor and donor must be at fair distance (1-10 nm); (iii) the transition dipole interactions of the donor-acceptor pair must be parallel to each other; (iv) The fluorescence life time of the donor should have enough duration for the FRET. According to Foster, the efficiency of FRET (E) is inversely related to the sixth power of distance between the donor and acceptor (r), according to the equation: $E_{FRET} = R_0^6/ (R_0^6+ r^6)$

where R_0 is the Förster radius at which half of the excitation energy of donor is transferred to the acceptor molecule. Therefore Förster radius (R_0) is referred to as the distance at which the efficiency of energy transfer is 50%.

(i)Principle of Fluorescence Resonance Energy Transfer (FRET):

During the process of FRET, the donor molecule absorbs energy because of the excitation of incident light and will transfer its energy to a nearby acceptor.

$$D + h\upsilon \longrightarrow D^*$$

$$D^* + A \longrightarrow D + A^*$$

$$A^* \longrightarrow A + h\upsilon'$$

Fig.4 depicts Jablonski diagram that demonstrates the coupled transitions between the donor emission and acceptor absorbance in FRET. In presence of proper acceptor, the donor fluorophores can transfer its excited state energy directly to the acceptor without photon emission. FRET leads to quenching of fluorescence of the donor and increase in fluorescence intensity of acceptor. However, if the acceptor species is non fluorescent, FRET will result in the intensity loss of fluorescence signal of donor molecule. Conversely, any process capable of removing the fluorescent donor from the quencher acceptor will increase the fluorescence intensity of the donor [7-9].

FRET has emerged as a powerful analytical tool for investigating the dynamics and structure of biomolecules, for visualization of intermolecular assays etc. As the energy transfer depends on the distance between the donor and acceptor, the distance can be measured from the intensity of the signal which depends on the spectral characteristic of the pair. Hence by attaching a known fluorophore onto molecules, the energy transfer data can serve as an ideal means for measuring the intra or inter molecular distances between molecules. The fluorophores used for this purpose are called probes. Exploiting all the intriguing features behind FRET, it finds

application as fluorescent sensors, fluorescent imaging, medical diagnostics, DNA analysis etc [10].

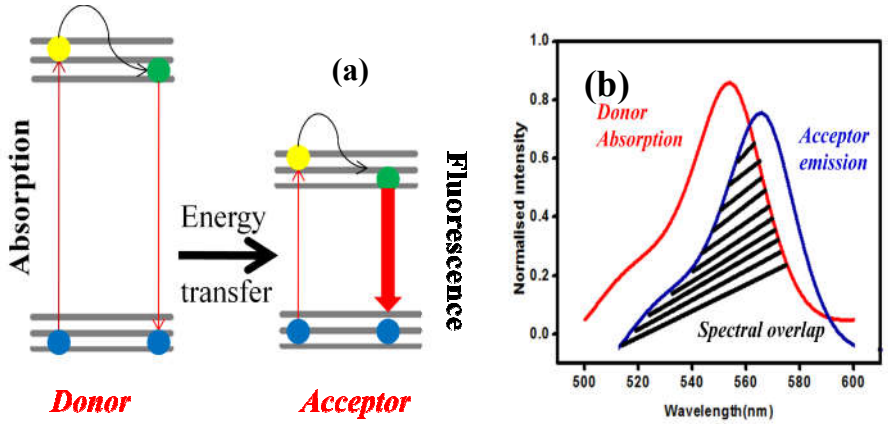

Figure 4. (a) Energy transfer leading to FRET; (b) Overlap of emission spectra of acceptor and absorption spectra of Donor.

3.5 Fourier Transform Infrared Spectroscopy (FTIR)

The FTIR spectra of GRO and GN are shown in Fig. 5. The spectrum of GRO presents numerous bands pointing to the presence of various functional groups on GRO. The bands at 1800 cm^{-1}, 1710 cm^{-1} (–C-O- stretching vibrations from carboxylic acid and carbonyl groups) and at 1100 cm^{-1} (–C–O stretching vibrations) testify the presence of oxygen containing functional groups. The strong bands at 3300 cm^{-1} (–O–H stretching vibration) can be correlated to that of adsorbed water molecules. The bands at 2979 cm^{-1} and 2866 cm^{-1} can be ascribed to the existence of $–CH_2$ and –CH groups in GRO. In comparison to the FTIR spectra of GRO, there is a drastic decrease / or disappearance in the intensity of IR bands in the FTIR spectrum of GN and hence the conversion is proved. The bands at 1710 cm^{-1}, 1707 cm^{-1}

and 1105 cm^{-1} almost disappear in GN. The presence of band indexed at 1551 cm^{-1} can be related to C=C stretch implying high degree of reduction of GRO [11]. The low intensity band at 955cm^{-1} can be ascribed to the C-O stretching vibrations of the carboxyl groups remaining after reduction.

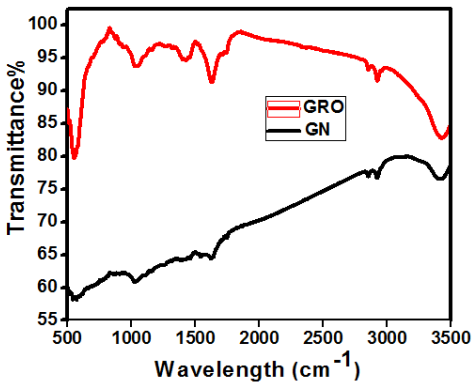

Figure 5. FTIR spectra of Graphene oxide (GRO) and Graphene (GN)

3.6 Raman Spectroscopy

Raman spectroscopy is an ideal nondestructive tool that can be employed for the qualitative and quantitative analyses of carbonaceous materials. The presence of conjugated and carbon-carbon double bonds will give rise to high intense Raman spectra. The Raman spectra for GRO and GN are shown in Fig.6. Two characteristic bands viz the D band and G band are seen for both GRO and GN. The D band can be related to the edge carbons, defects and disordered carbons. The D band arises due to out of plane vibrations (breathing mode) attributed to the presence of structural defects. On the other hand, the G band corresponds to in plane vibrations of sp^2 bonded carbons. Presence of

G band alone is the characteristic feature of pure graphite and pristine graphene sheets. The D and G bands of GRO are centered at 1360 cm^{-1} and 1613 cm^{-1} while that on reduction, the bands shift towards lower frequency region confirming reduction to Graphene. The I_D/I_G ratio of GRO and GN were 0.843 and 0.540 nm respectively indicating the reduction of oxygen functionalities in GRO on conversion to GN. The intensities of D and G band can give an idea regarding the extent of disorderness in the structure [12]. In addition to this, the intensity of D band compared to the G band has decreased pointing the rejenuvation of conjugation and fewer defects.When the D and G bands are of similar intensity, it is indicative of high quantity of defects.

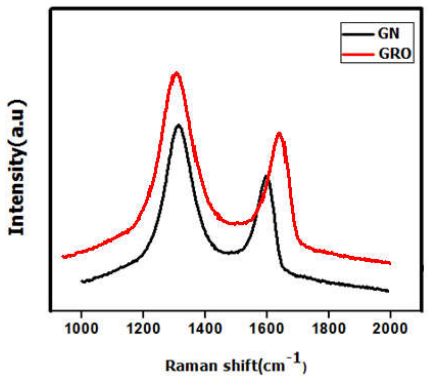

Figure 6. Raman spectra of GRO and GN

3.7 Scanning Electron Microscopy (SEM) and Transmission electron Microscopy (TEM)

Scanning Electron Microscopy images were taken to examine the morphology of the prepared Graphene sheets. Fig.7 (a) depicts the representative SEM image of GN sheets, which confirms the formation

of free standing 2D graphene sheets which are not perfectly flat but illustrates roughened surfaces and out of plane deformations with crumpled/wrinkled paper like appearance [13]. These features are characteristic of Graphene sheets and confirm the formation of Graphene sheets. The rippled structure arises due to the expulsion of gases in the form of Carbon Dioxide and Oxygen from the surface of GRO, and also due to the deformation during exfoliation and restacking.

Fig. 7(b) shows the TEM image of as-prepared GN sheets. Paper like appearance unique to GN sheets is well portrayed in the TEM image [14], which also indicated that the prepared system is composed of few layered GN sheets, typical observation for GN obtained via chemical reduction. From the high resolution TEM images [Fig.7c], the approximate number of GN layers was found to be 15, which confirms the formation of few layered GN sheets. The interlayer distance as obtained from SAED pattern (inset) was 0.41nm which is in agreement with the data obtained from XRD analysis.

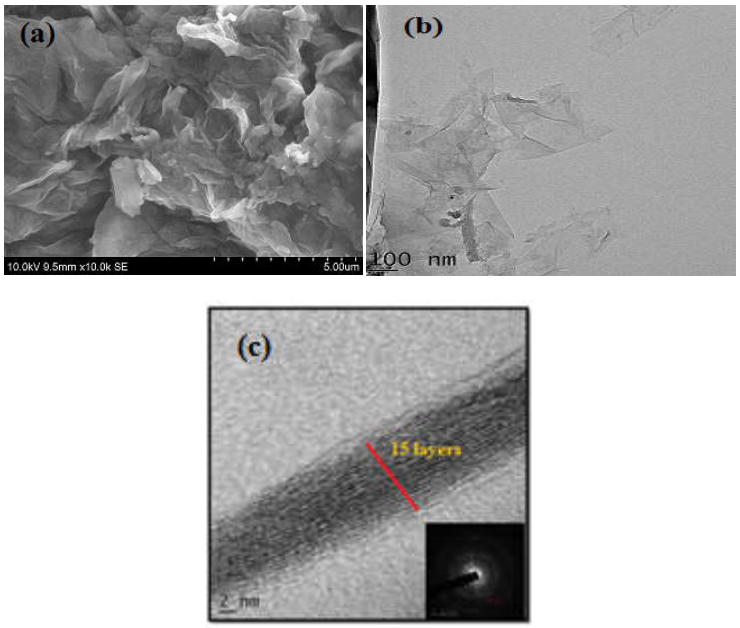

Figure 7. (a) Scanning Electron Microscopy image of Graphene, (b) Transmission electron Microscopy images of Graphene sheets (TEM) and (c) HRTEM images of GN sheets; Inset depicts the SAED pattern.

3.8 Thermogravimetry Analysis (TGA)

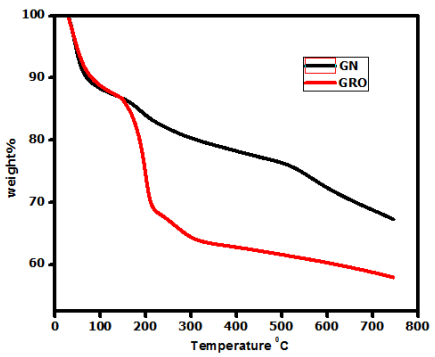

Figure 8. Thermograms of Graphite oxide (GRO) and Graphene (GN)

Fig.8 illustrates the TG curves of Graphene Oxide and Graphene. The TGA curve of GRO illustrates two major weight losses

which can be ascribed to the removal of physically adsorbed water molecules (below 100 ◦C) and due to the removal of oxygen functional groups as gases (in the range of 150 to 250 °C). In the thermogram of GN, weight loss in similar temperature range is negligible due to the absence of oxygen functionalities. Compared to GRO, GN depicts high thermal stability and slightly lesser mass loss underlining the removal of functional groups by Hydrazine Hydrate [15-16].

3.9 Conclusion

- Graphene sheets prepared by Hummers Method were well characterised by well known physiochemical techniques and confirmed the reduction of Graphene Oxide to Graphene.
- The XRD analysis hinted the conversion of Graphite oxide to Graphene as indicated by the disappearance of characteristic peak of Graphene Oxide.
- The FTIR spectral analysis indicated the removal of several oxygen functional groups namely epoxide groups and hydroxyl groups after reducing Graphene oxide to Graphene.
- Raman spectroscopy analysis indicates the presence of defects in Graphene structure.
- Analysis of Electron Microscopy images underlined the formation of crumpled/wrinkled Graphene sheets.
- All these characterisation techniques confirmed the formation of few layered Graphene sheets. It is to be noted that chemical

reduction of Graphene oxide does not yield pure graphene sheets as confirmed by the characterisation techniques adopted. Reduced Graphene Oxide is the actual product, however it is customary to represent Reduced Graphene Oxide as Graphene, hence we have adopted that practice and have referred Reduced Graphene Oxide as Graphene throughout our research work.

3.10.References

[1] B. J. Li, H. Q. Cao, J. Shao, M. Z. Qu and J. H. Warner,, *J. Mater. Chem*., 2011, 21, 5069

[2] S. Dubin, S. Gilje, K. Wang, V. C. Tung, K. Cha, A. S. Hall, J. Farrar, R. Varshneya, Y. Yang and R. B. Kaner, *ACS Nano*,2010, 4, 3845.

[3] S. Xu , L .Yong, and P. Wu, *ACS Appl. Mater. Interfaces* 2013, 5, 654.

[4] H. Guo, X. Wang, Q. Qian, F. Wang and X. Xia, *ACS Nano*, 2009, 32,653.

[5] K. P Loh, Q. L. Bao, G. Eda and M. Chhowalla, *Nat. Chem.* 2010, 2, 1015.

[6] Y. Hernandez, V. Nicolosi, M. Lotya, F.M Blighe and Z.Y. Sun De, *Nat Nanotechnol.,* 2008, 35, 63.

[7] V. G. Kozlov, V. Bulovic, P. E. Burrows, S. R. Forrest, *Nature,* 1997, 389 362.

[8] T. Förster , *Discuss Farady Soc*. 1959,27, 7

[9] D. M. Willard, L. L. Carillo, J. Jung and A. V. Orden, *Nano Lett*., 2001,1, 469.

[10] Jares- Erijman, E. A., and T. M. Jovin, *Nat. Biotechnol*. 2003,21,1387.

[11] S .Stankovich, D. A. Dikin, R. D. Piner, K. A. Kohlhaas, A. Kleinhammes, Y.Y Jia, Y .Wu, S. B. T Nguyen and R.S Ruoff *Carbon,*2007 45,1558.

[12] M. Qian , T. Feng, H. Ding, L. F. Lin, H. B.Li, Y.W. Chen and Z. Sun *Nanotechnology ,* 2009. 20, 425702.

[13] J. Nishijo, Ch. Okabe, O. Oishi and N. Nishi, *Carbon*, 2006, 44, 2943−2949.

[14] R. Sergiienko, E. Shibata, Z. Akase, H. Suwa, T. Nakamura and D. Shindo, *Mater.Chem. Phys*. 2006, 98, 34.

[15] K. Morishige and T. Hamada, *Langmuir* , 2005, 21, 6277.

[16] M. Bystrzejewski, S. Cudziło, A. Huczko, H. Lange, G. Soucy, G. Cota-Sanchez, W. Kaszuwara, *Biomol. Eng.,* 2007*,* 24, 555.

CHAPTER IV

GRAPHENE BASED SORBENTS FOR POLLUTION ABATEMENT

Contents

In this chapter, we have investigated the application of Graphene-Iron Oxide Hybrid as an adsorbent for water decontamination. This chapter is divided into two parts wherein, Part A deals with the application of Graphene-Iron Oxide nanotube hybrid as an adsorbent for Cr (VI) and MB dye. The superior adsorptive removal efficiency of the composite can be attributed to the synergistic effect between graphene and the iron oxide nanotubes. Adsorptive removal and magnetic separation were achieved quickly which highlights the efficiency of the prepared hybrid. In Part B, the prospects of Graphene-Iron Oxide incorporated Polyurethane foam as oil Sorbent was investigated. The micro/nano-textured structure of the graphene-iron oxide nano composite in combination with the micro-porous structure of the polyurethane foam creates a dually roughened surface, consequently switching the sponge's wettability from super hydrophilic to super hydrophobic. The as-fabricated sponge absorbs a wide range of oils and organics with high selectivity, appreciable recyclability and excellent absorption capacities.

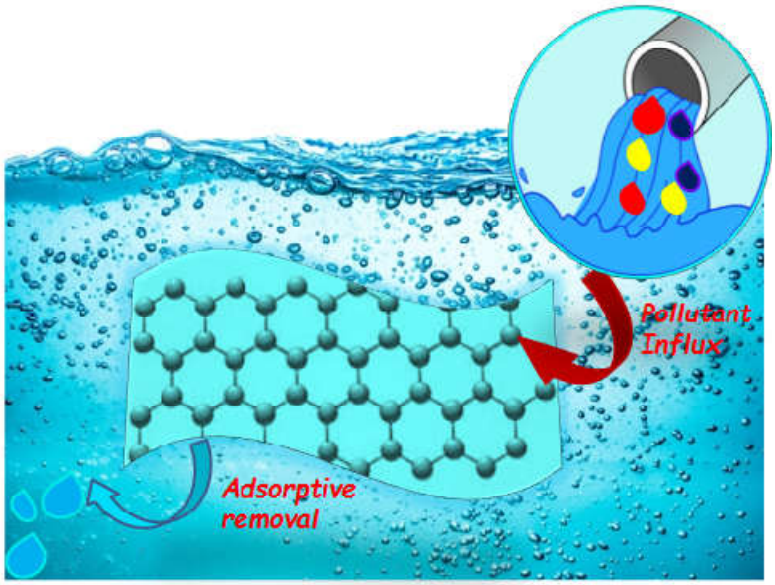

Graphene Hybrid as an elite adsorbent platform

4.1 Introduction

The 21st century has been coined as the Century of the Environment. The ever growing population, extensive industrial and agricultural activities, deterioration of land, air and water bodies, global warming have become the centre of political and scientific concern [1]. Currently, the scientific and political anxiety is directed towards understanding the issues affecting the environment balance and formulating policies and technologies to mitigate the hazards associated with this worrisome issue. The recent technological and scientific advancement in Graphene world have triggered the applications of this wonder material and its hybrids for environmental remediation. Graphene has been opted as a superior platform to develop new adsorbents, mostly because of their high surface area, non-corrosive nature, and presence of oxygen-containing functional groups, tunable surface chemistry, and scalable production [2]. The unique physiochemical properties, specifically high surface area, electron mobility and mechanical strength are the root cause for the interests in Graphene systems for environmental applications. The high surface area of graphene, the π electron cloud, the oxygen functionalities on graphene and its derivatives, the ease of functionalisation of graphene, efficient ability to host various nano materials etc. adorn graphene as a supreme candidate for environmental remediation techniques involving adsorption or surface reactions. Graphene based materials have become an indispensible entity for environmental applications, as building blocks for water

treatment membranes, adsorbent, electrode systems for contaminant removal and monitoring etc [3] .

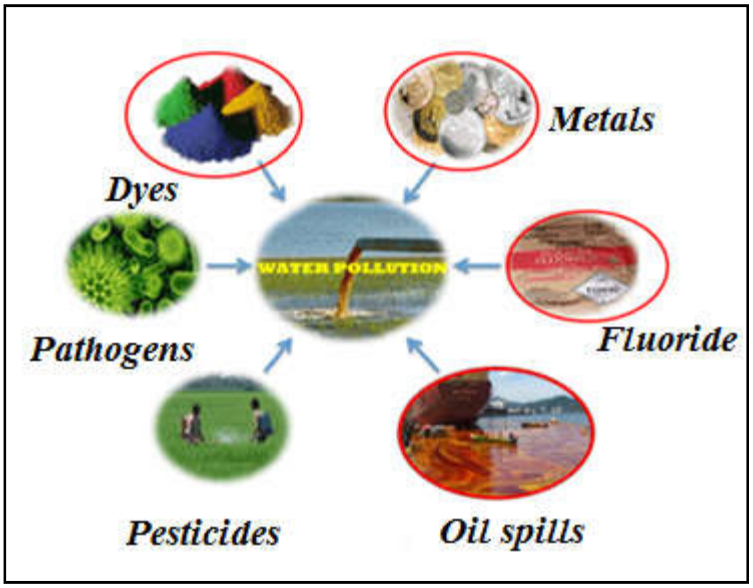

Figure 1. Various sources of Water Pollution

4.1.1 Graphene Hybrids for contaminant removal

The influx of diverse contaminants viz. organic dyes, heavy metals, organic compounds, pesticides, oils and organic solvents etc., into water bodies presents a dominant environmental issue of public concern [Fig.1]. Consequently, global efforts are directed to develop competent technologies to decontaminate pollutants from aquatic ecosystem. Table 1 presents the various technologies adopted for combating water pollution. Among the practiced decontamination technologies, adsorption presents itself as a fast, cost effective and dynamic method for the removal of pollutants from aquatic bodies [4].

Adsorption is a physiochemical process wherein the host matrix (adsorbent) holds the contaminant (adsorbate) by various interactions. Herein our work, we have chosen Methylene blue, Chromium (VI), oils and organic solvents as our target pollutants, which can serve as model contaminants and we have investigated the adsorption efficiency of the prepared Graphene hybrid for the removal of the aforesaid toxicants from aqueous solution.

Method	***Target***	***Advantages***	***Disadvantages***
Bioremediation	Dyes, oil	Eco friendly	Less efficient
Membranes	Oils & Heavy Metals,	High efficiency	High Cost, Fouling, Complex Process
Coagulation	Dyes, Oil & Heavy Metals	Efficient, simple sludge settling nature	Sludge volume is high
Photocatalysis	Dyes, heavy metal	Quick and efficient	Formation of toxicants much more toxic than parent pollutant
Adsorption	**Dyes, oil, heavy metal**	**Efficient for low concentration of target**	**Efficiency and feasibility is dependent on sorbent.**
Precipitation	Heavy metals, oils, dyes	Simple and cost effective	Fails when target concentration is too low
Burning	Oils	Quick removal is possible	Non Green

Table 1: A look into common Techniques to combat water pollution

(i) *Graphene and its hybrids as dye adsorbent*

Dyes are organic compounds widely used in, leather, cosmetic, pharmaceutical, food industries, textile, rubber, plastic and paper industry as colorant and as functional additives. Their unruly discharge into aquatic bodies has raised serious concern owing to their non biodegradable, mutagenic as well as carcinogenic nature towards human and aquatic life, hence their prompt and steady

removal/treatment from water bodies is of great interest and a challenging task for the scientific community [5]. Several environmental agencies and regulatory bodies have laid down stringent rules to reduce the discharge of dyes into water bodies. Literature review suggests the monstrous potential of graphene and its derivatives for adsorptive removal of various dyes. The interaction of dyes and graphene depends on the structural properties like molecular conformation, functional groups on graphene and dye molecule etc. Yang and his group have documented the mechanism involved in the adsorption of organic molecules on Carbon Nanotube (CNT) and have suggested five different interactions for adsorption, which comprise of electrostatic interaction, hydrophobic effect, π–π bonding, covalent bonding and hydrogen bonding [6]. Similar mechanism can be suggested for the adsorption of dyes by graphene and its hybrids.

(ii) *Graphene oxide and Graphene as an adsorbent*

Electrostatic interactions are dominant when both the adsorbate and adsorbent are charged as in the case of adsorption of cationic dyes (Methylene Blue, Methyl violet) by graphene oxide over a wide pH range (6-10). Consequently, the adsorption of anionic dyes is not favorable in this pH range. Some studies, suggest the role of π-π interaction for adsorption of cationic dyes on Graphene Oxide. Few studies point that under conditions where pH was not adjusted, hydrogen bonding interaction dominate the adsorption of cationic dyes over Graphene oxide. It was found that the adsorption efficiency increases with increase in oxidation of Graphene oxide as investigated

by Cheng et al., wherein the adsorption of cationic Methylene blue dye increased to a greater extent when highly oxidized Graphene oxide layers were employed [7]. Apart from the role of electrostatic interaction, Van der Waals interactions between the aromatic rings of adsorbent and adsorbate also play a vital role in the adsorption of dyes. Hydrogen bonding interactions are also decisive in adsorption especially when the adsorbent possess functional groups such as amine, hydroxyl, carboxyl etc. In this context, hydrogen bonding has been involved in the adsorption of polar hydrocarbons like naphthol, and 1-naphthylamine by GRO-based hybrids. In addition to this, hydrophobic interactions and the sieving effect are believed to involve in the adsorption of non-polar hydrocarbons on Reduced Graphene Oxide or Graphene sheets. Liu et al. investigated the adsorption dynamics of Methylene blue adsorption by graphene [8]. Their study indicated the dependence of adsorption on adsorbent dosage, contact time and temperature. The adsorption data fitted with Langmuir isotherm and the thermodynamic parameter revealed the adsorption to be endothermic and spontaneous. Similar report was done by Wu et al., suggesting the role of π-π interaction for adsorption of Methylene blue [9]. In a study conducted by Zhao et al., Graphene sponges act as efficient sorbents for a wide range of cationic and anionic dyes [10]. Graphene-sand composite prepared using asphalt as the carbon precursor was employed as an adsorbent for the removal of Rhodamine 6G by Sreeprasad et al. [11]. The ability of Graphene-carbon nanotube composite to adsorb MB from aqueous solution was reported by Ai et al. and the prepared composite demonstrated an adsorption capacity of

81.97 mgg^{-1} [12]. Copper oxide-graphene composite and Magnesium hydroxide- graphene composite were synthesised by Li. et al. for the adsorption of Methylene Blue and Rhodamine B [13]. The ability of Graphene oxide to adsorb Methylene blue, Methyl violet, Rhodamine B and Orange G from aqueous solution was investigated by Ramesha et al. [14] . They suggested that the electrostatic interaction between the dyes and Graphene Oxide is responsible for adsorption and the adsorption followed Langmuir model.

Kim et al. investigated the use of reduced graphene oxide for the adsorptive removal of Methylene blue and acid red. The adsorption efficiency was found to be 302.11 mgg^{-1} for MB and 28.51 mgg^{-1} for Acid red. MB adsorption data fitted with Langmuir model while that of acid red with Freundlich model [15]. Tiwari and group employed three dimensional RGO based hydrogels for the adsorptive removal of MB and Rhodamine B (RB) and their hybrid demonstrated approximately 100 % removal efficiency for MB and 97% removal efficiency for RB. Strong π-π interaction and anion –cation interaction is responsible for the increased adsorption efficiency of Reduced Graphene Oxide hybrid [16]. Recyclability studies using ethylene glycol underlined the high regeneration ability of the said hydrogel. Nguyen-Phan et al. conducted an investigation employing RGO–titanate hybrids for the adsorptive removal of MB from aqueous solution [17]. The optimum adsorption capacity was found to be 83.26 mgg^{-1} at 10 mgL^{-1} initial concentration. RGO- ZnO composite prepared by Wang et al. was used for the removal of Rhodamine B [18]. The maximum adsorption capacity for RB was found to be 32.6 mg g^{-1}. Chen et al. conducted an investigation

to remove Methylene Blue dye and Eosin Y from aqueous solutions using Graphene oxide–Chitosan hydrogel [19]. UV-Visible spectral method was employed to determine the adsorption mechanism of the dyes and it was concluded that the electrostatic interaction was vital for the adsorption of dyes by the hydrogel.

An innovative technique that has received utmost interest is the application of magnetic materials for separation. Magnetic separation is advantageous in several aspects like it can treat large amount of polluted water within a short span of time and its easy phase of separation. Recently, magnetic materials have been employed in the removal of organic and inorganic contaminants from water. Iron nanomaterials are suitable entrants in this direction and literature query suggests the ample potential and applications of iron nanomaterials as an adsorbent in conjugation with carbon based sorbents like Graphene, CNT, activated carbon etc. The synergistic interaction between carbon based sorbent and iron nanomaterials have crowned these composites as efficient adsorption platform. The synergistic combination of adsorption capacity of graphene and the magnetic responsiveness of iron nanoparticles bestows the composite with unique ability to separate the adsorbed dye from solution

Yao et al. have employed magnetic Fe_3O_4–graphene composite for adsorptive removal of Methylene Blue and Congo red (CR) from aqueous solution. The system exhibited admirable adsorption efficiency of 45.27 mgg^{-1} and 33.66 mgg^{-1} for MB and CR respectively [20]. A facile one-step solvothermal method for the synthesis of

graphene nanosheets (GNS)/magnetic (Fe_3O_4) composite was reported by Ai et al. wherein the prepared composite was employed for the removal of MB [21]. Their studies revealed that the kinetics and adsorption can be described by the pseudo-second-order kinetics and Langmuir isotherm model, respectively. Wang and coworkers employed magnetic sulfonic graphene nanocomposites as an adsorbent for batch adsorption of three cationic and three anionic dyes namely neutral red, safranin T, victoria blue, methyl orange, brilliant yellow, and alizarin red [22] . The as synthesized composite depicted excellent adsorption capacity towards cationic dyes as when compared to anionic dyes. A facile covalent binding methodology to prepare Fe_3O_4/SiO_2–GRO was reported by Yao et al. and they employed the aforesaid composite for adsorptive removal of MB dye [23]. The composite proved out to be an efficient adsorbent at higher temperatures. A one step solvothermal method to synthesise RGO-ferrite (MFe_2O_4, M ¼ Mn, Zn, Co, and Ni) hybrid was carried out by Bai et al [24]. Within a contact time of 2 minutes and dye concentration of 5 ppm, the hybrid could achieve 100 and 92 % removal efficiency for MB and RB respectively.

Moreover, the hybrid could also function as a photocatatlyst for the photocatalytic removal of the said dyes. In a similar report, Sun and coworkers could synthesize magnetic reduced graphene oxide nanocomposites and it was tested for its adsorption capacity towards dyes [25]. The composite portrayed admirable adsorption capacity towards RB and methyl green. Moreover the recyclability of the hybrid was also commendable. Xie et al. reported the application of super

paramagnetic GRO-Fe_3O_4 as a distinguished adsorbent for the removal of MB and neutral red (NR) [26]. The composite showed adsorption capacities of 167.2 and 171.3 mgg^{-1} for MB and NR respectively. The application of as-synthesised magnetic cyclodextrin-GRO as a superior adsorbent for MB was reported by Li et al. [27]. The composite displayed an adsorption capacity of 261.78 mgg^{-1} and the adsorption followed Langmuir isotherm model. The interplay of high surface GRO sheets, hydrophobicity of cyclodextrin and magnetic responsiveness of Fe_3O_4 in the composite are the key factors for the admirable adsorption efficiency of the composite.

(iii) Application of graphene and its hybrids as heavy metal sorbent

Industrialization has paved the route for the indiscriminate discharge of water lodged with heavy metals (Cr, Cd, Hg, Pb and As) that have detrimental effect on our ecosystem and human health. Heavy metals are toxicants that will reach the aquatic ecosystem from anthropogenic activities like mining, tanning, soldering etc. as well as from natural processes such as volcanic eruption, soil erosion etc. Several techniques have been adopted to remove these toxic heavy metals from aquatic bodies which include reverse osmosis, electro precipitation, adsorption, ion exchange etc. Adsorption occupies a special place among the aforesaid techniques as the current era demands quick, robust and efficient methods with admirable recyclability for the sorbent [28]. Though activated carbon is a widely acclaimed sorbent for heavy metal sorption, it failed to show its capacity at low concentration of heavy metals. As mentioned earlier,

Graphene has emerged as a superior sorbent for heavy metal removal on account of its unique surface features. Incorporation of magnetic nanomaterials onto graphene sheets enhances its performance as an adsorbent to a very large extent. Iron nanomaterials are suitable candidates in this direction as they impart magnetism onto the composite as well as serve as an effective media to remove heavy metals from aqueous system. Graphene sheets provide physical support to stabilize Iron nanomaterials preventing its oxidation. Immobilization of magnetic nanoparticles on graphene offer rapid and efficient separation of heavy metals from aqueous solution. The mechanism of metal ion adsorption on graphene surface can be related to electrostatic interactions and sorption between metal ions and oxygen functional groups. In addition to electrostatic interaction, the attraction between the delocalised π clouds in the sp^2 network of graphene will function as Lewis base that can donate electrons to metal atoms (Lewis acid). A good quantum of research has been devoted to the applications of graphene and its hybrids for the adsorptive removal of heavy metal [29].

Wu et al. have synthesied cetyl-trimethyl ammonium bromide (CTAB)-modified graphene for the adsorptive removal of Cr (VI) from aqueous solution. It was observed that the mutual interaction of CTAB with the oxygen functional groups on graphene surface has greatly enhanced the adsorption of Cr (VI). The adsorption data and kinetic data fitted well with Langmuir isotherm model and pseudo second order kinetics [30]. Thermodynamic study indicated that the adsorption process was exothermic and spontaneous in nature. As already stated, magnetic separation is of great implication for the adsorptive removal

of Cr (VI). Several reports throw light on the application of Graphene based magnetic sorbents for Chromium adsorptive removal. The integration of magnetic graphene nanocomposites with a core of double shelled nanoparticles composed of iron oxide and amorphous silica (crystalline iron core, iron oxide inner shell, and amorphous Si–S–O compound outer shell: graphene/Fe@Fe_2O_3@Si–SO) resulted in the formation of an excellent adsorbent as reported by Zhu and co workers [31]. The composite turned out to be an excellent sorbent for Cr (VI) with an adsorption capacity of 1.03 mgg^{-1} at an initial concentration of 1g L^{-1}. Bhunia et al. synthesized iron-iron oxide matrix dispersed RGO as an adsorbent for an array of metals including Cr(VI), As(III), Hg(III), Pb(II) [32] . The adsorption process Langmuir isotherm model and the sorbent displayed admirably high sorption capacity. To examine the adsorption of Cr (VI) from aqueous solution, Li and coworkers synthesized GRO-Polypyrrole composite using sacrificial template polymerization technique. The composite depicted an adsorption capacity of 9.56$mmolg^{-1}$ and the adsorption followed Langmuir model with pseudo-order kinetics [33].

(iv) *Application of graphene as oil sorbent*

Owing to the frequent occurrence of water pollution by oil spills in the past few decades, there is an ever growing demand to devise facile techniques for quick and selective removal of oils from water surface. Oil spill occurs accidently, during extraction, transportation and storage of oil. In 2010, a massive oil spill accident shocked the Gulf of Mexico, wherein an estimate of 4.9 million barrels

of oil spilled into the sea waters. This is believed to be the largest oil spill ever in the history of mankind which had grave impact on the marine eco system. Among the 322 species, 53 species became in the category of threatened and 29 nearly threatened. Similarly in 2014, around 3000 barrels of oil spilled into the waters of the Sunderbans which blackened the whole shoreline, killing large number of fishes, birds, dolphins and mammals.

Oil spill has more grievous impact on the sea than on the land as the spilled oil must be removed quickly to prevent the oil spread and diffusion by sea waves and wind. Oil spill can cause wide spread environmental hazards viz. permanent damage to wildlife and their habitats, threat to the existence of flora and fauna, chemical toxicity etc [34]. Oil in the industrial waste water also stands as a pollutant in the ecosystem, which also need to be resolved. To address this concern, currently three different mode of oil spill cleanup is adopted viz. (a) Chemical, (b) Mechanical and (c) biological methods. Chemical clean up includes employing chemical dispersants and solidifiers. Chemical dispersants assist in breaking oil slick into droplets, thus helps in easing the mix of oil and water, and consequently hastens the natural biodegradation [35]. Mechanical methods are primary line of defense against oil spills with the use of skimmers, booms, barriers, natural and synthetic sorbents. Bioremediation envisages the use of microorganism to degrade, alter or breakdown hydrocarbons of oil into smaller safe molecules. Adsorption is celebrated as one of the most successful approaches for oil spill remediation on account of their cost effectiveness, ease of fabrication, high selectivity, environmental benignity and recyclability. In this direction, substances with super

hydrophobic and super oleophilic nature are promising platforms as oil adsorbent due to its capacity of selective absorption of oils or organics from water. Carbon materials are considered as the supreme candidates for oil adsorption with super hydrophobic and super oleophilic surfaces due to their high oil uptake ability and environmental benignity. Graphene based materials have gained interest in oil spill clean up owing to the intrinsic hydrophobicity, high surface area and admirable mechanical and thermal stability. Spongy graphene prepared by Bi et al. could adsorb dodecane in the rate of 0.57 gg^{-1} and adsorption capacity of 20-86 times its own weight [36]. They reported that the presence of few hydrophilic groups increased the interaction of polar solvents with graphene sheets and consequently increased the adsorption capacity. Iqbal et al. employed thermally reduced graphene for adsorption of oils and organic solvents and it was observed that with the increase in C/O ratio, the adsorption capacity increases [37]. A green strategy for the reduction of graphene oxide using several phenolic acid was proposed by Wang et al. They demonstrated that the graphene could absorb oils with an absorption capacity of 115-1260 mgg^{-1} [38]. Graphene aerogels synthesied by several methods like solvent exchange, freeze drying, hydrothermal cross linking and polymerization, oil bath etc. have shown huge potential in the oil spills attributing to their ultra lightness, compressibility, porosity and surface area.

Graphene being inherently hydrophobic, can be coated on sponges, cotton and fabric by dip coating, hydrothermal and grafting polymerization and was employed as efficient oil sorbent. Ultra light density, cost effectiveness and high adsorption capacity make these

sorbents ideal oil adsorbents. However, these sorbents need to be modified to tune their wettability to super hydrophobic while maintaining their adsorption capacity. Gupta et al. reported melamine sponges coated with graphene which demonstrated super hydrophobic and super oleophilic properties depicting high adsorption capacity of 54-165 times its own weight [39]. Reduced Graphene oxide coated cotton demonstrating an adsorption capacity of 11-25 times its own weight was reported by Sun et al. [40]. The same group also prepared 3D super wetting graphene mesh film on stainless – steel girds. They observed that the water droplet took a spherical shape and did not slide even if the film was kept in vertical position. Due to these traits, these meshes can be used to separate oil from water.

In the present work, we have synthesied a novel hybrid based on Graphene-Iron oxide nanostructures and have exploited it as an adsorbent for Chromium (VI), Methylene Blue and Oil. The target heavy metal and dye employed for the study is Chromium (VI) and Methylene Blue (MB). For Oil spill removal studies, commercially available oils and organic solvents were chosen. This chapter is divided into two sections dealing individually with each of the contaminants. Graphene-Iron Oxide nanotube composite was employed as sorbent for removal of Cr (VI) and MB dye from aqueous solution. As our efforts to utilize Graphene-Iron Oxide nanocomposites as oil sorbent did not yield fruitful results, we incorporated Graphene-Iron Oxide nanocomposite onto Polyurethane foam and examined its applicability as sorbent for organic contaminants and oils.

Part A

Graphene-Iron oxide Nano tube Hybrid as sorbent for Chromium (VI) and Methylene Blue Dye

4.2 Introduction to Chromium (VI) and relevance of its removal

The top-most miscreant among the water pollutants are Heavy Metals. The term Heavy metal is generally coined for all those metals and metallic elements whose densities fall higher than 3.5gcm^{-3} and are toxic even at low thresh holds. Prominent candidates in this category include mercury (Hg), chromium (Cr), arsenic (As), cadmium (Cd), thallium (Tl), zinc (Zn), nickel (Ni), copper (Cu) and lead (Pb) [41]. Their adverse nature has been recognized due to their non biodegradability and accumulation in the biotic system. Both natural and anthropogenic sources contribute to heavy metal pollution and every metal is believed to possess specific physiochemical features that bestow to its unique toxicological effect, which is not fully known till date. Based on the extent of toxicity, arsenic, cadmium, chromium, lead, and mercury have been ranked as the top most five toxicants. All these elements are considered to be systematic toxicants, capable of inducing multiple organ failure, neural disorders, cancer etc.

Chromium is a naturally occurring element in the earth crust with valence states from I to VI. Trivalent Cr is the most stable and abundant form of Chromium, followed by Cr (VI). Both natural and man-made sources permit the entry of Cr into the environmental matrix. Metal processing industries, tannery, mining industries, stainless steel production, and chrome pigment production industry are

the major anthropogenic sources of Cr. The adverse hazards on exposure to Cr are greatly linked to its oxidation state ranging from less toxic Cr (II) to almost lethal Cr (VI). Hexavalent Cr is the most dominant state of Cr released by anthropogenic sources and is classified as a potential carcinogen by several regulatory agencies. Exposure to Cr levels over permissible limit causes grave damage to various organs namely renal system, cardiovascular, gastrointestinal, hematological, hepatic, respiratory tract, nervous system and skin. Cr is considered to modify DNA transcription process leading to severe chromosomic aberrations [42].

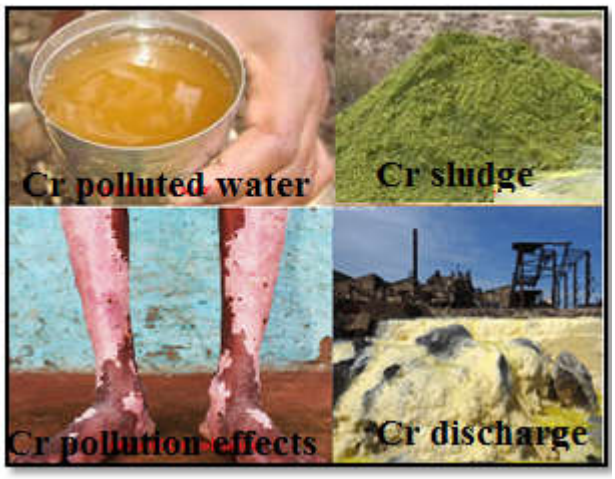

Figure 2. Chromium discharge and its adverse effects [Adapted from various sources from the internet, https://goo.gl/images/tawBJ3]

The bioaccumulation of Cr severely damages the ecological balance of the flora and fauna [Fig.2]. Over dosage of Cr in aquatic plants retards their growth and affects the photosynthesis. Even animals are not safe from the toxic hands of Cr as they develop ulcers,

anemia, and infertility on Cr intake. Cr poisoning in fishes alters their reproductive cycle and may also lead to mutations. As mentioned earlier, oxidation state and solubility play a central role in the governing the toxicity of Cr compounds. Cr (VI) compounds are more toxic, corrosive and irritating than Cr (III), on account its strong oxidizing capacity. This variation in toxicity can be related to the ease of penetration of Cr (VI) into our skin and its consequent reduction to intermediates. As Cr (III) is poorly adsorbed by human skin, the toxicity of Cr generally refers to that rooted on Cr (VI). Under physiological conditions, Cr (VI) can easily enter cells and can be easily reduced to form reactive intermediates like Cr (IV), Cr (V) radicals and ultimately Cr (III). All the aforesaid intermediates can attack cellular DNA and can destroy cells easily leading to fatal diseases. Cr (VI) acts as a sensitizer and irritant to skin. Moreover, occupational and environmental exposure to Cr will lead to Allergic Contact Dermatitis (ACD) in skin [43]. If Cr containing air is inhaled, it can deposit on respiratory tract leading to lung cancer. Owing to the toxicity concerns, the Environmental Protection Agency (EPA) has set 100 μg/L as the permissible amount of Cr in drinking water [44]. Conventional techniques like cyanide treatment, precipitation, reverse osmosis, ion exchange etc. have been adopted for Cr removal before discharge. Toxic intermediate formation, sludge formation, high operational cost, limited operating pH range stands as a hurdle for the widespread application of the aforementioned technologies. Summing up the adverse effects of Cr, removal of this heavy metal stands as the

need of the hour. Consequently, adsorption stands out as a feasible and alternative methodology for removal of Cr ions.

4.3 Introduction to Methylene Blue and relevance of its removal

"Everything goes fine with colour". From times immemorial, mankind has employed the art of colouring to enhance the beauty and quality of any substance. Colour is the central attraction to any commercial product and without colour it fails to appeal us. Dyes are natural and synthetic colourants that exhibits high fondness to the surface on which it is applied and renders the surface coloured. The discovery of synthetic dyes by William. J. Perkins in 1856 has revolutionsed textile industry as synthetic dyes offered fast, bright and brilliant colours. Methylene Blue, Rhodamine, Acridine orange, crystal violet etc are the common dyes widely used in textile industry. Synthetic dyes exert toxic effects on all forms of life [45]. Dyeing industry is one of the most chemically intensive industries contributing 20% of industrial pollution. Dyes impart undesirable colour to water bodies, obstructing sunlight and hence retarding photosynthesis and affecting aquatic environment. Most of the dyes have aromatic ring structure in their framework imparting non biodegradability and fatal toxicity. In addition to this, degradation of dyes can yield several free radicals which are more lethal than the parent dyes.

Methylene Blue (MB) is a cationic, thiazine dye crowning an invincible position for its application in textile and paper industry. MB, discovered by Caro in 1878, is a stable heterocyclic aromatic compound with chemical formula $C_{16}H_{18}N_3SCl$ and is characterised by

a strong absorption at 660 nm. It appears as a dark green odourless solid and yields a blue solution when dissolved in water. MB finds application as photo sensitizer in solar cells, as an antiseptic and as a surface modifier of semiconductor colloids [46]. In spite of its widespread application, MB has far reaching adverse effects on human health as well as on ecosystem. On account of its chemical inertness and high solubility in water, efficient removal of MB from aqueous system continues to be a tedious task [Fig.3]. Accumulation of MB will lead to grave disorders like hypertension, dizziness, fever, headache and mental confusion, skin irritations, nausea, abdominal pain and anemia. Taking all these facts into account, prompt and efficient removal of MB continues to be a challenging task to researchers.

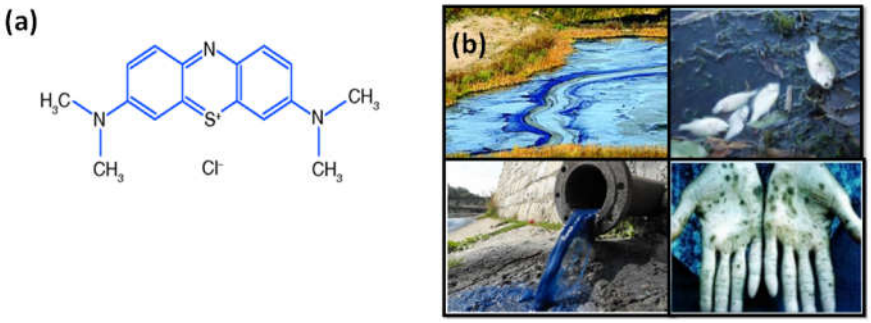

Figure 3. (a) Structure of Methylene blue dye: (b) Discharge of Methylene Blue into water bodies and its consequences *[Photographs obtained from the internet, https://www.slideshare.net/Vsonu/water-pollution-effects-1-1]*.

4.4 Results and Discussion

Details regarding the adopted experimental procedure are dealt in Chapter 2.

4.4.1 Characterisation of the prepared composite

The prepared graphene-iron oxide nanohybrid was adequately characterized through the following characterization techniques.

(a) X-Ray Diffraction analysis

As explained in Chapter 3, the XRD pattern of Graphite oxide exhibits an unique peak centered at 2θ value 10.37°, which corresponds to the reflection from (001) plane of the material [47, 48] . Fig. 4b shows the XRD pattern of graphene iron oxide composite. The sharp peak of Graphite oxide disappears on reduction, which clearly indicates the formation of graphene. The peak at 28.4° corresponds to the turbostratic arrangement of RGO stacked sheets [49, 50]. This peak indicates the successful incorporation of graphene back bone. Other characteristic peaks appeared at 32.89°, 38.7°, 47.53°, 56.31°,59.1° and 62.49° can be indexed to the reflections from (220), (311), (422), (440) and (511) planes of cubic phase of γ-Fe_2O_3 respectively [51]. [JCPDS 89-3854].

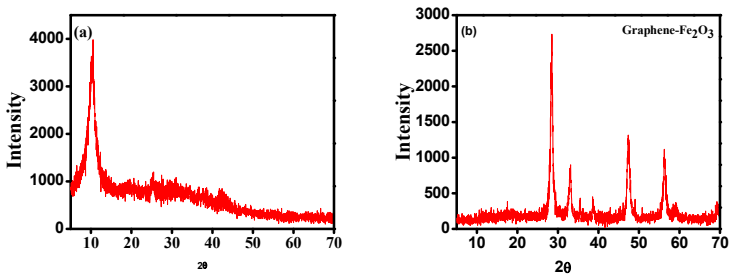

Figure 4. XRD pattern of Graphite Oxide (a) XRD Pattern of Graphene-Fe_2O_3 (b)

(b) Fourier Transform Infrared Analysis (FTIR)

Fig.5 displays the IR spectra of graphene – iron oxide nano composite. Addition of Hydrazine Hydrate leads to the reduction of functional groups on GRO as evident by comparing the FTIR spectra of GRO presented in Chapter 3. The band near 1730 cm^{-1} is indicative of the - C=O group in carbonyl and carboxyl moieties. The skeletal vibrations of unoxidised graphitic domains are characterized by the peaks around 1630 cm^{-1} and the peak at 1060 cm^{-1} is attributed to the stretching vibration of C-OH vibration of epoxy group [52]. The stretching vibration frequency of C-O moiety in the epoxy functional group has disappeared. However stringent the experimental conditions may be, it is not possible to reduce all the functional groups on graphene which makes the material as reduced graphene oxide. The skeletal structure of graphene is considerably modified on incorporating Iron oxide as is shown in the IR spectra. The peak centred at 470 cm^{-1}accounts for the Fe-O stretching vibration in the composite system.

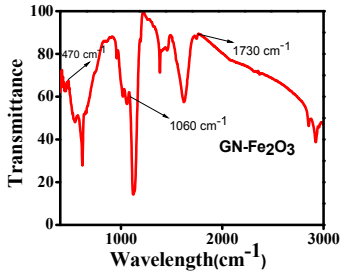

Figure 5. IR spectra of Graphene –Iron Oxide nano composite (GN-Fe_2O_3).

(c) Electron Microscopy Analysis (Scanning Electron Microscopy & Transmission Electron Microscopy)

Fig. 6a shows the SEM image of Graphene iron oxide nano composite. The change in morphology indicating the formation of 1D iron oxide structures in the composite is evident from the SEM image [53]. The exact morphology of the synthesized hybrids was clear from the TEM image [Fig. 6b], which is in agreement with the data derived from SEM analysis. Voile like Graphene nanosheets covering Fe_2O_3 nanotubes can be clearly seen from the SEM images. The TEM image illustrates that GN sheets are well decorated with nanotubes of average diameter 15 nm and length in the range of 135 -150 nm. TEM image in the inset of Fig.6b clearly shows the hollow structure of the iron oxide nanotube incorporated on graphene sheets. It is noteworthy that till date no reports exist on Graphene iron oxide nanotube formation via a template free route.

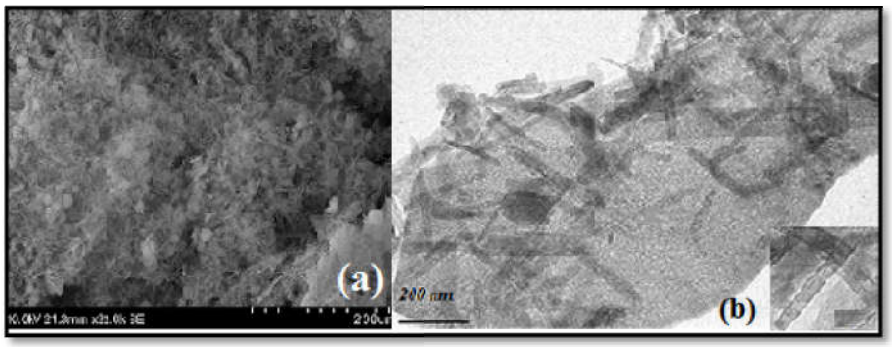

Figure 6. (a) SEM image of Graphene –Fe_2O_3 nanohybrid (b) TEM image of Graphene –Fe_2O_3 nanohybrid. Inset: Fe_2O_3 nanotube.

(d) VSM analysis

The magnetic property of the prepared hybrid was measured using Vibrating Sample Magnetometer (VSM). Magnetic hysteresis loop of the composite is an S-like curve [Fig. 7] and the saturation magnetisation of is 11.2 emu/g which is sufficient for magnetic separation as supported by the literature report. The magnetic intensity of the hybrid was lower than that of bulk iron oxide due to the presence of GN as well as due to the small size of incorporated iron oxide nanostructures [54, 55]. This observed decrease in saturation magnetization reflects the standard practice of normalizing the magnetization by magnetic constituent's mass [55]. Thus, the contribution of the nonmagnetic GRO layer to the total magnetization may be responsible for the decrease in the saturation magnetization .The magnetic coercivity or remnant was nearly zero indicating no remaining magnetization upon removal of the external magnetic field. Therefore, super-paramagnetic behaviour of the composite was established.

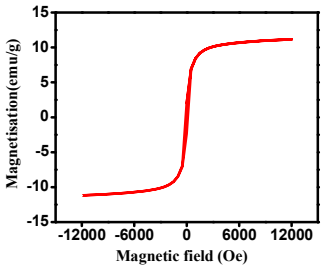

Figure 7. Magnetisation curve of Graphene-Fe_2O_3 composite.

(e)Evolution of iron oxide nanotubes

As template free synthesis of 1D hollow nanostructure is practically nil, our interest was directed to the factors that lead to the evolution of tube morphology of iron oxide. We propose a Kirkendall type mechanism for the formation of iron oxide nanotubes. Kirkendall effect is a classical phenomenon in metallurgy. It refers to vacancy diffusion along a bimetallic interface so as to compensate for the unequal matter flow which arises due to the difference in diffusion rate of the constituent atoms [56]. Kirkendall effect is a well established route to direct nanotube formation ever since the synthesis of hollow Cobalt oxide and Cobalt sulphide nanoparticles by Alivisatos et al. in 2004 [57]. The pore formation during the growth of metal oxide films is due to the fast outward diffusion of cations through the oxide layer accompanying by an inward flow of vacancies to the vicinity of the metal–oxide interface. The void formation accompanying Kirkendall diffusion will coalesce into a single hollow nano core leading to the fabrication of hollow nanotube. Zeng et al. have synthesised Copper

oxide nanotube from direct metal oxidation due to the preferential movement of copper ions to the surface [58]. You et al. have reported the fabrication of Cerium oxide nanotube based on a solid-liquid interface reaction between Ce $(OH)CO_3$ nanorods and NaOH solution. Accordingly $Ce(OH)CO_3$ acted as a reactant and template for assisting the nanotube formation. The diffusion of Ce^{3+} from the interior complemented by the opposite flow of vacancies has directed the formation of nanotubes [59]. Other reports include $Cu(OH)_2$nanorods via ascorbic acid assisted route involving diffusion of Cu^{2+} ions, [60] formation of porous Iron oxide nano structure using Zinc oxide nanostructure as sacrificial template. All these methods for fabrication of nanotubes demand surfactants, protracted reaction condition, multi step reaction etc. However, herein our procedure we could synthesise hollow iron oxide nanotube through a facile, template free and cheaper route at ambient reaction conditions. We could clearly monitor the synthesis of template free iron oxide nanotube achieved via a modified Kirkendall route.

In order to get a clear understanding of the growth mechanism, we have conducted the time dependent experiment for the hydrothermal synthesis of iron oxide nanotubes without adding graphene. The transition in morphology and the composition of the synthesized sample were well monitored and characterized using XRD and TEM. The TEM images were recorded after every 2 hours from the start of the reaction. Within two hours after the start of the reaction, short nano rods are formed in the reaction mixture, as is evident from the TEM image [Fig. 9a]. The corresponding XRD pattern confirmed

the sole formation of FeOOH nano rods at 2 hrs [Fig. 8 a]. Prominent characteristic peaks at 31.58, 34.56, 36.42, 48.0, 56.9, 52, 62.92, 68.14, 68.88, and 77.09 degrees correspond to reflections from (130), (021), (111), (131), (041), (211), (221), (002), (002), and (112) planes [JCPDS 81-0464]. The formation of FeOOH entity can be described as follows [61]. The acetate ion in the reaction mixture hydrolyses to form hydroxyl anion (OH^-) and this in turn interacts with Fe^{2+} and oxygen (O_2) according to the following reaction:

$$CH_3COO^- + H_2O \longrightarrow CH_3COOH + OH^-$$

$$Fe^{2++} OH^- + O_2 \longrightarrow 4FeOOH + 2H_2O$$

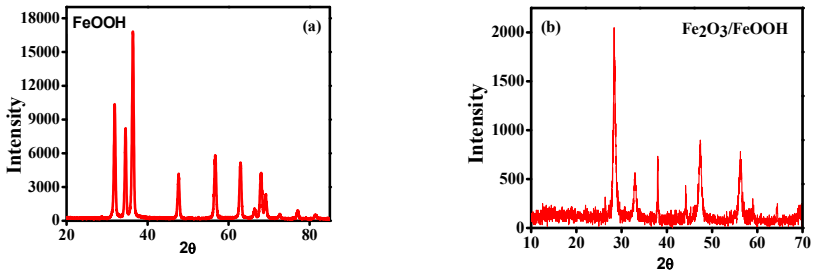

Figure 8. XRD pattern taken after 2hr from the start of the reaction and (b) XRD pattern taken after 4 hours. The data confirms the presence of both Fe_2O_3 and FeOOH.

As time elapses i.e. after 4 hours, empty spaces have commenced to form inside the rod structure [Fig. 9b]. The sharp contrast between the interior of nanorod with the surface in the TEM image [Fig.9c] indicates formation of a new layer on the surface of FeOOH initially formed, as time progresses further which is more vivid in Fig.9d. The XRD pattern at this stage indicated the presence of

both FeOOH and Fe_2O_3.The formation of hollow structure can be inferred from the high contrast between the dark edges and the pale interiors [Fig.9e & 9f]. The XRD data of final product confirms the presence of Fe_2O_3 only. The conversion of FeOOH to Fe_2O_3 in nearly neutral pH was reported by Robins et al [62].

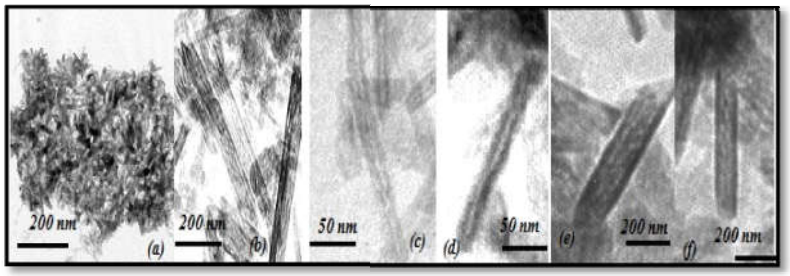

Figure 9. TEM images depicting the time dependant evolution of iron oxide nanotube.

(f) The Kirkendall effect in Reaction pathway

A survey through the literature hinted to a mechanism suggested by Kirkendall in 1942. The super saturation of lattice vacancies due to different diffusivities of atoms in a diffusion couple is the core of Kirkendall effect. Atomic jumps will be enhanced on diffusion of substitutional lattice atoms. Subsequently condensation of these super saturated vacancies will lead to the formation of void spaces called "Kirkendall voids" near to the interface and also within the fast diffusion side creating hollow structure [63, 64]. Though the formation of mixed oxides through the Kirkendall route has been suggested for several mixed oxides, the effect is rarely reported for single oxide systems. We suggest a modified Kirkendall type mechanism for the formation of hollow Iron oxide nanotube and subsequent incorporation on Graphene sheets. The Fe^{2+} ions in FeOOH

initially formed starts diffusing from the interior of nanorod and reaches the surface, where it is oxidized to Fe_2O_3. Under an oxidizing condition, Fe_2O_3 is the most stable form of iron oxide. We suggest the formation of a small layer of Fe_2O_3 on the surface of nanorods. This Fe_2O_3 layer separates the inner Fe^{2+} from the surrounding mixture [65, 66] thus preventing a direct chemical reaction. Similar Copper oxide layer formation was reported by Lee et al. Consequently outward diffusion of Fe^{2+} and inward diffusion of OH^- via vacancy exchanges occurs in a similar way as suggested in the formation of hollow nanospheres of Cobalt Sulphide by Ha et al. [67]. As the oxidation reaction increases, the outward diffusion of Fe^{2+} ions increases and an inward flow of fast moving vacancies to the vicinity of the oxide and FeOOH interface results. Thus pores are formed leading to the breakage of structures leading to hollow nano tubes. Thus a modified Kirkendall type counter diffusion of Fe^{2+} ions and voids during the conversion of FeOOH nanorods to Fe_2O_3 nanotubes is confirmed. The scheme for the proposed route is provided in Fig.10.

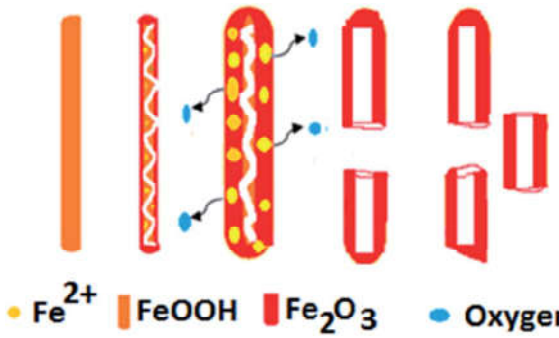

Figure 10. Pictorial representation of the modified Kirkendall mechanism for the formation of iron oxide nanotube.

4.4.2 The composite as Chromium (VI) and Methylene Blue (MB) adsorbent

Adsorption isotherm helps to understand the way in which the adsorbate are distributed between the liquid phase and solid phase when at equilibrium. Langmuir model and Freundlich model are widely employed for probing the nature of adsorption [68-69]. Isotherms indicate the nature of interaction between adsorbate and adsorbent. According to Langmuir model, monolayer adsorption occurs on homogeneous surface and the adsorbed molecules will not interact with each other. Freundlich model assumes heterogeneity of adsorption sites and the isotherm is based on an exponential distribution of adsorption sites.

$$\text{Langmuir equation} \quad \frac{C_e}{q_e} = \frac{1}{bq_m} + \frac{C_e}{q_m}$$

$$\text{Freundlich equation} \quad \ln q_e = \ln K_f + (1/n)\ln C_e$$

Where q_e is the amount adsorbed at equilibrium (mg g^{-1}), C_e is the equilibrium concentration of the Cr (mg/L), b is related to equilibrium constant (L /mg), q_m is the Langmuir monolayer adsorption capacity (mg /g), K_f roughly represents adsorption capacity and 1/n represents adsorption intensity.

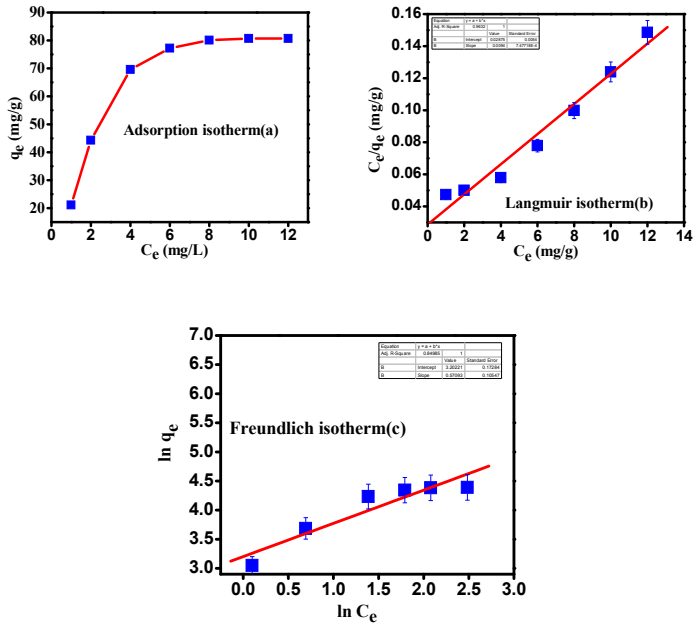

Figure 11. (a) Adsorption isotherm of Cr (VI) on the composite (b) Langmuir adsorption isotherm and (c) Freundlich isotherm. **[**Reaction conditions: Temperature: 27^0C, pH: 7.2, Concentration: 80 mg of adsorbent in 60 ppm chromium solution]

The adsorption data for Cr (VI) and Methylene Blue removal were fitted into the above mentioned adsorption isotherms. For Cr (VI), the regression coefficient [R^2] value as calculated from Langmuir isotherm is 0.9845 while that of Freundlich isotherm is 0.9382. The higher value of regression coefficient R^2 from Langmuir isotherm suggests that the Langmuir adsorption isotherm fits better than Freundlich isotherm [Fig.11 b & c]. In agreement with the Langmuir isotherm model, assuming monolayer coverage, the amount adsorbed increases with the concentration of the solution and the amount adsorbed attained a limiting value at higher concentration of the Cr (VI) solution [70-71]. The limiting amount of adsorption at equilibrium

for the prepared composite was found to be 80.7 mg/g. which is commendable when compared to earlier studies conducted at similar experimental conditions [Fig.11a]. Comparing the maximum limiting amount adsorbed (q_{max}) value of Cr (VI) on other sorbents like RGO-Montmorillinite nanocomposites (12.86 mg/g), Graphene oxide functionalised with Chitosan and cyclodextrin (67.66 mg/g), surface modified sand (6.24 mg/g), PEI modified activated carbon (20.05mg/g), and our composite could achieve a much commendable limiting amount of adsorption [72-74].

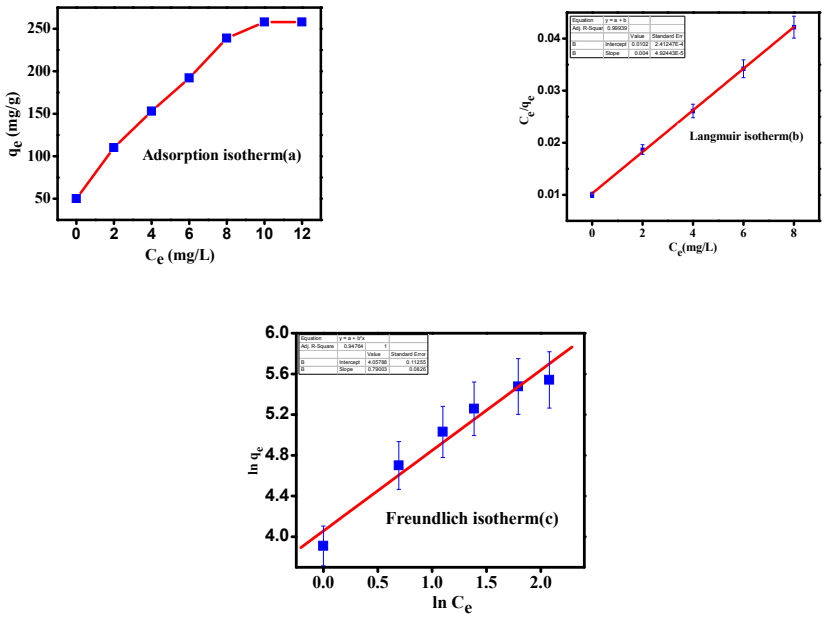

Figure 12. (a) Adsorption isotherm of MB on the composite [MB dye concentration 25-100mg/l]: (b) Langmuir adsorption isotherm and (c) Freundlich isotherm. **[**Reaction conditions: Temperature: 27^0C, pH: 6.6±0.3, Concentration: 80 mg of adsorbent in MB solution]

The adsorption data were applied to both of the aforementioned isotherms for MB removal also [Fig.12a]. The regression coefficient [R^2] value as calculated from Langmuir isotherm is 0.9996 while that of Freundlich isotherm is 0.9994. The higher value of regression coefficient R^2 from Langmuir isotherm suggests that the Langmuir adsorption isotherm fits better than Freundlich isotherm [Fig.12b & 12c]. In agreement with the Langmuir isotherm model of assuming monolayer coverage, the amount adsorbed increases with the concentration of the solution and the amount adsorbed attained a limiting value at higher concentration of the dye solution. The corresponding maximum adsorbed amount was 250 mg/g which was much higher compared to earlier reports highlighting the merit of the prepared composite [75].

(a) Mechanism of adsorption

Generally, the adsorption capacity of GN-Fe_2O_3 depends on the nature of adsorption sites viz. surface oxygenated groups, defects, porous nature etc. Pollutants could be adsorbed on the composite surface through various interaction (i) electrostatic interaction and coordination with the lone pair of electrons on the oxygen functional groups (ii) π-π stacking interaction (iii) adsorption by the dopants or nanomaterials incorporated on GN sheets and (iv) binding of heavy metals with the π cloud on the graphene basal plane (Lewis base) to form the electron donor−acceptor complexes. High surface area of GN sheets greatly enhances the adsorption capacity. Incorporation of porous materials further adds to the adsorption efficiency.

Electrostatic attraction between the positively charged amino groups and negatively charged oxygen containing (-OH,-COOH)

surface groups and the π-π interaction between the π cloud of dye molecule, lone pair of electrons and the aromatic cloud of GN plays a decisive role for the adsorptive removal of MB. The possible mode of interaction between GN and MB dye is depicted in Fig.13. In addition to this, Fan et al., Sohn et al., and Bandara et al. proposed several possible decolurisation reaction mechanisms [76-78]. According to them the reaction between iron oxide and H_2O or H^+ can generate atomic [H] which can affect the chromophore group of the dyes. Moreover, the porous structure of the incorporated Fe_2O_3 nano tubes further adds to the adsorptive removal. The high-performance of the absorbent may be attributed to the large specific surface area of graphene nano sheets, which could provide excellent conditions for adsorption to occur. Moreover, MB has aromatic structure and the adsorption capacity will be greatly enhanced due to the π-π stacking between dyes and π-conjugation regions of the graphene sheets. Graphene is characterized by the presence of several oxygen containing functional groups which render negative charge to graphene due to ionization of functional groups at the studied pH.

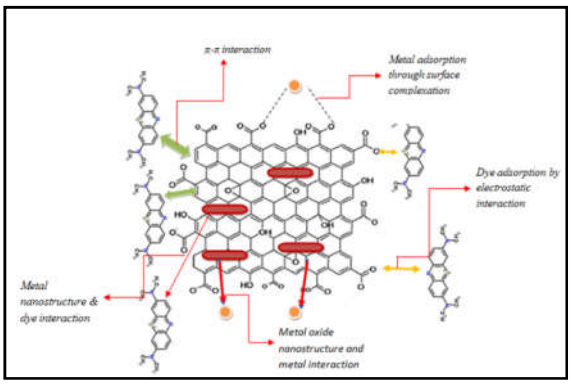

Figure 13. Possible modes of interaction of Graphene sheets with Cr (VI) and MB dye.

Chromium in solution exists as chromate (CrO_4^{2-}), dichromate ($Cr_2O_7^{2-}$) and hydrogen chromate ($HCrO^{4-}$) according to the pH of the solution and the total chromium amount. The oxygen functional groups in the GN hybrid, like,-OH –COOH etc act as electron donors in 'Cr' solution and will help the reduction of Cr (VI) oxy anion to Cr (III) ions. Electron rich acidic groups present in hybrid surface acts as Lewis bases at lower pH values and attracts the Cr^{3+} ion thus generated leading to increased adsorption. In addition to this, at higher pH, the electrostatic interaction between the electron rich oxygen functional group on the GN sheets and the electron deficient heavy metal ion have a vital role. The oxygen functional groups will donate the lone pair of delocalized π electrons to the chromium ion, forming a surface oxide compound [79], Cr (OH)] $^{2+}$ - A^-], ('**A**' is the acidic groups like carboxyl, hydroxyl etc. present on the hybrid surface). This complex formed will be attracted to the oxygen functional groups on GN and will lead to the enhanced removal of Chromium ions from solution [80]. The π electron cloud of GN sheets will act as Lewis base to form electron donor-acceptor complex with metal ions [81-82].

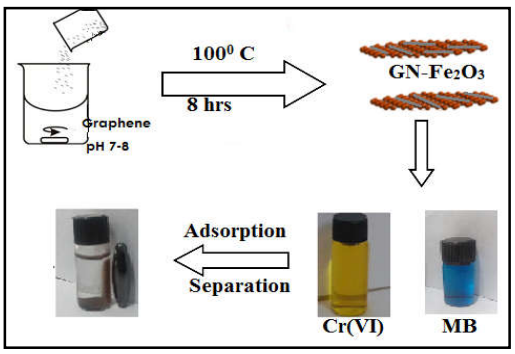

Scheme 1: Schematic representation of adsorptive removal of Cr (VI) and MB dye.

(b) Effect of pH

As mentioned earlier, Cr ion exists as chromate (CrO_4^{2-}), dichromate ($Cr_2O_7^{2-}$) and hydrogen chromate ($HCrO^{4-}$) according to the pH of the solution and total chromium amount. Normally, $HCrO^{4-}$ dominates in solution at a pH lower than 6.8, while above 6.8, Cr exists as CrO_4^{2-}. Oxygen functional groups in the GN hybrid like,-OH –COOH etc act as electron donors in 'Cr' solution and will help the reduction of Cr (VI) oxy anion to Cr (III) ions as per the equation: $HCrO_4^- + 7H^+ + 3e^- \leftrightarrow Cr^{3+} + 4H_2O$

In the alkaline pH, the electrostatic interaction between the electron rich oxygen functional group on the GN sheets and the electron deficient heavy metal ion have a vital role, the oxygen functional groups will donate the lone pair of delocalized π electrons to the chromium ion, forming a surface oxide compound [83] . Hence at alkaline pH, the Chromium ion exists mostly as $[Cr(OH)]^{2+}$ species. At higher pH, $[Cr(OH)]^{2+}$ ••••••A^-) complex formed will be attracted to the oxygen functional groups and will lead to enhanced removal of Chromium ions from the solution This can be illustrated by the following reaction:

$Cr^{3+} + H_2O + HA \leftrightarrow$ ($[Cr(OH)]^{2+}$ ••••••A^-) + $2H^+$,

('A' is the acidic groups like carboxyl, hydroxyl etc. present on the hybrid surface).Electron rich acidic groups present in hybrid surface acts as lewis bases at lower pH values and attracts the Cr^{3+} ion thus generated leading to increased adsorption [84] [Fig.14].

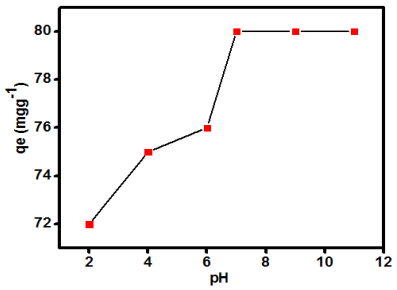

Figure 14. Effect of pH in the adsorptive removal of Chromium (VI)

The varied extent of adsorption of MB dye was probed by changing pH of the initial solution. pH has a decisive role in influencing the electrostatic interaction between the negatively charged Graphene and the cationic MB dye. pH range from 2-11 was examined in the present study. The low value of adsorption at low pH can be attributed to the competition between dye molecules and protons for available adsorption sites. It can be seen from the figure that as pH increases the electrostatic interaction increases, culminating in high adsorption [Fig.15].

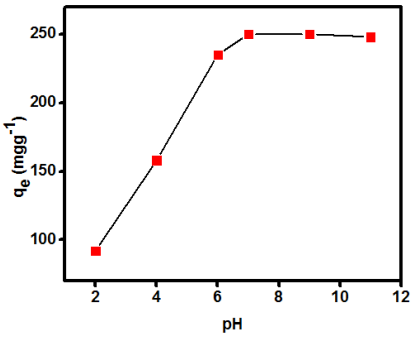

Figure 15. Effect of pH in the adsorptive removal of Methylene blue dye.

(c) Desorption Studies

Desorption of the adsorbate is one of the important property of an adsorbent which underlines the versatility and commercial significance of the adsorbent. The prepared hybrid was employed for examining the reusability studies. Reusability test was carried out using Conc.HCl as the eluent. This may be due to the decrease in the electrostatic interaction between the adsorbent and adsorbate when in acidic solution [85]. Fig.16 illustrates the reusability cycles of the prepared composite. It is evident that the adsorption capacity decreased after each cycle. Markedly, there was only a nominal decrease in adsorption capacity even after six successive cycles which adds to the merit of the prepared hybrid over other similar systems reported earlier.

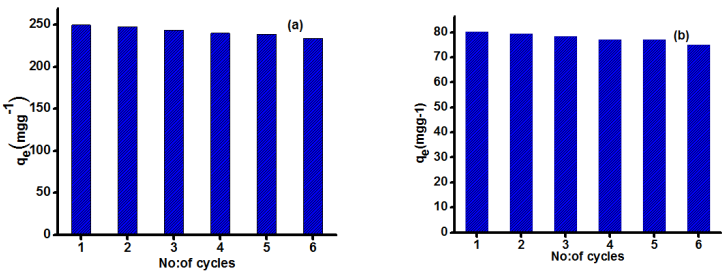

Figure 16. Adsorption capacity of Methylene Blue and Chromium (VI) on the adsorbent in six successive cycles.

4.5 Concluding Remarks

- Summarizing, we demonstrate the first ever nano-manipulation of hollow iron oxide nanotube by a modified Kirkendall effect and its subsequent incorporation on graphene sheets.

- We have adopted a facile template free hydrothermal approach for the synthesis of graphene–iron oxide nanotube composite. Iron oxide prevents the aggregation of graphene sheets thereby maximizing the surface area of graphene sheets.

- The physical characterization techniques adopted confirms the formation of hollow iron oxide nanotubes of length 75–100 nm and diameter 10–15 nm well dispersed on graphene sheets.

- Time dependant TEM studies and XRD data point to a mechanism akin to Kirkendall type, for the formation of hollow iron oxide nanotube.

- This involves counter diffusion of Fe^{2+} ions and voids along the metal–oxide interface.

- The composite being super paramagnetic in nature, it can be easily manipulated in an external magnetic field for the adsorptive removal of toxic Cr(VI) and MB dye and subsequent magnetic separation, which was achieved within few minutes.

- The maximum adsorption capacity (q_{max}) calculated from the Langmuir isotherm plot was 106.38 mg g^{-1} and 250.3g mgg^{-1} for Cr (VI) and MB dye respectively, which is very much appreciable in magnitude when compared to previous reports.

- The composite provided a better fit to the Langmuir isotherm model. The synergistic effect between graphene and the hollow

iron oxide nanotube plays the key role in the adsorptive removal of the toxic heavy metal Cr (VI) and MB dye.

- We also believe that our novel composite can be a representative candidate for various applications as catalyst, adsorbent, electrode etc.

4.6 References

[1] F. Fu and Q. Wang, *J. Environ. Manage*, 2011, 92, 407.

[2] J. Xu, S. T. Yang and J. Lao, *Rev. Inorg. Chem*., 2013, 33, 139.

[3] S. K. Y. Some, E. Hwang, H. Yoo and H. Lee, *Chem.Commun.* 2012, 48, 7732.

[4] K. Wang, J. Ruan, H. Song, J. Zhang, Y. Wo, S. Guo and D. Cui, *Nanoscale Res. Lett.*, 2011, 6, 8.

[5] Z.-H. Huang, X. Zheng, W. Lv, M. Wang, Q.-H. Yang and F. Kang, *Langmuir*, 2011, 27, 7558.

[6] J. Zhao, Z. Wang, J. C. White and B. Xing, *Environ. Sci.Technol.*, 2014, 48, 9995.

[7] H. Yan, X. Tao, Z. Yang, K. Li, H. Yang, A. Li and R. Cheng*, J. Hazard. Mater.*, 2014, 268, 191–198.

[8] L. Liu, C. Li, C. Bao, Q. Jia, P. Xiao, X. Liu and Q. Zhang, *Talanta*, 2012, 93, 350.

[9] T. Wu, X. Cai, S. Tan, H. Li, J. Liu and W. Yang, *Chem. Eng.J.*, 2011, 173, 144.

[10] G. Zhao, W. T. C. Chen and X. Wang, *RSC Adv.*, 2012, 2, 9286.

[11] T. S. Sreeprasad, S. M. Maliyekkal, K. P. Lisha and T. Pradeep, *J. Hazard. Mater.*, 2011, 18, 921.

[12] L. Ai, C. Zhang and Z. Chen, *J. Hazard. Mater.*, 2011, 192, 1515.

[13] Z. J. Li, F. Chen, L. Y. Yuan, Y. L. Liu, Y. L. Zhao, Z. F. Chai and W. Q. Shi, *Chem. Eng. J.*, 2012, 210, 539.

[14] G. K. Ramesha, A. V. Kumara, H. B. Muralidhara and S. Sampath, *J. Colloid Interface Sci.*, 2011, 361, 270.

[15] P. C. Ma, J. K. Kim and B. Z. Tang, *Carbon*, 2006, 44, 3232.

[16] J. N. Tiwari, K. Mahesh, N. H. Le, K. C. Kemp, R. Timilsina, R. N. Tiwari and K. S. Kim, *Carbon*, 2013, 56, 173.

[17] T.D. Nguyen-Phan, V. H. Pham, E. J. Kim, E.-S. Oh, S. H. Hur, J. S. Chung, B. Lee and E. W. Shin, *Appl. Surf.Sci.*, 2012, 258, 4551.

[18] J. T. T. Wang, B. Tang, X. Hou, L. Sun and X. Wang, *ACS Appl. Mater. Interfaces,* 2012, 4, 3084.

[19] Y. Chen, L. Chen, H. Bai and L. Li, *J. Mater. Chem. A*, 2013, 1, 1992.

[20] Y. Yao, S. Miao, S. Liu, L.-P. Ma, H. Sun and S. Wang, *Chem.Eng. J.*, 2012, 184, 332.

[21] L. Ai, C. Zhang and Z. Chen, *J. Hazard. Mater.*, 2011, 192, 1515.

[22] X.-J. Hu, Y. Liu, H. Wang, A. Chen, G. Zeng, S. Liu, Y. Guo, X. Hu, T. Li, Y. Wang, L. Zhou and S. Liu, *Sep. Purif.Technol.*, 2013, 108, 189.

[23] Y. Yao, S. Miao, S. Yu, L. P. Ma, H. Sun and S. Wang, *J.Colloid Interface Sci.*, 2012, 379, 20.

[24] S. Bai, Z. X. Shen, Y. Liu, G. Zhu, X. Xu and K. Chen, *Carbon*, 2012, 50, 2337.

[25] H. C. L. Sun and L. Lu, *Nano Res.*, 2011, 4, 550.

[26] G. Xie, P. Xi, F. Liu, L. Huang, Y. Shi, F. Hou, Z. Zeng,C. Shao and J. Wang, *J. Mater. Chem.*, 2012, 22, 1033.

[27] L. Li, L. Fan, H. Duan, X. Wang and C. Luo, *RSC Adv.*, 2014,4, 37114.

[28] M. Machida, T. Mochimaru and H. Tatsumoto, *Carbon*, 2006, 44, 2681–2688.

[29] G. Zhao, J. Li, X. Ren, C. Chen and X. Wang, *Environ. Sci.Technol*., 2011, 45, 10454.

[30] Y. Wu, H. Luo, H. Wang, C. Wang, J. Zhang and Z. Zhang, *J.Colloid Interface Sci.*, 2013, 394, 18.

[31] C. J. Madadrang, H. Y. Kim, G. Gao, N. Wang, J. Zhu, H. Fen,M. Gorrring, M. L. Kasner and S. Hou, *ACS Appl. Mater.Interfaces*, 2012, 4, 1186.

[32] P. Bhunia, G. Kim, C. Baik and H. Lee, *Chem. Commun.*,2012, 48, 9888.

[33] S. Li, X. Lu, Y. Xue, J. Lei, T. Zheng and C. Wang, *PLoS One,* 2012, 7, e43328.

[34] M. O. Adebajo, R. L. Frost, J. T. Kloprogge, O. Carmody and S. Kokot, *J. Porous Mater.*, 2003, 10, 159.

[35] H. Bi, X. Xie, K. Yin, Y. Zhou, S. Wan, L. He, F. Xu, F. Banhart, L. Sun and R. S. Ruoff, *Adv. Funct. Mater.*, 2012, 22, 4421.

[36] M. Iqbal and A. Abdala, *Environ. Sci. Pollut. Res.*, 2013, 20, 3271.

[37] H. Li, J. Wang, L. Yang and Y. Song, *Adv. Funct. Mater*., 2008, 18, 3258.

[38] R.Gupta and G. U. Kulkarni, *ChemSusChem*., 2011, 4, 737.

[39] X. Yi, S. Yu, W. Shi, S. Wang, N. Sun, L. Jin and C. Ma, *Desalination*, 2013, 319, 38.

[40] K. P. Nickens, S. R. Patierno and S. Ceryak, *Chem.-Biol.Interact.*, 2010, 188, 276.

[41] J. H. Duffus, *Pure Appl. Chem*., 2002, 74, 793.

[42] D.A. Benoit, *Water Res.* 1976, 10, 497.

[43] S. Marshal, Hazardous and Toxic Effects of Industrial Chemicals, *NDC Publication,* USA, 1979,137.

[44] T. Nandy, S.N. Kaul, P.P. Pathe and B. Malika, CEW XXV,1990, 2, 90.

[45] Teo Peik-See, Alagarsamy Pandikumar, Lim Hong Ngee, Huang Nay Ming and Chia Chin Hu, *Catal. Sci. Technol*., 2014, 4, 4396.

[46] J.L. Gong, B. Wang, G.M. Zeng, C.P. Yang, C.G. Niu, Q.Y. Niu, W.J. Zhou, and Y. Liang,, *J. Hazard. Mater,* 2009, 164, 1517.

[47] B. J. Li, H. Q. Cao, J. Shao, M. Z. Qu and J. H. Warner, *J. Mater. Chem*., 2011, 21, 5069.

[48] S. Dubin, S. Gilje, K. Wang, V. C. Tung, K. Cha, A. S. Hall, J. Farrar, R. Varshneya, Y. Yang and R. B. Kaner, *ACS Nano*, 2010, 4, 3845.

[49] L. J. Cote, R. Cruz-Silva and J. Huang, *J. Am. Chem. Soc*., 2009, 131, 11027.

[50] B. T. Hang, T. Doi, S. Okada and J. Yamaki, *J. Power Sources*, 2007, 174, 493.

[51] J. Guo, R. Wang, W. W. Tjiu, J. Pan and T. Liu, *J. Hazard. Mater*. 2012, 225, 63.

[52] J. Zhu, S. Wei, H. Gu, S. B. Rapole, Q. Wang, Z. Luo, N. Haldolaachige, D. P. Young and Z. Goo, *Environ.Sci. Technol.,* 2012, 46, 977.

[53] Jixin Zhu, Yogesh Kumar Sharma, Zhiyuan Zeng, Xiaojun Zhang, Madhavi Srinivasan, Subodh Mhaisalkar, Hua Zhang, Huey Hoon Hng, and Qingyu Yan, *J. Phys. Chem. C* 2011, 115, 8400.

[54] K. Turcheniuk, M. Khanal, A. Motorina, R. Boukherrouba and S. Szunerits, *RSC Adv*., 2014, 4, 865.

[55] K. S. Suslick, M. Fang and T. Hyeon, *J. Am. Chem*. Soc., 1996, 118, 11960.

[56] N. A. D. Burke, H. D. H. St€over and F. P. Dawson, *Chem. Mater*., 2002, 14, 4752.

[57] H. J. Fan, U. Gçsele and M. Zacharias, *Small,* 2007, 3, 1660.

[58] Y. Yin, R. M. Rioux, C. K. Erdonmez, S. Hughes,G. A. Somorjai and A. P. Alivisatos, *Science,* 2004, 304, 711.

[59] Y. Chang, M. L. Lye and H. C. Zeng, *Langmuir*, 2005, 21, 3746.

[60] G. Chen, S. Sun, X. Sun, W. Fan and T. You, *Inorg. Chem*., 2009, 48, 4.

[61] J. Xu, Y.-B. Tang, W. Zhang, C.-S. Lee, Z. Yang and S.-T. Lee, *Cryst. Growth Des.,* 2009, 9, 4525.

[62] B. Zhao, R. Liu, X. Cai, Z. Jiao, M. Wu, X. Ling, B. Lu and Y. Jiang, *J. Appl. Electrochem.,* 2014, 44, 53.

[63] R. G. Robins, *J. Inorg. Nucl. Chem*., 1967, 29, 431.

[64] H. L. Guo, X. F. Wang, Q. Y. Qian, F. B. Wang and X. H. Xia, *ACS Nano*, 2009, 3, 2653.

[65] L. Zhang, J. C. Yu, Z. Zheng and C. Wan Leung, *Chem. Commun.*, 2005, 21, 2683.

[66] J. C. Wren, G. A. Glowa and J. Merritt, *J. Nucl. Mater.,* 1999, 265, 161.

[67] C. Zhang, J. Zhu, X. Rui, J. Chen, D. Sim, W. Shi, H. H. Hang, T. M. Lim, Q. Yan, L. Zhang, J. C. Yu, Z. Zheng and C. W. Leung, *Cryst. Eng Comm.,* 2012, 14, 147.

[68] D.-H. Ha, L. M. Moreau, S. Honrao, R. G. Hennig and R. D. Robinson, *J. Phys. Chem. C*, 2013, 117, 14303.

[69] Langmuir, *J. Am. Chem. Soc*., 1918, 40, 1361.

[70] H.M.F. Freundlich, Z. *Phys. Chem.* 1906, 57, 385.

[71] G. K. Ramesha, A. Vijaya Kumara, H. B. Muralidhara and S. Sampath, *J. Colloid Interface Sci.,* 2011, 361, 270.

[72] S. M. Lee, W. G. Kim, C. Laldawngliana and D. Tiwari, *J. Chem. Eng. Data*, 2010, 55, 3089.

[73] Z. Ai, Y. Cheng, L. Zhang and J. Qiu, *Environ. Sci. Technol*., 2008, 42, 6955.

[74] G. S. Alvarez., *J. Mater. Chem*., 2011, 21, 6359.

[75] L. Fan, C. Luo, M. Sun and H. Qiu, *J. Mater. Chem*., 2012, 22, 24577.

[76] W.J. Weber and R.K. Chakravorti, *J. Am. Inst. Chem. Eng.*, 1974, 20 228.

[77] J. Fan, Y.H. Guo, J.J. Wang and M.H. Fan, *J. Hazard. Mater.,* 2009, 166, 904.

[78] K. Sohn, S.W. Kang, S. Ahn, M. Woo and S.K. Yang, *Environ. Sci. Technol*., 2006, 40, 5514.

[79] J. Bandara, J.A. Mielczarski and J. Kiwi, *Langmuir* 1999, 15 7670.

[80] W. T Tan, S. T. Ooi and C. K. Lee. *Environmental Technology*, 1993, 14, 277.

[81] S. Babel and T. A. Kurniawan. *Chemosphere*, 2004, 54, 951.

[82] Y. Nakano, K. Takeshita and T. Tsutsumi. *Water Res*earch, 2001, 35, 496.

[83] S. B.Lalvani, T. Wiltowski, A. Hubner, A. Weston and N. Mandich, *Carbon*, 1998, 36, 1219.

[84] Z. Reddad, C Gerenete, Y. Andres and P. Le Cloeiric, *Environmental* Technology, 2003, 24, 257.

[85] M. Chen, Y. Chen and G.W. Diao, *J. Chem. Eng. Data* 2010, 55, 5109.

[86] Juang R.S, Wu F.C and Tseng R.L, *Colloids Surf A*, 2002,201 191.

Part B

Graphene-Iron Oxide incorporated Polyurethane foam as Sorbent for Oils and Organics

4.7 Introduction

Oil spills refers to the large scale release of crude oil or oil distilled products into water bodies by oil tankers, oil drilling rigs, offshore oil platforms and oil wells. The spilled oil will prevent penetration of sunlight through water affecting the balance of marine ecosystem [1-3]. The spilled oil can easily enter into the plumage and feathers of birds, making them heavier, which ultimately obstructs their flight and finally to their death via hypothermia. New born animals and birds starve to death as their parents cannot recognize their natural scent. The fauna cannot regulate their body temperature and it chokes them to death. Oil and chemical spills threaten the very existence of all forms of life, ranging from algae to higher mammals in the marine ecosystem [Fig.1]. Oil spills burdens the ocean with toxicants that detoriates the marine food chain. Oil spill pollution can directly affect human beings, especially the on-site workers and they will suffer from skin irritations, ulcers and severe abdominal diseases. Moreover, the spilled oil must be removed quickly as with time the volatile constituents evaporates, leaving a highly viscous residue nicknamed as chocolate cake which is detrimental to aquatic system [4]. In these grounds, to cope up with these grievous environmental issues, efficient oil sorbent is a necessity.

An ideal oil adsorbent must possess high surface area, fair chemical stability and cost effectiveness in addition to synergistic hyrophobicity and oleophilicity. Sorbents like wool, straw, clay, saw dust, activated carbon etc. all have been employed as adsorbents from ancient times due to their microporosity. However, most of these sorbents are marked by low selectivity, low adsorption capacity and poor reusability which restrict their widespread application [5-8]. Apart from the afore said sorbents, commercially available 3D porous materials like Polyurethane sponges (PU) and Melamine sponges have emerged as desirable choices for oil adsorption due to their high surface area [9-10] . However, the presence of amino and carboxyl groups on its surfaces renders them hydrophilic which inhibits their selectivity and overall performance. These sponges must be tuned to exhibit hydrophobic nature in order to avail their maximum adsorption efficiency. To selectively adsorb oil from water, substances must possess oleophilic and hydrophobic nature. In this regard, inorganic nanowire membranes [11], carbon based materials like carbon nanotubes [12] and carbon fibers [13] have drawn considerable attention and have been extensively used as they selectively separate oil from water. However, these substances have practical limitations on account of their cost along with complex fabrication procedures. Currently, membranes that selectively separate oil and water have enthused interest among researchers. However, they are vulnerable to surface and internal fouling which deteriorates their performance in practical operations [14].

Figure 1. Pangs of oil pollution [Adapted from various sources in the internet,http://www.theblackvault.com/documentarchive/wpcontent/uploads/2015/02/Oil-Rig-Explosion-in-Gulf-of-Mexico-10.jpg]

On account of its hydrophobic and oleophilic nature, GN has emerged as a staple adsorbent in oil spills[15]. Several reports suggest the application of 3D graphene foams and graphene coated polymer foams as oil adsorbent. A few representative studies include reports by Singh et al. who fabricated GN sponges which displayed high adsorption efficacy for petroleum products and organic pollutants [16]; GN coated melamine sponges designed by Ngyuen et al. [17] and GN coated PU foams were reported by Gao et al. [18]

Though these entities portrayed fair adsorption efficacy, few issues need to be addressed and optimized for their widespread application. The major hurdle in their practical application is in the collection and reuse of substrates saturated with oil and pollutants. Imparting magnetism onto these adsorbents stands as a promising remedy to address this issue. Once these adsorbents are magnetically

actuated, they can be easily driven to the target zone (spill areas) and can be fleetly removed after adsorption. In addition to this, the recyclability of the adsorbent is greatly enhanced and the adsorbents can be scaled up for quick and selective decontamination of water bodies [19-22].

Keeping all these facts, we have attempted to fabricate a simple GN coated magnetic PU sponge that could serve as an excellent platform for oil/organic chemicals separation from aqueous environment. PU sponge characterized by its micrometer scale reticulate network is switched from hydrophilic to a super hydrophobic moiety and by the inclusion of GN sheets and super paramagnetic by the incorporation of mesoporous iron oxide. The as prepared sponge, referred to as GPUF portrayed impressive adsorption capacity towards oil and other organic liquids. It exhibits long time stability, outstanding hydrophobicity, elasticity and fair magnetic responsivity, all these assuring GPUF as an elite pick among other established sorbents.

4.8. Results and Discussion

4.8.1 Characterisation of the prepared hybrid

(i) X-ray Diffraction analysis

The XRD patterns of PU, GPU and GPUF are shown in Fig.2 (a).The PU foam displayed a characteristic diffraction peak at 19.3°, which can be ascribed to the presence of short range ordered structure, and both soft and hard domains of amorphous PU. The XRD pattern of GPU and GPUF obliviously displayed the peak assigned to PU,

indicating that the PU framework remained intact after modification [23]. Moreover, there is no characteristic peak of graphene oxide at 10° assuring the reduction of graphene oxide to graphene. The presence of Iron Oxide cannot be deciphered from the XRD pattern as it is uniformly dispersed in the highly amorphous PU 3D network.

(ii)Fourier Transform Infrared Analysis (FTIR)

FTIR spectra of PU, GPU and GPUF are shown in Fig.2 (b). For PU, the bands at 2322 cm^{-1} is due to the asymmetric stretching of NCO. The bands at 1734 cm^{-1}, 1639 cm^{-1} and 1153 cm^{-1} can be ascribed to the C=O stretching vibration in amide, urea and ether respectively. The broad band near 3400 cm^{-1} corresponds to the OH stretching vibration, while the band at 2918cm^{-1} can be related to the C-H stretching in $–CH_3$ and $-CH_2$ groups [18, 24]. FTIR spectra of GPU, GPUF and PU displayed similar characteristic bands between 1000 cm^{-1} and 1800 cm^{-1}.The characteristic bands of PU underwent a marginal shift or variation in intensity in GPU and GPUF which may be due to the interaction between the additives and PU. No new bands are formed in GPU and GPUF ruling out the formation of chemical bonds among the additives and PU. The band at 600 cm^{-1} corresponds to the Fe-O stretching vibration in Fe_3O_4.

(iii) Thermogravimetry Analysis

The thermo grams of PU, GPU and GPUF are displayed in Fig.2(C).The trio depicted similar TG curves and have a substantial weight loss in the range of 200 -350 ^{0}C.This notable drop in mass is

due to the combustion of carbon skeleton.TG curves point a slightly higher stability for GPUF which displayed a mass loss of 30 % near 600 ^{0}C due to the decomposition of Fe_3O_4.

(iv) Vibration Sample Magnetometer Analysis

The magnetic property of GN-Fe_3O_4 was measured at room temperature and the result is depicted in Fig.2 (d). The saturation magnetization is found to be 30.07 emu/g which is sufficient enough for magnetic removal of the sorbent after adsorption [25]. The hybrid exhibited super paramagnetic nature with low remnant magnetization and low coercivity at room temperature assuring that the GPUF can be manipulated in an external magnetic field as depicted in Fig .3.

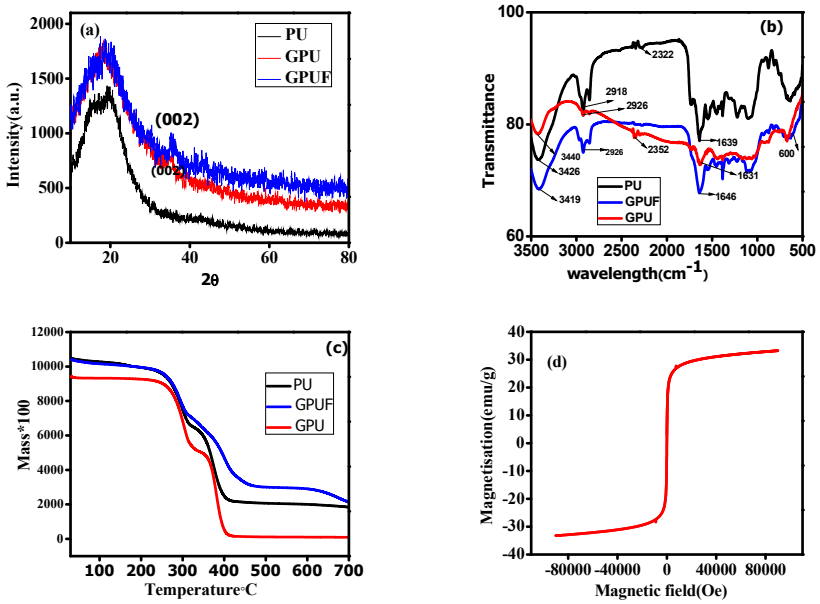

Figure 2. XRD patterns (a); FTIR spectra (b); TG curves of PU, GPU and GPUF(c); VSM analysis of Graphene-Iron Oxide composite (d).

Figure 3. Manipulation of GPUF by an external magnet.

(v)Super hydrophobicity

The water contact angle (CA) is employed to measure the wettability of surface that depends on solid-liquid, solid-vapour and liquid-vapour surface tensions. It can be expressed using the Young's equation:

$$\text{Cos } \theta = (\gamma_{SV} - \gamma_{SL})/\gamma_{LV}$$

Where θ is the contact angle and γ_{SV}, γ_{SL} and γ_{LV} are the interfacial tensions between solid and vapour, solid and liquid, and liquid and vapour, respectively. Based on the value of contact angle, surface properties can be classified as hydrophilic (θ is less than 90º), hydrophobic (θ is between 90º and 150º) and super hydrophobic (θ is greater than 150º).The wettability of any surface is dependent on the topography and chemical composition of the surface. Natural examples of hydrophobic materials include lotus leaf and Butterfly wings. Hydrophobic surfaces can be induced artificially by introducing roughness and low surface energy materials. There are two possible modes of wetting (i) the Wenzel state where the droplet can skip between the rough peaks and the drop is in complete contact with the surface leading to homogeneous wetting;(ii) the Cassie-Baxter state in

which the droplet can be suspended on the top of the asperities with the air trapped in between the asperities resulting in heterogeneous wetting.

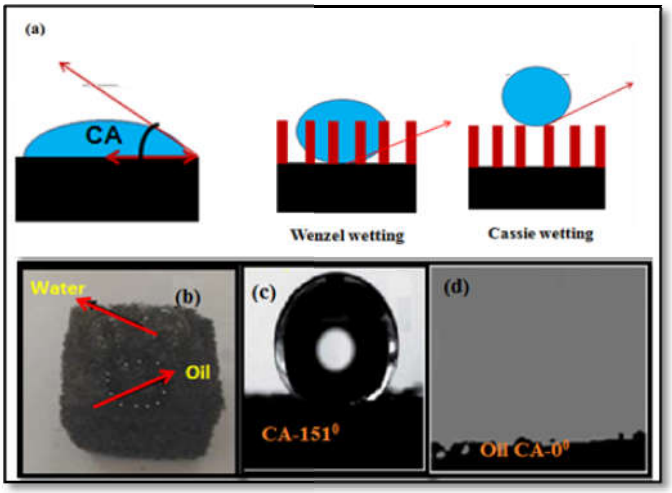

Figure 4. (a) Modes of wetting (b) Fig.3 (b) Digital images of water droplet and diesel oil droplet on GPUF: (c) Water contact angle of GPUF: (d) Oil contact angle of GPUF.

The digital images of water droplets on GPUF sponge portrays spherical shaped droplets hinting to the hydrophobic nature while oil droplet was instantaneously sucked into the GPUF depicting its oleophilic trait [Fig.4 (b)]. The super hydrophobicity and the super oleophilic feature of the as prepared GPUF were established using Contact angle measurements. The apparent contact angle of water and oil were 151° [Fig.4 (c)] and 0° [Fig.4 (d)]. The oil was instantaneously adsorbed into GPUF confirming its super oleophilic nature while it repelled water with high contact angle asserting its super hydrophobic nature. The selective absorption behavior arises from this super

hydrophobic and super oleophilic nature of the GPUF thus realizing its application in selective removal of oil and organic contaminants from water. The GPUF displayed super hydrophobic behavior in near neutral pH (6-8).Though the contact angle for water was decreased slightly the hydrophobic behavior (contact angle >120° i.e. hydrophobic nature) was still maintained in acidic and alkaline pH. This can be endorsed to the erosion of GN-Fe_3O_4 from the GPUF surface.

4.8.2 Adsorption capacity of GPUF and GPU in a variety of organic solvents

The above characterisation results suggest the super hydrophobicity and super oleophilicity of GPUF, which can render it as sorbent for oil and other organic solvents. The response of GPUF in organic contaminant / water separation and its adsorption capacity was evaluated in a wide range of organic chemicals and oils. It was observed that the GPUF sponge settled instantaneously in organic solvents (≤10s) and oil (≤30s). The adsorption capacity of GPUF and GPU varied from 90gg^{-1} to 316 gg^{-1} while that of GPU varied from 80 to 180gg^{-1}.The adsorption capacity followed the order: $CHCl_3$ >Diesel Oil> Lubricating oil> Bean Oil> Tetra HydroFuran> DimethylSulphoxide> Toluene> DimethylFormamide> Acetone [Fig.5a & 5b]. The swelling phenomenon was observed for a few solvents due to the diffusion of solvents onto GPUF. However, this did not alter the adsorption capacity of GPUF. The highest adsorption capacity was recorded for $CHCl_3$, which is highest among several

reported systems [18, 26, 27]. GPUF also have high adsorption capacity for oils which outshines the performance of many sorbents found in literature [28-30]. The absorption for organic liquids was so instantaneous that the equilibrium time could not be measured. Viscosity played a central role in determining the equilibrium time of oils as the rate of adsorption varied linearly with the viscosity of oils [Fig.5 (c)]. It is noteworthy that the sorption capacity does not follow a linear pattern with density as has been previously reported for other sorbents [18].

The adsorption capacity of GPUF was also assessed in the mixture i.e. oil/organic solvent: water. As and when a small piece of GPUF was forced onto $CHCl_3$, $CHCl_3$ was fleetly adsorbed [Fig.6 (a)]. In addition to this, GPUF instantaneously adsorbed diesel oil within 10 seconds, leaving completely clear water without any pollutant [Fig.5 (b)]. It was found that 80 mg of sorbent can readily remove 13 g of diesel oil of 0.5 cm thickness in 75 mL of DIW which is highly imperative. The adsorbed oil can be completely recovered by simply squeezing the sorbent. There was a nominal decrease (less than 5 %) in adsorption capacity in the studied system which can be accounted due to the competitive adsorption of water (which of course is negligible), presence of interfering ions and other foreign matter [31]. However, the adsorption capacity was still higher when compared to several other reports available in literature (Table 1).

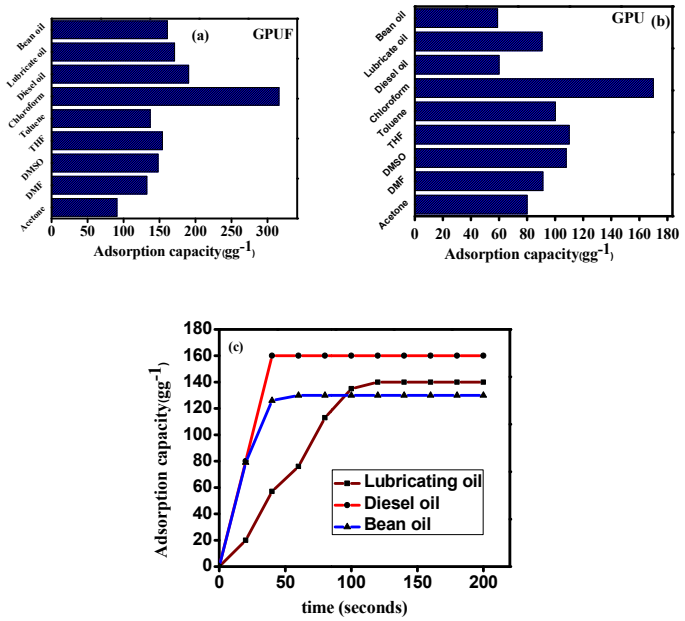

Figure 5. Adsorption capacity of GPUF (a) and GPU (b) in a variety of solvents and oils and (c) Adsorption capacity profile of GPUF against time.

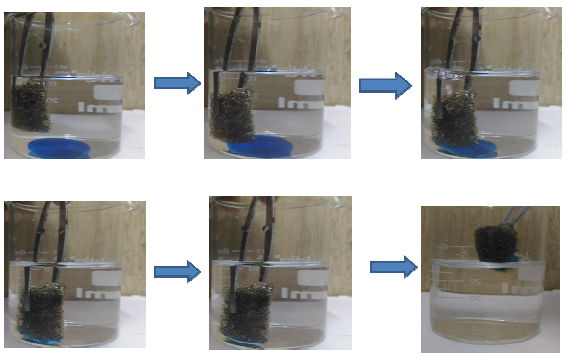

Figure 6. (a). Adsorptive removal of $CHCl_3$ (dyed blue) by GPUF within 5 seconds

.

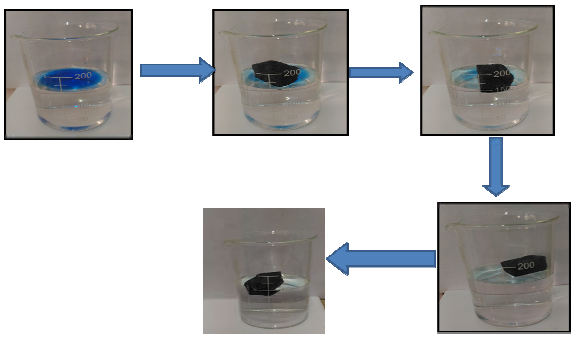

Figure 6. (b) Progression in selective adsorptive removal of diesel oil on water (dyed blue) within 10 seconds.

The microstructure of the GPUF sponge was analysed by Scanning Electron Microscopy (SEM). A wider investigation of the SEM images [Fig.7a to 7e] revealed the porous nature and the surface heterogeneity of GPUF. Detailing, Fig.7 (a) represents the SEM image of GPUF which portrays porous nature inherent to the PU framework. Adsorption occurs in voids of these porous materials. Fig.6b & 6c represent the SEM images of walls of the reticulate polymer network of GPUF decorated with wrinkled Graphene sheets. Zooming in on the wall reveals wrinkled Graphene sheets adorned with iron oxide nanoparticles. Further strengthening evidence is drawn from the TEM images [Fig.8a &8b] as it reveals the planar structure of Graphene with crumpled surfaces along with folding edges. It must be noted here that the structural roughness is of prior importance in wettability. Detailed analysis of the TEM images of GN-Fe_3O_4 composite reveals the successful incorporation of iron oxide on GN sheets as well as it point to the nature of the iron oxide nanoparticles [Fig.8b]. Size of the iron oxide nanoparticles as obtained from the TEM images was found to be in the range of 18-20 nm. Mesoporous nature of the Iron Oxide system

was also proved from the HRTEM images [Fig. 8b]. Investigation of wide angle XRD of GN-Fe_3O_4 composite established the amorphous nature of the composite and hints the presence of Fe_3O_4 nanoparticles of grain size of few tens of nanometer, ensuring a typical nano composite structure [Fig.9a]. The XRD pattern of Graphene-iron oxide composite depicting reflections characteristic of the planes in Graphene at 2theta values 21° and that of Fe_3O_4 at 30.5° and 41.1°[Fig.9a]. The small angle XRD pattern [Fig.9b] depicts a peak at low 2 theta value which further confirms the mesoporous nature of the incorporated iron oxide [32].

The whole credit for the imperative adsorption efficiency of GPUF can be solely laid to the optimized combination of surface heterogeneity, super hydrophobicity and porosity. As drawn from the microscopic analysis, GPUF presents a highly roughened surface with the addition of GN-meso iron oxide composite. Hydrophobic surfaces can be designed by the introduction of heterogeneity onto surfaces. Graphene, persistently known for its hydrophobicity will introduce nanoscale roughness that alters the PU network to a super hydrophobic moiety. The sub micrometer roughness of the exposed Graphene layers renders hydrophobic nature to the foam and hence water stays intrinsically at the exterior, while oleophilicity renders oil penetration to the material thus affecting separation of oil and water. Reports suggest that surface roughness can be correlated to hydrophobicity as the air trapped between the water droplet and solid surface minimizes the contact area [34, 35]. Sorption of oil to magnetic particle can be explained with fine particle-oil flocculation which is associated with an

electrostatic interaction between magnetic particles with charged surface and polar compounds in oil as well as in the polar solvents.[36]

The FESEM image[Fig.8e & 8f] of the iron Oxide nanoparticles depicted aggregated structures which are essential for super hydrophobicity [37] . The loading of Fe_3O_4 nanoparticles onto GN sheets benefits in adding to the roughness of GPUF and also facilitates the oil adsorption [38, 39]. As seen from the SEM images, stacked GN sheets with crumpled edges with protrusions projecting from various directions and decorated with meso iron oxide nanoparticles creates a fittingly roughened surface which is analogous to the lotus leaf leading to super hydrophobicity and super oleophilicity [33] . It is noticed that the water droplets attain a quasi spherical shape on the GPUF surface with a contact angle of 151° [Fig.9]. This novel GPUF is characterized by the presence of 3D structure with a wide range of micropores and mesopores within. The presence of mesoporous iron oxide nanoparticles further drives the oil adsorption. The oil is driven through the porous walls of the foam into the bulk via capillary action and the movement is further facilitated by the presence of oleophilic nanoparticles decorating the reticulate walls. The oil will be stored in the mesopores of the oleophilic iron oxide nano particles creating more volume for oil storage is due to the π-π interaction between GN sheets and π cloud in oils accounts for the selectivity of GPUF [40].

The intrinsic hydrophobicity of Graphene sheets clubbed with magnetic responsivity of Fe_3O_4 as well as porosity and oleophilicity of PU template lead to much high sorption capacity. Of course, the mesoporosity of Fe_3O_4 also has to be counted in this regard. Wenzel theory suggests that actual wetting area available on the surface of

solid increases proportionately with roughness. The projected Graphene sheets and Fe_3O_4 particles stage a highly roughened surface leading to super hydrophobicity. The synergistic action of inherent porosity, the super hydrophobicity and the inbuilt heterogeneity greatly facilitates the diffusion of oil into the sponge and results in appreciable adsorption efficiency. Preparation of iron oxide incorporated PU sponge alone was as done as a control. Though at the first instance, it displayed notable adsorption efficiency, the leaching of Fe_3O_4 was noticed, which rendered the system considerably unstable. This clearly points to the structural stability on incorporation of Graphene. The proposed GPUF foam competes and outshines with several established sorbents in terms of its cost effectiveness, simplicity and recyclability [41-43].

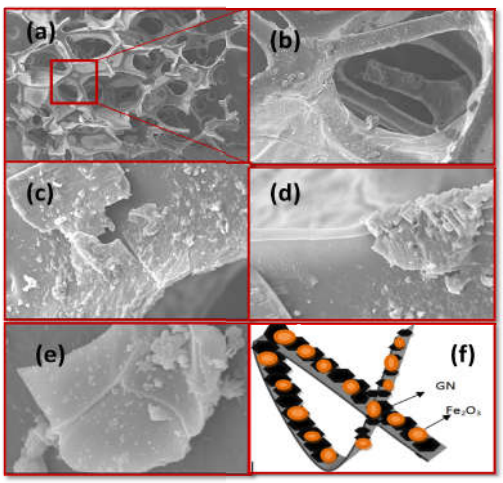

Figure 7. (a) SEM images of GPUF depicting the porous nature; (b-d) Walls of GPUF revealing the heterogeneity and incorporation of wrinkled Graphene sheets and Iron oxide;(e) SEM image confirming the incorporation of Iron oxide on GN sheets;(f) pictorial depiction of walls of GPUF adorned with GN and Fe_3O_4.

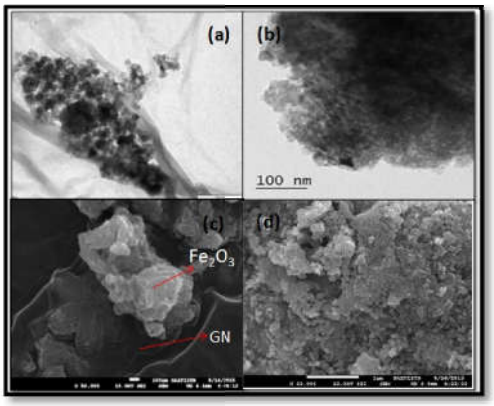

Figure 8. TEM images of Graphene-Iron oxide composite (a) ; Mesoporous nature of Iron oxide nanoparticles(b);FESEM images of Graphene-iron oxide composite (c); FE-SEM images of Iron oxide nanoparticles (d).

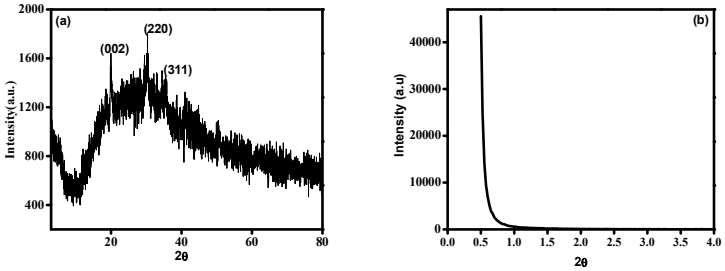

Figure 9. (a) XRD pattern of Graphene-iron oxide composite; (b) Low angle XRD of iron oxide nanoparticles.

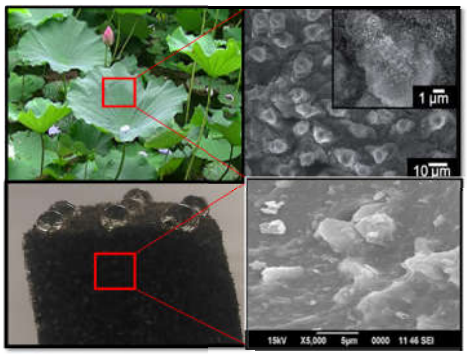

Figure 10. GPUF mimicking lotus leaf.

(i)Recyclability of the sorbent

Reusability of a sorbent is very significant for practical application in oil adsorption. The GPUF can be reharvested by reclamation by magnetic force and manual squeezing after sorption. To further elucidate the practical applicability of GPUF, it was employed to magnetically remove oil from water. Diesel oil (dyed blue) was dropped in water (oil: water, 1v:6v) and was magnetically actuated to move under the influence of weak magnetic force. The progress of the removal is shown in Fig.11. The oil was almost instantaneously removed by the magnetic sponge and it can serve as energy less strategy to allay the perils of collection of sorbent after adsorption.

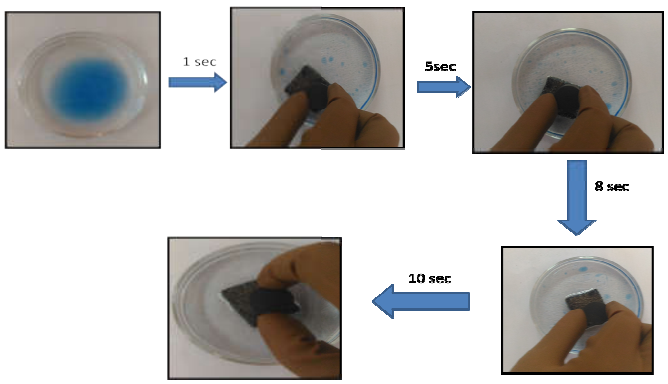

Figure 11. Progress in oil removal by magnetically driven GPUF

Owing to the intrinsic elastic nature of GPUF, the adsorbate can be easily removed by manual squeezing [Fig.12]. The adsorption capacity as a function of adsorption cycle for diesel oil and $CHCl_3$ is depicted in Fig12a & 12b. The adsorption capacity remained almost constant upto 120 cycles for diesel oil and 150 cycles for chloroform. Afterwards, there was a nominal decrease in adsorption capacity due to

the presence of slight traces of adsorbate in the sorbent which cannot be just removed by mere squeezing. Less than 2% weight remained in GPUF even after 100 cycles for both oil and $CHCl_3$, establishing the highly stable reusability of GPUF. Squeezing of the sorbent stands as a promising route for recyclability when compared to other techniques like burning, extraction etc as it is does not lead to structural damage when subjected to heat treatment and can also be employed for organic solvents and oils. The recyclability behavior is nearly analogous for all the investigated solvents and oils. It is noteworthy that, the recyclability is highest among other reported polymeric sorbents and carbon based sorbents [44-46] .Cyclic performance studies asserts its easy to recover and reuse capacity.

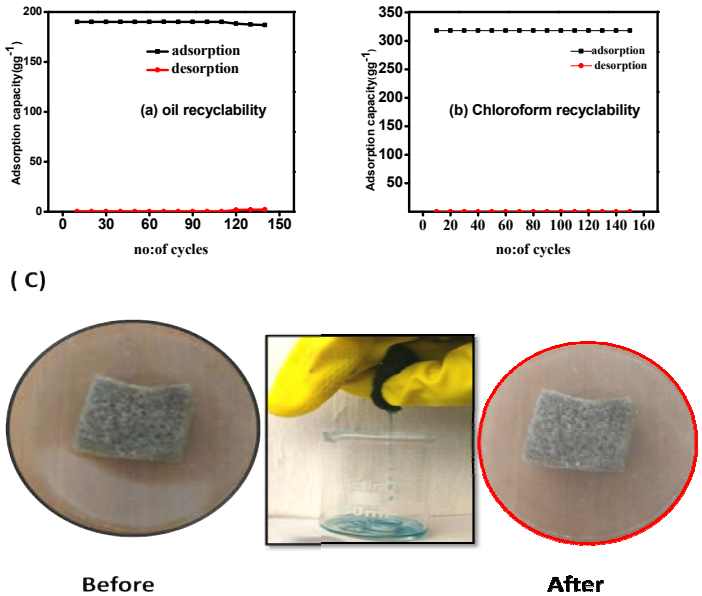

Figure 12. Adsorption capacity of GPUF in cycles of adsorption and desorption (a) Diesel Oil, (b) Chloroform; Digital images of GPUF before and after reusability studies in diesel oil(c).

We believe that GPUF presents itself as a feasible alternative over many of its other counterparts tabulated in Table 1.Though some reports are found on sorbents based on Nitrogen doped Graphene aerogel, Graphene foam etc which exhibited superior efficiency than our as prepared GPUF foam, they fail in competing with the efficiency, simplicity, cost effectiveness, reusability and user friendliness of the system projected herein.

Sorbent	**Capacity(gg^{-1})**	**Solvents**	**Cost**	**Reference**
PDMS	8	Organic liquids	medium	1
KG ppy	101	Diesel	medium	31
GN/CNT/Fe_3O_4	27	Diesel	high	47
Boron doped CNT	25-125	Oils& Organic liquids	high	48
RGO foam	5-40	Oils& Organic liquids	high	49
Graphene sponge	60-160	Oils& Organic liquids	high	50
TCF aerogel	50-192	Oils& Organic liquids	low	51
CNT sponge	50-102	Oils& Organics	high	52
Macroporous organo gel	50-102	Oils and solvents	medium	53
GPUF	90-316	Oils and solvents	low	This work

Table 1: Adsorption characteristics of various materials

4.9.Concluding Remarks

- To brief up, a novel and cost effective functional hybrid (GPUF) based on poly urethane as 3D architecture and Graphene-mesoporous Iron oxide composite as reinforcement material is fabricated and its water/oil separation characteristics is investigated in detail.

- Decked by Graphene-mesoporous iron oxide composite, this hybrid foam depicted hierarchical roughness and heterogeneity paving the lane for its admirably high adsorption capacity.

- GN and iron oxide, well known for its hydrophobic and oleophilic nature respectively, is believed to introduce nano and micro scale roughness, altering the PU scaffold into a super hydrophobic but super oleophilic moiety.

- The as prepared foam exhibited impressive traits like super hydrophobicity, super oleophilicity, and selectivity culminating in its extra ordinary high adsorption efficiency for a broad spectrum of oils and organic contaminants.

- Being magnetically actuated, GPUF can be driven easily with the help of a magnet to the target zones and can be recollected quickly after sorption. The recovered sponge can be reused for about 150 cycles maintaining its high adsorption capacity.

- We envision that the findings of our study projects a privileged sorbent, GPUF, that could be scaled up as a promising platform for large scale decontamination of pollutants in water.

4.10. References

[1] M. O. Adebajo, R. L. Frost, J. T. Kloprogge, O. Carmody and S. Kokot, *J. Porous Mater*., 2003, 10, 159.

[2] H. A. Aziz, M. A Zahed, M. H. Isa, L. Mohajeri and S. Bioresour. *Technol.* 2010, 101, 9455.

[3] A. Bayat, S. F. Aghamiri, A. Moheb and G. R Vakili Nezhaad, *Chem. Eng. Technol*. 2005, 2, 1525.

[4] H. L. Li, J. X. Wang, L. M. Yang and Y. L. Song, *Adv. Funct. Mater.*, 2008, 18, 3258.

[5] D. W. Wang, F. Li, G. Q. Lu and H. M. Cheng, *Carbon*, 2008, 46, 1593.

[6] M. M. Radetic, D. M. Jocic, P. M. Jovancic, Z. L. Petrovic and H. F. Thomas, *Environ. Sci. Technol.*, 2003, 37, 1008.

[7] D. Ceylan, S.Dogu, B. Karacik, S. D. Yakan, O. S.Okay and O. Okay, *Environ. Sci. Technol.* 2009, 43, 3846.

[8] S. Suni, A. L. Kosunen, M. Hautala, A. Pasila and M. Romantschuk, *Mar. Pollut.Bull.*, 2004, 49, 916.

[9] C. Wu, X.Y. Huang, X.F. Wu, R. Qian and P.K. Jiang, *Adv Mater.,* 2013,25,5658.

[10] Yu Yang, Huan Yi, and Chaoyang Wang, *ACS Sustainable Chem. Eng.*, 2015, 3, 3012.

[11] J. Yuan, X. Liu, O. Akbulut, J. Hu, S. L. Suib, J. Kong and F. Stellacci, *Nat. Nanotechnol.,* 2008, 3, 332.

[12] Huaiyuan Wang, Enqun Wang, Zhanjian Liu, Dong Gao, Ruixia Yuan, Liyuan Sun and Yanji Zhu, *J. Mater. Chem. A*, 2015, 3, 266.

[13] Zhen-Yu Wu, Chao Li, Hai-Wei, Liang Yu-Nin, Zhang Xin, Wang, Jia-Fu Chen and Shu-Hong Yu, *Scientific Reports* ,4, Article number: 4079 .

[14] T. C. Merkel, B. D. Freeman, R. J Spontak, Z. He, I.Pinnau, P.Meakin and A. J. Hill, *Science,* 2002, 296, 519.

[15] Y. Zhu, S. Murali, W. Cai, X. Li, J. W. Suk, J. R. Potts and R. S. Ruoff, *Adv. Mater*., 2010, 22, 3906.

[16] E. Singh, Z. Chen, F. Houshmand, W. Ren, Y. Peles, H. M. Cheng and N. Koratkar, *Small,* 2013, 9, 75.

[17] D. D. Nguyen, N. H. Tai, S. B. Lee and W. S. Kuo, *Energy Environ. Sci.,* 2012, 5, 7908.

[18] Yue Liu, Junkui Ma, Tao Wu,Xingrui Wang, Guanbo Huang, Yu Liu, Haixia Qiu, Yi Li, Wei Wang,and Jianping Gao, *ACS Appl. Mater. Interfaces*, 2013, 5, 10018.

[19] 19. A. B. Bourlinos, A. Simopoulos, N.Boukos and D. Petridis, *J. Phys.Chem. B,* 2001, 105, 7432.

[20] A. F. Gross, M. R. Diehl, K. C. Beverly, E. K. Richman and S. H Tolbert, *J. Phys. Chem. B* 2003, 107, 5475.

[21] W. S. Hummers Jr. and R. E. Offeman, *J. Am. Chem. Soc.,* 1958, 80, 1339.

[22] A. S. Poyraz, C.H. Kuo, S. Biswas, C. K. King'ondu and S. L. Suib, *Nat. Commun.* 2013, 4, 2952.

[23] Hu Liu, Mengyao Dong, Wenju Huang, Jiachen Gao, Kun Dai, Jiang Guo, Guoqiang Zheng, Chuntai Liu, Changyu Shena and Zhanhu Guo, *J. Mater. Chem. C*, 2017, 5, 73.

[24] M. Anju and N. K. Renuka, *RSC Adv.,* 2015, 5, 78648.

[25] Palanisamy Thanikaivelan, T. Narayanan, K. Bhabendra Pradhan and Pulickel M. Ajayan, *Sci.Reports,* 2012*,* 2.

[26] M.Husseien, A.A.Amer, A. El-Maghraby and N. Hamedallah, *J.Anal.Appl.Pyrol*. 2009,86,360.

[27] H.C. Bi, X. Xie, K.B Yin, Y.L. Zhou, S. Wan, L. B. He, F. Xu, F. Banhart, L. Sun and R.S Ruoff, *Adv.Funct.Mater.,* 2012, 21, 4421.

[28] D. C. Tuncaboylu and O. Okay, *Eur. Polym. J*., 2009, 45, 2033.

[29] G.Hayase, K. Kanamori, M. Fukuchi, H. Kaji and K. Nakanishi, *Angew. Chem. Int. Ed.*, 2013, 52, 1986.

[30] O.Carmody, R.Frost, Y. F. Xi and S. Kokot, *J. Colloid Interface Sci.*, 2007, 305, 17.

[31] Hua Li, Lifen Liu and Fenglin Yang, *J. Mater. Chem. A*, 2013, 1, 3446.

[32] M. P. Nikhila, A. K. Akhila, T. Divya, M. Anju, T. V. Arsha Kusumam and N. K. Renuka, *Cryst.Engg.Comm*., 2017, 19, 511.

[33] L. Feng, Z. Zhang, Z. Mai, Y. Ma, B. Liu, L. Jiang and D. A Zhu, *Angew. Chem., Int.Ed.* 2004, 43, 2012.

[34] S. Herminghaus, *Europhys. Lett.* 2000, 52, 165.

[35] G. McHale, N. J. Shirtcliffe, S. Aqil, C. C. Perry and M. I. Newton, *Phys. Rev. Lett.*, 2004, 93,036102.

[36] J. Zhang, W. Huang and Y. Han, *Macromol. Rapid Commun.* 2006, 27, 804.

[37] R. N. Wenzel, *Ind. Eng. Chem*. 1936, 28, 988.

[38] Liuhua Yu, Gazi Hao, Junjun Gu, Shuai Zhou, Ning Zhang and Wei Jiang. *J.Magnetism and Magnetic Materials* 2015, 394, 14.

[39] Y. W. Su, B. H. Ji, K. Zhang, H. J. Gao, Y. G. Huang and K. Hwang, *Langmuir* 2010, 26, 4984.

[40] M. Q. Zhao, J. Q. Huang, Q. Zhang, W. L. Luo and F. Wei, *Appl. Clay Sci.*, 2011, 53, 1.

[41] Xuchun Gui, Zhiping Zeng, Zhiqiang Lin, Qiming Gan,Rong Xiang, Yuan Zhu, Anyuan Cao, and Zikang Tang, *ACS Appl. Mater. Interfaces*, 2013, 5, 5845.

[42] Y. Zhao, C. Hu, Y. Hu, H. Cheng, G. Shi and L. Qu, *Angew. Chem. Int. Ed.*, 2012, 51, 11371.

[43] Hengchang Bi, Xiao Xie, Kuibo Yin, Yilong Zhou, Shu Wan, Rodney S. Ruoffb and Litao Sun, J. *Mater. Chem. A,* 2014, 2, 1652.

[44] H. Y. Sun, Z. Xu and C. Gao, *Adv. Mater.* 2013, 25, 2554.

[45] S. J. Choi, T. H. Kwon, H. Im, D. I. Moon, D. J. Baek, M. L. Seol, J. P. Duarte and Y. K. Choi, *ACS Appl. Mater. Interface* 2011, 3, 4552.

[46] R. Gupta and G. U. Kulkarni, *ChemSusChem*, 2011, 4,737.

[47] Sudong Yang, Lin Chen, Lei Mu and Peng-Cheng Ma. *Journal of Colloid and Interface Science*, 2014, 430,337.

[48] D. P. Hashim, N. T. Narayanan, J. M. Romo-Herrera, D. A. Cullen, M. G. Hahm, P. Lezzi, J. R. Suttle, D. Kelkhoff, E. Muñoz-Sandoval, S. Ganguli, A. K. Roy, D. J. Smith, R. Vajtai, B. G. Sumpter, V. Meunier, H. Terrones, M. Terrones and P. M. Ajayan, *Sci. Rep.*, 2012, 2, 363.

[49] Z. Niu, J. Chen, H. H. Hng, J. Ma and X. Chen, *Adv. Mater.*, 2012, 24, 4144.

[50] M. M. Radetic , D. M. Jocic, P. M. Jovanccic, Z. L. Petrovic and H. F. Thomas, *Environ. Sci. Technol.*, 2003, 37, 1008.

[51] H. C. Bi, Z. Y. Yin, X. H. Cao, X. Xie, C. L. Tan, X. Huang, B. Chen, F. T. Chen, Q. L. Yang, X. Y. Bu, X. H. Lu, L. T. Sun and H. Zhang, *Adv. Mater.*, 2013,41,5916.

[52] X. C. Gui, J. Q. Wei, K. L. Wang, A. Y. Cao, H. W. Zhu, Y. Jia, Q. K. Shu and D. H. Wu, *Adv. Mater.*, 2010, 22, 617.

[53] D. C. Tuncaboylu and O. Okay, *Eur Polym. J.,* 2009, 45, 2033.

CHAPTER V

GRAPHENE-DYE HYBRIDS AS SENSOR PLATFORM

Contents

This chapter presents the first ever prospective application of Graphene-Dye units (GD) as a colorimetric and fluorimetric sensor for Mercury ion (Hg^{2+}) ions and Fluoride ion. Rhodamine (RD) and Fluorescein (FLR) dye are opted as model dyes. The duality of Graphene to undergo π−π and dispersive interactions with the dye as well as to act as a selective adsorbent for Hg^{2+}/F^- is conceptualized in this study. The crux behind the sensing by the Graphene-Dye unit lies behind the decrease in absorbance/fluorescence intensity of the dye on complexing with graphene and the corresponding restoration of the optical response upon highly selective competitive adsorption of Hg^{2+} /F^-ions by graphene sheets. Quantification of these optical responses was attained by colorimetric and fluorimetric measurements, which yielded sub ppm ppb level assays for the test species, with Limit of detection values falling much below the permissible limit prescribed by Environmental agencies. The moiety is highly selective and specific for the analytes over their congeners and other possible interfering species. The significant advance in this investigation is the fabrication of a Graphene-Dye unit as a qualitative read out tool by immobilizing GD units onto filter paper strips for the visual detection of these ions through fluorescence in UV light.

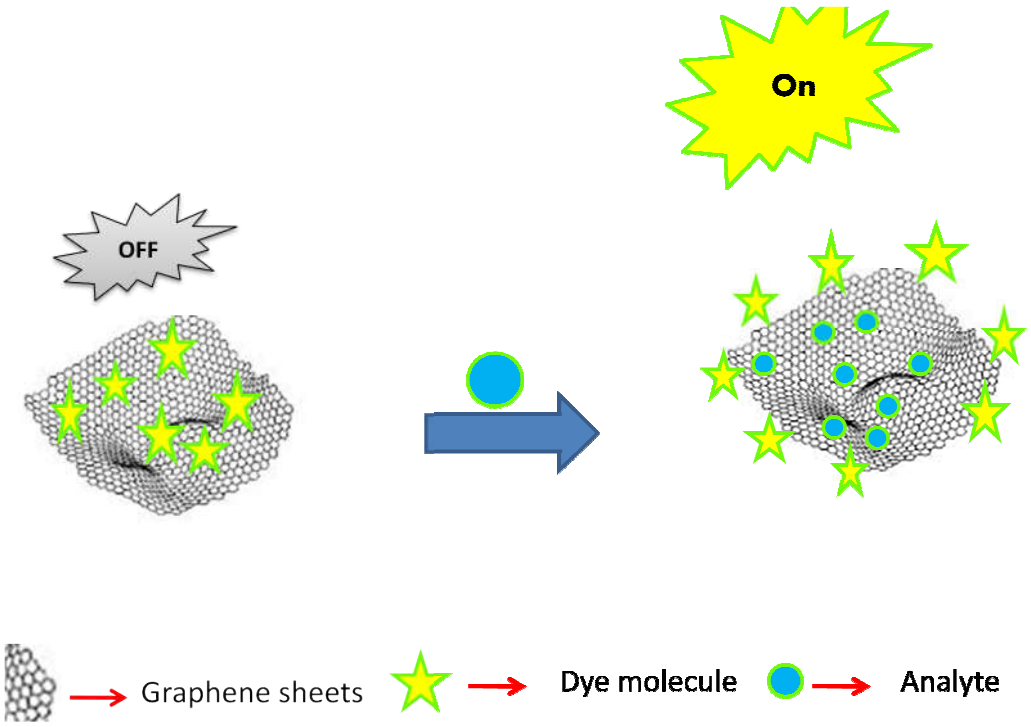

GRAPHENE-DYE HYBRID AS AN ELITE SENSING PLATFOEM

5.1 Introduction

Sensors can be identified as a systematic unit which when stimulated by any form of energy can undergo a transition in its state or characteristics that can be quantified and can be employed to analyse the stimulant. Depending on the nature of stimulus, sensors can be of two types viz. physical sensor and chemical sensor. Physical sensor is one which responds to change in physical property of the analyte and will quantify the change as an electrical signal. A sensor which quantifies an analyte with respect to a signal obtained through any chemical reaction is termed as a chemical sensor. Chemical sensors finds application in various fields namely for environmental monitoring, health diagnosis, food and beverages, security systems etc. Extensively used techniques in chemical sensors are optical absorption, fluorescence, redox potential etc. Among them, sensors based on optical absorption and photoluminescence are superior and is currently being widely investigated for a wide variety of analytes like heavy metals, bio molecules, explosives, anions etc. Herein, we have devised sensors based on Graphene-Dye hybrid and have investigated their performance as an optoprobe for Mercury ion and Fluoride ion.

In the Past few decades, 0-dimensional (Quantum dots) and 1 dimensional (nanowires, nanotubes) nanostructures have been the central impetus towards the development of novel sensors [1-3]. Ever since the emanation of Graphene, a one atom thick honeycomb like sp^2 hybridised Carbon allotrope, it has stimulated tremendous interests across many disciplines of nano technology and material science. Thanks to its intriguing physiochemical properties, GN has sparked

exceptional enthusiasm among the scientific community in the fields of energy storage and conversion [4, 5], sensing [6], nano electronics [7] etc. Despite its short history, GN has shown its mammoth potential in several novel sensors which exploits its unique traits viz. high mobility of charge carriers, high electron transfer rate, phenomenal ability to quench fluorescence, remarkable surface area, notable flexibility and robustness [8]. However, all these properties will emerge only when GN sheets exists without aggregation, which otherwise will limit its practical application as a sensor. Recent efforts in this direction have led to the functionalisation of graphene sheets with various entities like metal oxides, organic molecules, organic dyes, non metals etc. which would not only stabilize the graphene sheets but also pave the way for graphene based hybrid materials with astounding features and versatile applications. graphene together with GN Hybrids has carved an invincible stretch of novel and efficient sensors [9]. GN has been employed as physical sensor for mass, strain, photons, magnetic field and an electrochemical sensor for monitoring biomolecules, proteins etc [10-15]. Herein, we emphasis the application of graphene based systems as potential candidates for sensing a toxic heavy metal ion, Mercury ion (Hg^{2+}) and a biologically relevant anion, Fluoride ion (F^-). Before entering into the core of the chapter, the applications of graphene based chemo sensors will be briefly discussed here.

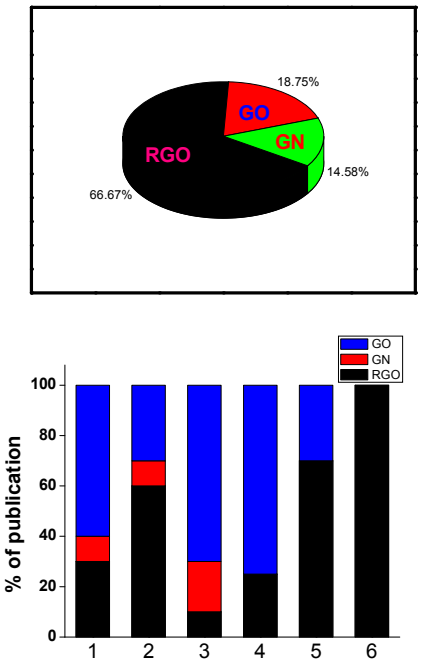

Figure 1. Statistical estimate of the publications on graphene and its derivatives work. Left: Nearly 68% of the reported work use reduced graphene oxide and only 14% use bare graphene sheets. Right: Evaluation of Graphene and its derivatives in various field of sensing; If divided into sensor types (1: plain sensors; 2: electro-chemical sensors; 3: field effect transistor-based sensors; 4: fluorescence based sensors; 5: chemiluminescence-based sensors; 6: colorimetric sensors) .The data shows that every GN derivative has its own sensing application area.

The statistical evaluation on the number of publications on graphene based systems for sensing various analytes clearly suggests the explosion of growth in this field over the years [Fig.1 (a)]. Pristine graphene, Reduced graphene Oxide and Graphene Oxide are utilized as efficient sensors for various analytes depending on the nature of the applications. Based on the data from Fig.1 (b), it is clear that every

graphene material has its own area of application and the selection of the host matrix depends on the task involved. For instance, pristine GN finds application, in transistor based sensors whereas its utilization as opto probes is practically nil. Plain sensors are those in which pristine graphene is used as the sensor moiety without any modification. They are found in Field effect transistor and physical sensors for detection of mass, strain, photons and magnetic field which demand high quality defect free graphene. As for bio and electrochemical sensing, the recent trend is to adopt Reduced Graphene oxide, a low quality variant of GN analogue, obtained by the reduction of Graphene Oxide and characterized by the presence of defects and few oxygen functional groups on its surface [16]. Though the relativistic charge transport and condensed matter effect are absent in Reduced Graphene Oxide when compared to that of pristine GN, its scalable preparation methods, tunable and unique properties make it a potential candidate for sensing application. The functional groups on the surface of Reduced graphene oxide can act as handles for covalent and noncovalent functionalisation of RGO which can serve as recognition ends towards specific targets which extends its prospects as a sensor [17]. Moreover, RGO is electrochemically superior to pristine GN on account of its defective basal plane and reactive centers along the edges. Graphene oxide, obtained after oxidation of graphite without further reduction, can act as a precursor for reduced graphene oxide as well as a sensing motif. In contrast to pure graphene, the most conspicuous feature of heterogeneous electronic structure of GRO and RGO is their near-infrared and visible fluorescence. The inherent and tunable fluorescence from Reduced graphene oxide and graphene oxide could open up impressive and previously unanticipated optical applications

for GN based nanostructures. Remarkably, Reduced graphene oxide and graphene oxide can also quench fluorescence. These obviously paradoxical properties are an indication of the heterogeneous structural, electronic and atomic features. It is well known that graphitic carbon can quench the fluorescence of the adsorbed dye. Similarly, RGO and GRO quench the fluorescence or more precisely optical characteristics of nearby species like dyes, polymers, quantum dots etc. [18, 19]. Investigations illustrated that the quenching of optical characteristics arises due to Fluorescence Resonance Energy Transfer (FRET) or non radiative dipole-dipole interaction between the fluorescent species and Graphene oxide or Reduced Graphene Oxide. Taking all these features into account, RGO and GRO can act as tunable, accomplished and capable platform for sensing applications. Reduced Graphene Oxide is a better nano quencher than Graphene oxide on account of the increase in sp^2 to sp^3 ratio and π-π coupling in Reduced Graphene Oxide due to reduction [20]. Hence, in our work Reduced Graphene Oxide was opted as sensor matrix.

As mentioned earlier, the aggregation of free standing graphene layers due to Van der Waals interaction stands as a major hurdle in the development and expansion of Graphene in sensor world. To circumvent this, various additives are incorporated on Graphene sheets and this has opened the door for Graphene Hybrids. To bestow sensing ability on Reduced Graphene Oxide/Graphene oxide, it is essential to functionalise it with recognition moieties that will bring the detection analytes onto the surface through interactions and may aid in signal transduction. Functionalisation induces and enhances its sensitivity, selectivity, loading efficiency etc. Covalent and noncovalent

approaches can be adopted to decorate GN and its derivatives with recognition elements. The presence of various oxygen functional groups on RGO surface act as handles for covalent functionalisation. A few strategies to functionalise graphene includes, introduction of Fluorine atom onto the GN surface and then substituting with various chemical moieties, addition of free radicals on sp^2 carbon atoms, cycloaddition reactions of dienophiles, biilups reaction, thermal or photochemical activated addition reactions, covalent functionalisation of linker molecules etc. results in functionalisation and ultimately enhances the overall sensing performance [21-23] . Non covalent functionalisation presents itself as an efficient synthetic propaganda for functionalisation of GN without disturbing its electronic structure. The extensive π system in GN plays a decisive role in the design of GN based electronic and optical devices.GN can be considered as a giant aromatic molecule which can adsorb several molecules without the aid of any coupling agents using various non covalent interactions like π-π interaction, cation-π interaction, anion –π interaction etc. These interactions do not alter the properties of the parent constituents and is retained as such. Different type of noncovalent interactions involves (a) Non polar Gas-π interaction that exists between an inert gas or non polar molecule and a polar molecule or lewis acid, (b)H-π interaction refers to a category of Hydrogen bonded interaction which occurs between a π cloud and H atom of electron deficient molecule, (c)The π-π interactions as the name points out occur throughout the GN system and can be fine tuned to functionalise GN and (d) Cation –π interactions refer to those supramolecular interactions that exist between a cation and π cloud and are considered as a potential route

for anion sensing. A detailed discussion on functionalisation of Graphene and its derivatives is provided in the introduction section.

5.2 Graphene-Dye Hybrids

As the name suggests, Graphene-Dye (GD) hybrids refers to heterogeneous GN based materials wherein dye molecules are embellished as reinforcement material on GN matrix via noncovalent or covalent forces. These hybrids enable new approaches towards the realization of high performance optoelectronic sensors and detectors. The interactions of GN with dye molecules leads to profound changes in the electronic structure of GN and can be modulated for various applications. The GN sheets can be exfoliated using dye molecules to prepare stable dispersion; Graphene-Dye units can serve as biological and chemical sensor; visualization of GN sheets can be done using Graphene-Dye systems which are emerging as desirable choices for bio imaging applications. Different modes of interaction are possible between Graphene and dye molecules depending on the extent of π conjugation and the nature of functional groups present on the system. Graphene-dye hybrids can function either as optical sensor or electrochemical sensor for various analytes ranging from heavy metals, biomolecules, anions etc. Graphene-dye hybrids work generally in two ways (1) Displacement approach:- A weak but stable supramolecular complex is formed between graphene and dye characterised by a specific optical response which is then modified with the advent of an analyte molecule. These modified optical responses can be quantified using spectroscopic techniques and hence a sensor is realized in practice [Fig.2 (a)]. Many advantages are associated with the

displacement strategy, namely, it does not demand covalent incorporation of the dye molecules (indicator) onto GN matrix or of analytes, the dyes can be exchanged and the sensing process is reversible. The second approach uses covalent linkage to bind with the dye molecule that will induce new optical signal or alters the existing optical response with the entry of analyte or target [Fig.2 (b)] [24].

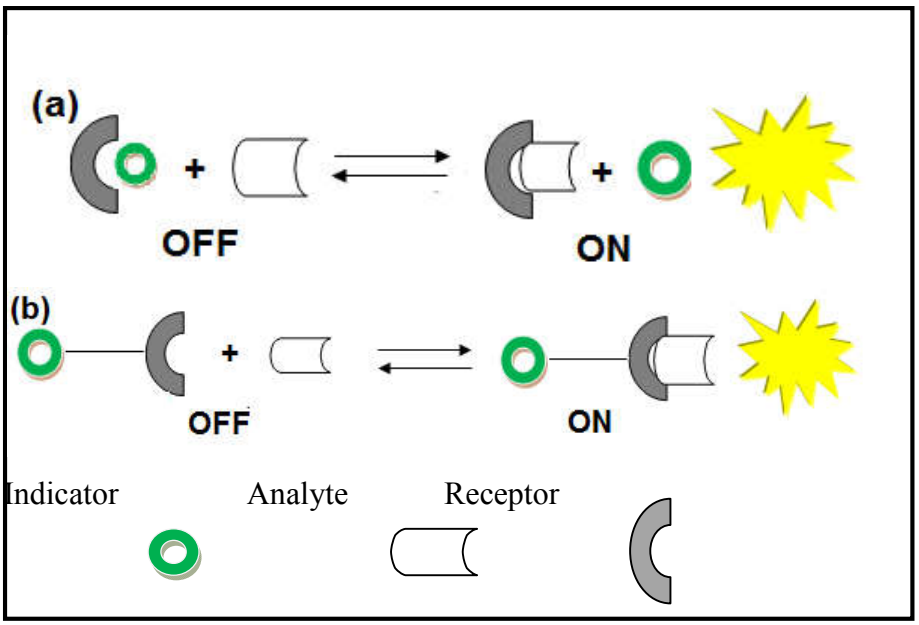

Figure 2. Approaches for working of Graphene-Dye Hybrids: (a) displacement approach (b) Sensor bearing a signaling subunit and a binding site.

GD hybrids offer themselves as promising sensing platform owing to the ability of GN sheets to undergo Fluorescence Resonance Energy Transfer (FRET). Photo physical calculations points the capability of Graphene to accept the energy transferred from excited dye molecules, and hence acts as an excellent quencher for the excited electronic state of dye molecule. FRET is extremely sensitive and is inversely proportional to the sixth power of distance between the donor

and acceptor. In GD hybrids, graphene act as a giant adsorbent capable of adsorbing dye molecules and bringing them at a minimum distance required for FRET. A thorough understanding regarding the interaction between GN and dye molecule is necessary before we proceed further into the topic. Various factors govern the interaction between GN and dye molecules, viz. the nature of functional group on dye molecules, number of GN layers, and conductivity of Graphene etc. Zhang et al. have investigated the photophysical features of several Xanthene [Rhodamine (RD), Pyronin Y (PYY) and Phthalocyanine(PC) dyes[Zinc Phthalocyanine and ZnPc(β-OPh)$_4$] in presence of GN sheets [25] . The UV-Vis and fluorescent response of the dye molecules were monitored after titration against graphene. Their investigations revealed the quenching of optical response of the dye molecules concomitant to the increase in concentration of GN. A new red shifted absorption band was seen for all Graphene-Dye systems which can be ascribed to the formation of a supramolecular Graphene-Dye complex (GD). The spectroscopic studies of all the Graphene-Dye complexes featured characteristics of charge transfer absorption bands viz. the bands are located in visible region, displayed boarder half width and weaker molar extinction coefficient. On comparing PYY with RD and ZnPc with ZnPc(β-OPh)$_4$, they have concluded that the phenyl ring does not affect the absorption of GD complexes but hinders the ease in the formation of GD complex. The photoluminescence (PL) spectra of PC and Xanthene dyes were also studied. Addition of GN quenches the fluoresnce intensity of dye molecules due to the formation of supramolecular Graphene-Dye complex which is weakly emissive as

confirmed by the life time measurement studies. Though the union of conventional organic dyes with GN sheets and its derivatives has enough ability to develop novel bio and chemo sensors, their potential is not fully exploited and there have been only few reports in this direction.

The graphene dispersion in aqueous solution acts as a polyaromatic platform of oxygen functional groups which has bright prospects in performing chemistry. The photo physical nature of GN and its derivatives enables it to be an efficient nano quencher and hence it is employed as an efficient sensor in bio applications, environmental fields, civil defense etc. Wang et al. has constructed a electrostatic optoprobe from Rhodamine and Graphene oxide for selective, sensitive and cost effective detection of DNA. The noncovalent interactions between Rhodamine and Graphene oxide lead to the quenching of the optical characteristics of Rhodamine on account of the formation of a noncovalent complex of $RD^{+}GO^{-}$. When in contact with DNA, this complex breaks due to the selective affinity of Graphene oxide towards DNA leading to the restoration of optical response. The selectivity of the system was assessed in presence of various metal ions and macromolecules and the linear calibration curve obtained in the range of 0.2 nM to 10 nM favoured the practical application of the unit in biofluids [26]. On similar grounds, Xu and coworkers constructed a Bovine serum albumin sensor based on chemically converted Graphene (CCG)-Squarine (Sq) Dye unit. Sq dyes are a class of cationic dyes which give rise to sharp and intense

absorption and fluorescent bands in the red region. [27] The non covalent interactions between cationic Sq dyes and anionic carboxylate groups of CCG leading to super quenching of the fluorescence of Sq dyes. Introduction of BSA triggers the restoration of the quenched fluorescence intensity with red shift in the emission wavelength.

DNAzymes based fluorescent sensors are celebrated as effective sensors for various metal ions, biomolecules etc. on account of their selectivity, sensitivity and efficiency. Exploiting the DNA cleavage -dependant GN/DNA interaction and the catalytic activity of DNAzymes, researchers have developed various fluorescent functional DNA sensors. Pyrene derivatives known for its noncovalent interactions with GO was employed for bio sensing by Balaparnu and group [28]. The as synthesied 4-(1-pyrenylvinyl)-N-butylpyridinium bromide (PNPB) can interact with negatively charged GRO to form a supramolecular charge transfer complex ($PNP^{+}GRO^{-}$). The quenched optical response of $PNP^{+}GRO^{-}$ unit was restored on with the introduction of DNA molecules and hence acting as a specific and sensitive sensor for DNA. A genaralised senstive and selective GRO based fluorescent platform for biomolecule sensing was reported by Yang et al. [29] . Binding of target molecule alters the conformation of dye labelled DNA and disturbs the contact between dye labelled DNA and GRO. These interactions will lead to the desorption of dye labelled DNA from GRO , resulting in the recovery of quenched fluorescence. An aptasensor based on Reduced Graphene Oxide and Acridine Orange which facilitates selective and specific ON-OFF sensing of

Hemin was developed by Shi and group [30]. Reduced Graphene Oxide quenches the fluorescence of AO due to the formation of AO-RGO complex by π-π interactions. The said complex breaks with the advent of hemin aptamer (PS2.M, 50-GTGGGTAGGGCGGGTTGG-30), a G-rich oligonucleotide sequence that can form G-quadruplex structure in presence of Na (I) or K (I). The complex can be broken because of the competitive binding of AO with G-quadruplex. When this unit is incubated with the target hemin, the specific binding of hemin with PS2.M breaks the AO-PS2.M complex resulting in the reunion of AO and RGO leading to the restoration of fluorescence intensity.

Conjugation of graphene with functionalised aptamers can be used as a sensing tool for the detection of thrombin. Li et al. has constructed a biosensing platform based on Fluorescein amidite labeled aptamer on graphene. The noncovalent assembly induced by π-π stacking interactions between dye labeled aptamer and GN guarantees the proximity of dye labeled aptamer with graphene surface. The nearness of dye labeled aptamer to graphene quenches the fluorescence of dye following FRET from dye to GN. When thrombin is added, it binds with dye labeled aptamer and makes the dye far away from graphene surface, restoring the fluorescence. The graphene FRET aptasensor can detect 31.3 pM thrombin with good selectivity [31]. Huang et al. constructed a novel, sensitive, rapid, label free fluorescent strategy for detecting Tartazine (Tz) by preferential binding to Reduced Graphene Oxide over fluorescein. The adsorption of fluorescein on RGO surface substantially quenches the fluorescence of

dye due to Fluorescence Resonance Energy Transfer (FRET). Upon addition of Tz, the quenched fluorescence intensity was regained due to the selective affinity of RGO towards Tz over fluorescein. The detection range was found to be 0.53 ng mL^{-1} [32]. Meng Liu and coworkers devised a general method for label free sensitive sensing of Cu (II) ions based on self assembled GN/DNAzyme complex and a fluorophore Gel Red. When Cu (II) specific DNAzymes is introduced onto graphene sheets a complete quenching of FLR is observed due to the proximity of graphene and Gel Red by π-π interactions. Addition of Cu (II), cleaves the DNAzyme due to Copper specific reaction, altering the DNA/GN conformation. The conformational change is accompanied by the release of gel red turning on the quenched response [33].

Devising highly sensitive and selective sensors for heavy metal ions have attracted keen interests among the researchers due to the perils they pose to our eco system. Among the heavy metals, Mn^{2+} is a typical entity with paramount importance to human health and ecosystem. Conventional fluorescent probes for Mn^{2+} sensor fails in practical application and hence there is an urge to develop fluorescent probes for Mn^{2+}. A novel pyrene derivative i.e. 1, 2-bis-(2-pyren-1-ylmethylamino-ethoxy) ethane (NPEY) and Graphene based Mn^{2+} sensor were fabricated by Mao et al. Pyrene –GN turned out to be an OFF-ON fluorescent switch to Mn^{2+}. The quenched fluorescence of NPEY-GN unit was turned ON when in contact with Mn^{2+} ion. It was found that the imino group and multi ethylene groups in NPEY binds

with Mn^{2+} as a result the electron transfer between NPEY and GN is blocked and the fluorescence is rejeunvated. The recognition ability of GO was sensitive in a concentration range from 1 $\times 10^{-5}$ to 10 $\times$ 10^{-5} with a detection limit of 4.6 $\times$ 10^{-5} M [34] .

In this chapter, we have investigated the application of Graphene-Dye Units as sensors for Mercury Ion and Fluoride Ion.

PART A

Graphene-Dye Hybrids as Potential Sensor for Mercury Ion in Aqueous Solution

5.3 Introduction and Relevance of Mercury ion sensing

Heavy metal pollution is regarded as one of the most grievous environmental issues, which undermines global sustainability. Metals whose density is higher than 3.5 g cm^{-3} falls under the class of heavy metals and is noted for their latent toxicity at low thresholds. Mercury, Lead, Cadmium, Zinc etc. are some representative elements amongst heavy metals. Hg^{2+}, ranked sixth, is a cumulative toxicant of global concern owing to its non biodegradability, long range transport in the atmosphere, persistence in the environment and its biomagnification through the food chain [35-40]. Hg^{2+} is released into the environment via both natural and anthropogenic sources. Mercury causes undesirable effect to central nervous system, brain, lungs, kidney, etc. If ingested by pregnant women, mercury can cause developmental delays in children. Hg^{2+} ion has a tendency to accumulate in vital organs of humans and animals that will lead to hematological destruction. Besides being the most common contaminant among heavy metals, the ecological effects and biomagnifications of Mercury ion through the food chain have led to a demand for proper sensing and removal of Hg^{2+} ion. Mounting evidence from various studies underlines the adverse influence of Hg^{2+} ion on human health, which demands the trace detection of Hg^{2+} ions [Fig.3] [41–43]. Though the detrimental effect of mercury ion has roused serious concern, the world's

contamination with this toxic metal has increased in an alarming rate over the past few decades. Alarmed by the perils of Hg^{2+}, the international World Health Organization (WHO) and the U.S. Environmental Protection Agency (EPA) have set 2 ppb as the maximum allowable amount of Hg^{2+} in drinking water. The actual peril associated with Hg^{2+} arises when once they are introduced into aquatic bodies, as mercury ion will be solvated instantaneously to form solvated Hg^{2+} which is one of the most stable forms of inorganic mercury. Hence there is always an urge to develop selective, sensitive and efficient Hg^{2+} sensors in aqueous systems. The obvious limitation for direct Hg^{2+} ion detection by spectroscopic technique is due to the lack of significant optical response from Hg^{2+} ion, on account of its closed d-shell configuration.

Figure 3. Pangs of Mercury poisoning [*Adapted from various sources from internet]*

Past few decades have witnessed remarkable progress in the development of Hg^{2+} sensors [44-47]. Many attempts were directed to design portable Hg^{2+} ion sensors, which include colorimetric, fluorescent and electrochemical methods [48-49], Probes based on organic molecules [50-53], polymeric materials [54-57], Au and Ag nanoparticles, etc., have been extensively investigated for this purpose. Poor solubility in aqueous solution and tedious preparation and purification steps limit the use of organic and polymer probes, whereas the high cost of noble metals holds back their widespread application. In this direction, GN-based systems have received considerable attention for the detection of heavy metal ions, notably Mercury ion [58-60]. Colorimetric approaches reported for Hg^{2+} ion detection mainly employ Au and Ag nanoparticles. Nay Ming Huang and co-workers designed Graphene oxide based silver system for this purpose [61]. Dithia and Diaza stabilized Au nanoparticles [62] and Tween 20-stabilized Au nanoparticles [63] have also been reported for Hg^{2+} ion detection. However, high cost of these systems limits their practical applications, and demands alternatives for them. Though the aforesaid nano sensors help us to monitor and detect analytes even with naked eyes and limit down to pico molar levels, there is always a cry to substitute cuvette based approach for sensing with solid phase sensors. Conventional cuvette based strategy is inconvenient and cannot be employed as a portable layman's tool for real on site detection of analytes and hence, there lies huge prospects of solid phase portable sensors. Alternatively, creating immobilized solid sensors could be another approach for the colorimetric detection of Hg^{2+} ions, while also

providing excellent stability and usability, especially from a practical point of view. Solid phase sensor strips have huge prospects as it can be employed in basic laboratory kit and in household use as commercial indictors. Several small molecules have been reported for their detection of Hg^{2+} upon chemical immobilization onto a substrate surface, despite of the tremendous development in material science, only few reports are available on the fabrication of solid phase sensors for Hg^{2+} [64-67] .

Recently, the union between GRO/RGO with organic dye has carved a new formula for sensing Hg^{2+} ions. In this direction, graphene, more scientifically GN derived by chemical reduction, has exceptional optical properties to its credit. Graphene based materials exhibits high optical transparency, high surface to volume ratio and can exploit non covalent interactions to interact with many molecules. All these traits project the capacity of graphene materials in optical sensing of various analytes. Motivated by the potential of Graphene-Dye hybrids, we intended to fabricate GN-dye hybrids as a sensor for relevant analytes. Graphene enters into noncovalent interactions with dye molecules forming supramolecular assemblies which can be fine tuned to sense various biological and chemical analytes. Our present study has its roots in a work reported by Zhang et al. wherein they have revealed interesting interactions between GN and various organic dyes. Quite a good quantum of research has been devoted to the use of Graphene and its hybrids as optical sensors based on fluorescence resonance energy transfer (FRET) as well as on its selective absorption

capacity [68]. The proposed detection through optical methods is based on the interaction of GN between the dye and the Hg^{2+} ions, which relys on the layman's phenomenon, adsorption. Literature survey hints to the extensive use of these dyes as sensors for several moieties notably in heavy metal sensing. We have opted Rhodamine (RD) and Fluorescein (FLR) as model dyes, as they are well acclaimed surface active compounds for optical sensing because of π–π interaction and other noncovalent interactions. RD and FLR based probes exhibit excellent variations in absorption and fluorescence intensity on interaction with metal ions. Besides, these dyes are readily available and are quite convenient to monitor their absorption spectra. This study exploits the unique ability of GN in selectively adsorbing Hg^{2+} over RD and FLR. It is a well-known observation that the interaction of GN reduces the intensity of optical characteristics of RD and FLR. Our efforts are directed to break this weak physical interaction between GN and RD with Hg^{2+} ion, an entity capable of replacing dye molecules by entering into interaction with Graphene. This forms the basis of the optical sensing protocol.

Herein, we project Graphene-Dye hybrids [Graphene-Rhodamine unit (GRD) & Graphene-Fluorescein unit (GFU)] that offer quick, selective and sensitive optical response to the presence of a noxious heavy metal ion, mercury (Hg^{2+}) in aqueous solution. The working of the sensing unit was followed using UV-Vis absorption spectroscopy and Fluorescence spectroscopy. The selectivity of the systems toward other interfering ions was also examined. In addition to

this, a reversible INHIBIT logic gate dependent on Hg^{2+} ions and EDTA has also been designed. Subsequently, an attempt is demonstrated here to tailor the GN-Dye immobilized solid phase sensor as chemical strips for visual detection of ultra trace amount of Hg^{2+} ions. A detailed discussion about the Experimental procedure and the methodologies adopted for Hg^{2+} sensing is provided in Chapter 2.

5.4 Results and Discussion

5.4.1. Graphene–Dye Array Based Colorimetric Hg^{2+} Ion Sensing Strategy

The projected sensing strategy through optical methods is based on the non covalent interaction of GN between the dye and the Hg^{2+} ions, which works on the layman's phenomenon, adsorption. The conjugation of GN with Dye molecules significantly quenches the optical characteristics (UV-Vis absorption and Fluorescence) of the dye molecules owing to the formation a supramolecular complex between GN sheets and the dye molecules. The possible noncovalent modes of interaction between GN and Dye molecule is illustrated in Fig.4. Any entity capable of breaking this supramolecular complex brings significant changes in the optical response of the complex and hence the Graphene-Dye unit can act as a sensor for the said moiety. Interestingly our investigations revealed that Hg^{2+} ion could break this supramolecular complex and could rejenuvate the quenched optical response of the dye and this forms the crux of the sensing strategy. As mentioned earlier, Rhodamine 6G and Fluorescein was taken as our model dyes for the sensing unit. Fig.5 (a) & 5 (b) depicts the UV-Vis response of RD and FLR on titrating with GN solution. The

absorbance intensity decreases with increase in concentration of GN and this stage is designated as 'turn off' state [71]. The high efficiency quenching is believed to be the result of noncovalent binding of the dye molecules on the graphene surface leading to the formation of a supramolecular complex of graphene and dye according to the equation:

$$nD + GN \leftrightarrow (GN \cdot \cdot \cdot D)n$$

With the addition of GN, the absorbance of dye molecules decreases due to the formation of a non covalent complex of Graphene-Dye unit. As the addition of GN continues, a sandwich type complex is formed. The interplay between π-π stacking forces and dispersion forces of GN with dye molecules guarantees the close proximity leading to effective adsorption of dye and quenching of optical response.

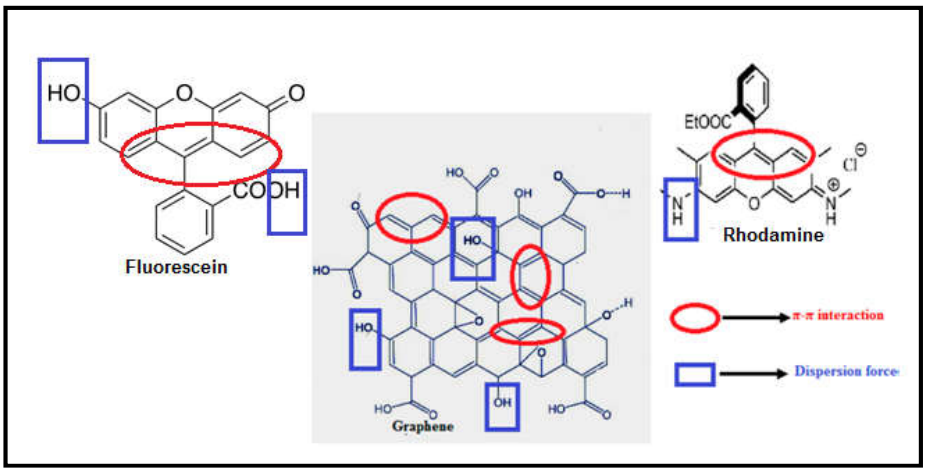

Figure 4. Possible modes of noncovalent interaction with Graphene and Dye molecules

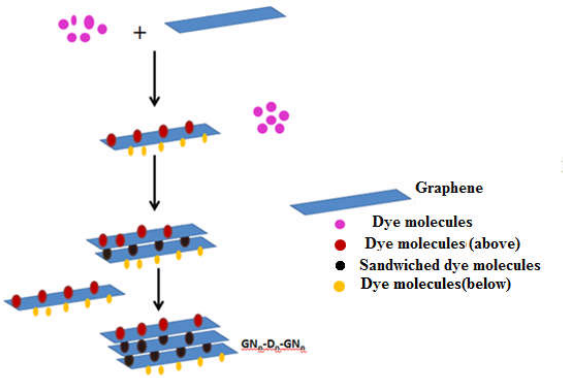

Scheme 1: Schematic representation of the complex formation between graphene sheets and dye molecules.

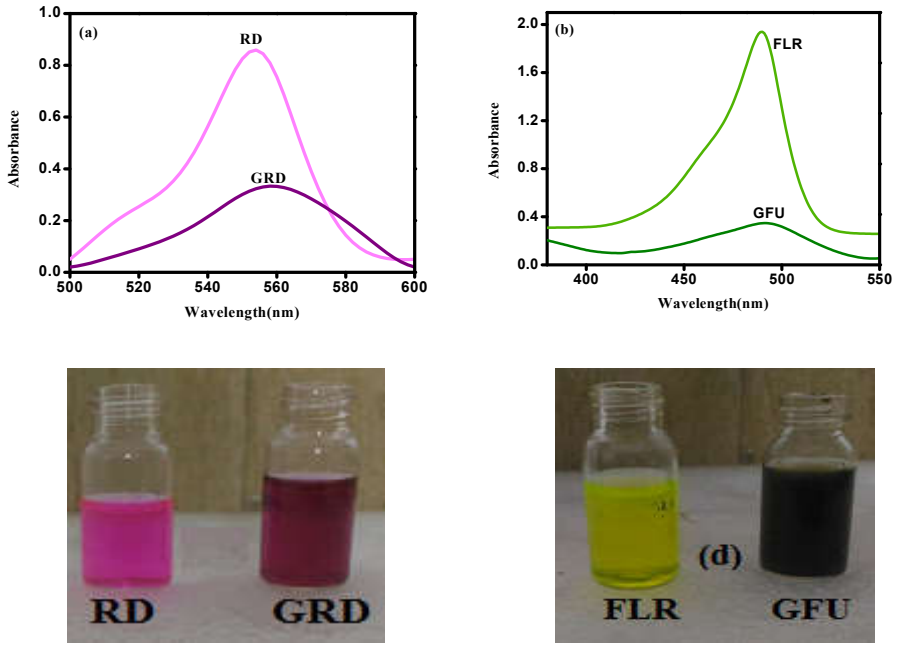

Figure 5. (a) UV-VIS spectra of RD on addition of GN [RD (10μM, 1mL) + GN (140μL)]; (b) FLR (10μM, 1 mL) on addition of aliquots of GN (110 μL); (c) Digital images of RD and GRD and (d) FLR and GFU.

(ii)Selectivity of Graphene-Dye unit

To start with, various ions (Hg^{2+} , Cd^{2+} , Pb^{2+} , Cu^{2+} , Zn^{2+} , Na^{+} , Ca^{2+} , Fe^{3+} , K^{+} , Sr^{2+} , Ba^{2+}, and Ni^{2+}) have been screened for the affinity towards GD unit. Surprisingly, no ion except Hg^{2+} could affect considerable restoration of the absorbance spectra of GD unit [Fig. 6a & 6b]. The suppressed absorbance of GD unit was almost rejeunvated to its initial value on titrating with Hg^{2+} ions. Although the congeners of mercury i.e. Cd, Pb, Zn and also K restored the suppressed absorbance intensity, the restored intensity was practically negligible (less than 2%) when compared to that affected by Hg^{2+}. For interference testing, all metal ions (including and excluding Hg^{2+} ions) were mixed to form solution and were titrated against GD. Mixed solution without Hg^{2+} failed to revoke the suppressed absorbance value of GD, whereas the mixed solution with Hg^{2+} could affect restoration of the absorbance maxima. These investigations assessed and underlined the selectivity of GD towards Hg^{2+} ions over other common interfering metal ions. The selectivity of the proposed system is found to be commendably superior as when compared to similar systems for mercury sensing, which further increases the relevance of the study**.** The coordinating ability, appropriate ionic radius, and charge density of Hg^{2+} ions are suggested to be decisive behind this highly selective response [72]. It is quite clear that the unit exhibited admirable selectivity towards Hg^{2+} in presence of other interfering ions, pointing the ability of the projected appliance to function in a complex environment [73].

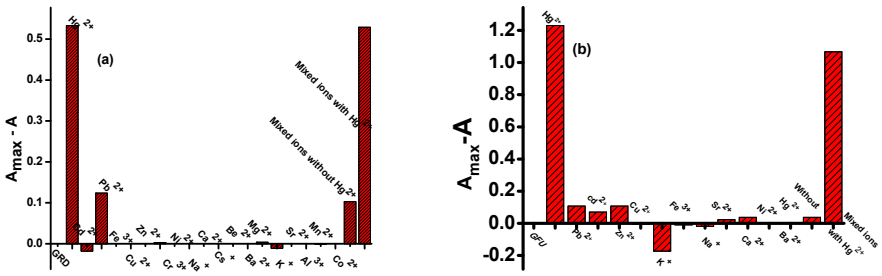

Figure 6. Selectivity of (a) GRD [metal ions: 160 µL, 100 µM)] and (b) GFU [metal ions: 150 µM, 180 µL] sensor toward Hg^{2+} ion over other metal ions and in a mixture of metal ions. A_{max} represents the absorption maxima of the restored curve of GRD/GFU array after addition of Hg^{2+}. A represents the absorbance maxima after addition of metal ions.

(iii)Graphene-Dye unit as optical probe for Hg^{2+}

(a)UV-Vis spectrometric route

The mercury ion sensing ability of Graphene-Dye (GD) assay was thoroughly investigated from the variation of absorbance intensity of GD unit when in the contact with the test ion. The intensity of absorbance of Rhodamine and Fluorescein centered at 554 nm and 489 nm respectively, enhanced upon addition of Hg^{2+} ions. A turn on state is recognized with the titration of Hg^{2+} ions against the GD unit as the absorption spectra of dye restored its original path, illustrating that colorimetric strategy can be successfully adopted for detecting the presence of Hg^{2+} ions [Fig.7 (a) and (b)]. The viability of the sensing route was elucidated using EDTA as the coordinating ligand. The removal of dye molecules from Graphene by Hg^{2+} ions was examined

by eliminating Hg^{2+}ions using ethylene diamminetetraacetic acid (EDTA) as the coordinating ligand, which due to its strong affinity toward metal ions, remove Hg^{2+} ions from Hg^{2+} /GN system [74]. This in turn enables the reunion of GN and Dye (turn-off state), thus lowering the intensity of absorbance maxima again [Fig.7 (c) and7 (d)]. Nitrogen atoms on EDTA have a greater tendency to form metal complexes by donating the lone pair of electrons when compared to the oxygen functional groups on Graphene. Moreover, according to the trend in electro negativity, formation of complex will be more facile from Nitrogen atom than Oxygen atom. Hence, EDTA preferentially binds to Hg^{2+} ion, releasing the ion from Graphene. To probe the sensitivity of the GD unit toward Hg^{2+}, the change in absorbance of the solution in the presence of various concentrations of Hg^{2+} was investigated, maintaining all other experimental parameters the same. The variations in intensity of the absorbance maximum were carefully investigated to ascertain the sensitivity and detection limit of the array. Both the dye systems yielded a linear calibration curve enabling the service of GD units as a quantitative readout tool for Hg^{2+} sensing. For GRD unit, the proposed array exhibited a perfect linear variation in absorbance over Hg^{2+} concentration of 0 nM to 1000 nM enabling its use as a quantitative tool for determination of Hg^{2+} at very low concentrations [Fig. 7(e)]. The lower limit of detection as calculated by 3 δ /m rule (δ is the standard deviation and m is the slope) was found to be as low as 2 ppb which is highly commendable when compared to

similar systems for Hg^{2+} detection. Further investigation using higher amount of graphene in RD solution of the same concentration (so as to lower the absorbance maximum of the dye solution) indicated that this linear variation is valid in higher concentration range also.

In the case of GFU unit, a linear correlation existed between the absorbance intensity and the concentration of Hg^{2+} [Fig. 7(f), R^2=0.98].The GFU exhibited Limit of detection (LOD) of 240 ppb as calculated by 3δ/m rule and the projected unit can function as a colorimetric quantitative tool for Hg^{2+} determination in unknown samples. The LOD value exhibited by the unit was almost comparable or further lower than several of the colorimetric sensors reported previously [75-84]. The Graphene-dye units outweigh the performance of other reported colorimetric sensors as it is highly specific with a notable LOD value and it does not demand complex modification steps, masking/buffering agents.

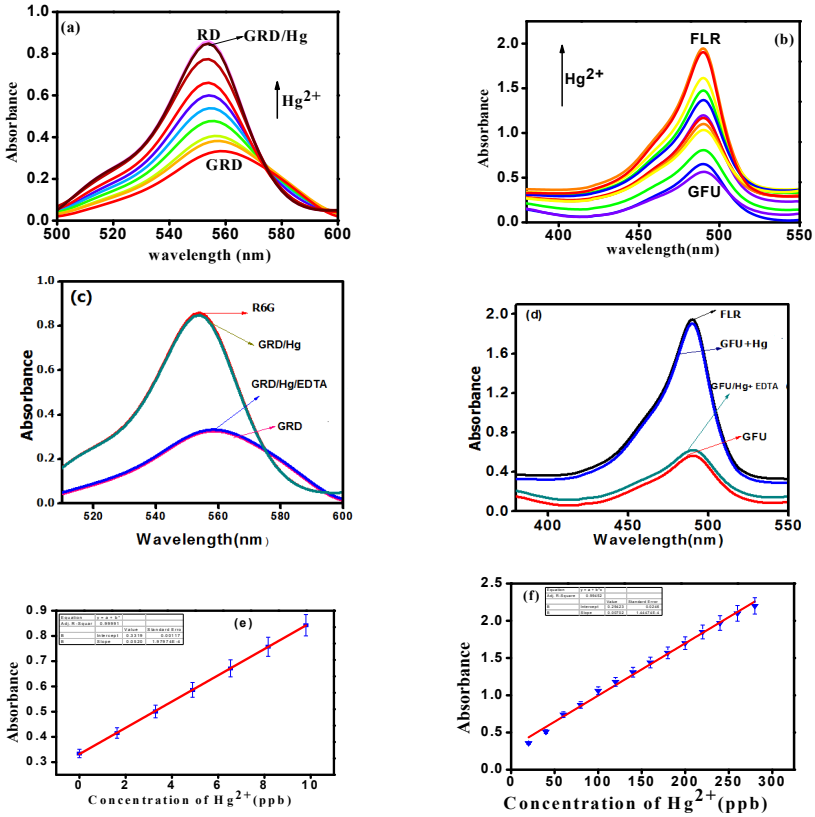

Figure 7 . Restoration of absorbance maxima of GRD (a) & GFU (b) array on addition of Hg^{2+} ions. [Concentration of Hg^{2+} from bottom to top :GRD unit: 0 ppb, 1.63 ppb, 3.29ppb, 4.89 ppb, 6.53 ppb, 8.16 ppb, 6 ppb, 9.17 ppb, 12 ppb; GFU unit:20, 40, 60, 80, 100, 120, 140, 160, 180, 200, 220, 240, 260, 280 ppb] Elucidation of sensing mechanism by addition of EDTA (c) GRD unit (EDTA: 150 µM, 100 µL) & (d) GFU unit. [EDTA: 200µM, 250µL] .Quantitative variation in absorbance of GD units and concentration of Hg^{2+} ion (e) for GRD unit [concentration of Hg^{2+}0 ppb, 1.63 ppb, 3.29ppb, 4.89 ppb, 6.53 ppb, 8.16 ppb, 6 ppb, 9.17 ppb and (f) GFU[20, 40, 60, 80, 100, 120, 140, 160, 180, 200, 220, 240, 260, 280 ppb].

(b) Fluorimetric Route

To extend the workability of the sensing unit in a more sensitive and reliable scenario, the spectral measurements were investigated using Fluorescence spectroscopy by following the same procedure. The fluorescence characteristics of GD unit were significantly modified by the presence of Hg^{2+}. Fig. 8(a & c) represents the fluorescence restoration of GD on addition of Hg^{2+}. Complete restoration of quenched fluorescence intensity was achieved upon addition of ppt amount of Hg^{2+} ions (turn –on state). The calibration graph drawn by plotting the variation of photoluminescence intensity followed a linear fashion with the concentration of Hg^{2+} ions [Fig.8(c & d)]. This proves the prospects of GD units as a quantitative fluoroprobe for Hg^{2+} ion detection in unknown samples. The system exhibited very high selectivity toward the ion of our interest, and the trend in selectivity toward other metal ions chosen followed the same order as that of colorimetric approach. Being a more sensitive technique, fluorimetry yielded a much low LOD value of 380 ppt and 780 ppt for Graphene-Rhodamine unit and Graphene-Fluorescein unit respectively. This significantly low LOD value asserts the supremacy of GD units in mercury sensing when matched with previously reported Hg^{2+} fluorimetric chemo sensors [85-88]. Notably, the LOD exhibited by the unit was much lesser than the LOD prescribed by European Union. This significant low LOD value asserts the exceptional efficiency of GD units in the heavy metal ion sensing scenario.

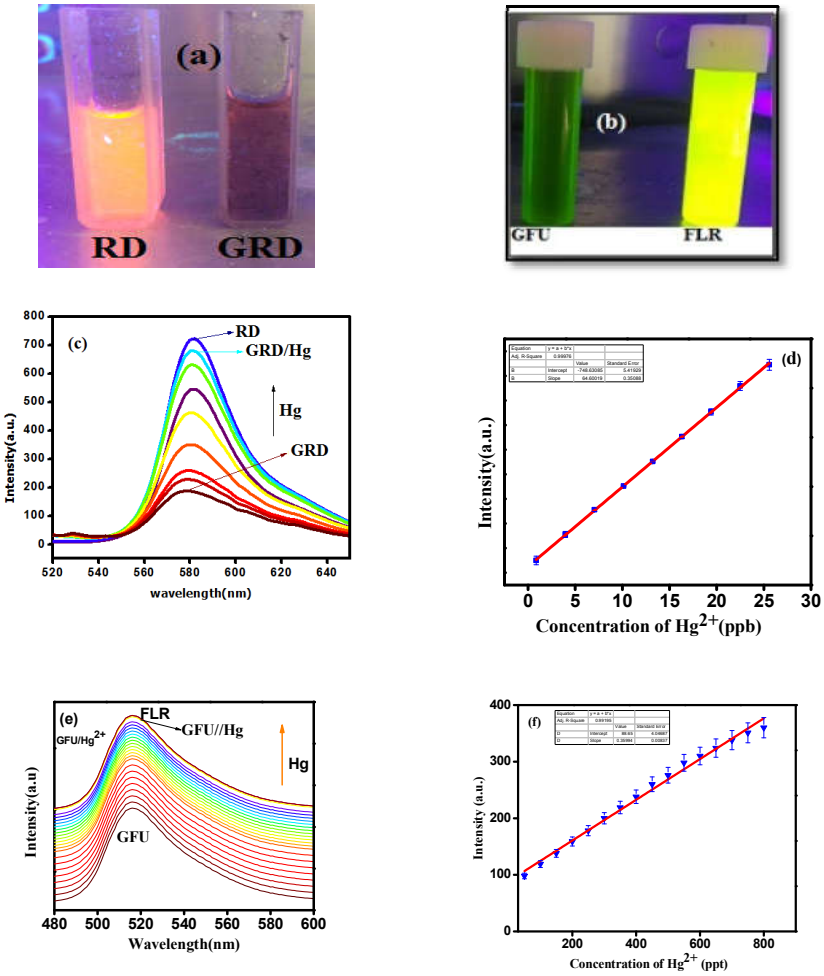

Figure 8. Digital images of (a) RD and GRD; (b) FLR and GFU under UV light. Restoration of fluorescence intensity of GRD (c) and GFU (e) array on addition of Hg^{2+} ions. [GRD unit:RD (1 µM,1 mL), GN (140 µ L), [Hg^{2+}] from bottom to top 0 ppt, 870 ppt, 3.87 ppb, 6.1 ppb, 9.23 ppb, 12.01 ppb, 15.20 ppb, 18.33 ppb, 21.0 ppb; Excitation wavelength: 550 nm, Slit width: 1nm; [GFU:FLR (1 µM,1 µL),GN(150 µ L) ,[Hg^{2+}] from bottom to top 50, 100, 150, 200, 250, 300, 350, 400, 450,500, 550, 600, 650, 700, 750, 800 ppt; Excitation wavelength: 460 nm, Slit width: 1nmVariation of fluorescence intensity of GRD (d) and GFU(f) with and concentration of Hg^{2+} ion.

Fig.9 shows the impact of various ions on GFU in day light. There was a visible colour change in the GFU from dark green to pale green on addition of Hg^{2+} ion along with the separation of Graphene sheets. No such observation was true for other ions selected (chosen randomly) and also for GRD unit. Interestingly, an amount of Hg^{2+} at a concentration as low as 20 ppm could be detected using this moiety. This opens up a route for visual naked eye detection of the ion, as drastic colour variation was observed for the GFU solution in presence of the said ion.

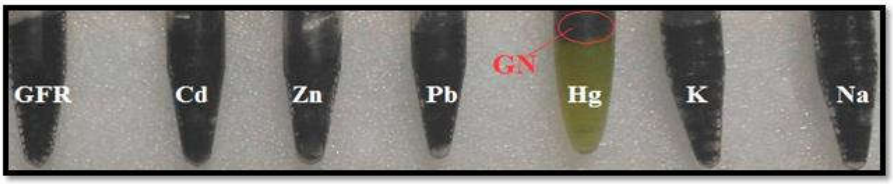

Figure 9. Impact of some environmentally relevant ions on GFU. A visual colour change from dark green to pale green is noted on addition of Hg^{2+} ions. (FLR: 1 µM, 10 µL), GN (2 µL), Metal ions (15 ppm).

(iv)Sensing Mechanism

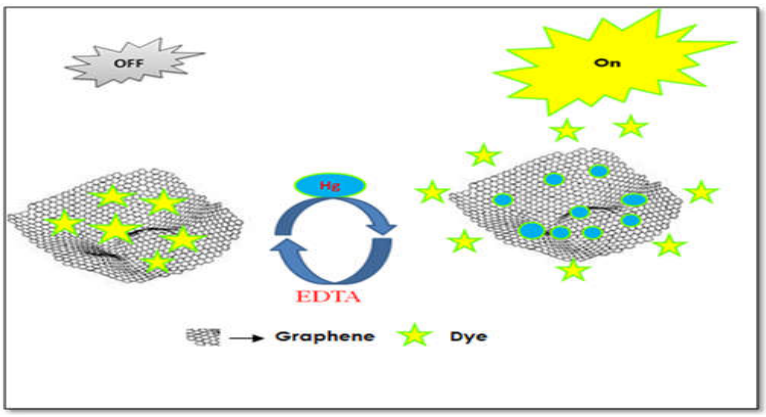

Scheme 1: Schematic representation of the sensing mechanism

The probable sensing can occur via the displacement of dye molecules from the GD unit with the entry of Hg^{2+} ion as a result of selective adsorption on graphene sheets. The principle underlying this sensing strategy relies on the nature of Graphene sheets to act as an absorbance/fluorescence nanoquencher and a highly specific nanosorbent. Initially, Graphene binds with dye molecules by noncovalent forces forming a supramolecular assembly i.e. $(GD)_n$. The noncovalent forces responsible for the formation of GD unit is the (i) π-π interaction between the aromatic clouds of Graphene and Dye molecules; (ii) the dispersive interaction between negatively charged functional groups on Graphene and the chromophore of dye molecules [89]. As a result of adsorption of dye molecules by GN, the excited state energy of the dye molecule is transferred to Graphene and hence quenches fluorescence via FRET. As the selective adsorption of Hg^{2+} ion disrupts this weak interaction between Graphene and Dye, the absorption spectra of Dye is restored as the concentration of free dye increases with increase in concentration of Hg^{2+} ions. The evolution of GD will leads to the suppression of absorbance and fluorescence intensity of dye (turn-off state), as the amount of free dye molecules in the solution decreases. When the strong competitor i.e. Hg^{2+} with higher affinity towards Graphene sheets than dye (weak competitor) is added to GD, Hg^{2+} will be preferentially adsorbed over dye by GN. As dye molecules are gradually desorbed from the surface of the supramolecular assembly, the absorbance and fluorescence intensity will be restored [Fig.10]. The π electrophilicity of Hg^{2+} towards the π cloud of graphene plays a pivotal role for the absorption of Hg^{2+} ion.

Graphene can selectively adsorb Hg^{2+} ion leading to the restoration of optical characteristics of dye. It was found that there were no significant changes in the absorption spectra of dye even after addition of 200µL of Hg^{2+} ion, which rules out the possibility of interaction between the dye and metal ion. The reason behind the unusual affinity of graphene towards Hg^{2+} is not clear till date. Theoretical calculations suggest that Hg^{2+} are adsorbed on T-site of graphene and the equilibrium distance of Hg^{2+} from graphene surface is with the interlayer distance of graphene obtained from XRD and SAED analysis, which favours the adsorption of Hg^{2+} on GN surface. The binding energies obtained also assist the adsorption of Hg^{2+} ions. Moreover, the coordinating ability, appropriate ionic radius, and charge density of Hg^{2+} ions are suggested to be decisive behind this highly selective response.

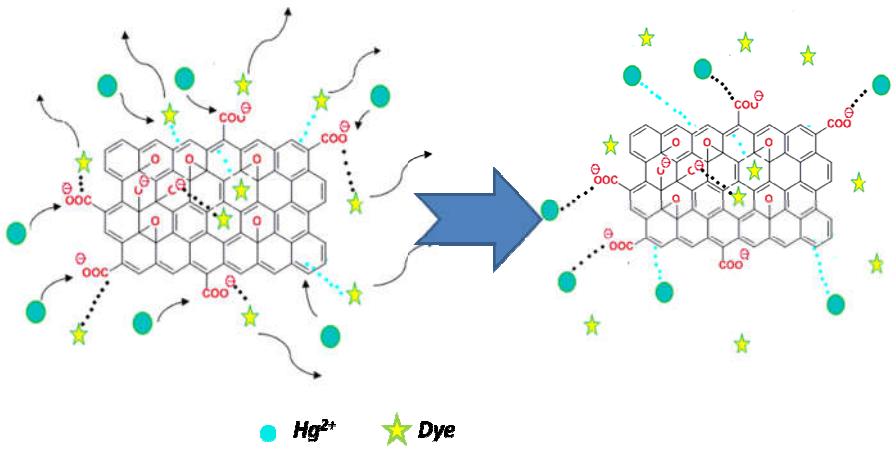

Figure 10. Pictorial representation depicting the interaction between Graphene sheets, Dye molecules and Hg^{2+}. Hg^{2+} interacts with GN and displaces dye molecules.

On account of the structural similarity between Fluorescein and Rhodamine as well as similar interactions with GN, we felt that a comparison between the two GD systems will be highly logical. The limit of detection (LOD) values exhibited by the Graphene-Rhodamine array were 2 ppb and 380 ppt for colorimetric route and fluorimetric route respectively, while Graphene-Fluorescein unit exhibited higher LOD values (240 ppb and 780 ppt by colorimetric and fluorimetric route respectively) than the graphene –rhodamine array making GRD more appreciable. This can be justified in the manner as explained hereafter. It is obvious that Rhodamine with more π conjugation will interact more strongly with graphene. This is again verified by the change in optical properties of the dyes with the addition of graphene. Fig.11 reveals that the same amount of graphene led to more depression of absorbance in the case of Rhodamine than that of Fluorescein for the same concentration of dyes. This in turn indicates that same amount of GN released from the graphene-dye complex in presence of a definite amount of Hg^{2+} ion will restore the absorbance maximum to a higher extent in the case of Rhodamine [Fig.11]. It is quite clear that this will lead to a lower value of LOD in the case of graphene-rhodamine array. This also opens up the scope of examining the interaction of graphene with dyes having more extensive π conjugation, which may pave way to more brilliant Hg^{2+} sensors.

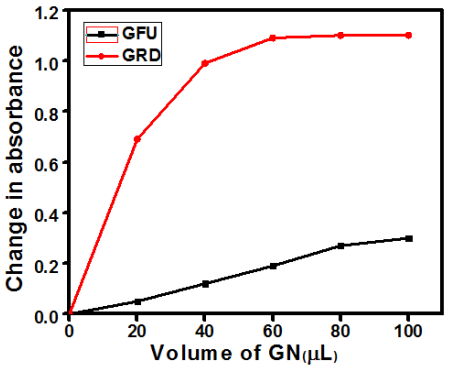

Figure 11. Simultaneous changes in absorbance of GFU & GRD on addition of GN [RD:10μM,1 mL:FLR:10μM,1 mL]

(v)Graphene-Dye immobilised solid phase sensors for Hg^{2+}

Encouraged by the above results, we immobilised the graphene-dye units onto filter paper strips, which paved the way to easy to use strip sensors. Immobilisation of GD array on filter paper strip was achieved as explained in the experimental section. As shown in Fig.12 (a) & (b), under UV illumination the filter paper strips restored its colour (turn on) with the addition of Hg^{2+}. It was noticed that the OFF stage with the immobilization of Graphene-dye unit on the filter paper strip was turned ON with the addition of Hg^{2+} ions. The proposed filter paper strip serves as an elite and handy solid phase sensor for Hg^{2+} ion, which demands the mere presence of a UV source to selectively spot the presence of Hg^{2+}. The limit of detection for Graphene-Rhodamine strip and Graphene-Fluorescein strip under UV light illumination was found to be 870 ppt and 20ppb respectively, which outweighs the performance of several other Hg^{2+} strips in terms of its performance, cost effectiveness, simplicity, stability etc. The

restoration of purple and greenish yellow emission for GRD and GFU respectively revealed the successful service of this solid phase sensor in ppt and ppb level detection of mercury ions. The projected graphene-dye filter paper strips serves as an elite and handy solid phase sensor for Hg^{2+} ion, which demands the mere presence of a UV source to selectively identify the latter. To the best of our knowledge, no report is there in the literature till date, which focuses on GD based solid phase Hg^{2+} sensors. Though some reports are there using other systems based on bis (ferrocenyl) azine, porphyrin, conjugated polymer etc, they fail in competing with the simplicity, efficiency, cost effectiveness and user friendliness of the system reported herein [78-80]. The filter paper strips yielded Hg^{2+} ion-sensing recognition for both cost- and energy-saving systems. We believe that these opto strips can revolutionize the consumer and industrial world with the introduction of the probe surface-mount naked-eye graphene-dye strips.

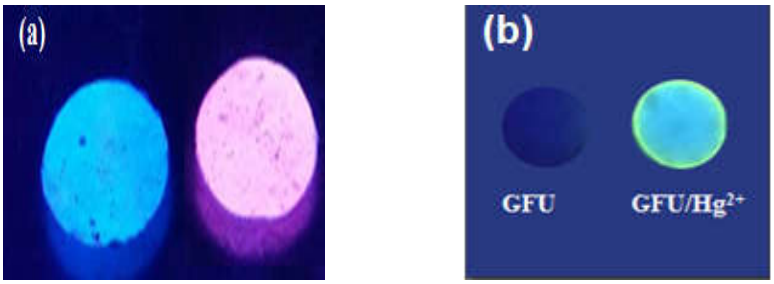

Figure 12. Performance of GRD (a) and GFU (b) unit as a fluorimetric sensor strip for Hg^{2+}. The fluorescence restoration was attained with 870 ppt and 20 ppb of Hg^{2+} ion for GRD and GFU unit respectively under UV light.

(vi) Graphene-Dye unit as real time Mercury ion sensor

As the proposed unit exhibited excellent selectivity and sensitivity in deionised water, the practicability and analytical capability of graphene-dye units were tested with tap water by spiking a known amount of Hg^{2+} ion into tap water and well water. Fluorescence being the more sensitive technique, we opted it for the real sample analysis. Consequently, the fluorescence response of graphene-dye was followed on addition of aliquots of tap water and well water contaminated with mercury ion. It was demonstrated that the suppressed fluorescence intensity of graphene-dye was restored on addition of tap/well water spiked with Hg^{2+} ion. The restoration of optical characteristics by fluorimetric techniques indicates the utility of the proposed graphene-dye in real samples. It was quite soothing to note that the error % of the analysis was less than 5% [Table 1].

GRD			GFU		
Source	Actual (ppt)	Measured (ppt)	Source	Actual (ppb)	Measured (ppb)
Tap Water	800	810	Tap Water	10	12
Well Water	800	820	Well Water	10	20

Table 1: Graphene-Dye units as real time sensor

The findings of our investigation suggest the efficiency of the proposed sensor moiety and establishes its supremacy over several established probes as shown in Table 2.

Sensing Unit	*Limit of detection*	*Reference*
Fluorescent aptamer-functionalized graphene oxide	0.18 ppb	90
Glucose-Based Rhodamine Fluorescent sensor	1 ppb	91
Silver@graphene oxide	100μM	92
Metal-oxo clusters	30 ppb	93
Rhodamine-based fluorescent chemosensor	1ppb	94
Au-based Rhodamine sensor	20 ppb	95
Rhodamine based silyl probe	20 ppb	96
Reduced Graphene Oxide with Functionalized Gold Nanoparticles	40 ppb	97
Graphene-Rhodamine unit	380ppt	This work
Graphene-Fluorescein unit	780 ppt	This work

Table 2. Comparision of graphene-dye probes over other established sensors

(vii) Graphene-Dye logic gates

In addition to this, a reversible INHIBIT logic gate dependent on Hg^{2+} and EDTA has also been designed, which will be usable for extending the potential of the proposed system. The advent of molecular logic gates has set the way for molecular scale computers and automated chemical systems [98]. In this article, we propose a molecular logic inhibit gate using Boolean algebra. The INHIBIT gate has two inputs (A, B, which in the present case represents Hg^{2+} and EDTA) and an output (here, the absorbance maximum of GD). The criterion for the INHIBIT logic gate is that when either input is on, the gate is off. Switching on input A turns the gate on. Turning on input B alone does not switch the gate on. In addition, switching both inputs on

makes the gate in the off position. Thus, input B inhibits the gate from responding to input A. Here, Hg^{2+} (input 1) and EDTA (input 2) are the two inputs which function through the GRD array. The presence of the inputs is defined as 1 while their absence as 0.The absorbance was defined as the output (1 or 0, corresponding to maximum absorbance and minimum absorbance) (Fig.13a). The truth table for the proposed INHIBIT logic gate is shown in Fig. 13b. The four possible input combinations for $Hg^{2+}$and EDTA are (0, 0), (1, 0), (0, 1), and (1, 1). Without Hg^{2+}or EDTA (corresponding to (0, 0), the absorbance maximum (Abs max of graphene-dye array (output) is 0 (Abs max decreases).On addition of Hg^{2+} alone to the graphene-dye array (1, 0) the Abs max increases sharply leading to an output (1) [turn-on]. Addition of EDTA alone (0, 1) does not increase the absorbance maxima of graphene-dye array, leading to an output value (0).On subjecting the two inputs simultaneously (1, 1), the output was zero. Thus, the requirements for an INHIBIT gate are met with.

(a)

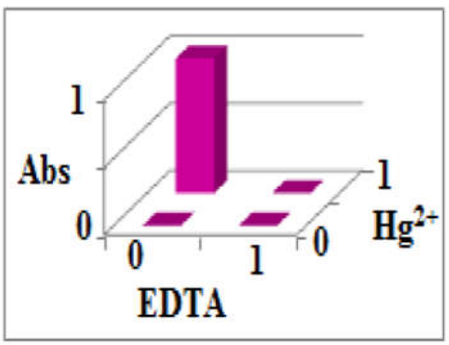

(b)

INPUT		OUTPUT
Hg^{2+}	EDTA	Abs_{max}
0	0	0
1	0	1
0	1	0
1	1	0

Figure 13. (a) An INHIBIT logic gate system based on GRD using both $Hg^{2+}$and EDTA as inputs and (b) Truth table for the inhibit logic gate

5.5. Concluding Remarks

- We have illustrated that Graphene-Dye units (Graphene-Rhodamine and Graphene-Fluorescein unit) can effectively function as an effective Hg^{2+} ion sensor via colorimetric and fluorimetric channels.

- The dual nature of Graphene to undergo noncovalent interactions viz. π-π and dispersive interactions with the dye molecules and to act as a specific adsorbent for Hg^{2+} is conceptualized in this study.

- The core behind the sensing of Hg^{2+} ion by the Graphene –dye unit lies in the decrease in absorbance/fluorescence intensity of the dye on combining with GN sheets and the corresponding restoration of the optical response upon highly selective competitive adsorption of Hg^{2+} ions by graphene sheets.

- The credibility of the mechanism was proved using EDTA as the complexing ligand. It is to be noted that all the optical variations occurred in the visible scale of the electromagnetic spectrum.

- Quantification of these optical responses was attained by colorimetric and fluorimetric measurements, which yielded ppb level and ppt level mercury ion assay.

- The linear calibration curve obtained by plotting absorbance/fluorescence intensity against the concentration of

Hg^{2+} ion facilitated the service of the unit as a quantitative readout tool for detection of Hg^{2+} ion in unknown samples.

- The limit of detection for Graphene-Rhodamine unit was found to be 2 ppb and 380 ppt via colorimetric and fluorimetric route respectively.

- The limit of detection for Graphene-Fluorescein unit was 240 ppb and 780 ppt through colorimetric and fluorimetric channels respectively.

- The commendable selectivity of the array towards Hg^{2+} ion has been investigated by observing the optical response in presence of other environmentally relevant metal ions.

- The significant advance in this investigation is the fabrication of Graphene- Fluorescein unit as a qualitative read out tool for naked eye detection of Hg^{2+} ion in ppm levels noting the colour and for the visual detection of ppt levels of Hg^{2+} through fluorescence in UV light.

- A highly efficient Graphene-Dye immobilized filter paper strip was developed which could sense Hg^{2+} under UV light in a concentration as low as ppt level and ppb level for Graphene-Rhodamine and Graphene-Fluorescein unit respectively.

- The fabrication of these optoprobes into ordered nano sensor strips transformed the graphene-dye systems into smart, simple and portable laboratory assays.

- A reversible turn off and turn on INHIBIT logic gate has been proposed which extends the scope of the designed array for the development of automated chemical systems.

- Our investigation warrants the bright prospects of Graphene-Dye units as an effective detection tool for the hazardous metal ion, Hg^{2+}.We believe that the scope of examining the interaction of graphene with dyes having more extensive π conjugation, will pave way to more brilliant Hg^{2+} sensors.

5.6 References

[1] Y. X. Huang, D. Cai and P. Chen, *Anal. Chem*., 2011, 83, 4393.

[2] T. Asefa, C. T. Duncan and K. K. Sharma, *Analyst*, 2009, 134, 1980.

[3] Y. X. Huang and P. Chen, *Adv. Mater.,* 2010, 22, 2818.

[4] Y. Q. Sun, Q. O. Wu and G. Q. Shi, *Energy Environ. Sci*., 2011, 4, 1113.

[5] D. A. C. Brownson, D. K. Kampouris and C. E. Banks, *J. Power Sources*, 2011, 196, 4873.

[6] Y. Q. Wu, Y. M. Lin, A. A. Bol, K. A. Jenkins, F. N. Xia, D. B. Farmer, Y. Zhu and P. Avouris, *Nature*, 2011, 472, 74.

[7] B. Arash, Q. Wang and W. H. Duan, *Phys. Lett. A*, 2011, 375, 2411.

[8] Perry T. Yin, Shreyas Shah, Manish Chhowalla, and Ki-Bum Lee, Design, *Chem. Rev*, 2015, 115, 2483.

[9] P.Avouris and C.Dimitrakopoulos, *Mater.Today* 2012,15, 86.

[10] F. N. Xia, T. Mueller, R. Golizadeh-Mojarad, M. Freitag, Y. M. Lin, J. Tsang, V. Perebeinos and P. Avouris, *Nano Lett*.,2009, 9, 1039.

[11] S. Pisana, P. M. Braganca, E. E. Marinero and B. A. Gurney, *IEEE Trans. Magn*., 2010, 46, 1910.

[12] B. Arash, Q. Wang and W. H. Duan, *Phys. Lett. A*, 2011, 375, 2411.

[13] A. Sakhaee-Pour, M. T. Ahmadian and A. Vafai, *Solid State Commun.,* 2008, 145, 168.

[14] Y. Wang, R. Yang, Z.W. Shi, L. C. Zhang, D. X. Shi, E. Wang and G. Y. Zhang, *ACS Nano*, 2011, 5, 3645.

[15] Hongmin Ma , Dan Wu , Zhentao Cui , Yan Li , Yong Zhang , Bin Du and Qin Wei, *Analytical Letters*, 2013, 46,1.

[16] W. Gao, L. B. Alemany, L. J. Ci and P. M. Ajayan, *Nat. Chem*.,2009, *1*, 403.

[17] Emanuele Treossi, Manuela Melucci, Andrea Liscio, Massimo Gazzano, Paolo Samorı`and Vincenzo Palermo Treossi, *J. Am. Chem. Soc.* 2009,131, 15576.

[18] Y Wang, D. Kurunthu, G. W Scott and C.J. Bardeen, *J. Phys. Chem. C,* 2010,114, 4153.

[19] H. Dong, W. Gao, F. Yan, H. Ji, and H. Ju, *Anal. Chem.* 2010, 82, 5511.

[20] J.Kim, L. J. Cote, F. Kim and J. Huang, *J. Am. Chem. Soc.,2010,* 132, 260.

[21] P. Singh, S. Campidelli, S. Giordani, D. Bonifazi, A. Bianco and M. Prato, *Chem. Soc. Rev*., 2009, 38, 2214.

[22] B. K. Gorityala, J. M. Ma, X. Wang, P. Chen and X. W. Liu, *Chem. Soc. Rev*., 2010, 39, 2925.

[23] Y. Wang, Z. H. Li, J. Wang, J. H. Li and Y. H. Lin, *Trends Biotechnol*., 2011, 29, 205.

[24] Xiaoding Lou, Daxin Ou, Qianqian Li and Zhen Li, *Chem. Commun*., 2012, 48, 8462.

[25] Xian-Fu Zhang, Su-Ping Liu and Xiao-Na Shao, *Spectrochimica Acta Part A: Molecular and Biomolecular Spectroscopy* ,2013, 113,92.

[26] Xue Wang, Shuhua Zhong, Yu He and Gongwu Song, *Anal. Methods*, 2012, 4, 360.

[27] Yongqian Xu, Andrey Malkovskiyb and Yi Pang, *Chem. Commun*., 2011, 47, 6662.

[28] Janardhan Balapanuru, Jia-Xiang Yang, Si Xiao, Qiaoliang Bao, Maryam Jahan,Lakshminarayana Polavarapu, Ji Wei, Qing-Hua Xu, and Kian Ping Loh, *Angew. Chem*. 2010, 122, 6699.

[29] Chun-Hua Lu, Huang-Hao Yang, Chun-Ling Zhu, Xi Chen, and Guo-Nan Chen, *Angew. Chem. Int. Ed.,* 2009, 48, 4785.

[30] Yan Shi, Wei Tao Huang, Hong Qun Luo and Nian Bing Li, *Chem. Commun*., 2011, 47, 4676.

[31] Haixin Chang, Longhua Tang, Ying Wang, Jianhui Jiang, and Jinghong Li, *Anal. Chem.* 2010, 82*,* 2341.

[32] Sheng Tian Huang, Yan Shi,a Nian Bing Li and Hong Qun Luo, *Chem. Commun*., 2012, 48, 747.

[33] Meng Liu, Huimin Zhao, Shuo Chen, Hongtao Yu, Yaobin Zhang and Xie Quan, *Chem. Commun.,* 2011, 47, 7749.

[34] Xiaowei Mao, Haiyan Su, Demei Tian, Haibing Li, and Ronghua Yang*, ACS Appl. Mater. Interfaces*, 2013, 5, 592.

[35] P. B.Tchounwou, W. K.Ayensu, N.Ninashvili and D.Sutton, *Environmental Toxicology,* 2003,18, 149.

[36] C. H. Lu, J. Li, M. H. Lin, Y. W. Wang, H. H. Yang, X. Chen and G. N. Chen, *Angew. Chem., Int. Ed*., 2010, 49, 8454.

[37] S. J. He, B. Song, D. Li, C. F. Zhu, W. P. Qi, Y. Q. Wen, L. H. Wang, S. P. Song,H. P. Fang and C. H. Fan, *Adv. Funct. Mater*., 2010, 20, 453.

[38] J. H. Jung, D. S. Cheon, F. Liu, K. B. Lee and T. S. Seo, *Angew. Chem., Int. Ed*., 2010, 49, 5708.

[39] C. H. Lu, H. H. Yang, C. L. Zhu, X. Chen and G. N. Chen, *Angew. Chem., Int. Ed*., 2009, 48, 4785.

[40] W. L.Clevenger, B. W.Smithand and J. D.Winefordner, *Crit. Rev. in Anal. Chem*., 1997, 27, 1.

[41] K. P. Carter, A. M. Young and A. E. Palmer, *Chem. Rev.*, 2014, 114, 4564.

[42] D. Sareen, P. Kaur and K. Singh, *Coord. Chem. Rev*., 2014, 265, 125.

[43] P. B. Tchounwou, W. K. Ayensu, N. Ninashvili and D. Sutton, *Environ. Toxicol*., 2003, 18, 149.

[44] K.Leopold, M.Foulkes, and P. Worsfold, *Anal. Chim. Acta*, 2010, 663, 127.

[45] D. Karunasagar, J. Arunachalam and S Gangadharan, *J. Anal. At. Spectrom*., 1998, 13,679.

[46] R. K., Mahajan, I .Kaur and T. S. Lobana, *Talanta*, 2003, 59, 101

[47] R. Puk and J. H, Weber, *Anal. Chim. Acta* , 1994, 292, 175.

[48] Z. Zhu, Y.Su, J. Li, D.Li, J.Zhang, S.Song, Y.Zhao, G. Li, and C. Fan, *Anal. Chem*., 2009, 81, 7660.

[49] A. Singh,S. Kaur, N.and Singh, N. Kaur, *Org. Biomol. Chem*., 2014, 12, 2302.

[50] Y.K. Yang, K.J. Yook and J. Tae, *J. Am. Chem. Soc.* 2005, 127, 16760.

[51] W.Huang, X. Zhu, D.Wua,C. He, X.Hu and C. Duan, *Dalton Trans*. 2009, 48, 10457.

[52] N. Kumari , N.Dey and S.Bhattacharya, *Analyst* , 2014, 139, 2370.

[53] S. H.Lee, A.Parthasarathy and K. S. Schanze, *Macromol. Rapid Commun*. 2013, 34, 791.

[54] L.Feng, J. Sha,Y. He, S. Chen, B. Liu, H. Zhang and C. Lü, *Microporous Mesoporous Mater.* 2015, 208, 113.

[55] T.M. Geng, Y.Wang and R.Y. Huang, *J. Fluoresc.* 2014, 24, 1207.

[56] T.M.Geng and D.Y.Wu, *Luminescence* 2015, 30, 1263

[57] J. Lee, H. Jun and J. Kim, *Adv. Mater*. 2009, 21, 3674.

[58] X.Cui, L. Zhu, J.Wu, Y. Hou, P. Wang, Z.Wang, Z and M. Yang, *Biosens. Bioelectron.* 2015, 63, 506.

[59] T. Zhang, Z. Cheng, Y.Wang, Z. Li, C. Wang, Y. Li and Y. Fang, *Nano Lett.* 2010, 10, 4738.

[60] J.H.An, S.J Park, O.S. Kwon, J. Bae and J.Jang, *ACS Nano,* 2013, 7, 10563.

[61] K.Zangeneh Kamali, A.Pandikumar, S.Jayabal, R.Ramaraj, H.N. Lim, B.H. Ong, C.S.D.Bien, Y.Y. Kee and N.M. Huang, *Microchim. Acta*. 2016, 183, 369.

[62] W.Chansuvarn and A. Imyim, *Microchim. Acta* 2012, 176, 57−64.

[63] C.Y Lin, C.J Yu, Y.H. Lin and W.L Tseng, *Anal. Chem.* 2010, 82,6830.

[64] Y. Zou, M. Wan, G. Sang, M. Ye and Y. Li, *Adv. Funct.Mater.,* 2008, 18, 2724.

[65] J. Lee, S. Mahendra and P. J. Alvarez, *ACS Nano*, 2010, 4, 3580.

[66] C. D´ıez-Gil, R. Mart´ınez, I. Ratera, A. T´arraga, P. Molina and J. Veciana, *J. Mater. Chem*., 2008, 18, 1997.

[67] E. Coronado, J. R. Gal´an-Mascar´os, C. Mart´ı-Gastaldo, E. Palomares, J. R. Durrant, R. Vilar, M. Gratzel and M. K. Nazeeruddin, *J. Am. Chem. Soc*., 2005, 127, 12351.

[68] Xian-Fu Zhanga and Fangfang Li, *Journal of Photochemistry and Photobiology A: Chemistry* ,2012, 246, 8.

[69] W. F. Linke, *Inorganic and Metal-Organic Compounds, American Cynamid Co*., 1958, 1, 1245.

[70] R. Spence, M. I. Morris and J. Barton, *Waste Management Conference*, 2003.

[71] Hui Ren, Dhaval D. Kulkarni, Rajesh Kodiyath, Weinan Xu, Ikjun Choi, and Vladimir V. Tsukruk, *ACS Appl. Mater. Interfaces* 2014, 6, 2459.

[72] J.Luo, S. S. Jiang, S.H Qin, H.Q Wu, Y. Wang, J.Q. Iang and X.X Liu, *Sens. Actuators, B.,* 2011, 160,1191.

[73] W. T Huang, Y.Shi, W.Y .Xie, H.Q. Luo and N.B Li, *Chem. Commun*., 2011, 47, 7800.

[74] S.Erdemir, O. Kocyigit and S. Malkondu, *J. Photochem. Photobiol., A* 2015, 309, 15.

[75] K. M. Shafeekh, M. K. A. Rahim, M.C. Basheer, C.H. Suresh and S. Das, *Dyes Pigm.,* 2013, 96, 714.

[76] A. A. G. Al Abdel Hamid, M. Al-Khateeb, Z.A. Tahat, M. Qudah, S.M. Obeidat and A.M. Rawashdeh, *Int. J. Inorg. Chem*., 2011, 2011, 1.

[77] A. Santhana Krishna Kumar and S.J Jiang, *RSC Adv*. 2015, 5, 6294.

[78] Y. Haiguang, X. Yuhao, Z. Peng, S. Linjing and Y. Fanggui, *Anal. Methods*, 2015, 7, 4596.

[79] M. R´emi, L. Isabelle, L. B´en´edicte and B. Valeur, *J. Mater. Chem.*, 2005, 15, 2965.

[80] Z. Wang, J. Heon Lee and Y. Lu, *Chem. Commun*., 2008, 45, 6005.

[81] Q. Zou, L. Zou and H. Tian, *J. Mater. Chem.,* 2011, 21, 14441.

[82] G. Aragay, H. Monton, J. Pons, F.-B. Merce and A. Merkoci, *J. Mater. Chem.,* 2012, 22, 5978.

[83] M. Li, Q. Wang, X. Shi, A. Hornak and N. Wu, *Anal. Chem*., 2011, 83, 7061.

[84] Y. Tachapermpon, P. Piyanuch, N. Prapawattanapol, K. Sukrat, K. Suwatpipat and N. Wanichacheva, *J. Chem*., 2015, 1.

[85] S. Erdemir, O. Kocyigit and S. Malkondu, *J. Photochem. Photobiol*., A, 2015, 309, 15.

[86] E. Coronado, J.R. Galan-Mascaros, C. Marti-Gastaldo, E. Palomares, J. R. Durrant, R. Vilar, M. Gratzel and M. K. Nazeeruddin, *J. Am. Chem. Soc*., 2005, 127, 12351.

[87] D. G. C´esar, A. Caballer, I. Ratera, A. T´arraga, P. Molina and J. Veciana, *Sensors*, 2007, 7, 3481.

[88] Z. Guo, J. Duan, F. Yang, M. Li, T. Hao, S. Wang, D. We and Z. Guo, *Talanta*, 2012, 93, 49.

[89] X. F. Zhang, S. P. Liu and X. Shao, *Spectrochim. Acta, Part A*, 2013, 113, 92.

[90] Ming Li, XuejiaoZhou, Weiqiang Ding, Shouwu Guo and Nianqiang Wu, *Biosensors and Bioelectronics*, 2013, 41, 889.

[91] Longxia Li and Zhijie Fang, Spectroscopy Letters, 2015, 48,578.

[92] K. Zangeneh Kamali, A. Pandikumar, S. Jayabal, R.Ramaraj, H. N. Lim, B.H. Ong, C.S.D. Bien, Y. Y Kee and N. M Huang, *Microchim. Acta.* 2016, 183, 369.

[93] Kun Chen, Shan She, Jiangwei Zhang, Aruuhan Bayaguud and Yongge Wei, *Scientific Reports* doi.10.1038/srep16316.

[94] Yao Liu, Er-Bing Yang , Rui Han , Di Zhang ,Yong Ye and Yu-Fen Zhao, *Chinese Chemical Letters*,2014,25,1065.

[95] C.C. Huang and H.T. Chang, *Anal. Chem.*, 2006,78,8332.

[96] Namita Kumari, Nilanjan Deya and Santanu Bhattacharya, *Analyst*, 2014, 139, 2370.

[97] Kehung Chen, Ganhua Lu, Jingbo Chang, Shun Mao, Kehan Yu, Shumao Cui, and Junhong Chen, *Anal. Chem*. 2012, 84, 4057.

[98] K. S.,Park,C. Jung and H.G. Park, *Angew. Chem., Int. Ed.* 2010, 49, 9757.

Part B

Graphene-Dye hybrids as potential sensor for fluoride ion in aqueous solution

5.7 Introduction and relevance of Fluoride ion sensing

The outstanding and tunable optical properties of Graphene crown it as an indubitable sensor motif for a bunch of analyte molecules namely heavy metals, anions, biomolecules etc [1] . Owing to the established roles of anions in a wide range of chemical and biological process, the development of chemosensors for anion recognition has become the need of the hour. Anions play vital role in DNA regulation, enzyme synthesis, hormones transport, protein synthesis etc. As representative examples, Fluoride, Cyanide, Halides etc. have aroused considerable interests in the field of chemosensors among the researchers. To devise easy to use sensors for the detection of anions like Fluoride, Cyanide, Iodide, Pyrophosphate etc. is a key research theme due to the pros and cons they present to our ecosystem [2] . Among the interests, Fluoride ion (F^-) being the smallest and the most electronegative anion is of pivotal significance owing to its established role in biological and chemical processes [3,4] . Fluoride is the most reactive anion is extensively found in all biological systems. Fluorides are released to the eco system by both natural and manmade sources. Naturally containing Fluoride in drinking water and fluoridated water comprises the major fluoride source to human beings. The prominence of Fluoride ion in drinking water is an issue of serious health concern. Optimum amount of fluoride will guard teeth from dental cries and increases the mineral deposition in bones. Skeletal

fluorisis will cause severe pain in joints and will lead to paralysis. Chronic ingestion of large doses of F^- causes grave neurodegenerative diseases affecting cellular metabolism even culminating to cancer, while deficient intake leads to dental cries, osteoporosis, kidney disorders etc. [Fig.1] [5] . Alarmed by this scenario, the Environmental Protection Agency and the World Health Organisation have laid down 1.5 ppm as the permissible amount of Fluoride ion in drinking water [6] . Summing up the adverse effects of F^-, a huge deal of attention has been devoted to the development of portable F^- sensors. The conventional and the widely used techniques namely Ion electrode analysis and F^{19} NMR analysis have never been celebrated as a layman's probe for F^- recognition on account of its low sensitivity, slow response time as well as the demand for well equipped laboratory with trained personal [7,8] . In this line, opto probes (Colorimetric and/or Photoluminescence sensors) have emerged as feasible alternatives to sense and monitor F^- levels. Generally, these opto probes rely on hard lewis acidity of F^- , wherein it acts as a disrupter or a participant for any F^- induced reactions that will generate a new optical signal or quenches / restores the inherent optical response of the unit (UV absorption/ Photoluminescence signal (PL)) which can be deciphered qualitatively and quantitatively to sense the presence of F^-. To quote a few representative studies in this regard, systems based on Boron-Fluoride interactions, silyl ether –fluoride interactions, π-π interactions and Hydrogen bonding interaction involving urea and thiourea, organometallic reactions involving metal ion binding sites etc.[9-15]. Though these recognition units are much idolised from economical and sensitivity view point, several issues needs to be addressed, namely complex organic reaction steps, interference from congeners and

inefficiency to operate in aqueous environment as its sensing is accomplished mainly from tetrabutylammonium fluoride (TBAF) as the source as well as in a mixture of organic–aqueous solution [16,17] . Faced with these limitations, researchers are in continuous effort to develop facile alternative routes that warrant comprehensive probe for selective, sensitive, quick, quantitative and qualitative recognition of F^- in aqueous solution. Current trend in the fabrication of sensors exploits supramolecular assemblies formed by non covalent interactions which can be fine tuned to evoke optical response specific to any target molecule, and thus realizing a sensor in practice. These sensors allow onsite, real time quantitative and qualitative detection of anions without the aid of any sophisticated and complicated instrumentation.

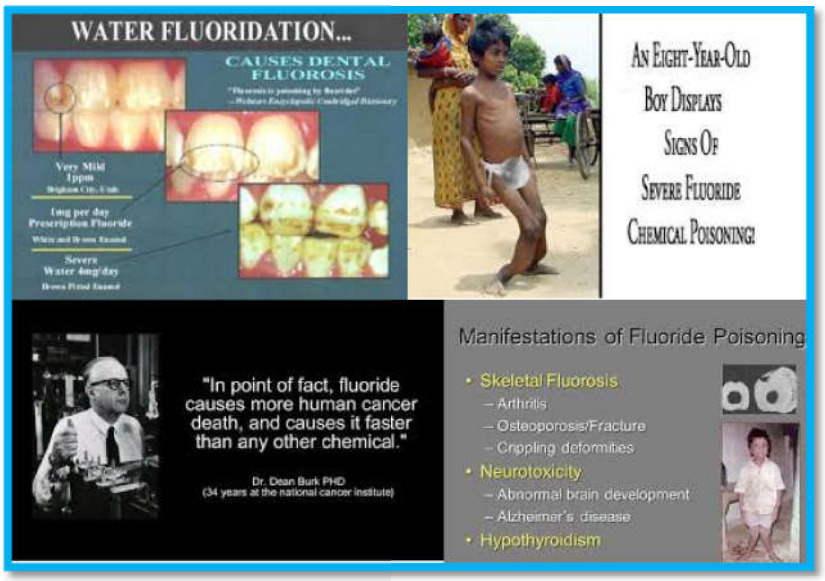

Figure 1. Adverse effects of Fluoride ion. [Adapted from various sources from the internet]

Herein, we present a sensor setup for Fluoride ion based on Graphene (GN) and mediated by organic dyes viz. Rhodamine6G and Fluorescein. Inspired by the reports based on Graphene-dye units as opto probes from Li.et al. [18] and from our own group [19,20] and also aiming at a continuation of our studies on sensors based on graphene-dye assemblies, we have worked on a novel displacement strategy for F^- recognition and sensing in aqueous solution.The counter ion of the Fluoride was chosen in such a way that it affects nil change to the optical response of graphene-dye unit. Hence Na^+ has been selected as the counter ion for all the anions. Briefly, a displacement approach tailors an anion binding sites i.e receptor and signaling unit (indicator) to form a supramolecular non covalent but stable assembly [21] . The binding of the indicator with receptor modifies the optical characteristics of the indicator by either quenching or enhancing the optical signal which is then modified (by restoring or suppressing the optical signal) specifically when in contact with the target ion. Quantification of these optical responses with Fluorimetry or UV spectrometer can serve as a tool for sensing and monitoring the presence of the test ion. Herein, we propose a displacement strategy based on Graphene and Rhodamine/Fluorescein supramolecular assembly that could sense parts per trillion and parts per billion amounts of F^- by fluorimetry and UV spectroscopy respectively. Further extension of the work has led to the fabrication of a solid phase sensor that can serve as a portable layman's tool for sub ppb level detection of the test anion. The sensory motif consists of Graphene-Dye unit at pH 4.3± 0.4 that will respond colorimetrically to the

presence of Fluoride ions. We have opted Rhodamine and Fluorescein dye as our indicators and Graphene as receptor. RD and FLR dye were chosen as they are much-admired surface active compounds noted for its noncovalent interactions with molecules. [22,18] A detailed discussion about the experimental procedure and the methodologies adopted for F^- sensing is provided in Chapter 2.

5.8 Results and Discussion

5.8.1 Graphene-Rhodamine dye unit as Fluoride ion sensor

(a) UV-Vis spectrometric route

Incremental addition of GN to Dye i.e Rhodamine solution led to progressive decrease of the absorbance band of their absorbance maxima centered at 557 nm as illustrated in Fig.2a. This can be ascribed to the formation of supramolecular assembly of graphene-Rhodamine dye unit at the expense of noncovalent interactions between graphene and Rhodamine molecules as reported earlier [18, 23-24]. π-π forces and dispersive forces operate in the formation of this supramolecular assembly. This diminished optical response was restored, and was enhanced upon the addition of fluoride ion, thus serving as a selective opto probe for fluoride ion as depicted in Fig. 2b. To establish the applicability of our approach for the quantative detection of F^- , we studied the UV-Vis response in presence of varied amounts of F^- and a working curve was established by plotting the absorbance (at 557nm) versus F^- concentration as shown in Fig. 2c. The restoration of absorbance intensity progressed in a linear fashion

with the concentration of F^- enabling the service of GRD unit as a quantitative read out tool for determining the concentration of F^- in unknown solutions. The Limit of detection (LOD) as calculated from 3 δ /m rule was 11 ppb which suggests the potential of this sensing strategy for F^- ion [25-27].

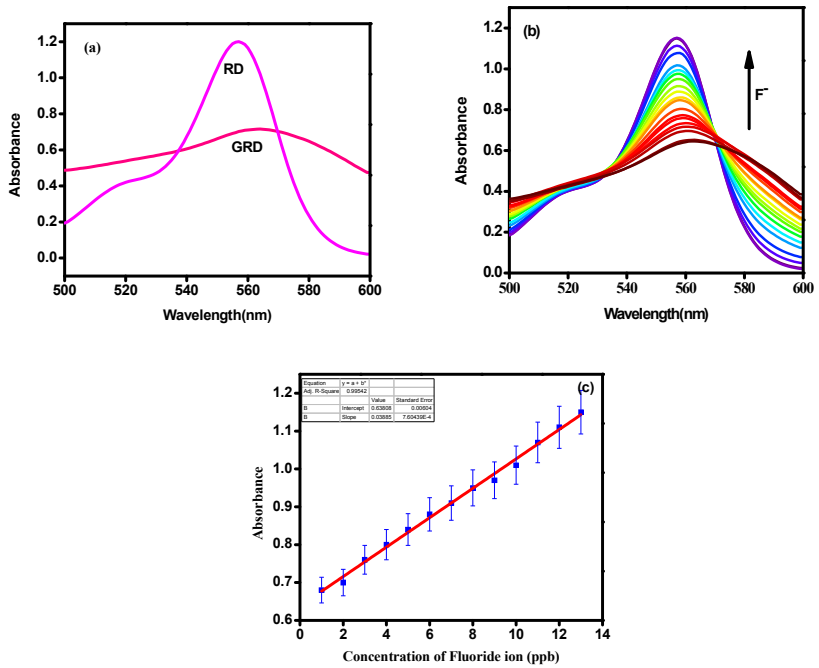

Figure 2. (a) UV−vis spectroscopic titration of RD with GN; (b) GRD unit with Fluoride ionand (c) Plot of absorbance intensity of GRD array with the concentration of F^- viz. 1.2ppb,2.4 ppb,3.1 ppb,4.4ppb,5.7 ppb,6.4ppb,7.1ppb,8.2 ppb,9.0 ppb,10.4 ppb,11.2 ppb,12.3 ppb,13.0 ppb & 14.5ppb.[RD-1.5mL,5μM:GN-140μL]

(b) Fluorimetric route

For applicability in more realistic and sensitive scenarios, the sensing performance was monitored with Fluorescence emission spectroscopy. As expected, the fluorimetric response went parallel with the UV-Vis response and it was found that the fluorescence of rhodamine centered at 584 can be effectively quenched and nullified by GN, was successfully restored with the introduction of aliquots of F^- [Fig.3a & 3b]. It is to be noted here that the fluorescence intensity was almost restored to the original intensity of pure rhodamine dye. A good linear relationship between the emission intensity indexed at 584 nm and F^- concentration, illustrated in Fig. 3c, suggests the potential of the projected system for F^- sensing in aqueous solution. The limit of detection (LOD) can be extended to 890 ppt using fluorescence spectroscopy as calculated by 3δ/m rule, which is much lower than the enforceable drinking water standard for F^- prescribed by EPA (Environmental Protection Agency) [28]. To the best of our knowledge, we believe that the proposed sensor motif outweighs the performance of most fluorimetric probes reported till date in terms of its Limit of detection, ease of operation in aqueous media, cost effectiveness and simplicity [29-34]. Though, the fluorescence color restoration upon the addition of 890 ppt of F^- is too small to be directly visualized with naked eye it can be clearly discerned with the aid of mere UV light [Fig.4]. The permissible amount of F^- in drinking water is 1-4 ppm and hence the projected assay is sensitive to serve as qualitative sensor for practical detection of F^-.

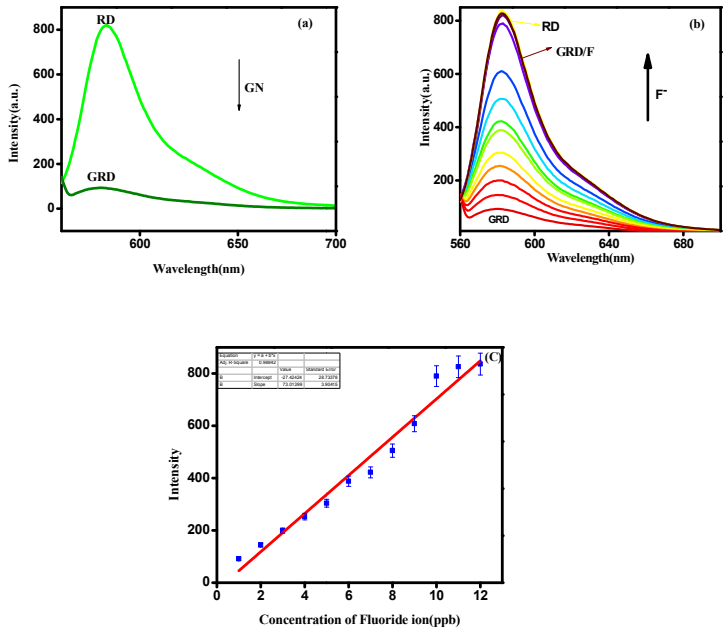

Figure 3. Fluorescence titration of RD with GN (a); (b) GN – RD with Fluoride ion and (c) Plot of fluorescence intensity of GN-RD array with the concentration of F^- viz. 1.1 ppt,2.0 ppt, 3.3ppt, 4.7ppt, 5.0ppt, 6.8ppt, 7.3ppt, 8.1ppt, 9.3ppt, 10.1ppt, 11.0ppt & 12.4ppt.[RD-1.5mL,5µM:GN-90µL; Excitation wavelength: 550 nm, Slit width: 1nm].

Figure 4. Colorimetric response of GRD array in presence of Fluoride ion in UV light (b) [RD-1.4mL; GN-150µL; Fluoride ion-900 ppt]

The proposed recognition strategy has its roots in the preferential adsorption ability of GN sheets. Graphene, the honeycomb

like decorated Carbon moiety is characterized by the presence of various oxygen functional groups and extensive π cloud that can enter into interaction with specific analyte molecules. The union between graphene and Rhodamine dye increases with the progress in titration and concomitantly a notable decrease in the optical response of rhodamine is seen as mentioned earlier owing to the formation of a supramolecular assembly of GN and the dye unit. The noncovalent forces viz. π-π stacking forces and the dispersive forces have played a central role in the formation of this weak but stable supramolecular assembly. This stage, characterized as an OFF stage (Optical response is decreased) will be turned ON (Optical response is restored) with the addition of any analyte molecule that can break the supramolecular assembly and preferentially binds with graphene sheets leading to the desorption of Rhodamine molecule. As the titration with F^- proceeds, graphene will selectively adsorb F^- ions and concurrently the supramolecular graphene-rhodamine assembly breaks leading to the increase in number of free dye molecules. Fluoride ion being the smallest and most electronegative atom can easily enter into graphene-rhodamine supramolecular complex and engages into stronger intermolecular Hydrogen bonding as well as anion-π interaction with GN sheets as depicted in Scheme 1. [35-38]. At the studied pH of 4, the edge carboxyl group-COOH and basal C-OH of GN sheets will be protonated which further enhances the interaction and adsorption of F^- by graphene. Subsequently, the recovery of absorbance takes place due to the desorption of rhodamine from the supramolecular network due to free rhodamine molecules in the solution enabling F^- sensing. The

adsorption of Rhodamine by graphene sheets quenches the fluorescence of Rhodamine as the excitation energy of Rhodamine is dumped into graphene without further emission (Fluorescence resonance energy transfer). With the addition of F-, graphene preferentially adsorbs F^- leaving Rhodamine molecules and hence its energy transfer is not interrupted by GN sheets.

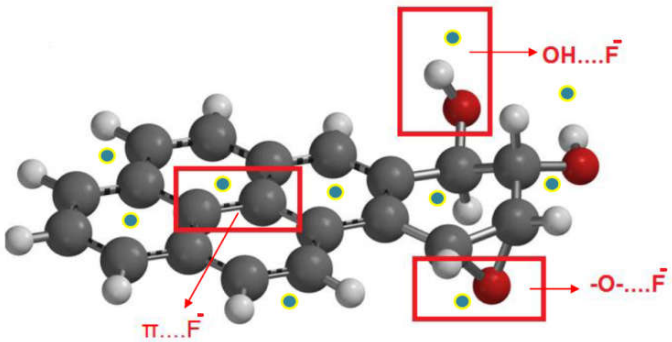

Scheme1 Possible modes of interaction between graphene and Fluoride ion

The lifetime measurements further strengthen the arguments for the proposed mechanism. Briefly, the adsorption of Rhodamine by graphene sheets quenches the fluorescence of Rhodamine as the excitation energy of Rhodamine is dumped into graphene without further emission (Fluorescence resonance energy transfer). With the addition of F-, graphene preferentially adsorbs F^- leaving Rhodamine molecules and hence its energy transfer is not interrupted by GN sheets. In the absence of GN sheets, the excited state life time of bare Rhodamine was 5.28 ns, which was reduced to 3.7 ns with the introduction of GN sheets. As F- ions are added, the excited state life-time increases to 5.17ns, underlining the sensing mechanism [Fig.5].

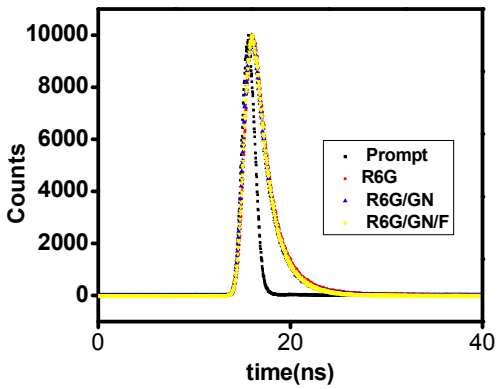

Figure 5. Fluorescence decays of RD, GRD and GRD/F measured by time-correlated single photon counting. Fluorescence monitored at corresponding emission maxima.

(ii) Graphene-Rhodamine unit as real time Fluoride sensor

The practical application of the projected sensor was explored by spiking a known amount of Fluoride ion in tap water and well water collected from neighbouring area. The sensing was performed by adopting the above described method using Fluorescence spectroscopy (concentration of F^- maintained at 850 ppt). As evident from Table 1, the potential utility of the sensor for onsite practical application is highly admirable as the measured concentration of fluoride ion fell within a small percentage error.

SOURCE	PL Method	
	Actual (ppt)	Measured (ppt)
TAP WATER	850	861
WELL WATER	850	885

Table 1. Analysis of Fluoride ion in real water samples

(iii) Selectivity of Graphene-Rhodamine unit

For further exploring the potential of the assay towards F^- sensing, the selectivity was investigated by the addition of 10 equivalents of common anions (such as Cl^-,Br^-,I^-,SO_4^{2-},NO_2^-,NO_3^- ,CO_3^{2-},HCO_3^-,CH_3COO^- in the form of K and Na salts) to the Graphene-Rhodamine assay and the absorption spectral changes were monitored. As depicted in the Fig.6, only F^- induced the restoration of the diminished absorbance while other anions lead to much weaker optical response substantiating the admirable selectivity of the unit for F^- recognition. Routine F- sensing systems face selectivity hurdles specifically from anions of similar basicity like carbonate and acetate but this current system could easily cross these issues [39-41]. The higher binding affinity of GN-dye unit to F^- than other anions is likely due to the high charge density and small size of F^- ion [42-43].

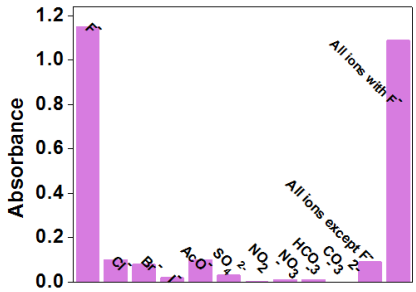

Figure 6. Absorbance of GN-RD unit in contact with selected anions

(iv) Graphene-Dye units as solid phase sensors

The cuvette based approach for F^- sensing is inconvenient and cannot be employed as a portable layman's tool for real on site detection of F^- and hence, there lies the huge prospects of solid phase portable sensors for F^-. Prompted by the above results, we have investigated the potential of Graphene-Rhodamine assay as a qualitative sensing tool for practical sensing of F^-. We have employed cellulose acetate strips stained with Graphene-Rhodamine solution as the matrix. The fluorescence of this modified strip was imaged under UV irradiation followed by the addition of F^- in varying concentrations. As depicted in Fig.7, no fluorescence was seen for GN-RD stained strip but the fluorescence can be easily restored with the addition of 950 ppt of F^- ion. It is to be noted that the fluorescence was recovered within few minutes after the addition of F^-. The strip showed a detection limit of 950 ppt, which is highly admirable as it falls much below the recommended F^- levels. Moreover, literature survey hints that this is the lowest LOD ever achieved for F^- strip sensor [44-46] .Though this dip strip is a simple proof of concept design for layman's qualitative tool for F^- detection in aqueous media, our study indicates

that the projected filter paper strips can serve as a potential candidate for environmental monitoring and control of Fluoride ion in aqueous systems. This study envisages that the use of this projected colorimetric strip for screening and in-laboratory assays will facilitate as a quick, simple and cost-alternative means to current, effective laboratory techniques for F^- detection.

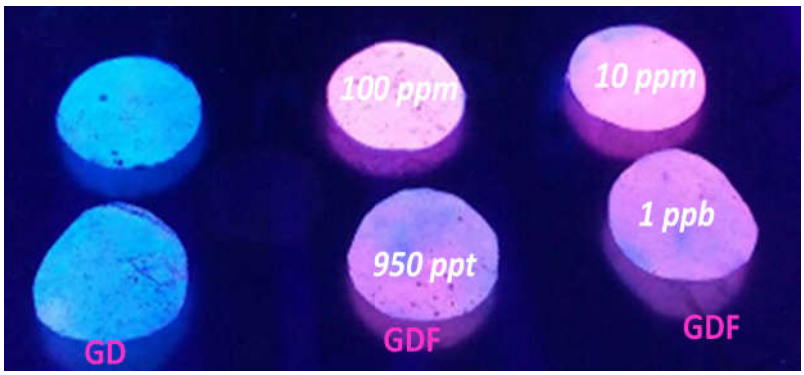

Figure 7. Digital images of paper strips dipped in F^- solution of varying concentration for depicting the visual detection limit of F^- ions under UV illumination.

5.8.2 Graphene-Fluorescein dye unit as Fluoride ion sensor

Inorder to extend the versatlity of the Graphene-Dye hybrid towards Fluoride sensing ,the performance of Graphene-Fluorescein unit was also investigated in a similar manner as adopted for Graphene-Rhodamine unit. As mentioned earlier, the extensive π conjugation in graphene sheets can be modulated for optical sensing. The noncovalent forces responsible for the formation of GD complex are (1) π-π interaction between aromatic clouds of graphene and dye and (2) dispersive interactions between functional groups on graphene and dye. Subsequently, there occurs a sudden decrease in the

absorbance/fluorescence intensity of fluorescein dye with the addition of GN to dye molecules due to the formation of graphene-dye supramolecular assembly [turn off state, Fig.8 (a & c)]. Secondly, when a strong competitor, F^- with high affinity for GN sheets comes into play, dye will displaced from the GD matrix and will be replaced by F^-. This in turn sets free dye molecules in solution restoring the quenched absorbance [Fig.8 (b & d)]. Moreover, it was found that a linear relationship exists between the restored absorbance and the quantity of the F^- added [Fig.8 (e & f)]. This calibration graph obtained can serve as a quantitative tool for determining the concentration of F^- in unknown samples. The limit of detection as calculated by 3 δ /m rule (δ is the standard deviation of the calibration graph and m is the slope) is found to be 4.8 ppm and 890 ppb through UV-Vis and Fluorimetric route respectively. This value is highly commendable as compared to several reported colorimetric sensors based on organic probes, graphene based systems, nanomaterials etc. and the proposed units could outweigh the performance of several fluorimetric sensors also. The performance of Graphene-Fluorescein immobilised filter paper strips was also studied. As shown in the Fig.9, the strips could detect 50 ppb of Fluoride ions under UV illumination.

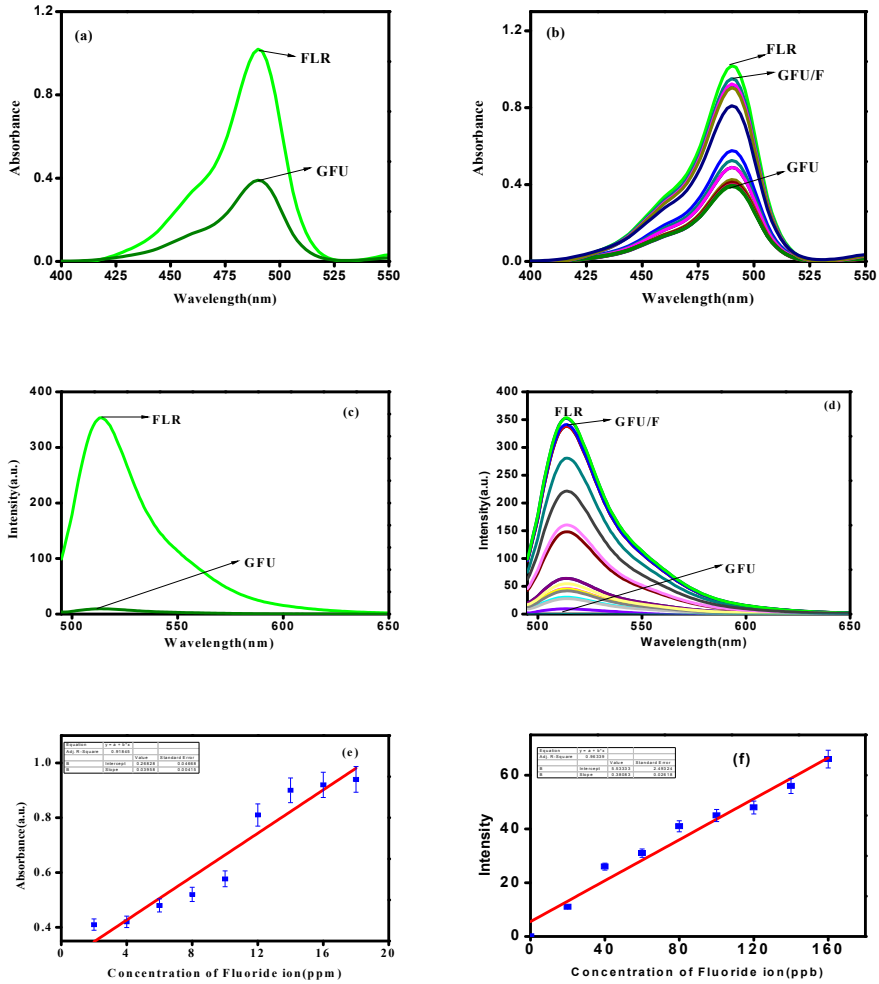

Figure 8. (a) Suppression of absorbance maxima of Fluorescein with the addition of Graphene;(b) Restoration of quenched response with the addition of Fluoride ion;(c) Fluorescence response of Fluorescein dye with the addition of Graphene [Excitation wavelength: 460 nm, Slit width: 1nm]; (d) Titration profile of GFU against Fluoride ion; quantitative variation of absorbance (e) and fluorescence(f) of GFU against Fluoride ion.

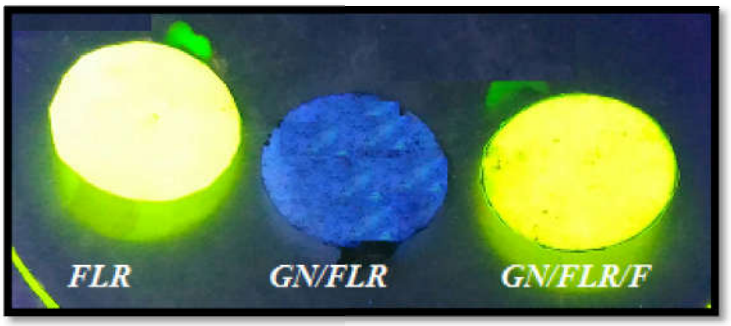

Figure 9. Fluoride sensing strips of Graphene-Fluorescein unit

Comparing the Fluoride ion sensing performance of various Fluoride probes reported in literature asserts the superiority of the projected GD unit as evident from Table 1.

Sensing Unit	Limit of detection	Reference
PEGylated Fluorescent Sensor	19 ppb	50
N-(3-(benzo[d]thiazol-2-yl)-4-(hydroxyphenyl)benzamide (3-BTHPB)	3.8 ppb	49
Anthraimidazoledione based sensors	0.038 ppm	48
Iridium(III) Cyclometalates	3.8 ppb	47
CdTe QD	5 ppm	27
Graphene-Rhodamine unit	850ppt	This work
Graphene-Fluorescein unit	890 ppb	This work

Table 1. *Comparison of GD units against other reported Fluoride sensors*

(vi) Graphene-Dye as a dual mode probe for Fluoride ion and Mercury ion

Graphene-Dye hybrids served as an excellent dual probe for Hg^{2+} and F^- ions. Hence there may be dispute on the selectivity of the sensor towards F^- in presence of Hg^{2+} and vice versa. However the significant difference in the pH of the sensing system for Hg^{2+} and F^- [which are ~ 7 and ~4 respectively] rules out the possible interference during their mutual presence. It was tested and verified that at pH 7, the sensing action towards F^- for Graphene-Rhodamine system was negligible. Same was the observation when Hg^{2+} sensing was attempted at pH 4.The zPc values of graphene solution obtained by Hydrazine Hydrate reduction is generally in the range of 3-4.At pH≤ zPc, the surface of the sorbent will be positively charged and hence is unfavourable for the adsorption of Hg^{2+}. Keeping this in mind, we have opted acidic pH for Fluoride sensing. Mercury adsorption is favourable at a pH>5. Literature survey suggests that anion adsorption process occurring through noncovalent interactions will vary inversely with the pH of the medium. It is to be noted that below the zPc value, the surface of the adsorbent is positively charged which facilitates the Fluoride adsorption. Hence we claim it as an added advantage of this sensing array, as it could successfully sense and quantify two hazardous species merely by varying pH of the medium.

5.9 Concluding Remarks

- A simple displacement approach for quick, selective and sensitive detection of F^- using Graphene sheets mediated by Rhodamine/Fluorescein dye is demonstrated here.

- The core of the sensing strategy lies on the preferential affinity of Graphene towards Fluoride ion over Rhodamine/Fluorescein.

- The findings of UV-Vis and Fluorescence titrations illustrates that through interactions between Graphene and Dye, an OFF state(optical response decreases) is established which can be turned ON specifically with the introduction of F^-, as dye is desorbed from the Graphene matrix.

- Quantitative detection of F- for Graphene-Rhodamine system in totally aqueous solution with a striking detection limit of 11ppb and 850 ppt was possible using this optoprobe via UV-Vis and fluorimetric studies respectively. Whereas Graphene-Fluorescein unit yielded 4.8 ppm and 890ppb through Uv-Vis and fluorimetric channels respectively.

- The proof of concept for this sensing strategy is demonstrated through paper-based testing strips with limit down to 950 ppt for Graphene-Rhodamine strips. Graphene-Fluorescein strips could sense 10 ppb of Fluoride ion in UV light.

- Investigations on real water samples spiked with Fluoride ion assures that the proposed sensor moiety can swiftly monitor the test ion levels in complex samples and affirm the utility of the system for practical applications.

- To the best of our knowledge, conventional chromogenic and fluorogenic sensors for F- fails to compete with the proposed sensory unit in terms of its LOD, simplicity, workability in aqueous systems, selectivity etc.

- Integrating the strip into a portable fluorescence reader would open the doors for further technological improvements so as to enable the service of this simple and sensitive testing strip for in situ detection of F^- in water as well as in samples of environmental and industrial interest.

5.10 References

[1] Hui Ren,, Dhaval D. Kulkarni Rajesh Kodiyath,Weinan Xu, Ikjun Choi, and Vladimir V. Tsukruk, *ACS Appl. Mater. Interfaces* ,2014, 6, 2459.

[2] F. P. Schmidtchen and M. Berger, *Chem. Rev.* 1997, 97, 1609-1646.

[3] K. L. Kirk, Plenum Press: New York, 1991; 58.

[4] M. Kleerekoper, *Endocrinol. Metab. Clin. North Am.* 1998, 27,441-452

[5] Waddington R and M.Langley *Connective tissue research*. 2003,44,88-95.

[6] E.Gazzano, L.Bergandi, C. Riganti, E. Aldieri, S. Doublier , C. Costamagna, *Curr Med Chem*. 2010,17,2431-2441.

[7] R.Hawkings, L.Corriveau, S.Kushneriuk and P. Wong, *Analytica Chimica Acta*., 1978,102, 61-83.

[8] M.V.B. Krishna, S.V. Rao, V.S.N. Murthy and D. Karunasagar , *Analytical Methods*, 2012, 4,1565-1572.

[9] S. Chandra, A. Rika, P. Vec and H. Lang, *Anal. Chim. Acta*, 2006,577, 91

[10] X.Y. Liu, D.R. Bai and S. Wang, *Angew. Chem*., 2006, 118, 5601.

[11] T.W. Hudnall and F.P. Gabbaï, *Chem. Commun*. , 2008,38, 4596.

[12] T.W. Hudnall, Y.-M. Kim, M.W. Bebbington, D. Bourissou and F.P. Gabbai, *J. Am. Chem.Soc.* 2008,130,108901.

[13] X.-F.Yang, *Spectrochim. Acta Part A Mol. Biomol. Spectrosc.* 2007,67,321.

[14] E.J. Cho, J.W. Moon, S.W. Ko, J.Y. Lee, S.K. Kim, J. Yoon and K.C. Nam, *J. Am. Chem. Soc.* 2003,125,12376.

[15] F. M. Hinterholzinger, B. Rühle, S. Wuttke, K. Karaghiosoff and T. Bein*, Scientific Reports*,2013, 3,25621-25627.

[16] Pichandi Ashokkumar, Hardy Weißhoff, Werner Kraus and Knut Rurack, *Angew. Chem*., 2014, 53,2225.

[17] R. Nishiyabu and P Anzenbacher, *Org. Lett.* 2006, 8, 359.

[18] Wei Tao Huang, Yan Shi, Wan Yi Xie, Hong Qun Luo and Nian Bing Li, *Chem. Commun.* 2011, 47, 7800−7802.

[19] Anju Mohan and Renuka Neeroli Kizhakayil, *ACS Appl. Mater. Interfaces*., 2016, 8, 14125.

[20] M. Anju, T. Divya, M. P. Nikhila, T. V. Arsha Kusumam, A. K. Akhila, V. A. Ansi and N. K. Renuka, *RSC Adv.,* 2016, 6, 109506.

[21] Xiaoding Lou,Daxin Ou,Qianqian Li and Zhen Li, *Chem. Commun*., 2012, 48, 8462.

[22] G.Lunn and B. E. Sansone, John Wiley & Sons Publication: New York.Wiley, 2ed, 1994.

[23] Xian-Fu Zhang, Su-Ping Liu and Xiao-Na Shao, *Spectrochimica Acta Part A: Molecular and Biomolecular Spectroscopy* 2013,113, 92.

[24] Ebru Bozkurt, Murat Acar, Yavuz Onganer and Kadem Meral, *Phys.Chem.Chem.Phys.,* 2014, 16, 18276.

[25] Eun Jin Cho, Byung Ju Ryu, Young Ju Lee and Kye Chun Nam, *Organic Letters*,2005,7,2607.

[26] Raziyeh Arabahmadi and Saeid Amani, *Supramolecular Chemistry*, 2014, 26, 21.

[27] Pooja Singh, Asmita A. Prabhune,Chandra Shekhar Pati Tripathi and Debanjan Guin, *ACS Sustainable Chem. Eng*. 2017, 5, 982.

[28] Yang Jiao, Baocun Zhu, Jihua Chen and Xiaohong Duan, *Theranostics* 2015, *5*, 173.

[29] Ravi Chavali , Naga Siva Kumar Gunda , Selvaraj Naicker and Sushanta K. Mitra, *Analytical Chemistry Research,* 2015, 6, 26.

[30] Sheng Xu, Kongchang Chen and He Tian, *J. Mater. Chem.*, 2005, 15, 2676.

[31] Yi Qu, Jianli Hua and He Tian, *Org.Lett*.,2010,12,3320.

[32] Rui Hu, Jiao Feng, Dehui Hu, Shuangqing Wang, Shayu Li, Yi Li and Guoqiang Yang , *Angew. Chem. Int. Ed.* 2010, 49, 4915 .

[33] Fangyuan Zheng, Fang Zeng,Changmin Yu, Xianfeng Hou and Shuizhu Wu, *Chem. Eur. J.* 2013, 19, 936.

[34] Namita Kumari, Nilanjan Deya and Santanu Bhattacharya, *Analyst*, 2014, 139, 2370.

[35] Hidekazu Miyaji and L. Jonathan. Sessler, *Angew. Chem. Int. Ed.* 2001, 40, 154.

[36] Yinhui Li, Yu Duan, Jing Zheng, Jishan Li, Wenjie Zhao, Sheng Yang and Ronghua Yang, *Anal. Chem.* 2013, 85, 11456.

[37] W. H. Slabaugh and B. C. Seiler*, J. Phys. Chem*. 1962, 66, 396.

[38] I.Dékány, R Krüger-Grasser and A. Weiss, *Colloid Polym. Sci*.1998, 276, 570.

[39] T. Mizuno, W.-H. Wei, L. R. Eller and J. L. Sessler, *J. Am. Chem. Soc.,* 2002, 124, 1134.

[40] C. J. Woods, S. Camiolo, M. E. Light, S. J. Coles, M. B. Hursthouse, M. A. King, P. A. Gale and J. W. Essex, *J. Am. Chem. Soc.*, 2002, 124, 8644.

[41] E. J. Cho,J. W. Moon, S. W. Ko, J. Y. Lee, S. K. Kim, J. Yoon and K. C. Nam, *J. Am. Chem. Soc*., 2003, 125, 12376.

[42] J. Y. Lee, E. J. Cho, S. Mukamel and K. C. Nam, *J. Org. Chem*., 2004, 69,943.

[43] W. Lu, H. Jiang, F. Hu, L. Jiang and Z. Shen, *Tetrahedron,* 2011, 67, 7909.

[44] Gandhi Sivaraman and Duraisamy Chellappa, *J. Mater. Chem. B*, 2013, 1, 5768.

[45] Zhi-hua Lin, Yong-gang Zhao, Chun-ying Duan, Bing-guang Zhang and Zhi-ping Bai, *Dalton Trans.*, 2006, 30, 3678.

[46] Binglin Sui, Bosung Kim, Yuanwei Zhang, Andrew Frazer and Kevin D. Belfield, *ACS Appl. Mater. Interfaces*, 2013, 5, 2920.

[47] Nguyen Van Nghia, Jihun Oh, Jaehoon Jung and Min Hyung Lee, *Organometallics*, 2017, 36, 14.

[48] Amrita Sarkar, Sudipta Bhattacharyya and Arindam Mukherjee ,*Dalton Trans.*, 2016, 45, 1166.

[49] Rui Hu, Jiao Feng, Dehui Hu, Shuangqing Wang, Shayu Li,Yi Li, and Guoqiang Yang, *Angew. Chem. Int. Ed*. 2010, 49, 4915.

[50] Fangyuan Zheng, Fang Zeng,Changmin Yu,Xianfeng Hou,and Shuizhu Wu, *Chem. Eur. J.* 2013, 19, 936.

CHAPTER VI

SUMMARY AND SCOPE OF FUTURE WORK

Contents

Chapter 6 summarizes the highlights of the research work carried out and projects the future scope and hope in extending the potential of graphene hybrids for several applications.

6.1 Introduction

The objective of this work was to utilize Graphene-Hybrids for environmental applications. Hence, we have attempted to explore the properties and applications of Graphene hybrids for environmental applications. Briefly, our research work aims at devising Graphene-iron oxide hybrids for adsorptive removal of relevant water pollutants and employing Graphene dye hybrids for sensing toxic analytes in water bodies. In this regard, we have fabricated Graphene-Iron oxide nanotube hybrid for adsorptive removal of toxic heavy metal Chromium (VI) and hazardous dye Methylene blue. Graphene-Iron Oxide coated Polyurethane sponge was employed for decontamination of aqueous system from oils and organics. Graphene dye hybrids (Graphene-Rhodamine Unit and Graphene-Fluorescein unit) were employed to monitor and detect the presence of toxic analytes Mercury ion and Fluoride ion in aqueous system. The synergistic interactions between the constituents of Graphene composites and their tunable optical properties have been vital for the performance of these hybrids in adsorbing/sensing the proposed targets of the study.

6.2 Summary

- The prospects of Graphene-Iron oxide hybrid as an adsorbent was evaluated by examining its ability to remove heavy metal Chromium (Cr (VI)) and Methylene blue (MB) dye from aqueous environment. In this regard, a magnetically separable graphene–iron oxide nanotube composite was synthesised for the first time via an adept template free hydrothermal route.

The physical characterization of the material was done using XRD, FTIR, SEM, TEM and VSM analysis. A mechanism analogous to the Kirkendall effect, involving the diffusion of Fe^{2+} ions and consequent expansion of voids leading to the formation of hollow iron oxide nanotubes has been proposed in accordance with the results obtained from XRD and TEM analysis. The composite turned out to be an excellent adsorbent for the removal of toxic Cr (VI) ions and MB dye. Adsorptive removal and magnetic separation was achieved quickly within few seconds which highlights the efficiency of the prepared hybrid. The isotherm analysis indicated that the adsorption data can be represented by the Langmuir isotherm model. The superior adsorptive removal efficiency of the composite can be attributed to the synergistic effect between graphene and the iron oxide nanotubes. Through this investigation, we have demonstrated an attempt for template free synthesis of iron oxide nanotubes and their incorporation on graphene sheets that yield an excellent adsorbent for removing Cr (VI) and MB.

- As our efforts to utilize Graphene-Iron oxide nanotube hybrid for removal of oils and organics from aqueous system failed, we diverted our study to use Polyurethane as a matrix for hosting Graphene-Iron oxide nanoparticles and have investigated its use for the removal of oils and organics. The fabricated Poly Urethane foam wrapped by a network of Graphene-Iron Oxide composite (GPUF) served as an elite sorbent for organic contaminants and oils. Anchoring

Graphene-meso Iron Oxide composite on poly urethane foam switches it to a super hydrophobic and super oleophilic moiety. Detailed structural, microscopic and wettability studies points the cooperative effect of the 3D porous poly urethane scaffold and the effect of Graphene-mesoporous Iron oxide composite on the adsorption dynamics. Benefitting from the hierarchical porous structure and heterogeneity, the as fabricated sponge manifested superior selective adsorption capacity for a wide variety of oils and organic pollutants in the range of 90-316 gg^{-1}. Application of GPUF was demonstrated by quick and selective removal of oils from water under magnetic field. In addition to this, after sorption the adsorbate can be released by simple squeezing without any deterioration in structure and performance, underlining the recyclability of the sorbent for over 150 cycles. The results of the study promise a novel sorbent which can be easily scaled for large scale treatment of oil spills.

- Lured by the tunable optical properties of Graphene-Dye hybrids, we have investigated their ability in sensing relevant analytes in aqueous system. We have revealed the first ever prospective application of Graphene-Dye array that offers a quick, selective and sensitive optical response to the presence of a noxious heavy metal ion, mercury (Hg^{2+}) in aqueous solution. A turn off and turn on optical response is envisaged by the unit on competitive adsorption of dye and target Hg^{2+} on graphene sheets. The crux behind the sensing of Hg^{2+} ion by

the Graphene-Dye unit lies behind the decrease in absorbance/fluorescence intensity of the dye on complexing with Graphene sheets and the corresponding restoration of the optical response upon highly selective competitive adsorption of Hg^{2+} ions by GN sheets. The duality of Graphene to undergo π–π and dispersive interactions with dye molecules as well as to act as a selective adsorbent for target ions is conceptualized in this study. Quantification of these optical responses was attained by colorimetric and fluorimetric measurements, which yielded ppb level and ppt level mercury ion assay. The moiety is highly selective and specific for mercury ions over alkali, alkaline earth metals and its congeners. The significant advance in this investigation is the fabrication of Graphene-fluorescein unit as a qualitative read out tool for naked eye detection of Hg^{2+} ions in ppm levels by noting the colour, and for the visual detection of ppt levels of Hg^{2+} through fluorescence in UV light. A highly efficient Graphene-Dye immobilized filter paper strip was developed which could sense Hg^{2+} under UV light in a concentration as low as ppt level. Moreover, investigations on tap water samples spiked with Hg^{2+} ions underlines that the GD units can swiftly monitor Hg^{2+} levels in complex solutions and demonstrates its potential utility in practical applications.

- Further investigation on exploiting the potential of Graphene-Dye hybrids leads to the fabrication of Fluoride ion sensor based on Graphene-Rhodamine unit and Graphene-Fluorescein

unit by mere variation of solution pH. We proposed and demonstrated a simple displacement approach based on Graphene and Dye assembly that could sense fluoride ion in aqueous solution. As mentioned in the case of Hg^{2+} assay, Graphene-Dye unit engages in the formation of a supramolecular complex between dye (indicator) and Graphene (receptor), followed by the displacement of the indicator with the advent of F^- ion. These changes alter optical characteristics of the supramolecular entity which can be quantified using spectroscopic techniques. The findings of UV-Vis and Photoluminescence analysis together with the life-time measurement studies reveal that the optical response of the dye is quenched through the interactions of Graphene sheets with dye which can be selectively restored by introducing traces of F^-. The detection limit was measured by UV-Vis and Photoluminescence studies respectively, falling admirably below the permissible F^- level in drinking water i.e. 1.5 ppm. The proof of concept for this sensing strategy is demonstrated through paper-based testing strips that can function as a portable layman's tool for sub ppb level detection of the test anion. Our investigation warrants the application of GD units as a dependable sensor for Mercury ion and Fluoride ion by switching the pH of the solution.

6.3 Scope of future work

The advent of Graphene hybrids has opened many doors for fabricating high performance composites. A lot of emphasis has been given to the applications of these hybrids in versatile realms. The results obtained from our study throw light on the mammoth potential on the synergistic interaction between the components of Graphene hybrids and their tunable properties. Literature survey and our findings underlines that there is still room for further development on the application of Graphene hybrids.

It was concluded that the Graphene-Iron oxide composites have huge potential as an adsorbent. The synergistic interaction between the constituents was crucial for their performance. We believe that fabricating magnetically responsive Graphene based 3D hydrogels and aerogels can function as superior sorbents for removal of wide array of water contaminants. The concomitant removal of the contaminants can also be carried out which further extends the application of these hybrids as elite sorbents.

Figure 1. Digital images of Graphene Hydrogels of varying composition which can be employed as adsorbent for various pollutants. Figure in the inset presents the freeze dried images of Graphene Hydrogel.

Our studies point to the commendable sensing capacity of Graphene Dye hybrids. Exploiting the sensing potential of Graphene-Dye hybrids, we believe that proper use of different dyes and other fluorescent probes capable of entering into interaction with Graphene will be able to sense a whole array of analytes ranging from biomolecules, proteins, food additives, metal ions, to relevant anions etc. We also believe that these probes can be employed for bio imaging applications.

However, researchers are still facing many challenges associated with the production and applications of Graphene based materials. The main problem associated with GN based hybrids is in their reproducibility and difficulty in obtaining uniform dispersion on GN matrix. Intense research and advancement in current synthetic methods must be directed for extending the large scale application of these hybrids and their commercialization. Though researches on developments of Graphene hybrids are growing exponentially, there is still space for extensive research for basic understanding of the subject and their future practical utilization.